WestminsterResearch

http://www.westminster.ac.uk/westminsterresearch

Impact of urban form on concentration of air pollutants within street canyons at pedestrian level

Ebadi Borna, M.

A PhD thesis awarded by the University of Westminster.

Impact of urban form on concentration of air pollutants within street canyons at pedestrian level

Mehrdad Borna

This thesis is submitted in partial fulfilment of the requirements of
the University of Westminster for the Degree of Doctor of Philosophy

December 2022

(This page is intentionally left blank)

Abstract

Recent estimates published by WHO reported that in 2018 air pollution caused eight million premature deaths worldwide. The same report highlighted that outdoor air pollution was responsible for 4.2 million deaths. This implies that further efforts and mitigations are needed to reduce individuals' exposure to harmful air pollutants. In this respect, governments around the world developed and published a number of air quality plans and frameworks. However, they either ignored or paid less attention to microclimate and urban form attributes and their impact on air pollution concentrations or dispersion in urban spaces, particularly within urban street canyons.

Considering the above, this study postulates that there is a correlation between urban form and air quality. Therefore, the core focus of this thesis is to investigate this relationship in greater depth and to propose a set of recommendations that can create a desirable microclimate within various urban street canyons capable of mitigating air pollution concentrations and thereby reducing its negative impact on human health. This thesis employs a variety of methods, including fieldwork, computational modelling, and correlation analysis, to measure the influence of various street canyon configurations on the concentration of air pollution.

The findings of this study confirmed several correlations between air pollution concentrations and urban form within street canyons. This study generated new knowledge on air pollution and microclimate behaviour within various street canyons. It provided recommendations for 30 distinct urban street canyon configurations in order to increase dispersion and protect pedestrians from harmful levels of air pollution. It also offered much-needed knowledge and recommendations for urban designers and planners to consider to make informed design decisions to encourage greater dispersion of air pollution within various urban street canyons, particularly in areas with high pedestrian traffic to reduce and limit public exposure to harmful air pollution.

Acknowledgements

I am extremely grateful to many people who have assisted me in various ways throughout this long but rewarding process of completing a PhD programme.

I am grateful to my incredible director of study and first supervisor, Dr Rosa Schiano-Phan, for her guidance, constructive criticism, and encouragement throughout the process that led to the successful completion of this study. Throughout my PhD programme, she has been a limitless source of inspiration and intellectual drive. Along with her brilliance, Rosa's kindness and humbleness have provided me with an example of decency that I hope to emulate throughout my life.

I'd also like to thank Dr. Krystallia Kamvasinou, my second supervisor. Her constructive feedback during group meetings has been unquestionably beneficial to my research. The feedback was always timely and useful in helping me improve my thesis. I appreciate her encouragement.

I would like to thank the staff at the University of Westminster, particularly those in the Graduate School and the School of Architecture and Cities, for their unending support, especially during the COVID-19 pandemic and lockdown. I am grateful to the University for providing a high-performance computing facility and to FabLab for the instruments and tools; without their assistance and support, I would not have been able to complete my research. I am also grateful to the Globally Engaged Research fund, the 125 Fund Award, and the Sustainable Cities and the Urban Environment Research Community at the University of Westminster for their funding and support. Without their assistance, I would be unable to present or publish on my research topic during my PhD journey.

I am grateful to all of my university colleagues, undergraduate and postgraduate students, PhD colleagues in the PhD office, and especially colleagues who supported me in establishing the first PhD Society, a social and supportive space for our doctoral community. Not to mention the support from the Graduate School and the university's vice-chancellor,

Dr Peter Bonfield; I could not have launched the society successfully without your help and faith in me.

Thank you to all of my friends in the UK and around the world (if you're reading this, you know who you are!) for your continued support. I will never forget the role each of you played. I am grateful to my parents for their unwavering love and support. I apologise for all of the stress and worry I have caused you, not to mention all of the family gatherings I have had to miss. Thank you for being there for me every step of the way; I couldn't have done it without you! You have raised me up to more than I can be.

Last but not least, I'd like to thank my lovely wife, Sunny, without whom I would not have begun, continued, or completed this project. Thank you for bearing with me through all of the ups and downs of this challenging journey. Thank you for the lengthy and in-depth discussions on my PhD topic and for ensuring that I don't go insane during moments of stress and frustration - I often wonder why you put up with me, but I am grateful that you do! You are everything to me, and I humbly dedicate this work to you.

And perhaps one more thanks to my faithful writing companion, who, despite being 9 years old still can't read or write! Therefore, may never read this! To my dog Hugo for the love, devotion and reasons to keep me mobile and sane.

Author's declaration
I declare that all the material contained in this thesis is my own work.

Table of contents

List of Figures

List of Tables

List of acronyms

AADF	Annual Average Daily Flow
ADMS	Atmospheric Dispersion Modelling System
AERMOD	American Meteorological Society-Environmental Protection Agency Regulatory Model
AQMA	Air Quality Management Areas
AQS	Air Quality Strategy
AURN	Automatic Urban and Rural Network
BSC	Building Site Coverage
CAZ	Clean Air Zones
CCZ	Congestion Charging Zone
CFC	Chlorofluorocarbon
CFD	Computational Fluid Dynamics
CO	Carbon Monoxide
CO_2	Carbon Dioxide
DCLG	Department for Communities and Local Government
DEFRA	Department for Environment, Food and Rural Affairs
DfT	Department for Transport
EEA	European Environmental Agency
EIT	Emissions Inventory Toolkit
EMEP	European Monitoring and Evaluation Programme
EU	European Union
EV	Electric Vehicle
FAI	Frontal Area Index
FAR	Floor Area Ratio
FDM	Finite Difference Method
FVM	Finite Volume Method
GIS	Geographic Information Systems
GLA	Greater London Authority
HDV	Heavy Duty Vehicle
HUDU	Healthy Urban Development Unit
IAQM	Institute of Air Quality Management
ISL	Inertial Sub Layer
LAD	Leaf Area Density
LAQM	Local Air Quality Management
LCZ	Local Climate Zone
LDV	Light duty vehicle
LEZ	Low Emission Zone
LTN	Low Traffic Neighbourhoods
MP	Member of Parliament
MRT	Mean Radiant Temperature
NAEI	National Atmospheric Emissions Inventory
NHS	National Health Service

NO	Nitric oxide
NO$_2$	Nitrogen Dioxide
NTC	Negative Temperature Coefficient
O$_3$	Ground Level Ozone
PDD	Predicted Percentage of Dissatisfied
PET	Physiological Equivalent Temperature
PHE	Public Health England
PM	Particulate Matter
PM$_{10}$	particulate matter with a diameter of 10 microns
PM$_{2.5}$	particulate matter with a diameter of 2.5 microns
PPM	Part Per Million
PTAL	Public Transport Accessibility Levels
PUD	Perceived Urban Density
QA	Quality Assurance
QC	Quality Control
RAG	Red-Amber-Green
RH	Relative Humidity
RL	Roughness Length
RSL	Roughness Sub Layer
RTF	Roads Task Force
SET	Standard Effective Temperature
SF6	sulphur-hexafluoride
SO$_2$	Sulphur Dioxide
SVF	Sky View Factor
TfL	Transport for London
UBL	Urban Boundary Layer
UCL	Urban Canopy Layer
UDD	Urban Demographic Density
UK-AQF	UK-Air Quality Forecast
ULEZ	Ultra Low Emission Zone
UNDESA	United Nations Department of Economic and Social Affairs
UNWUP	United Nations World Urbanization Prospects
URD	Urban Resources Density
USA	United State of America
UTCI	Universal Thermal Climate Index
VOCs	Volatile Organic Compounds
WHO	World Health Organisation
WMO	World Meteorological Organisation

Part 1

Introduction

Chapter 1

1 Introduction

Chapter 1
Introduction

This chapter introduces this research. It briefly discusses the background of the research, before describing the research aim and objectives. It includes an overview of the methodological and theoretical approach and outlines the structure of the thesis.

1.1 Introduction and background

In 2010 and for the first time, the World Health Organization declared urban air pollution a serious public health hazard. Since then, various efforts have been made to reduce air pollution to protect public health. However, according to 2018 data, eight million people died prematurely as a result of exposure to outdoor and indoor air pollution in 2016, accounting for one-eighth of all global deaths (World Health Organization, 2018). This implies that further efforts and mitigations are needed to reduce individuals' exposure to harmful air pollutants. The same report highlighted that outdoor air pollution was responsible for 4.2 million deaths worldwide. According to a recent report published by London Council (2020) pollutants like particulate matter (PM) and nitrogen dioxide (NO_2) caused 9,416 premature deaths in 2019 in a developed city like London. Furthermore, these pollutants have caused hundreds of thousands more individuals to suffer from major chronic health conditions, resulting in a 1.5-year fall in average life expectancy in the UK (Munzel et al. 2019).

The link between health and air quality has been well researched and established (Pope, Ezzati and Dockery, 2009; Cohen et al., 2017), and several studies show that living in an urban area with high pollution levels may exacerbate lung cancer, heart disease, stroke, and respiratory diseases like asthma (Kuo et al., 2006; Nawrot et al., 2006; Boffetta, Merler and Vainio, 1993; Lasley and Gilbert, 2000; Mandal, 2005; Schell et al., 2006). This situation is exacerbated for vulnerable people, such as the elderly, who have a higher risk of hospitalisation when there are high levels of pollutants in the air, and children, as they breathe faster than adults and thus absorb more pollutants. Moreover, children are shorter than adults, therefore, are closer to the ground and hence to car exhaust pipes. It is important to note that during the COVID-19 pandemic, numerous international studies have

also established a link between air pollution and COVID-19 morbidity and mortality; this highlights the urgency of addressing issues pertaining to air pollution and developing solutions to reduce human exposure to harmful levels of air pollutants (Borna et al., 2022).

The term "air pollution" refers to the degradation of air quality as a result of physical or chemical changes caused by natural processes or human activities (Cunningham and Cunningham, 2017). One of the primary causes of the increase in air pollution is our rapid urbanisation as a consequence of the rise in urban population. This growth in population has increased the use of non-renewable energy sources, motor vehicles, and excessive industrial activity resulting in excessive air pollution and degrading urban air quality to "unhealthy" levels (Wang et al., 2020; Hueglin et al., 2005). Unhealthy conditions occur when large amounts of pollution and other forms of waste are released into the atmosphere at a rate faster than the atmosphere can absorb and disperse them (Enger and Smith, 2016).

Throughout most of history, human populations have mostly lived in rural areas, relying on hunting and agriculture for survival (UNDESA Population Division, 2015). In 1800, cities accounted for only 3% of the global population. By 1900, nearly 14% of the population (220 million) lived in cities, despite the fact that only 12 cities had a population of one million or more. The urban population continued to grow, and a century later, the urban population rose dramatically and rapidly to 49%, equal to 3.2 billion inhabitants (Bocquier, 2005). According to statistics published by the United Nations' World Urbanisation Prospects in 2014, cities now house more than half of the global population for the first time since 2005, with over 400 cities with populations ranging from one to five million and 19 with populations exceeding ten million (UNWUP, 2014). The latest reports projected that, the Earth's population is expected to increase by 68% by 2050, to 9.7 billion people, a 2.8 billion increase in three decades (Fig. 01). That means the number of cities with populations of 1 to 5 million will rise to 560, with 43 mega cities with populations of more than 10 million (UNDESA Population Division, 2015). Certainly, we cannot deny the benefits of urbanisation and city growth in promoting quality of life, but it also has caused a series of major environmental and health problems globally (Wang et al., 2020). In the same vein, the governments across the globe are actively introducing bold new plans and policies to build more homes to respond to this fast-growing urban population and additional building stock

3

will be constructed in the near future worsening the associated environmental and air pollution issues with urbanisation in future years to come.
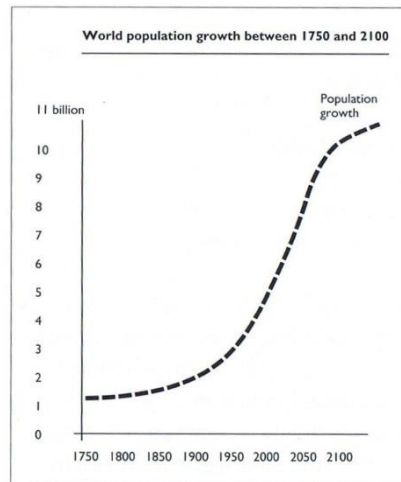
Fig. 01 - World population growth between 1750 and 2100 (Crewe, 2012).

In urban settings, the urban canopy layer which is a space between street level up to height of roofs, traps and concentrates pollutants. In urban areas, this urban canopy layer consists of multiple street canyons, which are narrow urban roads flanked by a continuous row of buildings (Fig.02). These street canyons suffer from issues pertaining to wind comfort for pedestrians as well as excessive pollution levels because they do not have adequate natural ventilation. This causes an increase in the concentration of pollutants that are related to both traffic and non-traffic sources (Oke, 1988; Chen and Ng, 2012; Evyatar, David and Terry, 2011). The short gap between the buildings prevents background wind from entering the street, resulting in lower wind speed in the street than outside, particularly when the background wind is perpendicular to the street (Oke, 1988).
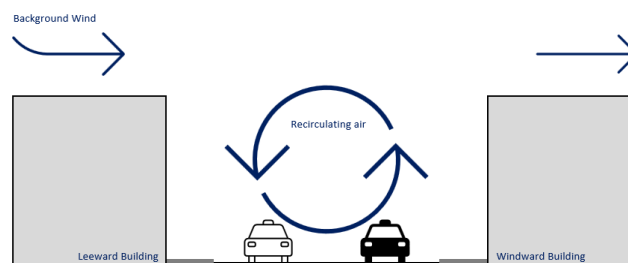
Fig.02 – Generic symmetrical urban street canyon and recirculation of airflow inside canyon when background wind is perpendicular to the street. Windward building is facing the upwind and leeward building is downwind and along the direction towards which the wind is blowing.

Typically, the concentration of pollutants in street canyons is higher than in the surrounding urban environment. For instance, in 2005, data collected at London's Marylebone Road revealed that the hourly concentrations of NO_2 had exceeded the hourly objective 853 times (Defra, 2008). These urban street canyons are where the majority of outdoor activities of urban residents occur. Pedestrians, vehicle drivers, and residents of nearby buildings that may get ventilation from the outside canyon environment are all subject to significant exposure in these areas.

On that account, over the past years number of studies have been carried out to link urban form with urban microclimate in various climates (Givoni, 1998; Krazter, 1956; Kubota et al., 2008; Grimmond et al., 2001; Mills et al., 2010; Oke, 1977; 1978, 1988, 2010, 2004; Steeneveld et al., 2014). Most of these studies focused on highlighting the desirable and undesirable conditions and possible design interventions that can improve pedestrian thermal comfort and lower building energy loads (Oke, 1981; Givoni, 1998; Santamouris, 2000; Cole, 2009; Edussuriya et al., 2011; Ren et al., 2011; Ng, 2012; Chatzidimitriou and Yannas, 2017; Jeanjean et al., 2017). In recent years, along with the development of air quality measuring devices and computational modelling, there has been an increase in research on the association between urban form and the concentration of air pollution, many of which are grounded in engineering and environmental science disciplines, with specific methodology and methods ranging from fieldwork and wind tunnel testing to computational modelling and correlation analysis (Zhu et al., 2022; Issakhov, Tursynzhanova and Abylkassymova, 2022; Buccolieri et al., 2022; Ehrnsperger and Klemm, 2022; Wen, 2017; Glover, 2015; Voordeckers et al., 2021; Jeanjean et al., 2015 and 2017; Zhong, 2016). When reviewing these works, there are very few studies that investigate the coupling of methodologies as well as the chemical and dynamical processes involving pollution mixing and transformation in street canyons. Furthermore, there is a lack of seasonal field research data to support theoretical assumptions and calibration of other methods. What's more, there are very few works that provide a comprehensive examination of street canyons with varying aspect ratios and consideration for symmetrical and asymmetrical configurations, as well as their relationship to in-canyon air quality. Another parameter that can impact the accuracy of the outcome of these studies is the type and resolution of computational modelling and the way various porous and solid urban attributes are represented. These

issues signify that there is a need for a multidisciplinary approach to improve the effectiveness of future strategies and bridge the knowledge gap between the science of air quality and urban planning. The stated knowledge gaps prevented the formulation of clear and applicable policy or design guidance, which is in high demand as a result of recent urban air quality issues and public health crises. In terms of policy and design recommendations, organisations such as WHO has recently introduced a framework with the goal of maintaining a healthy environment in the urban context; similarly, the European Commission designed the European air pollution policy to make significant progress toward the long-term EU goal of *"achieving levels of air quality that do not result in unacceptable impacts on, and risks to, human health and the environment"* (European Commission, 2005). The London Healthy Urban Development Unit (HUDU) (2015) and the National Health Service (NHS) created a checklist to promote healthy urban planning in London which encourages to take the wellbeing and health implications of major planning applications and local plans into consideration (the HUDU Model). The checklist is mainly compiled based on solutions and guidance produced by the London Plan (2016), The National Planning Policy Framework (DCLG, 2012) and the Institute of Air Quality Management (IAQM).

Similarly, in May 2017, the Department of Environment, Food and Rural Affairs and Transport published a new Air Quality Plan to combat illegal pollution levels and prevent further illness and premature death caused by poisonous toxins in the air that Londoners breathe. The Mayor of London expanded on these initiatives by enforcing some practical measures to promote public transportation, walking, and cycling. For example, the T-Charge, enforced in 2017, required all vehicles operating in central London to meet a minimum Euro emission standard. The T-charge was replaced in April 2019 by an even stricter regulation, Ultra Low Emission Zone (ULEZ), which discourages vehicles that do not meet Euro 4 (petrol) and Euro 6 (diesel) emission standards from entering central London. Other cities in the UK have adopted these regulations in the form of LEZs (Low Emission Zones) and CAZs (Clean Air Zones). Having said that and despite numerous efforts by central governments, city planners, and agencies, urban dwellers in London, Manchester, Swansea, Leeds, and many other big and small cities in the UK are still exposed to unacceptable levels of pollutant concentrations, which exceed national and international legal air quality obligations and objectives set by the European Environmental Agency (EEA) and the World

Health Organization. It is worth noting that air pollution limits set by the EU has technically remained in UK law after Brexit through the Air Quality Standard Regulation 2010 including the Ambient Air Quality Directive 2008 (2008/50/EC) which sets legally binding limits for outdoor air pollution concentrations that impact public health. Although the EU will no longer have a role in enforcing the UK government to adhere to these limits, which can be problematic, but at the same time that also present an opportunity for the UK to strengthen air quality standards in the UK by adopting revised limits based on World Health Organization guidelines which are driven solely by the available health evidence and set much tighter standards for a number of pollutants.

Though the aforementioned strategies and policies have been effective to some extent, a serious flaw with these policies is that they either failed or paid relatively less attention to microclimate and urban form attributes and their impact on air pollution concentrations in urban spaces. Parameters such as meteorological conditions (e.g., wind direction relative to the canyon axis; wind speed; surface temperature and air temperature) and variation in street canyon configuration (e.g. building coverage ratio; aspect ratio; floor area ratio; and sky view factor) and greenery (e.g. type, species, height and location of trees and greenery) and non-exhaust sources of pollution should have been considered. It is worth saying that the pollution from the latter i.e. non-exhaust sources is expected to rise as a result of regulations like ULEZ. While there will be an immediate reduction in exhaust emissions (primarily NO_x) caused by incomplete fuel combustion, this will not be the case for non-exhaust-related traffic particles. Even if petrol cars were replaced with electric cars they would still generate tiny pollution particles from tyre, clutch, brake, road surface wear and re-suspension of road dust due to traffic-induced turbulence. Shockingly, these tiny particles from tyre wear are almost 2,000 times worse than particulate matter emitted from car exhausts (Emissions Analytics, 2022). It's anticipated that proposals such as the ULEZ will result in a significant increase in electric/petrol cars entering the central London area, which in turn will increase the relative contribution of non-exhaust sources (PM_{10} and $PM_{2.5}$) (Denier Van der Gon et al., 2012; Amato et al., 2011; Bukowiecki et al., 2009). It is a missed opportunity that none of the mentioned policies made the consideration of the above parameters mandatory during the design and post design stages, and therefore, there are no indications of a specific framework or guidance to follow.

The following section of this thesis offers an overview of the study's aim and objectives, both of which are constructed to address the shortfalls that have been mentioned while also extending knowledge and filling knowledge gaps. Given that rapid urbanisation will have a greater impact on local climates and concentrations of air pollution, the timing of this study is critical, and its findings will help in the development of more comprehensive design guidance that takes into account factors affecting human health in the built environment.

1.2 Research aim

The aim of the present research is to outline a set of recommendations strategies that can be used to motivate a positive impact on urban microclimate, encourage greater air pollution dispersion, and avoid air pollution concentration within urban street canyons, thereby reducing its adverse impact on human health. In so doing, the research will seek to address the below objectives.

1.3 Research objectives

- To demonstrate that air pollution has a significant impact on human health
- To identify and explore the nexus between urban form and concentration of air pollution within urban street canyons
- To identify those urban form attributes that have the greatest impact on air pollution concentration within urban street canyons
- To outline a set of recommendations for improving air quality levels at pedestrian height within various urban street canyon types and configurations.

1.4 Research hypothesis

The contention that this thesis rests on is that a well-designed urban street canyon can create a desirable microclimate capable of mitigating air pollution concentrations and respectively reduce its adverse impact on human health.

1.5 Research methodology

The methodology of this study has been formulated based on the hypothesis that the urban form has a significant influence on the formation of undesirable microclimate which increases the concentration of air pollution in outdoor spaces and triggers an adverse impact on human health. On that account, this thesis employs a mixed methods approach, with an emphasis on quantitative data.

The methodology used is reflected in the thesis structure, which is divided into three parts. The first part (chapters 1, 2, 3, and 4) offer a critical review and discussion of the current condition of the problem as well as the motivation for doing this study. It then identifies knowledge gaps, strategies, and measures that promote healthy urban design. Chapter 2,3, and 4, in particular, reviews the existing literature on the impact of air pollution on human health and the influence of urban form on microclimate, as well as methods and tools to measure, model and assess air quality. Knowledge gained from the above reviews will form the theoretical framework of the research and will be largely used in parts 2 and 3 of the thesis to assess and respond to the research hypothesis. Part 2 (chapters 5 and 6) introduces the case study (fieldwork) follows by computational modelling and correlation analysis to assess the impact of various urban street canyons on air pollution concentration. The findings of part 2 are complemented by a thorough correlation analysis of computational simulation outputs in part 3 (chapter 7 and 8) to identify meaningful relationships between various metrics and parameters to offer new insights and reveal direct and indirect interdependencies to explain phenomena discovered in chapter 5 and 6. It then provides a conclusive discussion on the findings of the fieldwork (chapter 5), computational modelling (chapter 6) and correlation analysis to signify the impact of urban form on microclimate and concentration of air pollution within various urban street canyons. Based on this discussion, it then provides a set of recommendations on the most effective urban street canyon configuration(s) capable of eliminating or reducing undesirable microclimate conditions in urban outdoor spaces, thereby reducing air pollution concentrations.

1.6 Structure of the thesis

This thesis comprises of 3 main parts and 8 chapters (Fig.03). This section briefly describes the chapters that follow.

Chapter 1. Introduction

This chapter briefly introduces the research background and overview of the thesis. This includes the research aim and key objectives, as well as the presentation of the hypothesis and the methodology and concluding with the structure of the thesis.

Chapter 2 Impacts of air pollutants on human health – sources, actions and methods

This chapter reviews the existing literature on the health issues caused by excessive pollution released into the air as a result of rapid urbanisation and man-made activities to signify the urgency of tackling air pollution in cities. It then categorises the pollutants and their sources in order to identify the most harmful pollutants to urban dwellers and the significance of including them in further investigation in part 3 of this thesis. Furthermore, this chapter explores the common measures and methods employed by air quality professionals and authorities in the United Kingdom to identify knowledge gaps, strategies, and measures that promote healthy urban design.

Chapter 3 Urban Form, urban microclimate and air pollution

This chapter begins with a historical overview of human settlement and urbanisation, as well as issues related to urban population growth and activities that have exacerbated urban air pollution. This chapter defines urban street canyon as a dominant urban form and identifies urban attributes that influence urban microclimate and air pollution concentration inside street canyon. This chapter knowledge will be applied in chapters 6 and 7 to model various configurations of idealised urban street canyons.

Chapter 4 Air quality modelling in street canyons

This chapter reviews three major air quality models used by UK authorities and numerous research studies, namely physical models, deterministic models, and statistical models. This review contributes to a greater understanding of the advantages and shortfalls of such models in the micro-scale environmental investigation. It then highlights the knowledge gaps that this thesis seeks to address in order to improve the output of such models.

Chapter 5 Fieldwork and calibration Study

This chapter presents the methodology and result of the full-scale experiment (fieldwork) and computational modelling of a site within central London. It compares the results of the two methods and applies any necessary adjustment to calibrate the computational model to represent real world measurements. The knowledge gained in this chapter informs the steps that must be taken to model and calibrate the computational model outputs, enabling the study to model and simulate idealised and future scenarios across a variety of urban settings and seasons while ensuring the results are reliable and accurate predictions of real-world scenarios.

Chapter 6 Computational simulation analysis of pollutant dispersion in idealised urban street canyons

This chapter employs calibrated computational model to examine the impact of specific urban street canyons identified in Chapter 3 on the dispersion and concentration of air pollution. In order to ensure broader applicability for future studies, each urban street canyon is subdivided into six variations, each with a different aspect ratio, sky view factor and tree arrangement, including symmetrical and asymmetrical configurations. The findings of this chapter are discussed and complemented further in chapter 7, in which the gained knowledge is used to develop a set of recommendations to improve air pollution dispersion rate in various urban canyon configurations.

Chapter 7 Correlation analysis and recommendations

Correlation analysis is employed in this chapter to complement the previous chapters and identifies meaningful relationships between various metrics and parameters to offer new insights and reveal direct and indirect interdependencies to explain phenomena discovered in chapter 5 and 6. It then provides a greater discussion on the findings of the fieldwork (chapter 5), computational analysis (chapter 6) and correlation analysis (chapter 7), to signify the impact of urban form on microclimate and concentration of air pollution within urban street canyons. Based on this discussion, it then provides a set of recommendations on the most effective urban street canyon configuration(s) capable of eliminating or reducing undesirable microclimate conditions in urban outdoor spaces in order to reduce air pollution concentrations.

Chapter 8 Conclusions

This chapter concludes with a brief overview of the study, a summary of its key findings with reference to the research objectives, and a discussion of their contribution to knowledge, as well as potential future research directions.

Part 1 Introduction

Chapter 1
Introduction
1.1   Introduction and background
1.2   Research aim
1.3   Research Objectives
1.4   Research Hypothesis
1.5   Research Methodology
1.6   Structure of the thesis

Part 1 Literature review

Chapter 2
Impacts of air pollutants on human health – Sources, actions and methods
2.1 Past, present and future of air pollution
2.2 Air pollution and sources
2.3 primary Pollutant category
2.4 Air pollution and impacts on human health
2.5 Air quality in the UK (Regulatory context)
2.6 Air quality in London
2.7 Methods of monitoring air quality within urban setting
2.8 Conclusion

Chapter 3
Urban Form, microclimate and air pollution
3.1 Urbanisation
3.2 Urban morphology
3.3 Urban form, scales and morphological indices
3.4 Effect of street canyon configurations and orientations on microclimate
3.5 Urban canyon classification
3.6 Conclusion

Chapter 4
Air quality modelling in street canyons
4.1 Types of air quality model
4.2 Physical model
4.3 Deterministic model
4.4 Statistical model and correlation analysis
4.5 Conclusion

Part 2 Fieldwork & analytical analysis

Chapter 5
Fieldwork and calibration Study
5.1 Methodology of the fieldwork
5.2 Device calibration
5.3 Result of the fieldwork measurement
5.4 Methodology of computational simulation and calibration
5.5 Result of computational simulation and calibration analysis
5.6 Conclusion

Chapter 6
Computational model and analysis of pollutant dispersion
6.1 Methodology
6.2 Result and discussion of computational modelling of urban street canyons
6.3 Conclusion

Part 3 Discussion, recommendations and conclusions

Chapter 7
Correlation analysis and recommendations
7.1 Result and discussion of correlation analysis
7.2 Summary of correlation analysis findings
7.3 Recommendations
7.4 Conclusion

Chapter 8
Conclusions
8.1 Contributions to knowledge
8.2 Limitations and recommendations for future research

Fig.03 - Map of the chapters and their inter-dependency for this thesis

Part 1

Impacts of air pollutants on human health – sources, actions and methods

Chapter 2

Chapter 2

Impacts of air pollutants on human health – Sources, actions and methods

This chapter examines the health issues caused by excessive pollution released into the air as a result of rapid urbanisation and man-made activities by referring to historical events such as the Great Smog of London, which urged the UK government to pass the Clean Air Act in direct response to the lethal fog. It will also establish the severity of the issue of poor air quality by highlighting the recent data and literature published by authoritative organisations such as WHO and Public Health England on disease mortality related to short and long-term air pollution exposure, which can lead to a wide range of diseases such as stroke, aggravated asthma, trachea, chronic obstructive pulmonary disease, bronchus and lung cancers, and lower respiratory infections. It will then categorise the pollutants and their sources in order to identify the most harmful pollutants to urban dwellers and argue why strategies to mitigate air pollutants should be focused on primary pollutants, specifically the reduction and dispersion of NO_2, PM_{10}, and $PM_{2.5}$ within urban spaces. The current UK air quality policies and related regulations will then be assessed and examined in this chapter in order to identify strategies and measures that promote healthy urban spaces with clean air quality. This investigation is critical because it will confirm an apparent knowledge gap and provide an opportunity to evaluate and improve current regulations and policies in order to create an all-rounded approach to mitigating air pollution in our urban settings. The chapter asserts that current regulations, policies, and action plans, including the most recent Clean Air Strategy (2019), have paid insufficient attention to the potential of urban form and the arrangement of spaces between buildings as an effective long-term measure to reduce air pollution levels. Furthermore, the chapter delves into the common measures and methods used by air quality professionals and authorities in the United Kingdom to monitor and assess air pollution. The chapter then argues that no single measure or method will achieve the full attainment of the air quality objectives on its own and that a combination of measures and methods in the form of a package must be deployed to be more effective and provide more location-specific and long-term solutions to reduce air pollution. Finally, there is a chapter summary emphasising the gap in current policies and regulations, as well as an indication of topics that will be reviewed and explored in the following chapters.

2.1 Past, present and future of air pollution

The issue of air pollution is not a recent problem, but as technology advances, it is becoming increasingly clear that the modern atmosphere is chemically distinct from the atmosphere that existed prior to the industrial revolution in the 18th century. Naturally occurring events such as volcanic activity, forest or grass fires, evaporation, air movement, and normal biological processes can deplete oxygen sources and emit large amounts of smoke, soot, and other harmful particles and gases, thereby affecting air quality significantly. These processes have existed for millennia, and so-called air pollution predates the industrial revolution; as a result, the Earth and our atmosphere appear to have survived quite well prior to the industrial revolution and only became an issue when the atmosphere became incapable of removing the excessive pollution produced and emitted as a result of increased man-made activities. This excess of particles, gases, and aerosols resulted in pollution accumulating in both the atmosphere and our living environment, posing a serious threat to human health and the environment (Kemp, 2012; Public Health England, 2022). The atmosphere is vital because it performs a variety of functions that enable humanity to thrive and live nearly anywhere on the planet's surface (Kemp, 2012). The Earth's atmosphere is made up of a mixture of gases called air and water droplets, dust particles, salt and sulphate crystals, spores from fungi and bacteria, and other microscopic particles blown up from the Earth's surface.

It's worth noting that pure air is colourless, odourless, and tasteless and that if it does have a scent, it's due to a polluting substance, not the air itself (Allaby, 2009). The source of aerosols and particulate matter is depicted in Fig.04.
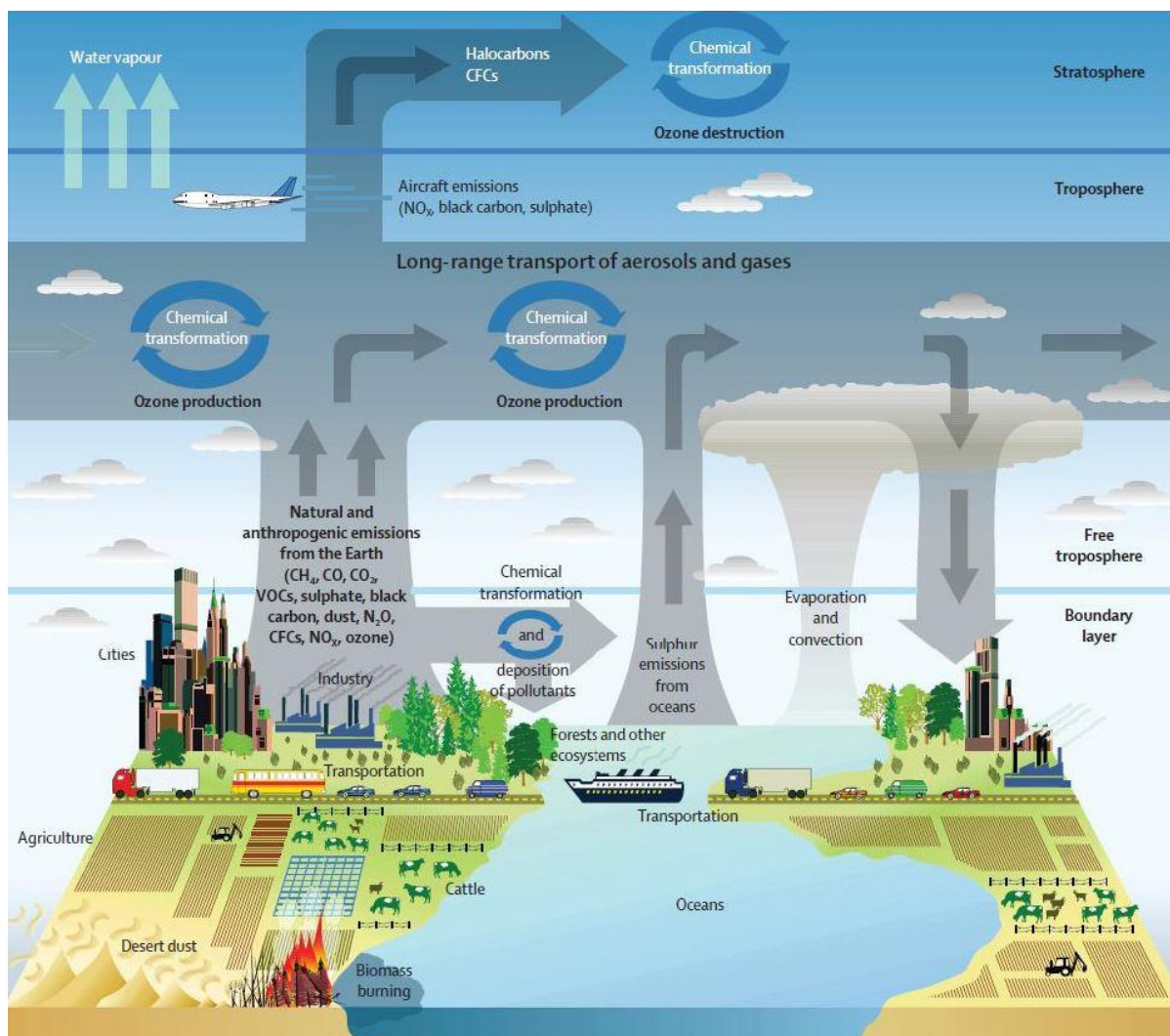
Fig.04 - Aerosol and particulate matter sources in the environment. Reproduced from the United States Climate Change Science Program (2013). CO_2 Carbon Dioxide, N_2O Nitrous Oxide, CO Carbon Monoxide, CFC Chloro Fluouro Carbon, NO_x Nitrogen Oxides, CH_4 Methane.

The origins of air pollution on Earth can be traced back to prehistoric times when man began cooking and heating in caves with firewood. It became a significant issue in the 18th and 19th centuries as the Industrial Revolution was based on the use of coal. At the time, the industries were often located in towns, and together with the burning of coal in homes for domestic heat, urban air pollution levels often reached very high levels. There were infamous episodes in history, but the serious ones were recorded in the mid-twentieth century when different cities in Europe and the US registered a large number of hospital admissions that resulted in deaths. For instance, London air pollution triggered by Sulphur Dioxide (SO_2) emissions caused the death of 4,000 people in London as a direct result of the

smog in 1952 (Bell et al., 2001). Additional research and re-evaluation of the London smog indicate that the total number of fatalities may have been significantly higher, with estimates ranging between 10,000 and 12,000 between 1952 and 1953. (Bell et al., 2004, Stone et al., 2002).

These recurrent winter smog episodes were linked to coal combustion and its emissions of sulphurous compounds and black particles into the atmosphere, as well as a lack of air movement between spaces, which means emissions from sources are not blown away as quickly as they should be, allowing polluted air to stagnate for a longer period of time and resulting in the formation of smog. As a result, numerous governments worldwide, including the United Kingdom, legislated a Clean Air Act in response to the lethal fog. The Act established smoke-free zones throughout the city and placed restrictions on the use of coal in both domestic and industrial fires.

Clearly, these regulations and laws are intended to bring SO_2 levels well below the legal limit. However, exposure to other harmful pollutants such as PM_{10}, $PM_{2.5}$, and NO_2 continues to be a major public health challenge in the UK and worldwide, shortening lives and adversely affecting the quality of life for many people. Additionally, it has a detrimental effect on the natural environment, affecting on waterways, biodiversity, and crop yields. For example, based on the latest Urban Ambient Air Pollution Database published by WHO (2016) (Fig.05), the vast majority of cities worldwide exceed the recommended particulate matter (PM_{10}) maximum annual mean levels of 20 $\mu g/m^3$ sets by WHO Air Quality Guideline.
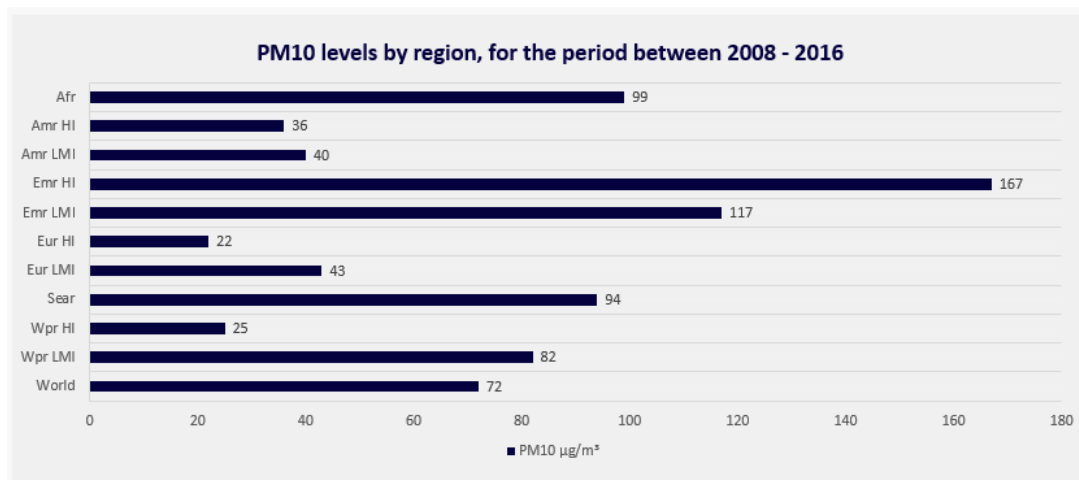
Fig.05 – Adapted from WHO Global Urban Ambient Air Pollution Database (2016)

Afr: Africa, Amr: America, Emr: Eastern Mediterranean, Eur: Europe, Sear: South-East Asia, Wpr: Western

Pacific LMI: Low and middle-income, HI: high-income.

As it can be seen in Fig.06, more than 91 percent of individuals living in cities are exposed to air quality levels that are higher than WHO guidelines.
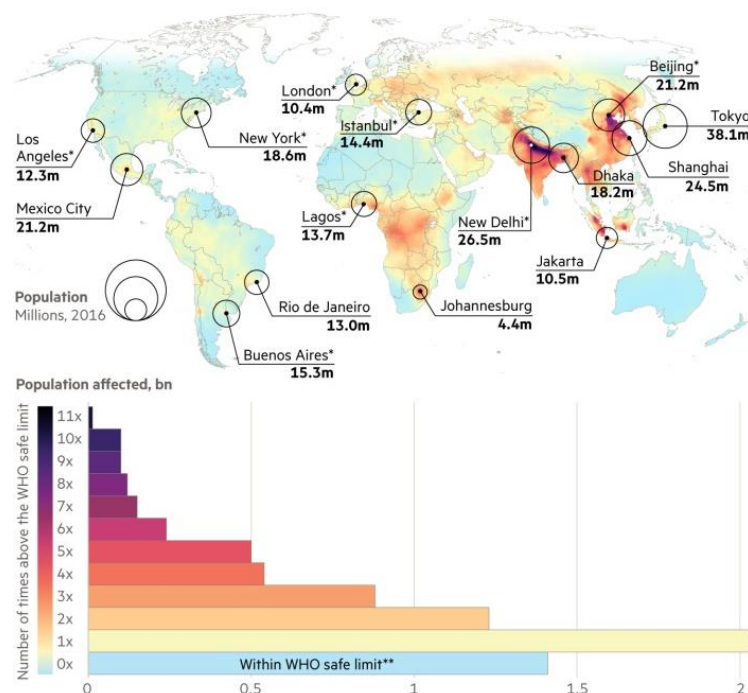
Fig.06 - 9 in 10 people in the world are breathing polluted air above the WHO's safe limit (World Health Organization, 2018).

A more recent study by Lelieveld et al. (2019) (Fig.07) estimated that 8.8 million people died as a result of indoor and outdoor air pollution in total. Moreover and according to 2014 EEA

(European Environmental Agency) report, illegal levels of fine particulate matter ($PM_{2.5}$) are responsible for over 450,000 premature deaths in Europe, despite the fact that neither the UK's National Air Quality Objectives nor the EU's Ambient Air Quality Directive 2008/50/EC contain $PM_{2.5}$ short-term exposure limits or target values for human health protection. In the United Kingdom, data indicate that between 28,000 and 36,000 deaths per year are attributed to long-term exposure to air pollutants such as NO_2, PM_{10}, and $PM_{2.5}$, with 9000 of those deaths occurring in major cities such as London (PHE, 2019).
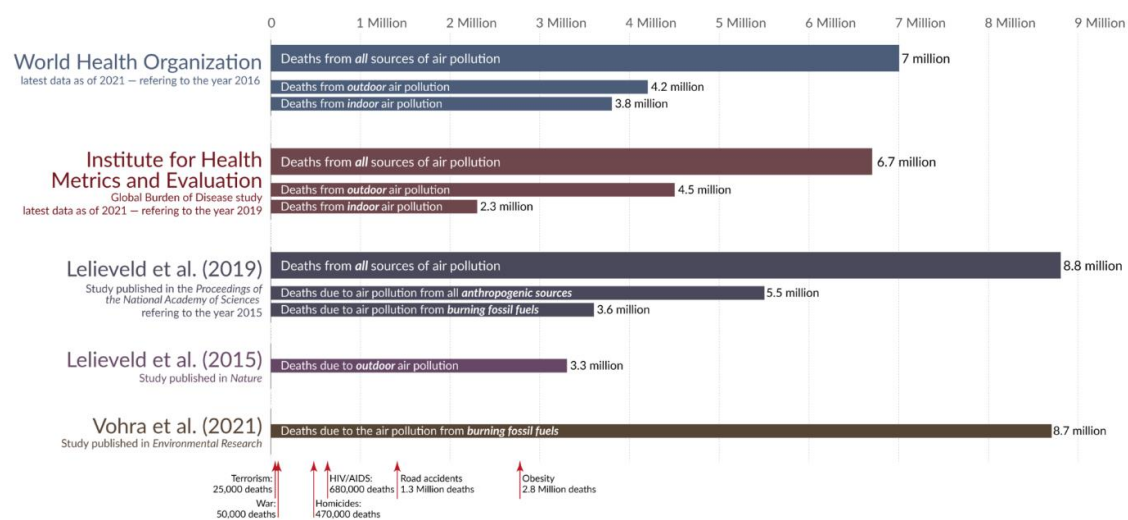
Fig.07 – Data on annual death tolls by various organisations and researchers (Max Roser, 2021).

Despite numerous efforts by central governments, city planners, and agencies, city dwellers around the world continue to be exposed to unacceptable levels of pollutant concentrations that exceed national and international legal air quality standards and objectives set by organisations such as the World Health Organization and the European Environmental Agency (EEA). The majority of these deaths from short- and long-term air pollution exposure could have been avoided if, first and foremost, pollution sources were reduced, and, equally important, our urban spaces were designed in such a way that promoted higher dispersion of pollution and thus had less impact on human health. The section that follows introduces and categorises various pollutants, as well as discusses their health implications. These will help to identify the number of key urban air pollutants that must be considered in future fieldwork and computational modelling studies.

2.2 Air pollution and sources

As previously stated, air pollution is most common in metropolitan cities with heavy automobile traffic and heavily industrialised activities. The majority of pollution is emitted as a result of cities' unsustainable housing, employment, commercial, and recreational structures, which has resulted in a reliance on road-based transportation, which contributes to high levels of urban air pollution and greenhouse gas emissions. Furthermore, emissions from power generation, home heating, construction, and even activities like cooking all contribute to the degradation of the air we breathe. Our environment is also incapable of accommodating and filtering the amount of pollution generated by a large number of people living in relatively small areas, as well as pollution emitted by natural causes such as windblown dust, wildfires, and so on; as a result, these pollutants will remain and concentrate in our living environment for far longer than they should, endangering human health and the environment (Kemp, 2012). As a result, natural and man-made pollutions have mixed into urban air, as shown in Fig.08, where they are transformed into even more hazardous pollutants via a variety of chemical processes.
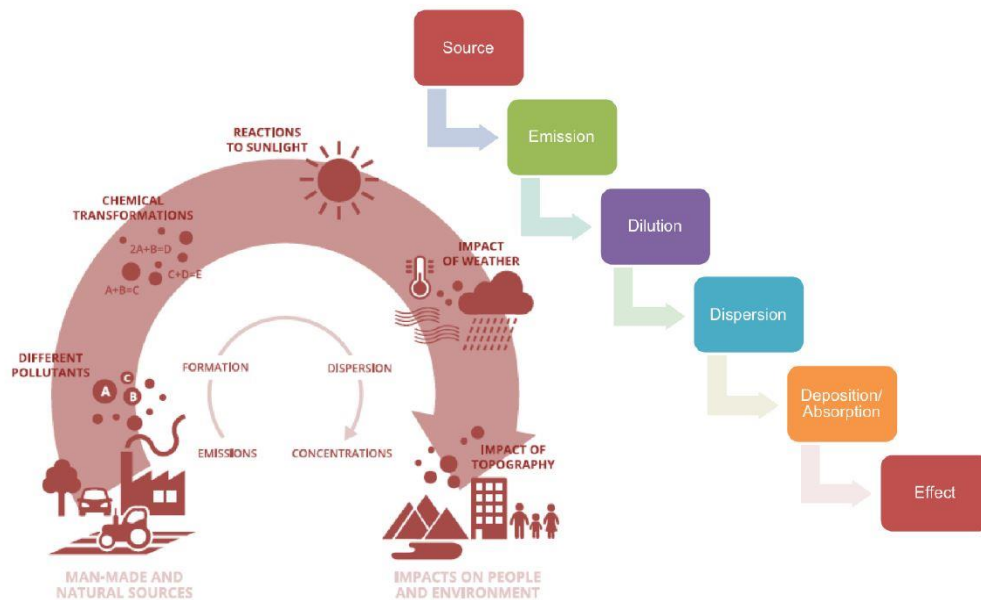
Fig.08 – Pollution pathway and its impact on human and environment

Air pollution is classified into three types: natural, primary, and secondary pollutants. Natural Pollutants are natural events that cause pollutants to enter the atmosphere. This

includes forest fires caused by lightning and pollen spread. Primary pollutants are pollutants that are discharged directly from the source and processed into the atmosphere. As a result, five primary pollutants can be released directly into the atmosphere in their unmodified forms in sufficient quantities to pose a health risk (Table.01). Particulates, nitrogen compounds, sulphur dioxide, carbon monoxide, and hydrocarbons are all examples of primary pollutants (Enger and Smith, 2016).

Pollutant	Sources
Particulates	Burning fossil fuels
	Farming operations
	Construction operations
	Industrial wastes
	Building demolition
Nitrogen compounds	Burning fossil fuels
Sulphur dioxide	Burning fossil fuels
	Smelting ore
Carbon monoxide	Incomplete burning of fossil fuels
	Tobacco smoke
	Construction operations
Hydrocarbons	Incomplete burning of fossil fuels
	Tobacco burning
	Chemicals

Table.01 - Primary air pollutant sources (Enger and Smith, 2016).

Secondary pollutants, as opposed to primary pollutants, are not released directly into the atmosphere. Instead, they formed in the lower atmosphere due to interactions or reactions between primary pollutants. For instance, nitrogen oxides (NO_x) emitted by vehicles and industries, as well as volatile organic compounds (VOCs) emitted by vehicles, solvents, and industries, react with sunlight to form ground-level ozone (O_3). That means controlling and limiting primary air pollutants can result in significant reductions in secondary pollutant formation. For that reason, only the primary pollutants and their categories will be explored

and discussed further in the following section, as any reduction in primary pollutants inevitably reduces secondary pollutants, but not the other way around.

2.3 Primary pollutant category

As previously stated, transportation emissions, fossil fuel combustion, industrial emissions, and building materials such as paints and adhesives all contribute to the changing composition of the atmosphere. Particulate matter and gaseous pollutants are the two major categories of primary air pollutants. Depending on their chemical composition, presence in the environment, and ability to be transferred over short or long distances, they can have a range of impacts on human health and the environment. The following section provides additional information on the various types of pollutants and their characteristics to offer a better understanding of their impacts on human health and the environment.

2.3.1 Particulate matter

Particulate matter is made up of various particle mixtures suspended in the air that include a wide range of chemicals and particle sizes. The primary sources of particulate pollution are naturally generated particles such as soil particles and particles released by the combustion of fossil fuels as a result of home heating and cooking, construction activities, power plants, fires, vehicles, and natural windblown dust, as well as a wide range of industrial processes such as trash incineration (Pöschl, 2005). PM_{10} refers to particles smaller than 10 micrometres, whereas $PM_{2.5}$ refers to particles smaller than 2.5 micrometres (Fig.09). Smaller particles penetrate deeper into the respiratory system and can reach the lung alveoli, whereas PM_{10} particles are mostly restricted to the upper respiratory tract. Ultrafine and fine particles are more harmful than larger particles produced by combustion sources as they can get deep into the lungs, and some may even get into the bloodstream.
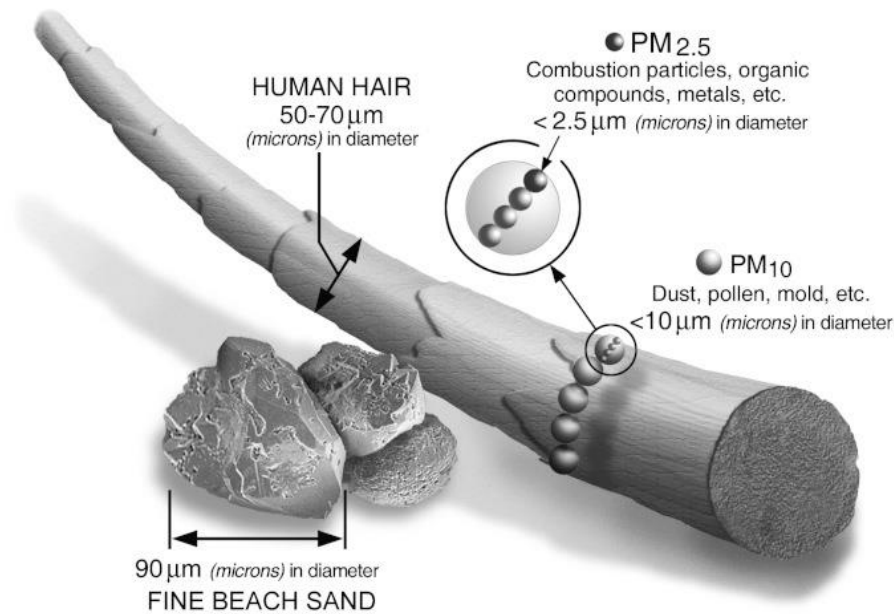
Fig.09 - Particulate matter – size comparison (U.S. Environmental Protection Agency, 2015)

2.3.2 Gaseous pollutants

Because of the combustion of fossil fuels, the air is invariably polluted; it is usually contaminated by primary gaseous pollutants such as NOx, CO, SO_2, and VOC. These gaseous pollutants play an important role in the formation of the atmosphere, which is primarily contaminated as a result of excessive emission and concentration of each of these pollutants. Nitrogen oxides (NO_x) are produced during high-temperature fuel combustion, most notably in motor vehicles (Boningari and Smirniotis, 2016). It is commonly used to refer to two gases: nitric oxide (NO), a colourless, odourless gas, and nitrogen dioxide (NO_2), a reddish-brown gas with a pungent odour. Nitrogen dioxide is formed when nitric oxide interacts and reacts with ozone and oxygen in the atmosphere (Altshuller, 1956). As a result, NO_2 is frequently used as a proxy for the overall level of air pollution emitted by motor vehicles such as cars, buses, and trucks, as well as power plants and off-road equipment. The recent trend shows that the level of this pollutant has decreased between 2010 and 2020 (DEFRA, 2022) as a result of stricter emissions regulations for road transport, but the UK continues to fail to meet national and international legal limits of nitrogen dioxide (NO_2) pollution, where the annual average concentration level cannot exceed 40 $\mu g/m^3$. As it was mentioned in chapter one, air pollution limits set by the EU has technically remained in UK

law after Brexit through the Air Quality Standard Regulation 2010 including the Ambient Air Quality Directive 2008 (2008/50/EC) which sets legally binding limits for outdoor air pollution concentrations that impact public health.

It is important to note that other primary gaseous pollutants such as VOCs, which are formed by incomplete fuel combustion, road travel, and building materials, and carbon monoxide (CO), which is a by-product of incomplete combustion, are the most important pollutants to measure and consider when it comes to indoor spaces. This is because it is highly unlikely that CO and VOC concentrations in the outdoor environment reach to high and dangerous levels. In general, CO levels inside buildings can rise to dangerous levels due to a faulty heating appliance and can cause health effects in enclosed and indoor spaces. Similarly, concentrations of VOCs are consistently higher indoors and in some cases up to ten times higher than outdoors. Similarly, Sulphur Dioxide, which is primarily produced by the combustion of sulphur-containing coal and heavy fuel oil, may not be a concern for countries that have transitioned away from the use of coal for energy production. Sulphur dioxide emissions in the United Kingdom have continued to fall as a result of the country's decreasing reliance on coal for energy generation. According to the most recent data published by DEFRA (2022), sulphur dioxide emissions from energy industries decreased by 87% between 2010 and 2020.

2.4 Air pollution and impacts on human health

Various disciplines have extensively researched and established the link between health and air quality. Poor air quality of urban spaces are increasingly being recognised as having an impact on wellbeing and human health in a variety of scientific disciplines, including psychology, ecology, biology, environmental health, horticulture, landscape and, of course, public health policy and medicine (Shahriyari et al., 2022; Dominski et al., 2021; Pope et al., 2020; Rao et al., 2013; Lieber and Rogers, 2009; The Royal Commission on Environmental Pollution, 2007; European Environment Agency, 2005; Hollander et al., 2003; van den Berg et al., 2003).

According to these studies, there is a clear link between health and air quality, and it is established that severe deterioration of air quality increases the risk of stroke, lung cancer, heart disease, and chronic and acute respiratory diseases, including asthma (Pope, 2009; Lim, 2010; Eze et al., 2014; kelishadi and Poursafa, 2010; Manucci and Franchini, 2017; Dockery et al., 1993). This situation is worse for the elderly and children, as their airways are limited as they often spend more time in the same outdoor locations. These studies recognise that the world's most pressing environmental problem is premature death and ill-health caused by biological agents in the human environment, which affects almost every country and causes serious environmental health problems for hundreds of millions of people who are exposed to unnecessary chemicals and physical hazards and suffer from respiratory and other diseases caused or exacerbated by poor air quality. According to a recent study by WHO published in May 2018, outdoor air pollution is responsible for 43% of all deaths and disease from chronic obstructive pulmonary disease, 17% from acute lower respiratory infection, 24% from stroke, 25% from ischaemic heart disease and 29% of all deaths and disease from lung cancer. As a result, individuals exposed to high levels of air pollution exhibit a range of disease symptoms. These effects are typically classified as either short- or long-term health effects. The most common short-term effects of exposure to air pollution are irritation of the skin, eyes, throat, and nose, coughing, wheezing, and chest tightness, as well as breathing difficulties that cause discomfort. Exposure to air pollution for a short period of time can also cause headaches, dizziness, and nausea. Having said that, depending on the environmental conditions, the level of concentration, and the individual susceptibility of those with asthma or other respiratory illnesses, this may be worse and can progress to more severe and serious conditions such as asthma, bronchitis, pneumonia, and heart and lung problems. These problems can be exacerbated by prolonged exposure to pollutants, which are harmful to the respiratory systems, the neurological and reproductive system, and causes cancer and even, rarely, deaths. The long-term effects of air pollution are chronic, lasting for years or the whole life and can even lead to death.

Pollutants such as particulate matter, specifically, can affect blood coagulation by causing pulmonary inflammation and systemic inflammatory alteration (Riediker et al., 2004). Additionally, when ozone and particulate matter penetrate the alveolar epithelium, they

cause lung inflammation, which exacerbates the condition of individuals with lung lesions or illnesses (Uysal and Schapira, 2003). Finer particles with a diameter of less than 10 micrometres cause the most concern, as they can penetrate deeply into the lungs and some may even enter the bloodstream. Particle pollution exposure is most likely to affect people with heart or lung diseases, children, and older adults Fig.10.
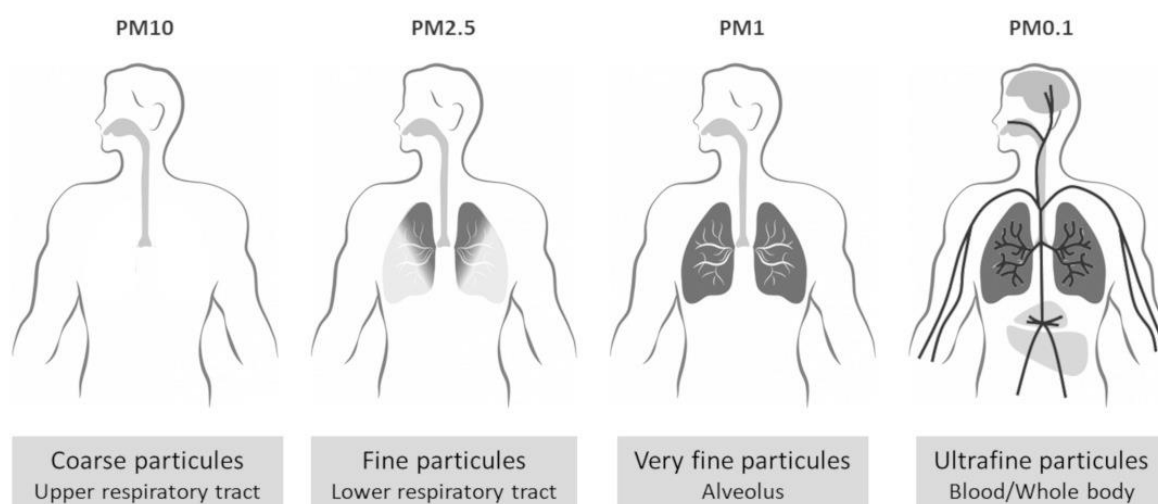
Fig.10 - Particle size and deposition in human body (Vincent, 2019)

In epidemiologic studies, dioxin exposure has been linked to an increased risk of death from ischemic heart disease. Furthermore, even at low concentrations, prolonged exposure can be harmful. Individuals exposed to excessive nitrogen oxides may experience irritation of the throat and nose, followed by bronchoconstriction and dyspnea (Balmes, 1987). Sleep difficulties, irritability, memory troubles, exhaustion, blurred vision, hand tremors, and slurred speech are all indications of dioxins and heavy metals such as mercury, lead, and arsenic damaging the nervous system (Ratnaike, 2003). Additionally, dioxins slow nerve conduction and damage children's brain development and impact on the digestive system cause liver cell damage, as evidenced by an increase in the levels of specific enzymes in the blood, as well as gastrointestinal and liver cancer. Figures 11 and 12 illustrate the primary sources of particulate matter ($PM_{2.5}$) and nitrogen oxides (NOx), as well as their impact on human health.
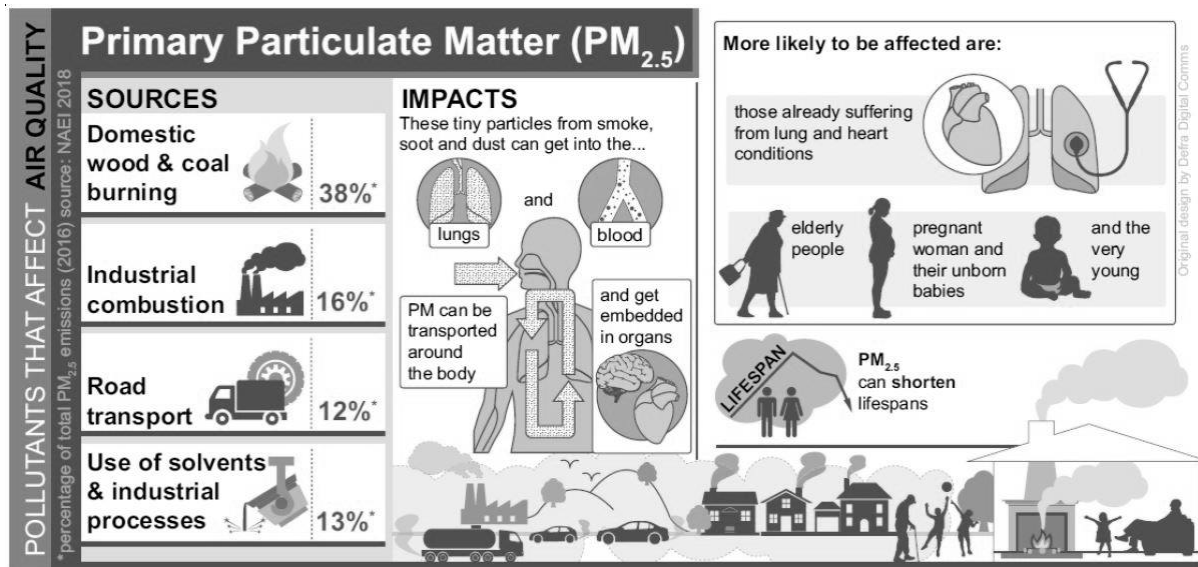
Fig.11 – Impact of primary particulate matter ($PM_{2.5}$) on human health. Source: DEFRA Digital Comms, 2018.
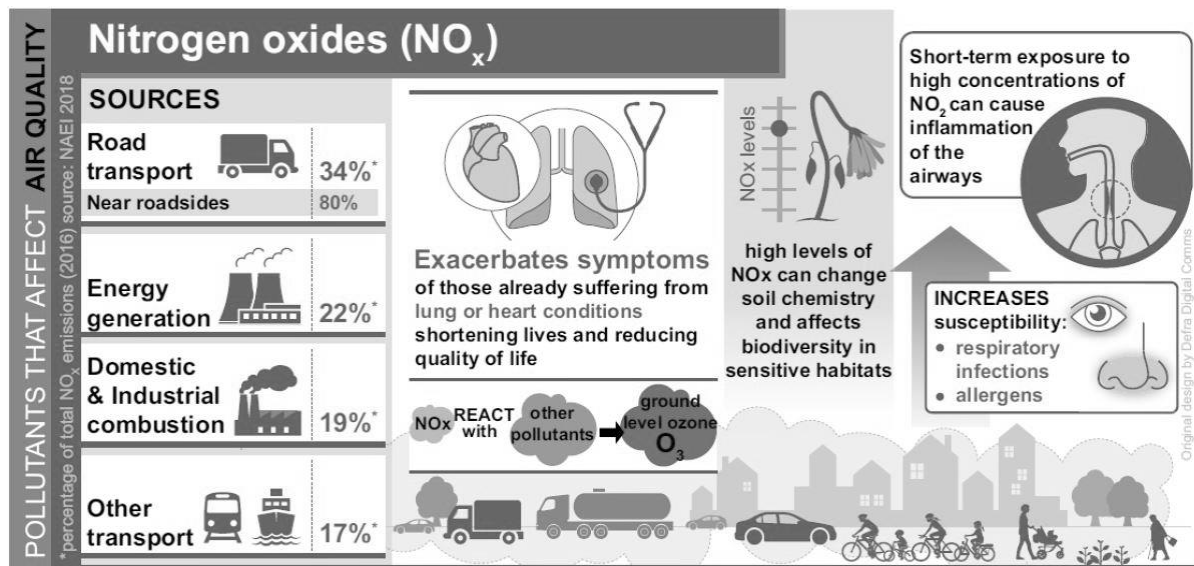
Fig.12 – Impact of Nitrogen Oxides (NO_x) on human health. Source: DEFRA Digital Comms, 2018.

Numerous studies have demonstrated the dangers of being exposed to air pollution both before and during pregnancy (Tozzi V et al. 2019). According to Lertxundi et al. (2015), prenatal residential exposure to PM and NO_2 has a detrimental effect on the motor and cognitive development of infants. The study estimated that, a 1 µg/m^3 increase during pregnancy in the average levels of $PM_{2.5}$ was associated with a -1.14 point decrease in motor and that a 1 µg/m^3 increase of NO_2 exposure was associated with a -0.29 point decrease in mental score Fig.13.

Fig.13 – Air pollution and adverse pregnancy outcomes. Often particles smaller than 2.5 are able to penetrate deep into the lungs and affect the body more systematically leading to cardiovascular disease and adverse pregnancy outcomes (Tsiaras, 2018).

Considering the above-mentioned concerns, PM_{10} and $PM_{2.5}$ will be considered for future fieldwork and computational modelling studies on this thesis; additionally, due to the fact that the United Kingdom has yet to meet legal NO_2 limits, this thesis will only consider NO_2 among other gaseous primary pollutants in future fieldwork and computational modelling studies.

2.5 Air quality in the UK (Regulatory context)

According to a recent World Health Organization report, residents of the United Kingdom are more likely to die from air pollution than residents of comparable countries such as Mexico, the United States, and Sweden (World Health Organization, 2017). Similarly, and according to a report commissioned by the UK Labour Party, over two-thirds (40 million people) of the UK population live in areas with dangerously high levels of air pollution. Additionally, tens of thousands of children in England are exposed to illegal levels of air pollution in schools and nurseries, according to Laville et al. (2017).

Two air pollutants, particulate matter and nitrogen dioxide, are responsible for between 40,000 and 50,000 premature deaths per year in the United Kingdom (Bolton, 2016). Since 2010, the amount of fine particulate matter ($PM_{2.5}$) generated by diesel vehicles has exceeded regulatory limits in nearly 90% of urban areas in the United Kingdom (Fig.14). This

toxic pollutant is projected to cause 23,500 premature deaths per year an associated loss to the population of 340,000 life-years, and as a result, in April 2016, a cross-party committee of MPs declared the issue a public health emergency (Carrington, 2016).
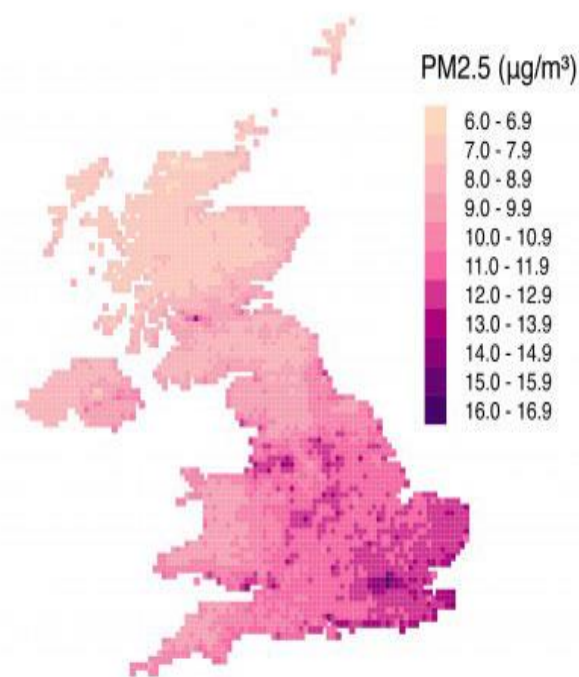
Fig.14 - Estimated UK air quality: 90% of the population of the UK lives in locations where outdoor pollution exceeds the WHO recommended limit of 10 micrograms per cubic metre. (World Health Organization, 2016)

It is worth noting that the UK government has always attempted to reduce emissions levels, albeit at a glacial pace, and in many cases, regulations need to be revised to include more ambitious standards and objectives. For example, under the Environment Act of 1995, the UK Government is required to develop a national Air Quality Strategy (AQS) for the UK, which outlines air quality standards, objectives, and measures for improving ambient air quality. The last comprehensive review of the strategy was published in 2007, with a review yielding some minor changes published in 2011. The Clean Air Strategy, published in 2019, primarily lays out the case for action and offers strategies, as well as indicating how devolved administrations intend to reduce emissions from transportation, homes, farming, and industry. The goal of these regulations is to limit and control human exposure to outdoor air pollutants by specifying 'limit values,' 'target values,' and 'long-term objectives,'

with the goal of bringing air quality as close to set standards and objectives as possible. Fig.15 shows the UK air quality management legislation under Environment Act 1995, part IV; while Fig.16 depicts the UK air quality organisational relationship.
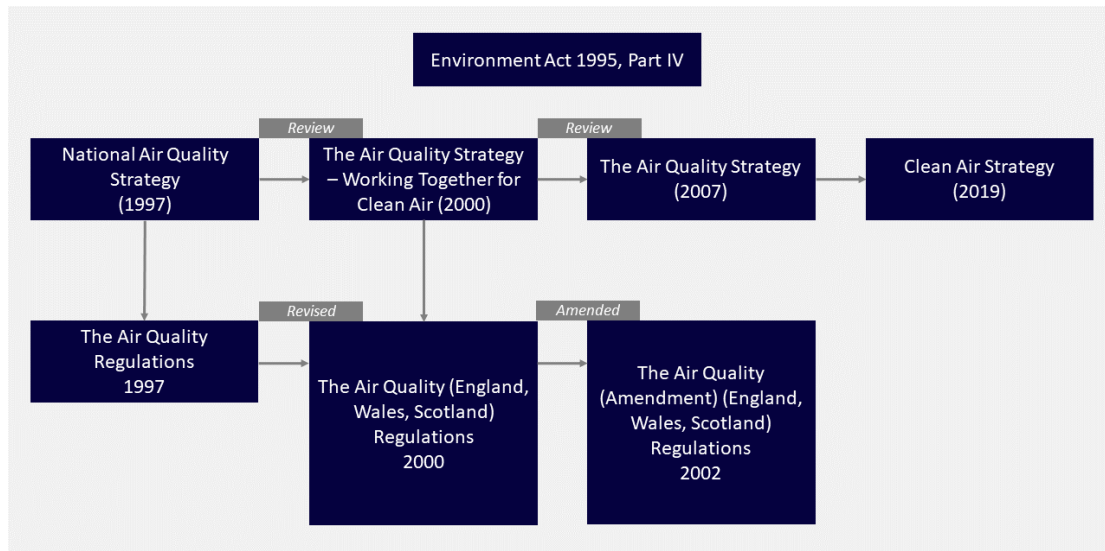
Fig.15 – UK Air Quality Management Legislation
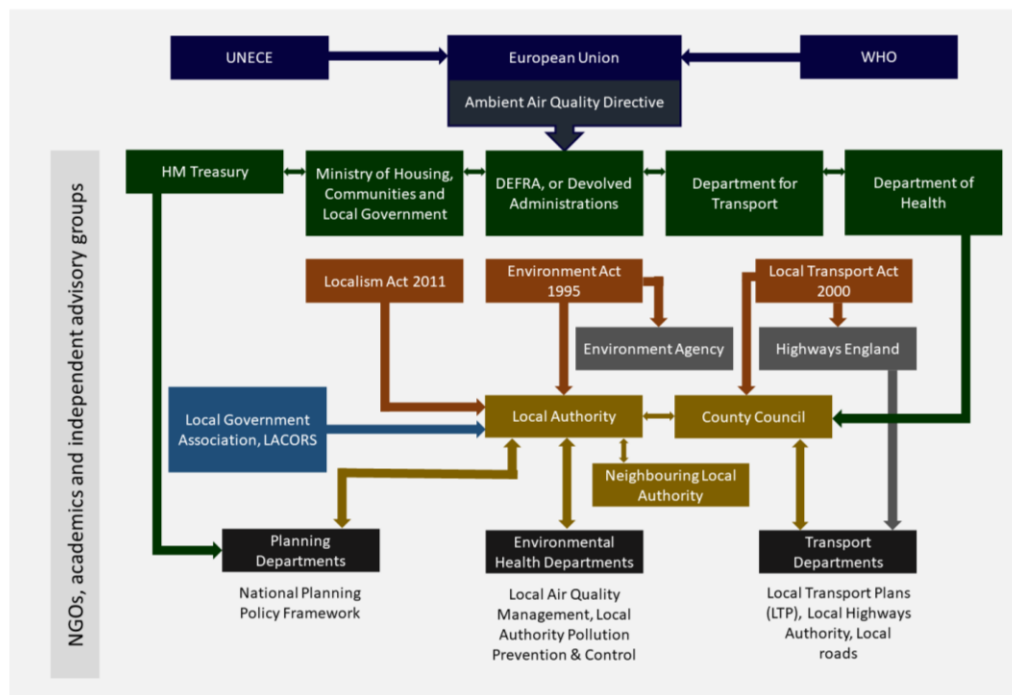
Fig.16 - UK air quality organisational relationship

Any exceedances of air pollutants, according to the regulations, will necessitate an air quality action plan to propose a set of measures to ensure that the exceedance period is eliminated or kept as short as possible. Table.02 shows the summary of these values for NO_2, PM_{10} and $PM_{2.5}$. The full list of national air quality objectives has been provided in appendix a.

Pollutant	Objective	Concentration measured as	Date to be achieved by (and maintained thereafter)
Particles (PM_{10})	50 µg/m³ not to be exceeded more than 35 times a year	24 hour mean	31 December 2004
	40 µg/m³	annual mean	31 December 2004
Particles ($PM_{2.5}$)	25 µg/m³	annual mean	2020
Exposure Reduction	(UK Urban area) Target of 15% reduction in concentrations at urban background	annual mean	Between 2010 and 2020
Nitrogen dioxide	200 µg/m³ not to be exceeded more than 18 times a year	1 hour mean	31 December 2005
	40 µg/m³	annual mean	31 December 2005

Table.02 - National air quality objectives and Directive limit and target values for the protection of human health objectives are policy targets often expressed as a maximum ambient concentration not to be exceeded, either without exception or with a permitted number of exceedances, within a specified timescale.

In the United Kingdom, the Secretary of State for Environment, Food, and Rural Affairs is in charge of meeting the limit values in England, while the Department of Environment, Food, and Rural Affairs (Defra) coordinates assessment and air quality plans for the entire country. Part IV of the Environment Act of 1995 requires local authorities in the United Kingdom to review air quality in their area and designate air quality management areas (AQMA) if necessary. Where an air quality management area is designated, local authorities are also required to work towards the Strategy's objectives prescribed in regulations (Amey, 2016). Following that, an air quality action plan describing pollution reduction measures must be implemented. These plans contribute to the achievement of local air quality limit values. Currently, more than 700 AQMAs (Fig.17) have been allocated by local authorities across UK and action plans have been put in place to address air quality, including any exceedances (Department for Environment Food and Rural Affairs, 2018).
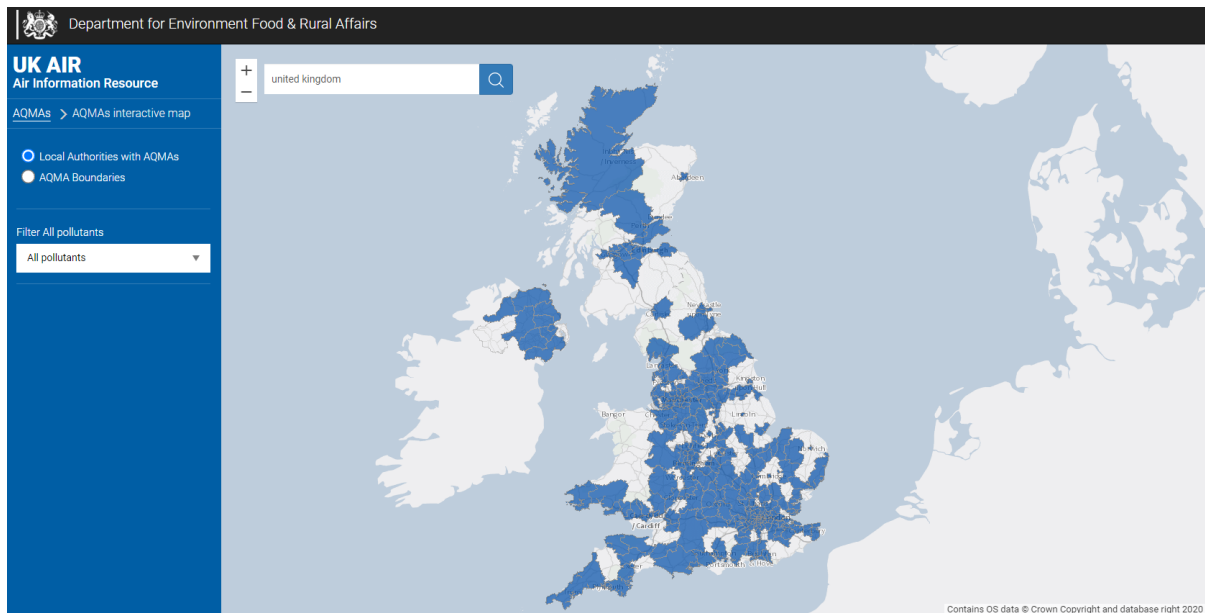
Fig.17 - Local Authorities with AQMAs across UK (2022)

These measures are the methods of achieving the objectives. However, it is important to note that no single measure will achieve the full attainment of the air quality objectives on its own, and thus a number of measures in the form of a package must be deployed to be more effective. To date, a variety of measures have been implemented by various councils throughout the country, including technological measures such as fitting pollution abatement technologies to road vehicles and industrial processes, as well as behavioural change measures such as smarter choices, traffic management measures, incentives for cleaner vehicles and road pricing, Low Traffic Neighbourhood and Clean Air Zones (CAZ). When reviewing these measures and regulations, objectives, and action plans, including the most recent Clean Air Strategy 2019, there is a consistent lack of awareness on the potential of urban form and the arrangement of spaces between buildings as an effective long-term measure to reduce air pollution levels. It's also worth noting that, thanks to the measures in place at the time, emissions have decreased in comparison to previous decades, but not enough to prevent the premature deaths of 40,000-50,000 people per year caused by poor urban air pollution (Johnston, 2016).

2.6 Air quality in London

The Great London Smoke, which occurred in 1952, will be commemorated on its 70th anniversary in 2022. The tragedy prompted significant changes in practices and legislation, most notably the Clean Air Act of 1956, which provided for the first time in London regulation of both residential and industrial smoke emissions. A thick layer of haze formed over London as a result of airborne pollution caused primarily by the use of coal. Cold temperatures, an anticyclone, and windless conditions were the key factors at the time, resulting in four days of severe air pollution (Davis et al., 2002). Despite the fact that London no longer suffers from the Smogs of the 1950s, and the city's air quality has significantly improved since then, the air quality remains below the requirements and standards set by the European Environmental Agency (EEA) and the World Health Organization, which exceed national and international legal air quality standards and objectives. Fig.18 depicts the complexities and pollution sources from both within and outside of London, which are all variables that influence the air quality in London.
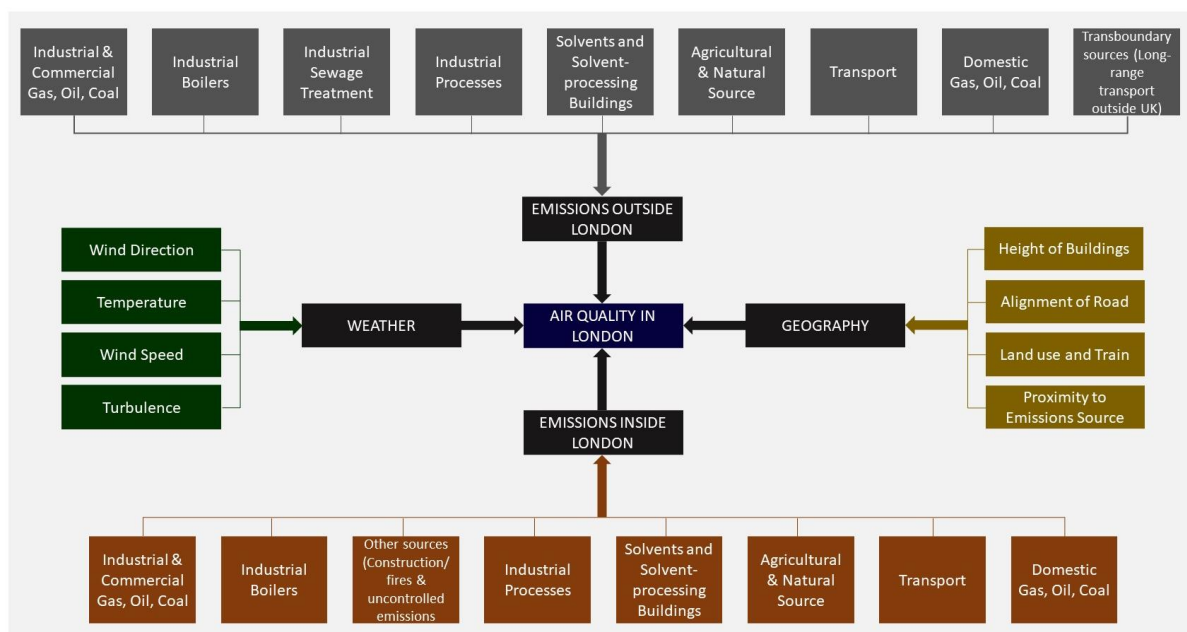
Fig.18 - Weather, topography, and pollution sources from both inside and outside London are all variables that influence London's air quality (Greater London Authority, 2010)

It is worth noting that London's air quality has improved year after year (London Borough of Camden Air Quality Annual Status Report for 2017) and is expected to improve even more

as a result of the London Mayor's recent air quality strategy known as ULEZ (Ultra Low Emission Zone), which took effect in April 2019 (Fig.19).

Fig.19 – Ultra Low Emission Zone expansion plan (TFL, 2019).

Although it is encouraging to see the Mayor of London actively implementing practical measures to boost the use of public transportation, walking, and cycling, the T-Charge or ULEZ only prohibits vehicles that do not meet the Euro 4 (petrol) and Euro 6 (diesel) emission standards from entering central London. Similar to the Low Traffic Neighbourhoods (LTN) and School Streets strategies, which only divert traffic to other parts of the neighbourhood or city, this can potentially lead to more significant air quality problems, even in neighbourhoods that previously had better local air quality. This pollution can then travel back from the outskirts of London to the heart of the city, exacerbating the problem. Furthermore, while such strategies will limit exhaust emissions (mostly NO_x) released as a result of incomplete fuel combustion, they will not limit non-exhaust traffic-related particulates. Even if we replaced petrol and diesel vehicles with electric cars, buses, and taxis, the tyres, clutch, brake, road surface wear, and re-suspension of road dust caused by traffic-induced turbulence would still emit microscopic pollution particles. Non-exhaust emissions accounted for more than 90 percent of PM_{10} and 85 percent of $PM_{2.5}$ emissions from traffic (Timmers et al., 2016). According to recent reports (2019) and as shown in

Fig.20, PM$_{2.5}$ emissions are increasing due to increased battery weight and torque on EV cars. This is an important graph that clearly shows that tyre emissions are increasing and, more importantly, that current policies, strategies, and regulations are inadvertently replacing one pollution source with another.
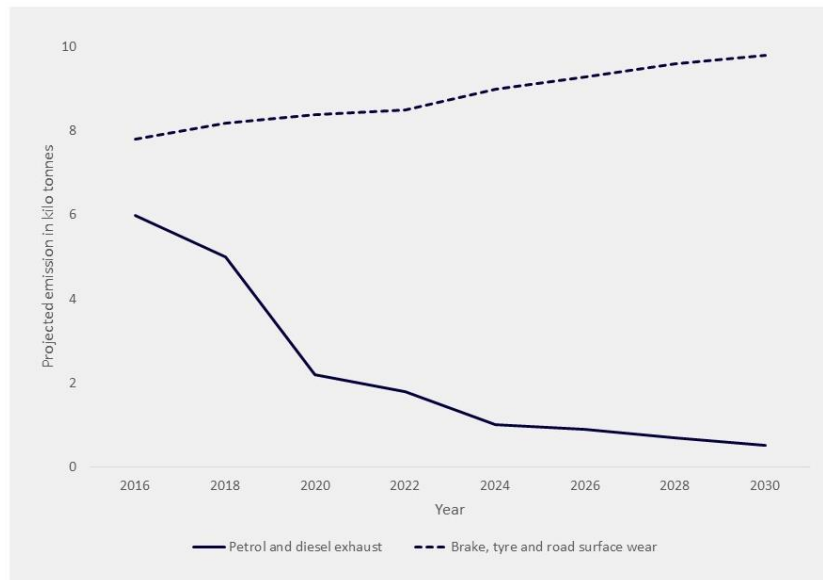
Fig.20 - Projected PM$_{2.5}$ emissions from brake, tyre and road surface wear, and exhaust emissions, 2015-2030 (Air Quality Expert Group, 2018).

Furthermore, initiatives like the Ultra Low Emission Zone (ULEZ) have already increased the number of electric/petrol cars entering central London, thereby increasing the relative contribution of non-exhaust sources to traffic-related emissions (PM$_{10}$ and PM$_{2.5}$) (Vaughan, 2021). Moreover, the COIVD-19 pandemic and lockdown demonstrated that it is possible to reduce pollutants such as NO$_2$ and particulate matter by limiting vehicle traffic to near zero (lock down scenario). This is very similar scenario to when all vehicles switched to electric vehicles (EV), where the NO$_2$ level is expected to drop significantly. However, given that the electric vehicles emitted nearly 2,000 times more particulate matter than car exhausts (Emissions Analytics, 2022), it is reasonable to conclude that the future of vehicle pollution will be caused by tyres rather than gas emissions.

2.7 Methods of monitoring air quality within an urban setting

There are two distinct types of air pollution monitoring generally in use - non-automatic and automatic. Non-automatic monitoring methods are often less expensive and easier to

implement, and as a result, they have been widely used in the UK by local authorities within their Air Quality Management Areas to measure ambient concentrations of nitrogen dioxide (NO_2). This is usually accomplished by placing a special tube in a specific location for 2-4 weeks before sending it to a laboratory for chemical analysis Fig.21.

Fig.21 – NO_2 diffusion tubes are used for ambient air monitoring within an urban setting, image by author, Euston Road in London.

Although non-automatic methods and diffusion tubes are inexpensive with wide spatial resolution and may be used to identify hotspots of air pollution concentration, this method has the lowest accuracy and cannot be used as a reference method; additionally, it has a low temporal resolution. This method only provides one value for the entire time it was in place, and there is also a delay in producing the measurements. That means that air pollution episodes cannot be tracked, and there is little to be learned from the impact of microclimate and its correlation with high or low pollutant concentrations. Continuous monitors, on the other hand, provide data with a higher temporal resolution (e.g., hourly or every 15 minutes) and a lower degree of uncertainty (+/-10-15%) than diffusion tubes (+/-20-25%). Defra recommends that local governments use continuous monitoring data whenever possible, either from the national Automatic Urban and Rural Network (AURN) or

from local monitoring campaigns, which report data hourly in real-time on the UK-AIR website(https://uk-air.defra.gov.uk/). However, due to the expense and inconvenience of locating continuous analysers at sites liable to relevant exposure, Defra accepts the use of diffusion tubes with appropriate QA/QC (Quality Assurance and Quality Control), and as a result, many local authorities tend to report on their air quality management area based on non-automatic methods, which unquestionably carry a greater uncertainty. A portable air pollution device, which has been used in many academic studies and by air quality professionals and many of the stakeholders involved in the use of small sensors for measuring air quality, is an alternative method for obtaining site specific air pollution data (World Meteorological Organization, 2008; Chen and Ng, 2011; Liu et al., 2011; Edussuriya, Chan and Ye, 2011; Williams et al., 2014; Chatzidimitriou and Yannas, 2017; Ventura, 2017; Sharag-Eldin, 2019; Kwak et al., 2018; Chatzidiakou et al., 2019). These devices are significantly less expensive than fixed station units and can provide higher real-time data resolution while also measuring a variety of pollutants. Furthermore, as air quality varies between urban settings, this mobile monitoring method will allow the user to respond quickly to these changes and capture variations in an individual's air pollution exposure. This method is a more effective way to measure air pollution and is widely accepted. It is important to note that data output from portable devices is only valid if the device is co-located and calibrated next to a maintained reference station, as shown in Fig.22. This allows for local correction via scaling and, more importantly, data validation (Billingsley, 2020)

Having said that, every local authority in the United Kingdom has access to fixed monitoring stations, which are mostly located in key locations. The AURN is the UK's largest automatic monitoring network and the primary network for reporting compliance with the Ambient Air Quality Directives. These stations regularly collect and measure various air pollutants at six different types of monitoring stations, including urban, suburban, rural, industrial, and roadside locations (DEFRA, 2017). Table.03 contains the definitions for each type. The samplings from urban and suburban regions are primarily the most densely populated and are, therefore, the most influenced by automobile emissions (Fig.22). Great London has

131 air quality monitoring stations scattered around the city. Fig.23 showing their locations within central London.

Kerbside	Sites with sample inlets within 1m of the kerb of a busy road. Sampling heights are within 2-3m of the ground.
Roadside	Sites with sample inlets between 1m and 5m of the kerbside. Sampling heights are within 2-3m of the ground.
Urban Background	Urban locations away from major sources and broadly representative of town/city-wide background concentrations, e.g. urban residential areas.
Suburban	Sites typical of residential areas on the outskirts of a town or city.
Rural	Rural locations distanced from major population centres, roads, industrial areas or other pollution sources.
Industrial	Sites where industrial emissions make an significant contribution to pollution levels.

Table.03 - Monitoring sites are divided into six different classes, depending on their proximity to major sources of pollution.

Fig.22 – Continuous Air quality monitoring equipment on Marylebone Road in London, England. Inside look of the station (Author, left image), Various environmental monitoring equipment on Marylebone Road meteorological station's rooftop (Greater London Authority, 2020).

Roadside   Suburban   Urban Background   Industrial
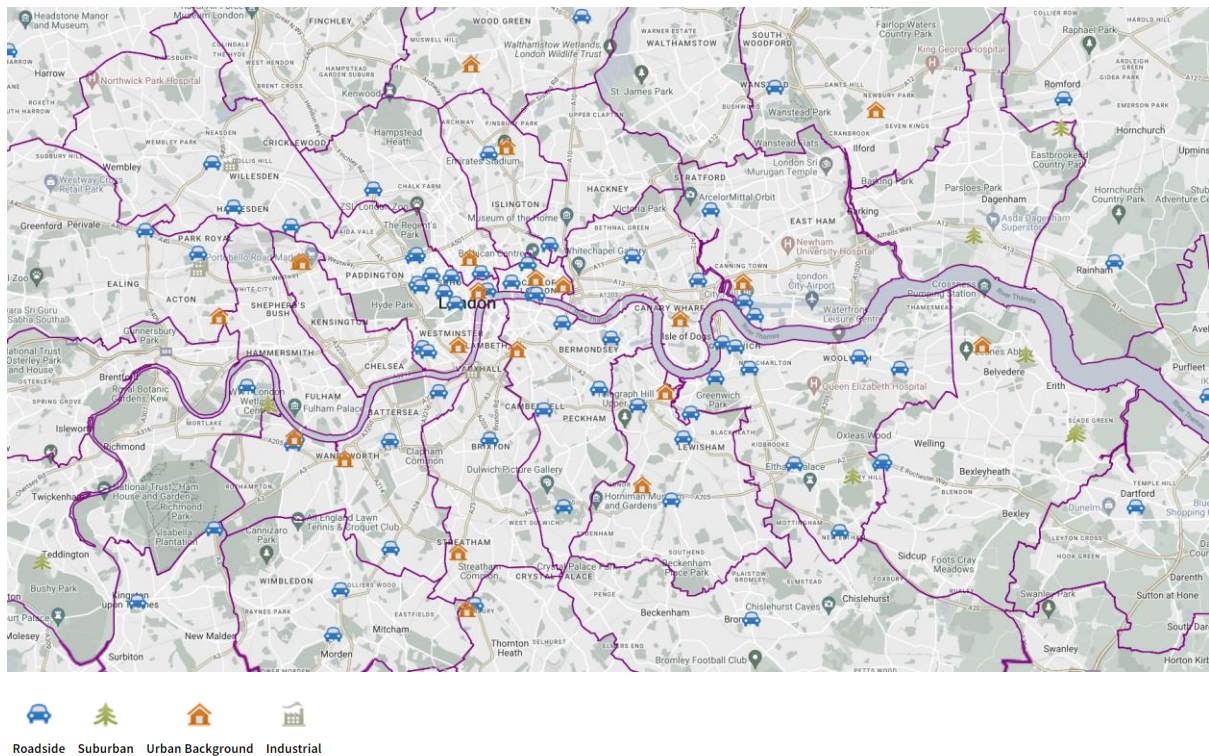
Fig.23 – Air quality stations within central London (London Air, 2021)

Aside from monitoring air pollution using the methods described above, air quality professionals and DEFRA use computational modelling to further evaluate air quality and estimate future predictions. Modelling is an important tool for evaluating air quality policy, and DEFRA uses it to assess compliance with UK directives and to inform negotiations on policy changes. DEFRA and researchers use a variety of modelling applications to provide a more comprehensive assessment and a better understanding of airborne concentrations, dispersion, deposition, and potential human exposure to polluted air. Chapter 4 of this thesis discusses these computational modellings in greater detail, along with their applicability for this thesis.

2.8 Conclusion

Air pollution has a significant impact on human health, triggering and inducing a variety of diseases that result in high morbidity and mortality, particularly in urbanised cities such as London. Air pollution is defined as a physical or chemical change caused by natural processes or human actions that degrades air quality (Cunningham and Cunningham, 2017). Large amounts of smoke and other types of pollution released into the atmosphere are

hazardous because the pollutants are released faster than the atmosphere can absorb them (Enger and Smith, 2016). Natural pollutants, primary pollutants, and secondary pollutants are the three types of urban air pollution. By reducing primary pollutants, secondary pollutants can be avoided, and as a result, NO_2 and PM_{10} and $PM_{2.5}$ have been identified as the most harmful pollutant at the pedestrian level, which will be considered in the future fieldwork and computational modelling stages of this thesis. These are the same pollutants that are responsible for the premature death of 40,000 to 50,000 people per year in the UK.

This chapter also explored the available methods in monitoring air quality within urban settings. Based on the current review, there are two distinct types of air pollution monitoring generally in use i.e., non-automatic and automatic. Although non-automatic methods and diffusion tubes are inexpensive with wide spatial resolution, but this method has the lowest accuracy with low temporal resolution. As a result, Defra recommends that local governments use continuous monitoring data (automatic) whenever possible. An alternative and less expensive method to measure air pollution is to use portable air pollution devices, which have been used in many academic studies and by air quality professionals. Given that air quality varies between urban settings, the mobile monitoring method will allow the user to respond quickly to these changes and capture variations in an individual's exposure to air pollution. As a result, during the fieldwork stage of this thesis, portable monitoring devices will be used to measure and capture air pollution levels. It should be noted that data output from portable devices is only valid if they are co-located and calibrated next to a maintained reference station.

As part of this literature review, UK government air quality policies and standards were critically discussed. Overall, it is encouraging to see the UK government and the Mayor of London actively introducing measures to control and reduce air pollution, but it is unfortunate that most of these policies primarily focused on transportation and cars as the primary focal point for proposing strategies to rectify or diminish urban air pollutants, and thus paid less attention to other potential factors such as urban physical form, urban planning, and microclimate. While the most effective strategy for combating air pollution is to reduce and eliminate pollutants at their source, and this should be the starting point for

any air quality policy and strategy, as previously discussed, no single measure on its own will achieve the full attainment of the air quality objectives, and thus a number of measures in the form of a package must be deployed to be more effective and provide a long-term solution to lower the air pollution. These measures can take the form of urban planning strategies and urban form manipulation to increase dispersion and decrease the concentration of various pollutants within urban spaces. The urban form has a significant impact on the formation of favourable and unfavourable local climates, particularly in terms of wind movement and its ability to disperse air pollution and create a type of microclimate conducive to human health.

As a result, reducing air pollution is not an either/or proposition. If there is an action that can be taken to reduce emissions by utilising or reforming urban spaces, as well as an action that can be taken to reduce the source of emissions, both actions must be taken if they will both reduce the illegal level of air pollution. This chapter confirmed that there is an apparent knowledge gap in current regulations and standards and provides an opportunity to investigate and evaluate the impact of urban form on microclimate and air pollution concentration to create a multidisciplinary approach to air pollution mitigation.

Based on the findings of this literature review, the following chapter will look into the potential of urban form to manipulate the urban microclimate in order to increase dispersion rate and improve the outdoor air quality. Moreover, it will provide an introduction to the factors that have influenced the formation of our cities to date, as well as speculate on their future struggle to remain in service of their inhabitants. The study will examine various urban forms and metrics to identify the most effective metrics for controlling urban microclimates in order to increase pollution dispersion and reduce concentrations of air pollutants between urban spaces.

Part 1

Urban Form, urban microclimate and air pollution

Chapter 3

Chapter 3

Urban Form, urban microclimate and air pollution

The term "urbanisation" refers to the increase in the proportion of people who live in towns and cities. It entails an increase in the degree to which a settlement is industrialised, as well as the number and extent of cities (Bowden, 2007). Grimm et al. (2008) characterise urbanisation as a dynamic and complex process involving multiple spatial and temporal scales. Cities undergo transformation and adaptation over time to accommodate changing conditions. Certain cities expand in size, while others contract in size as a result of economic, political, and environmental changes. However, they do so in markedly different ways, reflecting regional, national, and global responses to change. It's hard to overstate how important urbanisation has been in the last century, with far-reaching effects on many aspects of social, political, environmental and economic life (Shannon, Kleniewski and Cross, 2002; Macionis and Parrillo, 2010). Having said that, there is a sizable and growing body of literature which has examined the concept of human settlement in its current form and speculated on its future struggle(s) to remain in service of its inhabitants (Schellnhuber et al., 2010 ; Jacobs, 1961; Davis, 2006; Glaeser, 2011). Almost all of the world's largest cities transformed land cover and urban form through rapid urbanisation and consumption of water, energy, food, and land, thus, contributing to environmental and ever increasing air pollution, which has a detrimental effect on the health and quality of life of the urban population (Grimmond, 2007). It's worth noting that climatologists have been studying urban form and its impact on the environment and local microclimate conditions since the early 1950s (Mills et al., 2015; Krazter, 1956; Givoni, 1998; Oke, 1973, 1984, 2003; Steeneveld et al., 2014; Landsberg, 1970). For example, a number of studies led by Edward NG (Ren et al., 2012; Ng et al., 2011) have shown that urban form and, specifically, urban street canyons have a significant impact on urban microclimate through both field measurements and computational modelling. For that reason, this chapter defines urbanisation and provides a discussion of its positive effects as well as its downsides. The chapter will mainly focus on the impact of urbanisation on microclimate which has led to increase in concentration of air pollution in various urban settings, particularly within urban street canyons. It will then identify the urban morphological indicators that influence the concentration of air pollution within urban street canyons by reviewing the various

configurations and classifications of urban street canyons and their potential effect on microclimate and pollution dispersion. The knowledge gathered from these reviews will be used to frame the fieldwork study and computational modelling in order to fill a knowledge gap and provide a better understanding of air pollution behaviour in various urban street canyon configurations.

3.1 Urbanisation

Urbanisation and the city size, overcrowding, density and rate of development are not a new phenomenon; in fact, the earliest urban communities and human settlements can be dated back to about 6000 years ago in the Middle East, what is now present-day Iran and Iraq. That being said, these very small cities were heavily dependent on intensive farming and rural communities. Before the era of the Industrial Revolution, the pace and the size of the world's urban population remained relatively low. This was mainly due to limited food supply and the then crude nature of transportation. However, with the introduction of machine manufacturing in the mid-18th century, urbanisation gathered pace and urbanised territories expanded exponentially (Clark, 1998). Advancement during the Industrial Revolution and the significant evolution of machines in the manufacturing process changed the speed and volume of material production and manufactured goods. As a result, the lives of people who lived in cities, particularly in Europe and North America, were drastically altered. Additionally, transportation innovation and increased job opportunities in cities resulted in population redistribution, as evidenced by a shift from rural to urban areas (Fig. 24). However, it is critical to understand that, in comparison to the 'Industrial Revolution,' the rate of urbanisation increased with much faster pace. For example, it took 130 years for London population to grow from one million to eight million (Rasmussen, 1982), whereas Mexico City did so in less than 30 years (World Health Organization, 2008).
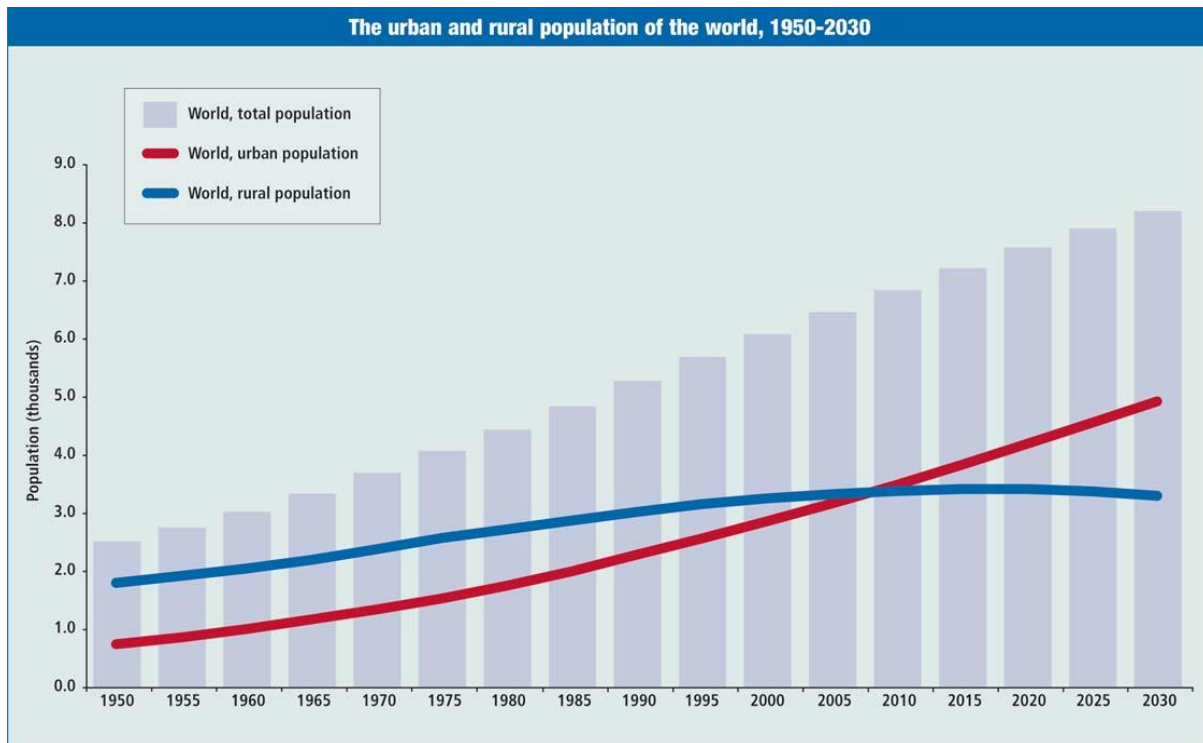
Fig. 24 - The urban and rural population of the world, 1950-2030 (United Nations Population Division, 2006)

Between 1800 and 1950, the world's urban population increased from 3% to 30% (732 million), and the number of cities with over 1 million people has increased to 83 (United Nations Population Division, 2006). Since then, the urban population has continued to grow exponentially, reaching 49 percent (3.2 billion) in 2005 (Bocquier, 2005). According to United Nations' World Urbanisation Prospects 2014, for the first time since 2005, more than half of the world's population now lives in cities, with more than 400 cities with a population of between one and five million and 19 with a population of more than ten million (UNDESA, 2016). According to the latest UNDESA (2018) report, global population is expected to increase to 68 percent by 2050, when it will be home to 9.7 billion people, an increase of 2.8 billion over the next four decades. Accordingly, the number of cities with populations of between one and five million will increase to 560, in addition to 43 megacities with populations exceeding ten million.

Numerous studies (Detwyler and Marcus, 1972; Smil, 1999; Institute for Population Studies, 2010; Farrell, 2013; Tal, 2013) have established that the world has experienced unprecedented urban growth and development in the last few decades in order to

accommodate and respond to this dramatic increase in urban population. In the long run, urban areas are expected to absorb and accommodate all of the projected population growth over the next decades. These cities are growing in population so rapidly that a central challenge for well-being in the coming decades is to make sure that those cities are viable, habitable, healthful, pleasant, prosperous, clean, and safe; in other words, to make sure that those cities are sustainable. In fact, such rapid urbanisation and population growth will inevitably increase demand for economically, environmentally, and socially sustainable planning. Fig. 25 depicts cities with a population of one million or more in 2016 and their projected growth through 2030.
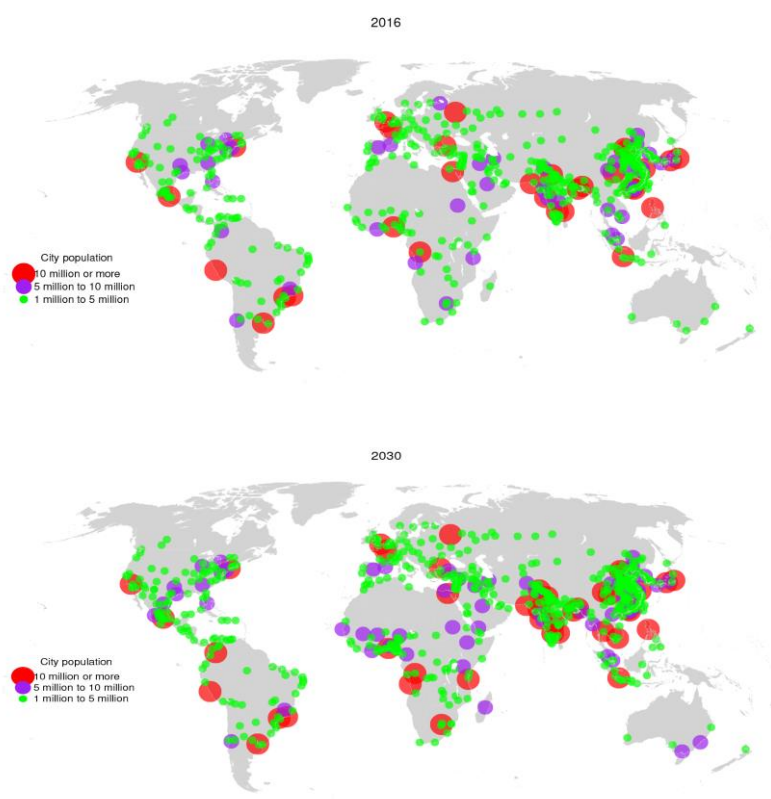
Fig. 25 - Cities with one million inhabitants or more, 2016 and 2030 (UNDESA Population Division, 2015)

The most apparent and obvious conclusion to be drawn from the preceding paragraph is that this population growth and escalating rates of urbanisation will increase human activities, and therefore the environmental problems associated with increased emission and air pollutants as a result of this growth will increase substantially (Haughton, G., & Hunter, 2003).

3.2 Urban morphology

The study of city forms and human settlements, as well as their process of transformation and formation, is referred to as 'urban morphology' (Kropf, 1996). It is concerned with the structure and shape of cities, towns and villages. Morphological studies, according to Rapoport (1990), are an attempt to organise and classify a set of objects in order to gain a better understanding of the built environment's common features and regularities, as well as the relationship between these components (objects) and our role as the agents who create and use them, as well as their arrangement and composition over time (Rapoport, 1990). In other words, these studies use thorough classifications of buildings and open spaces to explain the physical and spatial organisation of cities. The morphology of cities can be studied at several levels and scales. This can range from microscale, for example, buildings and their immediate spaces around them, i.e. plot, street and green spaces or from mesoscale, such as regions and districts and their arrangements and overall network connection of a city.

Among the many scholars and researchers who have studied the urban form, there are three distinct schools of thought on urban morphology, the Italian, English, and French (Lynch, 1981; Moudon, 1997; Larkham, 1997; Gauthier and Gilliland, 2006; Whitehand, J.W.R. and Larkham, 1992). While 'urban morphologists' generally agree on what they study, there is much disagreement over how urban forms and what urban morphological indicators should be investigated. In the mid-twentieth century, an Italian school led by Saurio Moratori and Gianfranco Caniggia focused on urban typology. All aspects of the built environment, including open spaces and the interaction between urban form and building typology, are addressed in the Italian method. The 'urban form' here refers to the plot, open space, and shape of the street network, while the 'building typology' refers to the types of construction, shape, and placement of the structure on the plot, as well as internal distribution. The English school paralleled the Italian school, is evidenced by work by Whitehand (1977), Conzon (1958), and Dickinson (1934), all of whom contributed significantly to the analytical technique of examining cities (Chiaradia, 2019). In 1960, M.R.G. Conzen proposed a complete concept for defining and analysing cities. He separated the study of urban form into three categories (Fig.26). First, the ground plan, which includes

the block layouts, street, plot and building's site. Then there's the building fabric and the three-dimensional form of the buildings, followed by building utilisation and land use. Subsequently, Conzen's work focused on putting these notions into practise in planning.

Fig.26 - The main elements of the city from the perspective of Conzen (Kostof, 1991)

The French school emerged in Paris in the late 1960s as a result of a renewed interest in urban morphology. With the involvement of disciplines other than architecture, including sociologists, planners, and historians, the French school advanced Muratorian views even further. As a result, the French School looked at the study of the urban morphology from a slightly different angle and debated the importance of social dimension of our cities in urban studies and argued that the physical spaces are meaningful only by their social activities, and these social activities force the spatial transformation of the urban fabric.

It is worth noting that, since the 1950s, motorised vehicles have transformed the logic of distance as a factor of accessibility and influenced the form of our settlement. Urbanisation largely led to a speed-oriented urban morphology including relatively tall buildings with the intention of maximising the space available by using the least amount of surface area and providing more space to vehicle traffic. This led to the creation of the most iconic and dominant urban form where the street is flanked by buildings on both sides creating a canyon-like environment known as urban street canyon (Fig.27).

Fig.27 – Pictures showing typical building and street network arrangements in Euston, London forming street canyons with various configurations. Image on the left, Euston Road. Image in the middle Tottenham court road looking towards Euston junction. The image on the right is Warren Street looking towards Fitzroy Street in London.

This strong and rapid evolution necessitated the development of new definitions of the urban domain, and various researchers influenced by the three main schools of urban morphology defined various urban scales through morphological indicators. The following section will review and identify the most appropriate scale and morphological indicators for use in this thesis.

3.3 Urban form, scales, and morphological indicators

Urban form is a combination of all physical characteristics of a city, including its size, configuration, and shape. Based on the three schools of urban morphology and despite differences in approach and methods of dealing with the subject of urban form, a common ground can be identified in these three schools, which are based on three basic principles: First, the urban form can be defined, understood and analysed with three basic physical elements: building/plot, street/block, city neighbourhood (Moudon, 1997); Second, the characteristics governing the urban form can be divided into three categories: two-dimensional shape (location), elevation (volumetric) and network connection characteristics; Third, three areas of study can be identified among the studies conducted: the study of physical characteristics with special emphasis on quantitative characteristics; historical study with emphasis on time and its effect on urban system; And the study of qualitative characteristics with emphasis on their effect on human behaviour. In light of this, in recent years, urban morphologists such as Kropf, who is influenced by the three main schools of morphology and a well-known urbanist in the subject of urban morphology, have introduced a combination of components offered by Conzon and Caniggia and created a

number of tools, strategies, and methodologies for examining and assessing the performance of urban environments as a habitat, as well as the suitability of different forms for various purposes and conditions. The most important concept in his view in morphological studies to describe urban form is the concept of urban tissue (fabric). Kropf enumerates seven primary elements as elements of the urban tissue (fabric) and introduces these elements at three different scales (Fig.28).
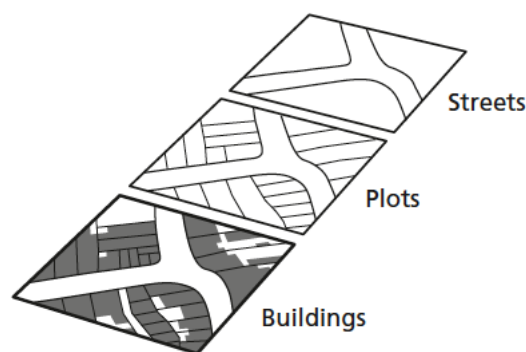
Fig.28 - The level of resolution introduced by Kropf for study of urban form in three scales, buildings, plots and streets (Kropf, 2017).

Each level in the multilevel diagram of generic structure represents recursive actions of aggregation, with each element moving up a scale, implying an increase in the amount of complexity of the elements (Fig.29). These diagrams indicate the importance of scale at which urban form can be considered or measured.

Fig.29 - The levels in the multilevel diagram of generic structure (Kropf, 2017).

Another urbanist, Rådberg in 1996, used percentage of built-up area, residential density (the ratio of the total residential area to land area) and building height (average number of storeys) as the main parameters to define and classify urban form. The level of analysis of the urban form is chosen as a set of buildings surrounded by adjacent streets. Further, he illustrated these three indicators in a logarithmic diagram and identified eight different types of urban forms (Fig.30) (Rådberg, 1996)

1	High density inner city blocks, 4–6 storeys
2	Blocks with planted inner courtyards, 4–6 storeys
3	High rise developments, point blocks or slab blocks 6–12 storeys
4	3–4 storey "walk-ups" (lamellas)
5	Preindustrial low rise traditional blocks
6	Garden suburbs, mixed developments
7	Small one-family houses (bungalows) on small individual plots
8	Villas on larger plots. (Rådberg, 1996)

Fig.30 – Urban density, building height and percentage of built-up area in eight Swedish urban types.

The vertical axis of Fig.30 is assigned to the net residential density index, the horizontal axis to percentage of land covered with buildings, and the diagonal lines to the number of floors in a block. In other words, the building site coverage and floor area ratio are used to determine the density variation. The building site coverage is the percentage of the ground area that is occupied by buildings (Fig.31) and is one of the most useful morphological index of a city and its ability to impact local wind velocity. In wind tunnel experiment carried out by Ng and Wong (2006) Indicates that the wind velocity of a city, in general, would halve if the building site coverage increased from 10 to 30 percent. This means, the higher the building coverage ratio, the lower the observable wind velocity ratio (Yoshie et al., 2013; Ng et al., 2011). Similarly, Kubota et al. (2008) found a strong correlation between building

coverage ratio and average wind velocity ratio, concluding that building coverage ratio is the most significant morphological index for mean street level (pedestrian-level) wind velocity. The floor area ratio (FAR), which is the total floor area of a building divided by the size of the plot of land on which it is constructed, is another morphological index that is being used by many planning authorities to apply certain FAR restrictions in order to classify various building typologies and their functions (Fig.31). A FAR of 1.0, for example, means that a one-story building can be built over the entire land, or a two-story building can be built over half of the land. In many studies, FAR is used to index the density and intensity of urban spaces (Yang et al., 2010; Razak et al., 2013; Jiang et al., 2008).
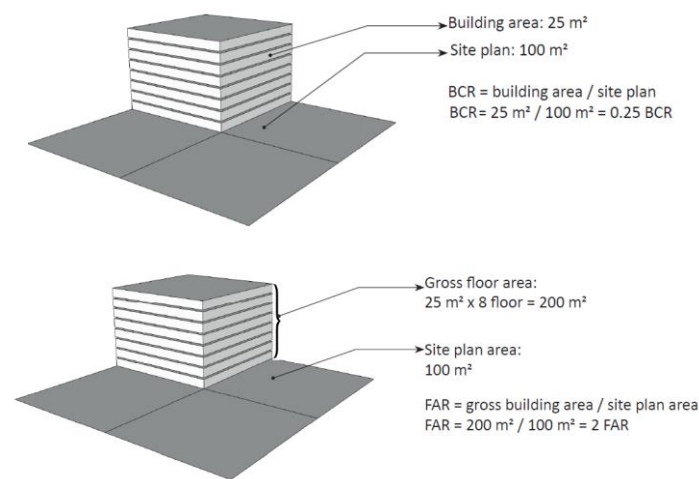
Fig.31 - Building Coverage Ratio (top) Floor Area Ratio (bottom)

In the same vein, Trache (2001) looked at the same elements from a slightly larger scale and dealt with elements of urban form such as the grid of streets and street blocks, building typologies with specific attention to the position of the building within the plot, and building heights differentials, an approach that was famously used by French architects (Fig.32).
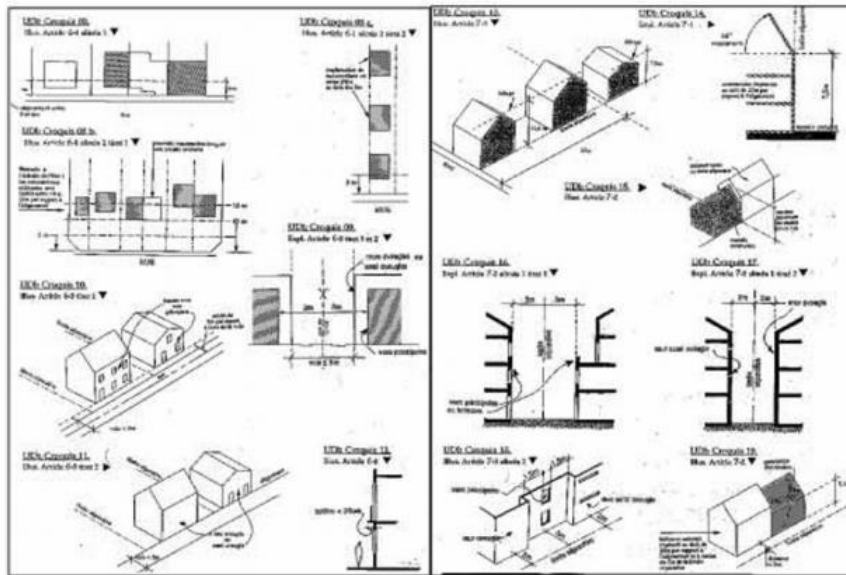
Fig.32 - Three-dimensional drawings were outlining siting and height prescriptions (Trache, 2001).

The building height differentials mentioned in Trache's works is another important morphological index for city ventilation. Based on Ng and Wong (2005) study, a city with larger differences between the taller and the lower buildings tends to have better city ventilation. This can be due to the downdraught effect on tall buildings and their ability to channel the wind downward. This downdraught effect not only happens on the windward façades of buildings, but it also happens on the leeward façades via spiralling vortexes towards the ground and leeward recirculation behind the building. Fig.33 indicates the schematic variation of air flow pattern around an isolated tall building.
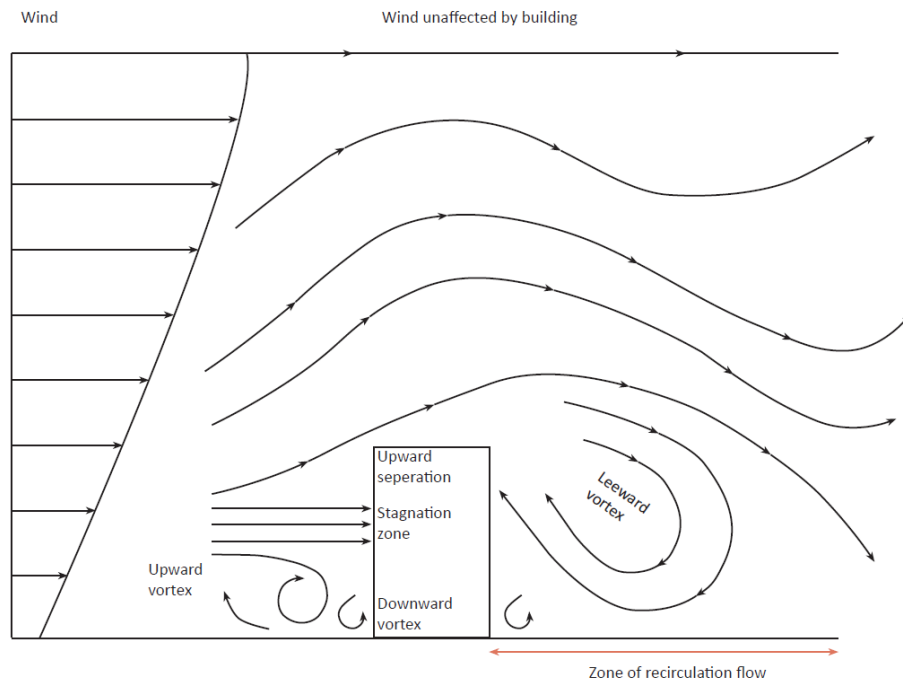
Fig.33 - Schematic airflow pattern around a tall building

In addition, buildings that are of different heights induce positive and negative pressures on the two sides of a slab-like building (Fig.34). This, in turn, creates air movement parallel to the building façades and improves urban city ventilation (Ng and Wong, 2005). Ng et al. (2011) used additional morphological indicators such as frontal area index to offer more details on urban ventilation at pedestrian levels. The FAI (Frontal Area Index) is the ratio of a building's frontal area to the overall area of a site (Fig.35), and it's linked to pedestrian ventilation and airflow. On a geographical scale of hundreds of metres, a 10 percent increase in FAI can result in a 2.5 percent drop in wind velocity ratio at the pedestrian level (Ng et al., 2011). For high-density urban situations, Razak et al. (2013) observed a similar link.
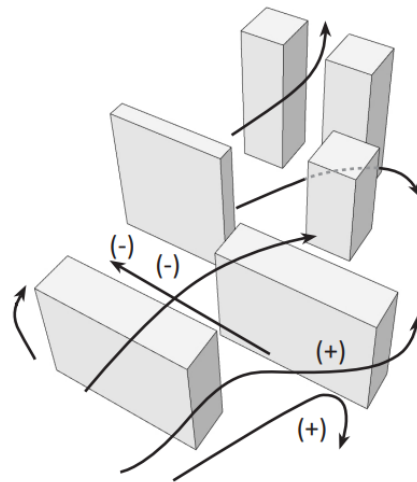
Fig.34 - Variation in building heights created positive and negative pressures; a city with greater building height differentials is preferable.
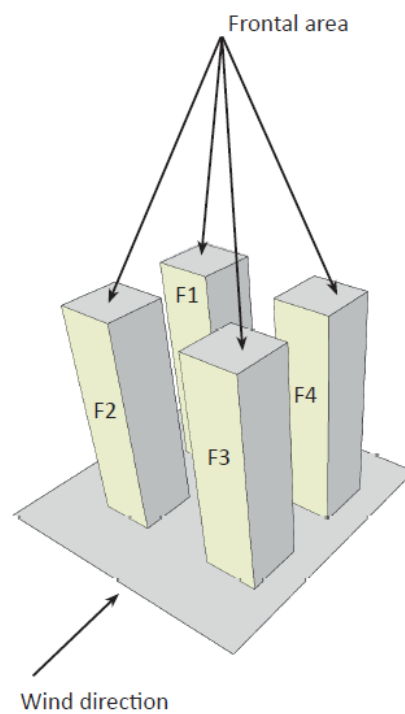
Fig.35 - The FAI (Frontal Area Index) is the ratio of a building's frontal area to the overall area of a site.

Oke (1982, 1987) refers to the similar scales as to other urbanists but through climatology lens. He claims that urbanisation has resulted in two unique climate conditions in cities. To begin with, the city as a whole alters regional climate conditions, resulting in a variety of climate conditions between the built-up and adjacent (countryside/rural) areas. This effect

may be seen in the climate above the city's rooftops, known as the Urban Boundary Layer (UBL), which is very stable across the city. Second, in contrast to the UBL, the climate beneath the city's roofs, in the gaps between buildings, and at the surface level can vary substantially even within a few metres (Fig.36). This medium is one of the most complex and least-understood scales in the formation of microclimate known as the Urban Canopy Layer (UCL). Fig.36 indicates the schematic of the typical layering of the atmosphere over a city, and table.04 indicates the classification of atmospheric layers comprising the urban climate system based on typical vertical length scales (Oke, 1984).
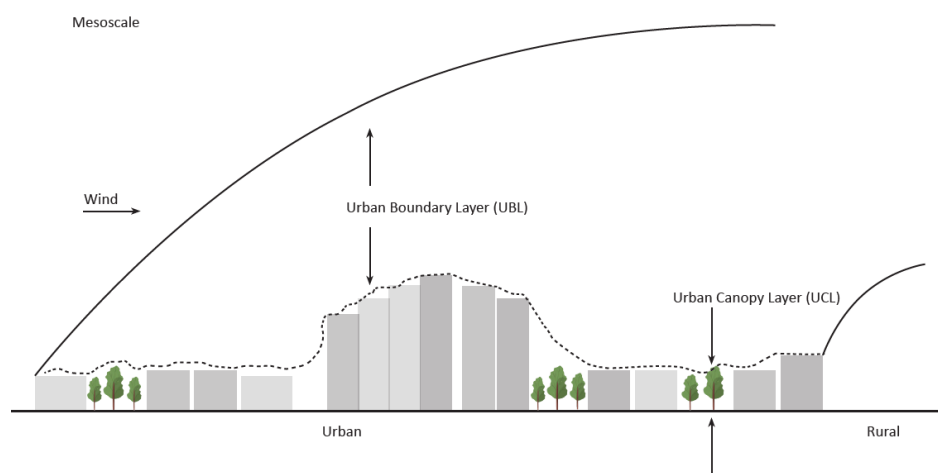
Fig.36 - Schematic of the Urban Boundary Layer and Urban Canopy Layer (revised by Oke and Rotach after a figure in Oke, 1997).

Name of layer	Definition	Typical vertical dimension	Scale
Urban canopy layer	From ground to the mean height of buildings/trees. It consists of exterior (outdoors) and interior (inside buildings) atmosphere.	Tens of metres	Micro
Roughness sublayer	From ground up to two to five times the height of buildings/trees including the UCL. In the RSL flow is affected by individual elements.	Tens of metres	Micro
Inertial sublayer	Above the RSL, where shear-dominated turbulence creates a logarithmic velocity profile and variation of turbulent fluxes with height is small (< 5%).	~25–250 metres	Local
Mixed layer	Above the ISL, where atmospheric properties are uniformly mixed by thermal turbulence and usually capped by an inversion.	~250–2,500 metres	Meso

Table.04 - Classification of atmospheric layers comprising the urban climate system based on typical vertical length scales, adapted from Oke (1984 and 2017).

Oke et al. (2017) then divided a number of urban units within the three mentioned climate scales, i.e. Meso, Local and Microscale. Table.05 shows the 7 classification of urban units

and their common built and green features. The spatial variability of these scales extends over distances from a few meters (a courtyard or wall) to tens of kilometres (whole cities).

Urban units	Built features	Green and water features	Climate scale
Facet	Roof, wall, road	Leaf, lawn, pond	Micro
Element	Residential building, high-rise, warehouse	Tree	Micro
Canyon	Street, canyon	Line of street trees or gardens, river, canal	Micro
Block	City block (bounded by canyons with interior courtyards)	Park, wood, storage pond	Local
Neighbourhood	City centre, residential (quarter), industrial zone	Greenbelt, forest, lake, swamp	Local
City	Built-up area	Complete urban forest	Meso
Urban region	City plus surrounding countryside		Meso

Table.05 – Classification of urban morphological units adapted from Oke (1984, 1989 and 2017).

Based on Oke's (2017) classification the local and meso climate scales are influencing larger urban climate phenomena such as urban heat island, which typically occurs over a large urban or metropolitan area when the temperature over urban areas are warmer than its surrounding rural areas as a result of human activities and built form. On the other hand, the microclimate scale is capable of influencing the immediate environment at the pedestrian level, which has a far greater impact on human thermal comfort and immediate exposure to air pollution. The microclimate scale's morphological indicators include built features such as rooftops, walls and roads and pedestrian paths, and green features can be as small as leaves, lawns and ponds. In terms of urban units, as it can be seen in Table.05 above, the 'element' urban unit, which is a step greater than the 'facet' urban unit, is regarded as the primary 3D unit, and its repetition across a city influences the urban climate. Urban elements can be buildings of all types, low to high rise and greenery are trees ranging from short to tall height with consideration for their species. The placement of buildings within the scale of 'element' and their repetition will create a specific microclimate for that area and can impact the wind behaviour, and lead to an increase in pollutant concentration and change in spatial pattern of temperature due to shade and wind effect. These changes in wind behaviour are explained in section 3.4 of this chapter.

Canyon is the largest urban unit within Oke's Micro climate scale classification and is the structure formed by the common arrangement of a street and its flanking buildings. The

urban canyon form and geometry is the most characteristic form of modern urban settlement and is usually echoed across the urban landscape and can influence many features of urban climates, including solar radiation, shade, wind flow behaviour and velocity, surface and ambient temperature within a canyon. Oke (2017) describes these canyons by their aspect ratio H/W (Fig.37) and characterises the openness of spaces towards the sun and sky as a morphological index to describe the ventilation rate inside the urban street canyon, known as the Sky View Factor (SVF).
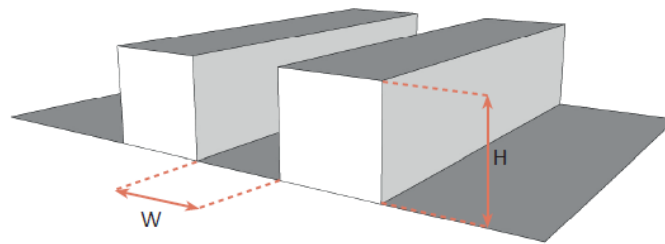
Fig.37 – Aspect ratio of urban street canyon H/W where H is the height of the building and W is the width between the two rows of buildings.

The SVF is a three-dimensional measure for a single point on a surface (Johnson and Watson, 1984). In other words, it defines the ratio of the sky hemisphere (above the urban canopy layer) visible from the ground. The SVF varies from 1 from a completely unobstructed land surface for example in flat terrain, to 0 for a completely obstructed land surface. When a location has buildings and trees, it will cause the SVF to decrease proportionally (Oke, 1977). This parameter is of major importance in urban climate investigations, whose aim is the exploration of the effects of a complex urban surface on climatological processes in built-up areas (Fig.38). This means that meteorological conditions and the urban canyon configuration can influence airflow and ventilation paths, which in turn control the behaviour of air pollutants and directly influence their concentration or dispersion within site. According to Mayer (1999), after air pollutants are released into the urban canyons, they follow one or more of the following processes: dispersion, dilution, deposition, and transformation. Dispersion refers to the movement of ambient air pollution after it is emitted from sources, and it is commonly used to express

the effectiveness of wind flow in clearing pollutants from the street canyon (Vallero, 2019). Dilution refers to when the air within street canyon mixes with the above the roof air which potentially can remove the polluted air from the canyon. Deposition refers to removal of air pollutants either through dry or wet deposition. The direct uptake of air pollutants by urban features such as trees, buildings, ground and urban surfaces is referred to as dry deposition and wet deposition occurs when pollutants mix with suspended water in the atmosphere and are then washed out through rain, snow or fog (WMO, 2008). Transportation refers to the physical and chemical transformation of air pollutants from the point of emission until they are deposited on the ground, waters, and vegetation, or are inhaled by humans and animals (European Environment Agency, 2020). A poorly designed urban canyon can also result in a fifth condition, which is the concentration of air pollution, which must be avoided in order to reduce the exposure of urban dwellers to air pollutants.
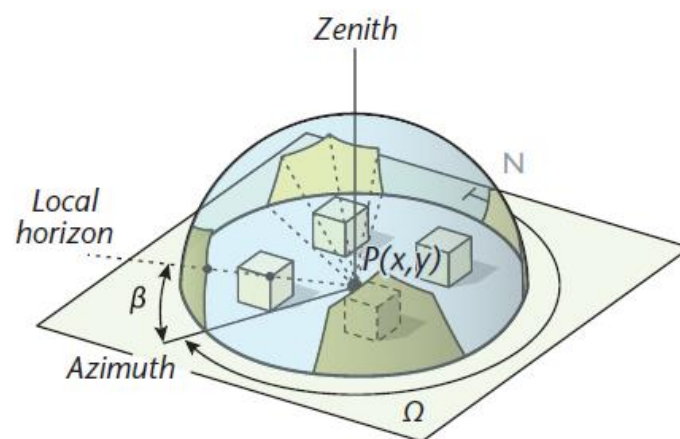
Fig.38 – The sky view factor conceptualised for a point P on the ground at an urban site (Oke et al., 2017)

Baruch Givoni, who is one of the most authoritative specialists in bioclimatic architecture, identified that the street orientations, height of buildings, urban density and availability of open and green spaces are important in controlling urban microclimate (1998). The green cover ratio here is the total area of greenery, including tree canopy and any vegetation to the total land area (Fig.39).

$$A_v$$
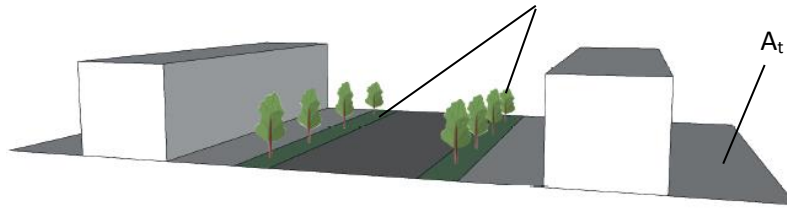
Fig.39 – Green cover ratio A_v/A_t which is the ratio of area of greenery (A_v) to the total land area (A_t).

The inclusion of greenery as one of the major morphological indicators is critical, as trees, vegetation, and green infrastructure in general are increasingly perceived as a promoted method for air pollution mitigation (Barwise and Kumar, 2020; Zhai et al., 2022; Claesen et al., 2021). Green infrastructure such as street trees, green roofs and walls are perceived to be depositing pollutants more efficiently onto vegetations than onto smoother, impervious, artificial surfaces (Fowler et al. 2009; Nowak et al. 2013; Neft et al. 2016). Greenery deposit pollutants and in particular particles via the dry deposition (through wind force) or wet deposition (through rain and snow). Meaning, polluting particles reach leaf surfaces through rain and snow (wet deposition) or wind force (dry deposition) (Vigevani et al., 2022; Bealey et al., 2007). Apart from that, strategic placement of trees in cities can cool the air, thus reducing the urban heat island effect and improving thermal comfort, boosting physical and mental health of urban dwellers, and flourishing urban biodiversity.

By contrast, a number of growing experimental and modelling research on trees and their negative impact on urban air quality have been published recently (Buccolieri et al., 2022; Xing and Brimblecombe, 2019; Jeanjean et al., 2017; Gallagher, 2015; Vos et al., 2013). These studies indicate increasing tree and vegetation numbers will change the urban configuration, which will have a direct impact on the urban microclimate, with a pronounced impact on urban wind flow and air volume, thus lowering air velocity around trees and leading to a higher concentration of air pollution. At the same time, research suggests that the influence of trees within urban canyon is complex, and can reduce or increase concentrations depending on the case i.e. wind speed, direction, deposition, buoyancy and urban heat island (Buccolieri et al., 2019). The use of hedgerows were also considered in various studies, for example Abhijith and Kumar (2019) studied the effectiveness of 2 meter hedgerows in open street configuration and their study showed a 63% reduction in pollution concentration. Given that many urban canyons have space

limitation hedgerow can be placed instead of trees or other type of greenery. In a similar study Santiago et al. (2019) found that green infrastructure barriers composed by a combination of hedgerows and trees were more effective than barriers with only hedgerows. Moreover, Ottosen and Kumar (2020) recommended coniferous hedges over deciduous hedges since the protection and performance of the latter will be reduced during its shedding season. It is worth noting that there is an obvious limitation in most of these studies as there is a great reliance on meteorological and air quality data that are extracted from a monitoring station far from the study site/s, with little attempt to undertake fieldwork spot measurements to calibrate the data from the stations. This raises the number of assumptions, and the little published research on this topic provides an opportunity to investigate this phenomenon in further detail and with finer resolution.

The next section of this thesis will review the effect of urban canyons on microclimate and air pollution in more details and a list of most influential morphological indicators on microclimate and air pollution within urban canyons will be provided. Table.06 provides a summary of all the morphological indicators reviewed thus far.

Researcher/study	Morphological indicators
Conzen, 1960	Ground plan (comprising streets, plots and block plans of buildings), building fabric, land use and building utilisation.
Rådberg, 1996	Building height, building area (site coverage), residential density (ratio of total residential area to area of land).
Kropf, 1997	Plots, street blocks, buildings, rooms and spaces, building structures and materials.
Maller, 1998	Linear elements (i.e. boundaries, arteries), enclosed elements (i.e. piazzas, streets), massive elements (i.e. blocks, parks) and edges (i.e. waterfronts, rail track frontage).
Thayer Jr, 1981); (Littlefair, 2000	Street network and orientation
Trache, 2001	Street grid (network) and street blocks, building typology, building orientation within the plot, building heights and internal layout.
Ganiggia,G., & Maffei, 2001	Buildings, urban tissue (urban fabric), cities (urban organism), and territories.
Ratti et al., 2003	Sky view factor, shape factor
Meta Berghauser Pont & Per Haupt, 2005	Building area (site coverage), Accessible open space coverage, number of floors and floor area ratio.
Arboit et el., 2008	Typology and orientation of building blocks
Allegrini et al., 2014	Average building height, street width, aspect ratio, building orientation.
Van Nes et al., 2012	Street width or distance between buildings, height to width ratio (urban canyon)
Oke 1988	Aspect ratio, length to height ration (L/H), frontal area ratio, plan areal fraction, canyon aspect ratio, street aspect ratio
Cionco and Ellefsen 1998	Topography/urban terrain, urban layout: layout, development, street form, open spaces, roof. Mineralisation factor/percentage of impervious surface, mean building height, wind angle to longer-street axis of buildings
Givoni 1998	Topography/urban terrain, urban layout: layout, development, street form, open spaces, roof. city size/quotient, roughness height, mean building height, air paths
Newton 2000	Topography/urban terrain
Santamouris 2000	Topography/urban terrain, altitude, street aspect ratio, mean building height, mean canyon width, wind angle to longer-street axis of buildings
Hawkes et al., 2002	Topography/urban terrain, altitude, distance from water body, urban density/floor area ratio/rugosity, mean building height, mean canyon width
Golnay 1996	Distance from water body, street aspect ratio, mean building height, mean canyon width, wind angle to longer-street axis of buildings
Theurer 1999	Urban layout: layout, development, street form, open spaces, roof. city size/quotient, plot ratio, street aspect ratio, canopy breadth ratio, mean building height, mean canyon width, wind angle to longer-street axis of buildings
Steadman, 2002, 2014	Building geometry and elements including building periphery (Parasite)
Adolphe, 2001	Mineralisation factor/percentage of impervious surface, compacity factor, mean contiguity factor, urban porosity, sinuosity, occlusivity, street aspect ratio, mean building height, mean canyon width
Grimmond and Oke 1998	Complete aspect ratio, frontal area density, urban density/floor area ratio/rugosity, roughness height, zero-plane displacement height, canyon aspect ratio
Ramponi et al., 2015	Building orientation, street width (or distance between buildings), average building height
Edward NG, 2009	Air paths, Deep street canyon, street orientations, aspect ratio, ground cover ratio, building height differentials, non-building area (open spaces ratio), Scale of podium, building disposition, projection obstructions (vertical & horizontal)

Table.06 – List of urban parameters and indicators of urban form from the perspective of various urban morphologist.

3.4 Effect of street canyon configurations and orientations on microclimate

As was previously mentioned, street canyons have an effect on the direction, movement, and speed of the wind, which in turn has an impact on the air quality and the temperature of the surrounding area. The speed and direction of the wind are both affected by the orientation of the street; when the wind is blowing in a parallel direction,

street canyon flow has an effect that is comparable to the channelisation effect (Louka et al., 2000; Yamartino and Wiegand, 1986). This condition frequently leads to an increase in wind speed due to the venturi effect (Blocken et al., 2008) which occurs when the wind is forced to pass through an opening that is relatively narrow. As a result, pollutants such as vehicle fumes can be effectively flushed out downwind along the street while also causing discomfort to pedestrians (Lawson, 2001). Kastner-Klein and Plate (1999) conducted additional research into the pollutant distribution in seven different wind directions. These wind directions had angles that ranged from 0 degrees to 90 degrees relative to the axis of the street. They were able to verify that the perpendicular wind was the most polluting condition, while the winds at 30 degrees and 45 degrees caused the second-highest concentrations of pollution in the street canyon. The performance of pollutant removal was best when the wind was blowing in a parallel direction, as the concentrations at most measuring points were approximately one-third of what they were when the wind was blowing in a perpendicular direction (Kastner-Klein and Plate, 1999). Therefore, ventilation of the street canyon is carried out more effectively when the prevailing wind is either parallel to the street or oblique (Fig.40a&b) to the street rather than when it is blowing in a direction that is perpendicular to the street canyon. The magnitude of its effects is dependent on the velocity of the wind, the length of the street, as well as the width and height of the canyon (Soulhac et al., 2008). For example, in a uniformed (symmetric) street canyon with the perpendicular wind blowing above the rooftop, a cross canyon vortex formed (Fig.39c) and with an increase in the height of the canyon two counter-rotating vortices formed (Fig.39d). That means any future investigation should be focused more on disadvantageous conditions where the wind volume is impacted by the configuration of the street canyon, i.e. configurations (c) and (d).
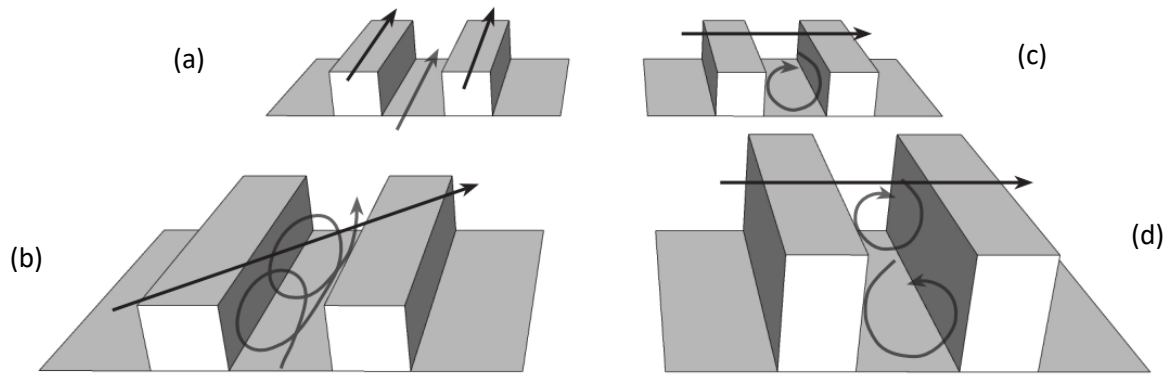
Fig.40 - Typical flow patterns in urban canyons: (a) along channelling and jetting along a canyon, (b) helical flow along a canyon, (c) cross canyon vortex, and, (d) multiple stacked vortices in a deep canyon (Modified after Oke, 1997; Belcher, 2012).

Oke (1987) defined three sub-flow regimes based on the wind direction blowing perpendicular to the street canyon axis. These are depicted in Fig.41 and Table.07, highlighting the complex wind behaviour and vortices that are closely related to the street canyon's aspect ratio (i.e. Hight to Width ratio: H/W).
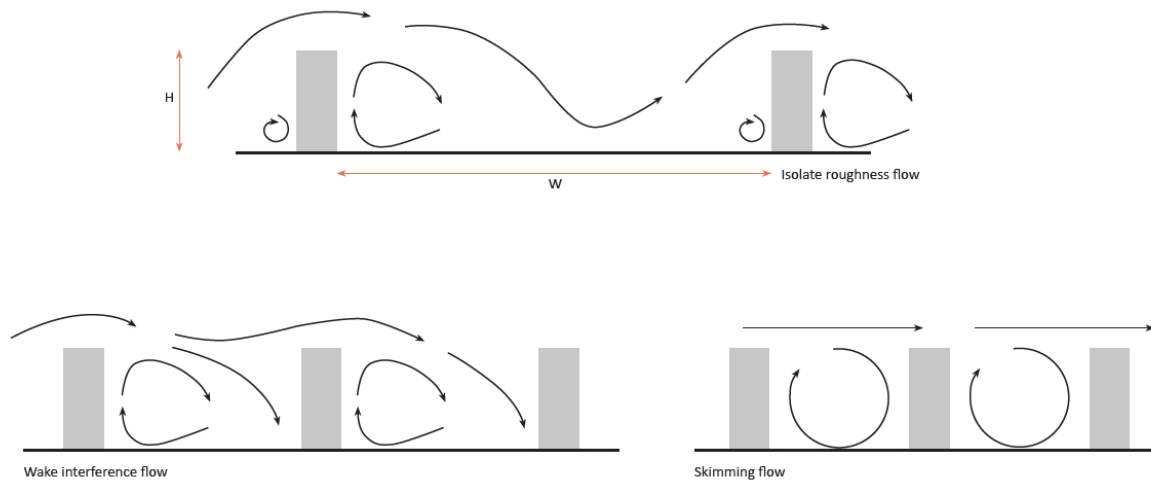
Fig.41 - Wind behaviour and pattern in the urban street canyon with wind perpendicular to the canyon axis, adapted from Oke (1987).

Flow regime:	Height to width ratio (H/W)	Characteristics
i) Isolated roughness flow	H/W < 0.5	The flow fields surrounding the buildings on either side of the street do not interact. Two co-rotative vortices can be formed.
ii) Wake interference flow	0.5 < H/W < 0.65	The flow around the upstream buildings starts to interfere with the flow around downstream buildings. One main vortex can be formed.
iii) Skimming flow	H/W > 0.65	The air above buildings hardly can interfere with the flow around downstream buildings inside the canyon. Circulatory or contra-rotative vortices can be formed.

Table 07 - Flow regimes type and characteristics in equal building heights canyons.

Another impact that street canyons have on the local climate is the amount of solar gain that occurs within urban street canyons. Depending on the geometry of the street this solar gain can either result in an increase or decrease in temperature of 2-4 degrees Celsius (Erell, Pearlmutter and Williamson, 2011). Those with an orientation that faces north to south are able to store the most energy, up to thirty percent of the radiant energy that is present during the day. This energy is then released at night when the temperature drops. Based on the surface material of buildings inside urban canyon some of the solar radiation will be reflected, and some of it will be absorbed. Ultimately the reflection coefficient or so-called albedo of the surface determines the amount of radiation that is either reflected or absorbed by the surface. Albedo is a nondimensional measure that is defined as the ratio of total-reflected to incident radiation and is determined by material surface properties. In general, light-coloured surfaces are expected to have the highest albedos. It is important to note that the sky view factor is one of the most important morphological indicators for the amount of solar radiation received by surfaces within an urban street canyon, and that an urban canyon with a lower SVF, i.e. with many obstacles such as urban furniture, vegetation, and green infrastructure, will have less diffuse and direct incident radiation. The height-to-width ratio, is another morphological index that influences the amount of sunlight that reaches the surface of the canyon. This is particularly important during the winter months when the sun is at its lowest point in the sky. As a result, wider canyons yield larger percentages of irradiation and when the H/W (aspect ratio) increases, global irradiation, which is the sum of diffuse and direct irradiation, decreases. Accordingly, the flow within the canyon is influenced by differential heating of the canyon surfaces during different times of the day and month. For instance, heating of the windward wall may cause a change

in the flow regime from one vortex skimming to two vortex skimming. This occurs because the thermal buoyancy opposes the downward flow movement, which in turn causes a flow reversal in the upper part of the canyon (Fig.42). Because thermal buoyancy and flow direction work in tandem, the flow in the canyon becomes more intense when a single vortex skimming flow regime is present (Kim & Baik, 1999; Sini et al., 1996; Cheng et al., 2009). Besides that, due to buoyancy, ground heating may cause a secondary counter-rotating vortex at the ground-level windward corner (Cheng et al., 2009). In addition to this, the heating of the ground surface causes recirculation of air within the centre of the canyon (Baik et al., 2007; Esch, 2015).
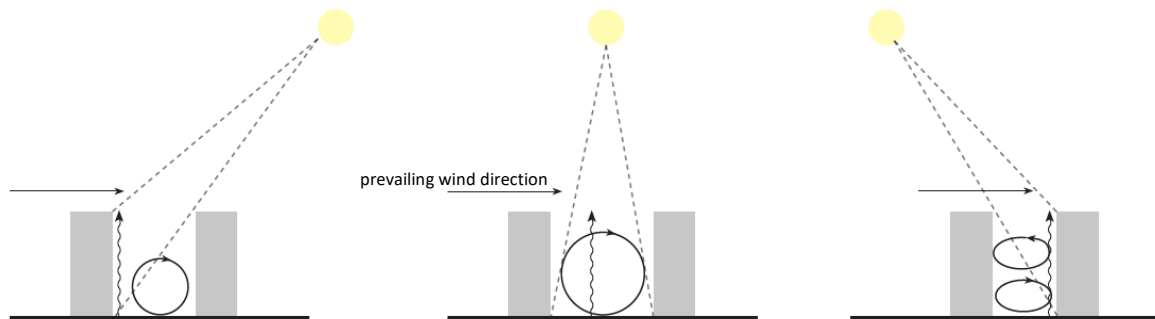
Fig.42 – Impact of canyon surfaces heat variation on the airflow pattern

At night, there is the potential for a thermally-induced canyon exchange due to the differences in radiation and heat storage between canyons and roofs, wall, floor, and air temperatures in canyons. In particular, canyons with large aspect ratios do not cool as rapidly as the temperature on the roof. As a result, canyon air is unstable in comparison to the level that is above the roof. Apart from the height-to-width aspect ratio and the orientation of the urban street canyon, the length to height ration (L/H) is an additional morphological index that influences the wind pattern and, more specifically, the wind speed along the street canyon. There is a strong likelihood that the wind speed will instantly increase from L/H = 12 to L/H = 4 before levelling off (Bottema, 1993).

The morphological indicators mentioned above have a large influence on microclimate and air pollution, and it is expected that the severity of this influence will vary as the canyon configuration changes. Therefore, it is important to analyse and study these changes in order to provide the best mitigation strategy for a various urban street canyon

configurations. For that reason, the following section reviews various types and classifications of urban street canyons in order to provide a better understanding of their urban form features and their significance and influence on air pollution dispersion and concentration.

3.5 Urban canyon classification

An urban canyon is a street that is relatively narrow and has tall, continuous buildings on both sides of the street. As was mentioned, this is the ideal configuration for an urban canyon. Having said that, the term "urban canyon" can refer to a wider range of geometrical formations. The aspect ratio (H/W) is one of the morphological indicators that can be used to categorise street canyons. This is the most significant geometrical aspect of a street canyon, and depending on the geometrical configuration, a canyon might be called regular if it has an aspect ratio that is roughly equivalent to 1 and there are no significant openings in the walls. An aspect ratio of less than 0.5 may be indicative of a canyon that is shallow (like an avenue), whereas a height-to-width value of 2 may be indicative of a canyon that is deep (Vardoulakis et al., 2003). Oke (1988) highlights another sub-classification of urban canyon based on the distance between two major intersections along the street, defined as the length (L) of the street canyon. To meet the dimensions of an urban canyon, the building length should be between 3 and 7 times its height. As a result, a short canyon has a building length that is three times its height, a medium canyon has a building length that is five times its height, and a long canyon has a building length that is seven times its height. The Manual for Streets (2007 and 2010) which complements planning policy statement 3 (Communities and Local Government: London, 2009) comprises technical guidance for various types of urban canyons in England and Wales. The manual divided the above three major urban canyon types into further classifications to define urban street types based on width and building heights. These are mews, residential streets, high streets, narrow high streets and boulevards. Table.08 illustrates the arrangement of the above street types and their respective urban canyon classification. The effect of these height and width variations also influences the flow regime within the canyon. The effect of this variation is illustrated in Fig.43.
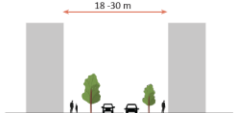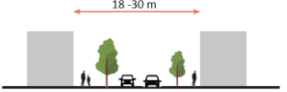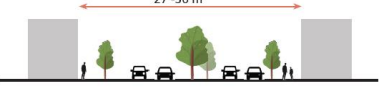
Canyon schematic diagram	Types of street	Urban canyon classification	Aspect ratio	Flow regime
7.5 - 12 m	Mews	Regular Canyon	1	Skimming Flow
12 - 18 m	Residential	Regular Canyon	0.6< and <1	Wake Interference flow
18 -30 m	Narrow High Street	Deep Canyon	>1.5	Skimming flow
18 -30 m	High Street	Avenue Canyon	≈0.5	Isolated Roughness flow
27 -36 m	Boulevard	Avenue Canyon	<0.5	Isolated Roughness flow

Table.08 – The types of street and their respective urban canyon classification, adapted from Vardoulakis, 2003 and manual for street (2007, 2010) and Oke (1987).
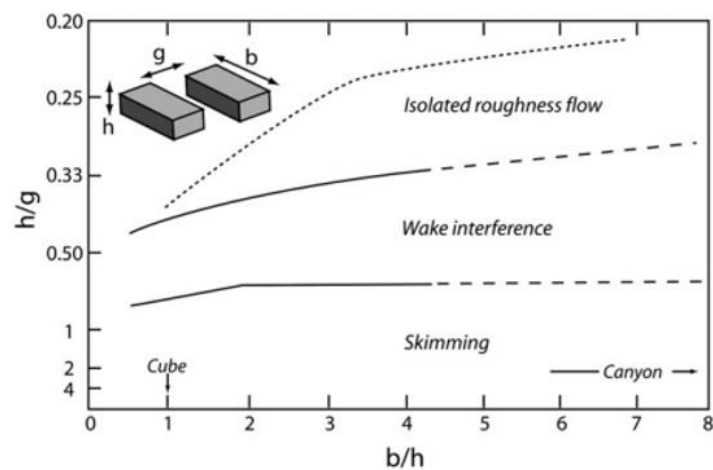
Fig.43 – The effect of urban canyon aspect ratio on the transition between flow regimes, adapted from Oke et al., 1987 and Hunter et al. 1992.

Another classification is based on the height of the buildings within street canyon, whereas when the buildings that makes the canyon have approximately the same height are referred to as symmetric urban canyons and if the buildings on either side of the street have significant height differences referred to as asymmetric street canyon. The asymmetric

69

canyon can be called step up canyon if the height of upwind building is less than the downwind building, and it is called step down if the upwind building is taller than the downwind building height. These differences between canyon geometry can greatly affect the local wind and air quality behaviour within street canyons. In a step-up canyon configuration, for example, the top of the vortex is stretched diagonally between the roofs of the aligning buildings, and the centre of the main vortex is shifted upwards and downwind. In the case of a step-down canyon configuration, the centre of the main vortex is moved upwards and is located at the roof level height of the lowest building, or even slightly higher, since the main vortex is weaker in this setting than in a symmetrical setting (Wania et al., 2012; Assimakopoulos et al., 2003; Xiaomin et al., 2006). Fig.44 illustrates these generic conditions based on a regular canyon aspect ratio and perpendicular wind to the canyon orientation. It is worth noting that it is expected by changing the aspect ratio, these compositions changes, and it would be an invaluable exercise to investigate the wind and air pollution behaviours in other urban canyons with different aspect ratios, as well as monitoring changes and include additional urban form features such as greenery to replicate the real-life complex conditions.
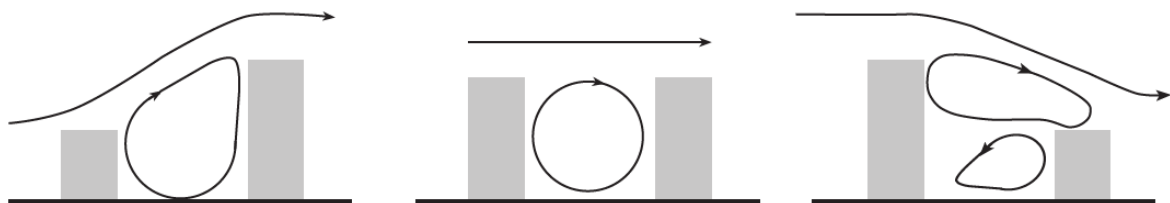
Fig.44 - Generic conditions based on a regular canyon aspect ratio and perpendicular wind direction to the canyon orientation.

In terms of pollution concentration, the windward façade of the step-up and the symmetric urban street canyon has the lowest pollution concentration. This occurs when the wind is perpendicular to the canyon axis. In this configuration, and depending on the aspect ratio, a relatively clean above-the-roof air volume enters the street canyon via downward vortex circulation on the downwind side of the canyon, removing part of the pollution (dilution effect), and pushing part of the pollution to the canyon's leeward façade. In contrast, the step-down canyon configuration has the lowest pollution concentration along the canyon's

leeward façade. This is due to the complex wind pattern and the formation of two counter-rotating vortices (Fig.45) (Baik & Kim, 1999; Kastner-Klein & Plate, 1999; Chan et al., 2001 & 2001; Assimakopoulos et al., 2003). It is worth mentioning that these diagrams and referred studies are primarily conducted in regular canyons with few to no physical obstacles such as trees or vegetation (Sotiris Vardoulakis et al., 2013; P. Edussuriya et al., 2014; Chao Yuan and NG, 2015; Buccolieri et al., 2011; Abhijith et al., 2017). To gain a better understanding of the validity of these effects in other urban canyons, additional studies on other classifications of urban canyons with varying aspect ratios are required. As a result, Chapter 6 of this thesis will look into this further to determine which urban form features have the greatest impact on increasing the dispersion rate within urban street canyons.
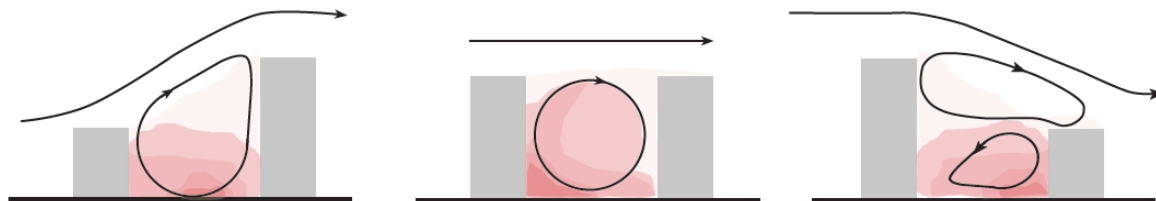
Fig.45 – Pollution concentration in asymmetric and symmetric regular urban street canyon. Adapted from Assimakopoulos et al., 2003 and Esch, 2015; Wen, 2017)

In summary, the above literature review identified that specific attributes of urban form have a significant impact on the formation of undesirable microclimate, which increases the concentration of air pollution in outdoor spaces, and that urban morphological indicators are essential for urban climatic analyses. According to studies on microclimate and air pollution, urban wind is the most important factor in determining pollutants dispersion because wind can carry pollutants from one location to another, increasing or decreasing air pollution concentrations within various urban canyon configurations. It has also been determined that not all urban morphological indicators are suitable for the study of wind and air pollution behaviour within urban canyons, and that only a few indicators that influence wind and air circulation in the city should be considered for fieldwork and computational modelling investigation. As a result, Table.09 includes a number of essential urban morphological and meteorological indicators that influence the microclimate and can be used to study air pollution and wind behaviour in urban street canyons.

Morphological & Meteorological indicators	Reference
Building Site Coverage	(Rådberg, 1996); (Meta Berghauser Pont & Per Haupt, 2005); (Ng and Wong, 2006); (Yoshie, 2013); Ng et al., 2011); (Kubota et al., 2008)
Floor Area Ratio	(Meta Berghauser Pont & Per Haupt, 2005), (Hawkes et al., 2002); (Grimmond and Oke 1998); (Yang et al., 2010); (Razak et al., 2013); (Jiang et al., 2008); (Park et al., 2020); (Reiminger et al., 2020)
Aspect Ratio	(J. Allegrini et al., 2011); (Oke, 1988); (Santamouris, 2000); (Theurer 1999); (Adolphe, 2001); (Grimmond and Oke 1998); (Edward NG, 2009); (Bottema, 1993); (Vardoulakis et al., 2003); (Oke et al., 2017); (Di Bernardino et al., 2018)
Frontal area index	(Oke, 1988); (Grimmond and Oke, 1998); (Ng and Wong, 2005); (Ng et al., 2011); (Razak et al., 2013); (Ratti et al., 2001)
Sky View Factor	(C. Ratti et al., 2003); (Oke et al., 2017); (Miao et al., 2020); (Edward NG, 2009); (Erell, Pearlmutter and Williamson, 2011)
Average Building Heights	(Cionco and Ellefsen, 1998); (Theurer, 1999); (Hawkes et al., 2002); (Ratti et al., 2001);(Santamouris, 2000); (Golany, 1996)
Building Height Differentials	(Trache, 2001); (Ng and Wong, 2005); (Edward NG, 2009); (Chen et al., 2015); (Nosek et al., 2016), (Reiminger et al., 2020); (Zhang et al., 2019); (Hoydysh and Dabberdt, 1988); (Ming et al., 2018); (Zajic et al., 2011); (Park et al., 2020)
Green Cover Ratio (green Infrastructure)	(Baruch Givoni, 1998); (Karttunen et al., 2020); (Buccolieri et al., 2018); (Abhijith and Gokhale, 2015 & 2017); (Di Sabatino et al., 2015); (Ng and Chau, 2012); (Buccolieri et al., 2009 & 2011); (Gromke and Ruck, 2009 & 2012 & 2007); (Abhijith et al., 2017); (Huang, Li et al., 2019); (Jeanjean et al., 2016); (Ottosen and Kumar, 2020); (Kristof and Papp, 2018); (Kumar et al., 2019); (Gromke et al., 2016); (Chen et al., 2015); (McNabola et al., 2009); (Vos et al., 2013)
Building and street orientation	(Thayer Jr, 1981); (Littlefair, 2000); (Trache, 2001); (Arboit et el., 2008); (J. Allegrini et al., 2011); (Ramponi et al., 2015); (Edward NG, 2009); (Louka et al., 2000); (Yamartino and Wiegand, 1986); (Oke, 1997); (Klein and Clark, 2007); (Xie et al., 2009); (Gromke and Ruck, 2012); (Becker et al., 2002); (Niu et al., 2018); (Voordeckers et al., 2021)
Air and surface Temperature	(Erell, Pearlmutter and Williamson, 2011); (Miao et al., 2020); (He et al., 2017); (Abdulsaheb and Kumar, 2010); (Nazarian et al., 2018); (Tan et al., 2019)
Relative Humidity	(Miao et al., 2020)
Wind speed and direction	(Assimakopoulos et al., 2003); (Xiaomin et al., 2006); (Baik & Kim, 1999); (Kastner-Klein & Plate, 1999); (Chan et al., 2001); (Cionco and Ellefsen, 1998); (Santamouris, 2000); (Golany, 1996); (Theurer, 1999)

Table.09 – Essential morphological and meteorological indicators that are impacting the air pollution concentration within urban street canyons.

3.6 Conclusion

Cities now house more than half of the world's population, with urban areas expected to house 60% of the world's population by 2030. Because of the rapid growth of urban development and population, human activities have increased, and the environmental problems associated with these activities have resulted in ever-increasing emissions and air pollutants.

Cities around the world responded to this rapid urban growth by developing more buildings and majority of urbanisation taking the form of a speed-oriented urban morphology and constructing relatively tall buildings with the intention of maximising the space available by using the least amount of surface area and providing more space to vehicle traffic which led to the creation of the most iconic and dominant urban form where the street is flanked by buildings on both sides creating a canyon-like environment known as urban street canyon. The urban canyon form and geometry is the most characteristic form of modern urban settlement and is usually echoed across the urban landscape and can influence many features of urban climates, including solar radiation, shade, wind flow behaviour and velocity, surface and ambient temperature within a canyon. The study of the urban form can be carried out at several levels and scales. This can range from microscale, for example, buildings and their immediate spaces around them, i.e. plot, street and green spaces or from mesoscale, such as regions and districts and their arrangements and overall network connection of a city. Based on the aforementioned reviews, it is concluded that the Urban Canopy Layer (UCL) and the microscale are the most relevant level and scale for the study of wind and air pollution behaviour within urban street canyons. It was also established that, the term "urban canyon" can refer to a wider range of geometrical formations. The aspect ratio (H/W) is one of the morphological indicators that can be used to categorise street canyons. This is the most significant geometrical aspect of a street canyon, and depending on the geometrical configuration, a canyon might be called regular, avenue and deep canyon. These scales divided into further classification to define urban street types based on width and building heights. These are mews, residential streets, high streets, narrow high streets and boulevards which is derived from the manual for streets (2007 and 2010) guidance.

This chapter also demonstrated that specific attributes of urban form have a significant impact on the formation of undesirable microclimate, which increases the concentration of air pollution in outdoor spaces, and that urban morphological indicators are essential for urban climatic analyses. It has also determined that not all urban morphological indicators are suitable for the study of wind and air pollution behaviour within urban canyons, and

that only a few indicators that influence wind and air circulation in the city should be considered for fieldwork and computational modelling investigation. As a result, a number of essential urban morphological and meteorological indicators were identified to be used for the study of air pollution and wind behaviour in urban street canyons. These are building site coverage, floor area ratio, aspect ratio, frontal area index, sky view factor, average building heights, building height differentials, green cover ratio, building and street orientation, temperature, relative humidity, wind speed and wind direction.

This chapter identified the meteorological and morphological parameters that must be considered when studying air pollution within urban street canyon. Having said that, it is essential to use the appropriate tools and methods in studying these parameters and investigate a measure the air pollution behaviour within various canyon configurations. Therefore, the following chapter will examine three major air quality models used by UK authorities and numerous research studies to provide a deeper understanding of the benefits and limitations of such models and tools in micro-scale environmental investigation. It then identifies the gaps in knowledge that this thesis intends to fill in order to improve the output of such models.

Part 1

Air quality modelling in street canyons

Chapter 4

Chapter 4

Air quality modelling in street canyons

As mentioned in the previous chapter, high pollution concentrations have been observed in urban street canyons as a result of increased traffic emissions and reduced natural ventilation. As a result, over the last few decades, various air quality models of varying complexity have been developed to assess urban air quality and support decision-making for pollution control and mitigation strategies in order to keep air pollution levels as low as possible. For that reason, in this chapter, this thesis will examine three major air quality models, namely physical models, deterministic models, and statistical models, which are used by UK authorities and various researchers. This investigation will aid in gaining a better understanding of the advantage of using these models for air pollution assessment, as well as highlighting their shortcomings in microscale environmental investigation and identifying potential knowledge gaps that this thesis can address, and improve the output of such models.

4.1 Types of air quality models

To measure air pollution levels or pollutant trajectories in urban areas, different organizations and disciplines employ various air quality modelling techniques. Given that air pollution has a direct impact on human health and the environment, greater precision and dependability are required to meet various regulations and standards imposed by local governments and international organisations such as World Health Organization. In the United Kingdom, every local authority follows their Local Air Quality Management (LAQM), which is the statutory process for monitoring, assessing, and taking action to improve local air quality. According to these regulations and standards, air quality models and their respective computational applications must be able to satisfy the following aspects: spatial scale (meso, local, and micro scale), temporal scale indicating short-term (maximum hourly concentrations) and long-term (yearly mean concentrations) exposure, and finally, type and volume of pollution source. The classification of these models may refer to the source type (point source, line source, area source), the scale used (meso or micro scale), the input type (deterministic models or statistical models) and the pollutant sources (gases or particles).

Having said that, there are three major types of air quality models: physical, statistical, and deterministic. The latter model is classified into four types, the Gaussian model, the dense gas model, the Lagrangian and the Eulerian model. The Gaussian model has been used since the 1930s (Sutton, 1932; Bosanquet, 1936) and is regarded as the oldest and very first air quality model. The dense gas model is mostly used to simulate the dispersion of dense gas pollution plumes, whereas the Lagrangian and Eulerian models are widely used in modelling turbulent dispersion and pollutant distribution in enclosed spaces. The above-mentioned three models will be discussed in greater detail in the following sections with the aim of justifying the use of one or multiple models for this thesis.

4.2 Physical model

Depending on the purpose of the study, physical models can take the form of reduced-scale or full-scale experiments. Reduced-scale experiments, also known as laboratory experiments, are those in which the scale of the physical model is reduced proportionally for practical and cost reasons and can be performed in a wind tunnel or a water tank facility. Reduced scaled experiments, particularly the wind tunnel method, are widely used in urban studies. For example, they are used to determine wind behaviours and flow structure between buildings and within urban street canyons (Uematsu and Isyumov, 1999), or to analyse pollutant dispersion in intersections and within urban street canyons (Ahmad et al., 2005), or to assess outdoor human wind comfort, such as near and beneath high-rise buildings (Kubota et al., 2008). Full-scale experiments, on the other hand, are conducted in a real urban street canyon (field experiments) or in a replica with the original and full scale size physical model with the same measurements as the real-world context (Vardoulakis et al., 2003).

As previously stated, reduced-scale modelling can be performed in a wind tunnel or a water tank facility. In microclimate studies, urban physics, and investigations where air pollution dispersion is the primary focus, wind tunnels have been used more frequently than water tanks to simulate pollutant dispersion. In this method, data is generated by observing air movement around objects (obstacles) and injecting sulphur-hexafluoride (SF_6) smoke or dye

into the tunnel. This process will then be videoed or photographed, allowing researchers to investigate the variety of possible flow and dispersion patterns obtained for different building configurations (Brown et al., 2006; Gromke et al., 2008). Concentrations at receptor sites throughout the canyon are also calculated using special tracer dispersion monitoring devices. A benefit of this model is that it permits isolating and studying each of the phenomena involved in microscale pollutant dispersion separately, as well as enforcing scientific control by testing a hypothesis in an artificial and highly controlled laboratory setting. (e.g. Halitsky, 1963; Huber and Snyder, 1982; Li and Meroney, 1983; Saathoff et al., 1995; Saathoff et al., 1998; Leitl et al., 1997; Meroney et al., 1999; Stathopoulos et al., 2002; Stathopoulos et al., 2004).

Brown et al., (2006) used a reduced-scale model in the University of Hamburg's controlled wind tunnel facility to show vertical profiles of wind speed for several realistic (Oklahoma City Central Business District) and idealised multi-building array configurations (Fig.46). According to their findings, the wind tunnel cannot simulate sudden changes in wind velocity or wind direction over a short distance (windshear) with a resolution that is useful or interpretable without the use of other models. As a result, when studying dispersion rate from tall buildings in a wind tunnel, this disadvantage will have a significant impact on the outcome and a full-scale experiment or a computational model is required to supplement and validate the study.
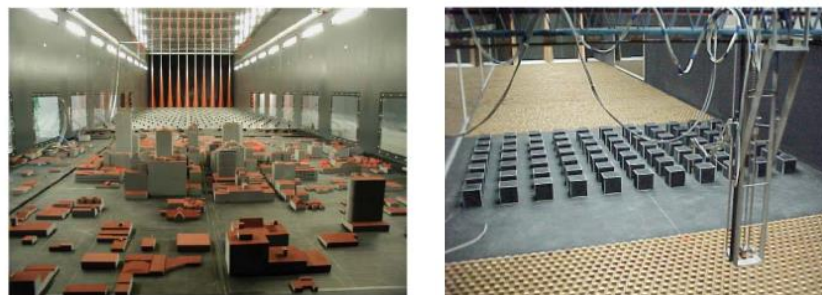
Fig.46 – Figure on the left showing the model of the Oklahoma City in wind tunnel and figure on the right showing idealised 7x11 cubical multi-building array configurations (Brown et al., 2006).

Sharma, Chaudhry and Chalapati Rao (2004) used a similar method in another study to investigate the complex vehicular pollution dispersion phenomena under various urban

environmental conditions for Indian traffic and climatic conditions. Although the findings of the study provided some insight into wind flow structure and air pollution dispersion in various urban settings, it was clear that wind tunnels are extremely difficult to operate at low wind speeds because wind tunnels are designed to operate efficiently at maximum speeds. Furthermore, measuring wind flow at those low speeds is difficult with standard instruments, necessitating more sensitive and costly instruments. As a result, to reduce errors, it is required to combine this model with fieldwork (full-scale experiments) and computational and statistical models. Gousseau et al. (2011), for example, calibrated and verified the output of a wind tunnel experiment with a high resolution CFD model (Fig.47). In addition to these drawbacks, the physical model has a size limitation, and in order to simulate large urban areas, everything must be scaled down, which changes the aerodynamic properties of the objects and the spaces between them. Moreover, wind tunnel walls have an effect on flow that must be taken into account during post-assessment calibration (Brown et al., 2006).
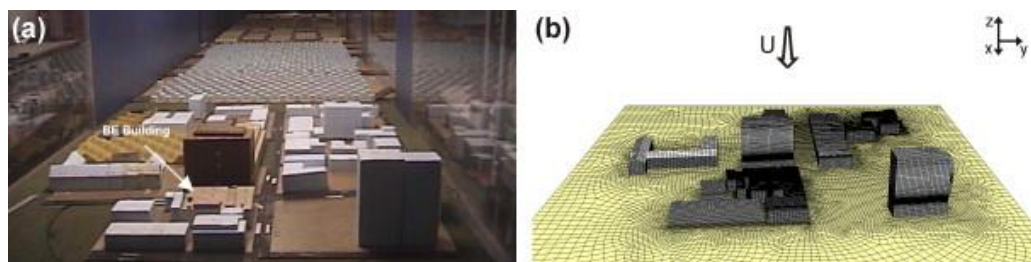
Fig.47 - Study of near field gas dispersion in downtown Montreal (a) physical wind-tunnel model (b) corresponding computational model (Gousseau et al., 2011).

In contrast to reduced-scale experiments, full-scale experiments are carried out in a real and existing context or under made-up look-alike conditions. These methods accurately depict urban conditions as well as the true complexity of the problem under investigation. This real complexity cannot be fully represented by wind tunnel measurements, statistical or computational models. As a result, field experiments (full scale experiments) are incredibly useful and, in many cases, required for validating or calibrating other models, such as reduced scale experiments and computational models, if conducted with great care and for a sufficiently long measurement period (Williams and Wardlaw, 1992; (Visser and Cleijne, 1994; Blocken and Persoon, 2009; Yoshie et al., 2007; Blocken et al, 2012).

When conducting a full scale physical model experiment, there are numerous measurement techniques which can be employed. DePaul and Sheih (1985, 1986), for example, conducted a full-scale experiment with tracer gas in an urban street canyon in Chicago (USA) to measure pollutant retention times and concentration levels. The mean wind speeds were calculated by analysing the trajectories of air balloons released into the street.

Nakamura and Oke (1988) investigated the climate of urban canyons in another study by collecting full-scale wind and temperature data from a real street canyon in Kyoto (Japan). These observations were used to create simple algorithms that relate the meteorological conditions above the roof (UBL, Urban Boundary Layer) to the meteorological conditions within the canyon (UCL, Urban Canopy Layer). The findings were used to develop an empirical expression for the relationship between pollutant concentrations inside and above the canyon's roof top. In another study, Chan and Kwok (2000) measured PM_{10} and $PM_{2.5}$ concentrations in two full-scale open streets and two full-scale canyon sites in Hong Kong. These measurements revealed that the street's aspect ratio and the prevailing wind direction influenced particulate matter dispersion and it showed that the PM_{10} levels decreased exponentially with buildings height. It should be noted that the accuracy of the above study's output is dependent on the accuracy and resolution of the data collected by measuring devices.

Recent studies with higher spatial and temporal resolution provided even more details on the investigated problem and allowed for more convenient and accurate study of microclimate within urban spaces. Glover (2015), for example, investigated the impact of trees on wind behaviour within symmetrical urban canyons using full-scale experiments (field measurements) and a CFD to gain a better understanding of wind flow structure and change patterns. The study used portable air quality monitoring devices to measure pollution levels in both non-tree-lined and tree-lined streets, and the results were compared with computational models to identify the configuration of an idealised urban geometry that minimises pollution concentration. Glover's study agrees with the Buccolieri et al., 2022; Xing et al., 2019; Jeanjean et al., 2017; Gallagher et al., 2015; Vos et al., 2013 in that

the addition of trees in street canyons can reduce the natural ventilation that occurs within street canyons, potentially resulting in the accumulation of pollutants.

It is worth noting that, unlike reduced scale experiments, where environmental parameters can be enforced in a quicker and shorter time to test multiple hypotheses, full scale experiments can take a year to complete because they are in a real-world context and the various parameters must be measured in different seasons to capture and measure the effect of seasonality changes on air pollution concentration. Therefore, if the research time frame allows, it is highly recommended to account for seasonality effects. Needless to say, that collecting more data in different environmental conditions will provide more knowledge and understanding of confounding variables and can be used to narrow down the causes and effects and avoid generalising phenomena.

Another advantage of full scale experiments over reduced scale experiments is that the results can be interpreted using real data rather than assumptions. Furthermore, unlike in a wind tunnel experiment, the geometries are in their actual size and with their details, whereas in a wind tunnel, the details are often not reproduced in the physical model and the geometrical forms are only equivalent to real-world conditions, which may result in distorted physical models that significantly affect the overall similarity between prototype and real-world conditions. Having said that, it is critical that the devices used to measure environmental parameters are co-located and calibrated next to a maintained reference station before and after investigation and each measurement cycle.

Field measurements, as previously stated, are point in time measurements, and for that reason, short field measurements provide a limited picture of the problem under study. Moreover, field tests can only be conducted on existing sites, therefore, it is impossible to make a prior assessment of a new urban development. This motivates the use of additional computational models.

The advantage of using computational models is that they can be calibrated/verified based on field measurements and then used to provide information beyond the point

measurements made in the field. Furthermore, computational models can provide results of flow features and pollution concentration at every point in space simultaneously, and they are significantly less expensive than fieldwork and wind tunnel experiments. They also offer repeatability which strictly does not occur in reality and fieldwork experiment due to largely uncontrolled (meteorological) conditions. This is another shortfall of full-scale experiments which can be addressed and complimented by further computational model. These issues have been discussed and demonstrated in detail by Schatzmann et al. (1997) and by Schatzmann and Leitl (2011). In light of the preceding understanding, deterministic and computational models will be discussed in detail in the following section to provide a better understanding of their benefits in assessing microclimate and air pollution concentrations in urban settings.

4.3 Deterministic model

Deterministic air pollution models are based on chemical and/or physical relations between the atmosphere and the pollutant concentration, and the output of the model is determined through the initial condition and parameter values. These models only require the average state of the atmosphere and a detailed output is calculated through mathematical equation (Randall, 2006; Jerrett et al., 2005; Lateb et al., 2016). It should also be noted that deterministic models, which are fed with emissions and meteorological data, can be used to predict concentrations at specific locations on a computational grid (Jimenez et al, 2003). Gaussian, Lagrangian, and Eulerian models are the most commonly used deterministic models. All of which are capable to estimate the downwind ambient concentration of air pollutants from various sources. As a result, the following section of this thesis gives a brief overview of each model and highlights the model that is a better fit for this thesis study.

4.3.1 Gaussian model

The greatest advantage of Gaussian Plume models is that they have an extremely fast, almost immediate response time and can be used to calculate pollution from multiple source types i.e. point source (pollution from smokestacks, discharge pipes, etc), volume source (pollution from uncovered gravel piles, sand piles, coal piles, etc) and area source (field burning, home heating, demolition site, etc). Their calculation is based solely on

resolving of a single equation for each receptor point, and the bulk of the computational cost associated with the model is taken up by the pre-processing of meteorological data and the parameterisation of turbulence. Depending on the level of complexity of these sub-modules, the runtime of the model can be drastically cut down, which paves the way for its application in real-time investigation and decision making, which is typically done for regulatory purposes.

The Gaussian model, which has been used in numerous studies since 1936 (Bosanquet and Pearson, 1936), is regarded to be the earliest air pollution dispersion model when high performance computers had an unreachable price for environmental protection organisations and authorities. This model, generally is used in large scale applications (Benson, 1984; Owen et al., 2000), as the plume models are calculated with steady state approximations and they do not take into account the time required for the pollutant to move from the source to the receptor. The atmospheric conditions are considered to remain constant during the dispersion from source to receptor, which is virtually instantaneous, and that is why the Gaussian dispersion formulas do not depend on time. The AERMOD (American Meteorological Society/Environmental Protection Agency Regulatory Model) and ADMS-Urban (Atmospheric Dispersion Modelling System), which is the second generation of urban-scale dispersion model that includes a street canyon module nested within the core Gaussian code, are two examples of Gaussian dispersion models. This application, developed by Cambridge Environmental Research Consultants in the United Kingdom, allows for rapid assessment over large areas, such as a few hundred metres or a few kilometres (Williams and Barrowcliffe, 2011) (Fig.48), making it an excellent choice for assessing and forecasting current and future air pollution levels within meso scale and large urban areas such as cities and towns (Vijay et al., 2021; Madiraju and Kumar, 2022; Di Sabatino et al., 2008).
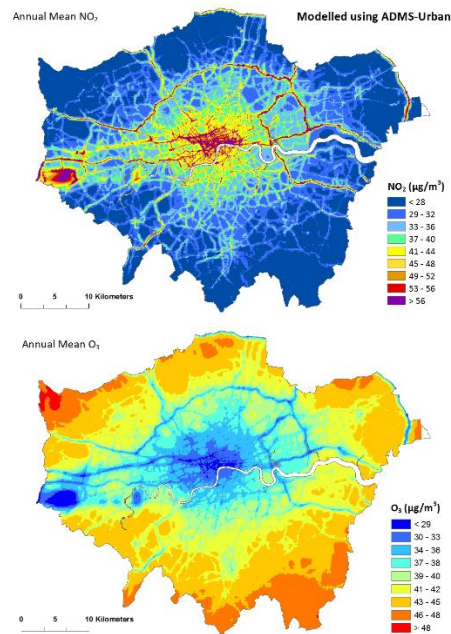
Fig.48 - Contour plot of London showing the annual average NO_2 and O_3 concentrations predicted by ADMS-Urban (Cambridge Environmental Research, 2006).

Over 80 local authorities in the United Kingdom are currently using ADMS to analyse and assess air quality levels as part of the LAQM (Local Air Quality Management) programme, as well as to develop air pollution remedial strategies and action plans. Additional toolkits such as Emissions Inventory Toolkit (EIT) (DEFRA, 2021) can be used in conjunction with ADMS to assess the effect of newly legislated emission reduction plans, i.e., Clean Air Zone (CAZ) and Ultra Low Emission Zones (ULEZ) on emissions (Fig.49). While the use of ADMS and especially its Road version is on the rise in the UK, as it was mentioned recent studies highlighted limitations of this programme that the ADMS tends to under-predict NOx concentrations within micro scale dispersion and under low wind conditions. Another shortfall is that within complex urban morphology where the microclimate of the given site is constantly influenced by building configurations, the application has some difficulty in simulating dispersion at pedestrian level (Williams and Barrowcliffe, 2011). Because of these mentioned shortfalls, the use of ADMS to model hyperlocal concentrations considered as not viable and it is not recommended to employ the above model for micro scale investigations.
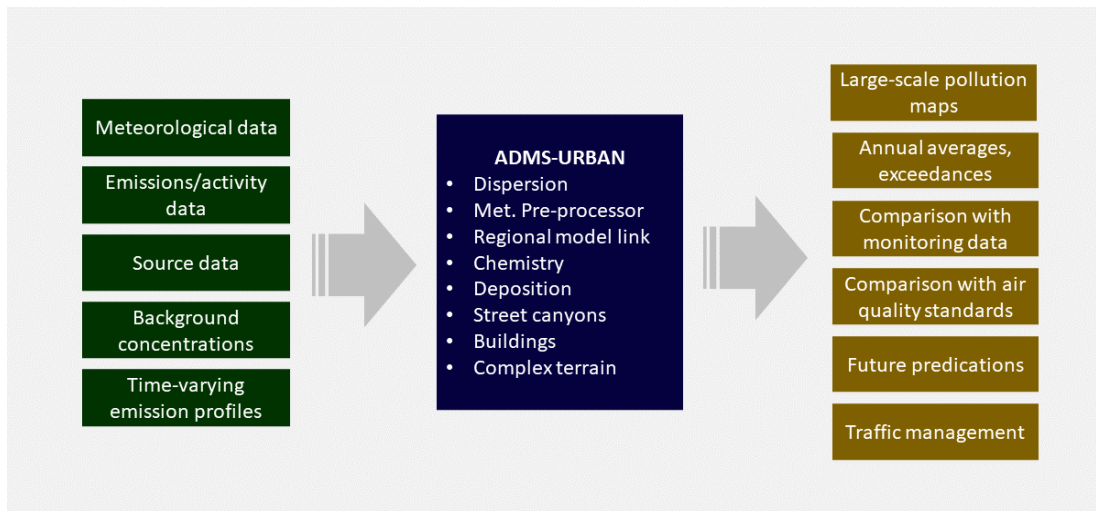
Fig.49 - This diagram shows some possible inputs to and outputs from the model, and some of the available modelling options. (Adopted from ADMS website)

4.3.2 Lagrangian model

Lagrangian model work well both for simplified and stable conditions over the flat terrain (Tsuang, 2003) and unstable conditions for the complex terrain (Jung, Park and Park, 2003). The Lagrangian model mathematically tracks pollution plume particles and uses actual turbulent velocity, wind, and arbitrary turbulent velocity to determine air pollution dispersion by computing statistics of a large number of pollution plume particle trajectories. The Lagrangian model is a good alternative with higher accuracy in situations where the Gaussian models are expected to perform poorly. Unlike Gaussian dispersion models, the Lagrangian model uses time-dependent simulation and are more physically valid than Gaussian models (Hanna and Britter, 2010). Lagrangian models are more physically valid than Gaussian models, which do not incorporate wind shear or inhomogeneity of the turbulence field, which makes this dispersion model a powerful tool for modelling atmospheric transport (Lin et al. 2012). Lagrangian models have minimal numerical diffusion and are able to analyse particle movement within microscale and match the resolution of the outcome with the resolution of the meteorological model grid.

The most significant drawback of Lagrangian models is their computation time requirements which are considerably higher than any other Gaussian and Eulerian models. They usually suffer for computational calculation, and they cannot be used for real time applications. The

Lagrangian model calculates the concentration of particles by averaging of particle residence time over a volume of space. In this process, tens of thousands of particles released in the space may not pass the target point; therefore, a greater number of particles might be required to predict (with reasonable accuracy) the concentration. In addition to this, if the volume area increased, the calculation of concentration will represent an average over a larger volume and will be less representative of the target point (Jeanjean et al., 2015; Nehrkorn et al. 2010; Brioude et al. 2012). CFD application such as OpenFOAM (Open Field Operation and Manipulation) which is an open-source software platform (freely available at http://www.openfoam.com) using the same dispersion model. The discrepancy between Jeanjean's work (2015) and their 2017 investigation (Jeanjean et al., 2017) is a good illustration of the limitations of the Lagrangian model. In their earlier study, they stated that trees reduce concentrations of road traffic emissions by 7 percent at pedestrian height. However, in their 2017 study, they found that trees actually increase pollution at pedestrian height. One reason for this variation was the difference in scale between the two studies, but the main reason was the inherent difficulty of the OpenFOAM in representing pollutants that are not directly released and assigning values to 'background' pollutants. It is therefore important to investigate this discrepancy further by other methods and computational software. The more accurate and finer-scale grids applications are the ones which are using more sophisticated and flexible models such as Eulerian which will be discussed in the next section.

4.3.3 Eulerian model

The Eulerian model is time-dependent, like the Lagrangian model, and can compute a huge number of air plume particles as they emerge from their initial source. The main distinction between the Lagrangian and Eulerian models is that the Lagrangian model moves the Cartesian grid with the plume movement, whereas the Eulerian model employs a fixed three-dimensional grid to show plume movement. As a result, 'nesting' and covering a larger horizontal geographic scale without employing too many grid cells is significantly easier and accordingly faster in producing outputs. This allows the model borders to be extended out from the research subject/s without wasting too many calculation cells, allowing the

simulation time to be reduced and making it more suitable for 'multi-pollutant' simulations (Vallero, 2021).

Furthermore, in recent years, authoritative organisations such as DEFRA (Department for Environment, Food and Rural Affairs) have shown a strong preference for using the Eulerian multi-scale, multi-pollutant model framework in their air quality modelling projects/plans, as this will allow Defra to quantify the influence of different policy scenarios on a variety of pollutants with a single high-resolution model run (Williams and Barrowcliffe, 2011).

The Eulerian model is widely used in various CFD dispersion applications by using flexible fine-scale grids which means it can compute complex-shaped geometry and other boundary conditions in a shorter time as compared to Lagrangian model (Davim, 2017). Some of the popular CFD applications which use the above model are ANSYS Fluent and ENVI-met, both of which using RANS equation as their turbulence modelling approach (Moonen et al., 2012). Both tools have been rigorously tested and validated against field measurement data in many experiments (e.g., Allegrini, Dorer and Carmeliet, 2015; Bruse & Fleer, 1998; Krüger et al., 2011; Toparlar et al., 2017).

ANSYS Fluent is developed to predict air flow (laminar and turbulent flow), extended with energy balance, radiation and evaporation module (Taleghani, 2014) and has been used in many urban outdoor studies (e.g., Blocken et al., 2008; Buccolieri et al., 2015; Toparlar et al., 2017). Apart from urban outdoor and climate studies ANSYS Fluent has a wide range of commercial use, such as aircraft, machine combustion, semiconductor, indoor air quality, etc. This is because ANSYS Fluent solvers are based on the Finite Volume Method (FVM) which enables this application to generate urban features and objects with high details and often curve line if needed. For that reason, the modelling with ANSYS Fluent is very precise, hence the computational time takes much longer than CFD applications which uses Finite Difference Method (FDM) like ENVI-met.

In contrast to the ANSYS Fluent, ENVI-met uses Finite Difference Method, also known as FDM, to solve the numerous partial differential equations in the model. ENVI-met is able to

use relatively large time steps while still maintaining its numerical stability because the atmospheric advection and diffusion equations are implemented in a fully implicit scheme (ENVI-met, 2020). But that also means modelling in ENVI-met will be limited to straight lines (2D) and cubes in three dimensional mode. This reduces computing costs and allows the ENVI-met model to run on any standard computer with less complication.

Another advantage of ENVI-met application is that every single pixel in the model site can be modified, and its impact can be calculated in understanding their effect on microclimate and specially air pollution dispersion or concentration. Although both applications allow for the creation and simulation of vegetations, ENVI-met allows for the modification of greenery properties down to the detail of leaves, allowing researchers to investigate the impact of foliage interaction on microclimate by calculating the interaction of leaf surface with respect to the actual meteorological, pollutants and plant physiological conditions for each grid box of the plant canopy. This includes calculating the wet and dry deposition of pollution on leaves, as well as the impact on wind behaviour around and near vegetation. Numerous ANSYS Fluent studies either did not account for vegetation or had to simplify the geometry and properties of greenery. This is because it increases cost and simulation time, and due to computational resource and meshing constraints, only tree canopies were created in the Ansys Fluent model, while tree trunks and leaf details had to be ignored (Fig.50) (Glover 2015; Wen, 2017).

In terms of pollutants, ENVI-met outperforms any other commercial CFD simulation application, as its pollutant dispersion model allows for the synchronous release, deposition and dispersion of up to six different pollutants, including reactive gases, passive gases and particles. Moreover, sedimentation and deposition at surfaces and vegetation, as well as the photochemical reaction between NO_2, NO and Ozone, are all taken into account. Furthermore, during the simulation process, background pollution can be added to provide a much more accurate representation of real-world conditions.
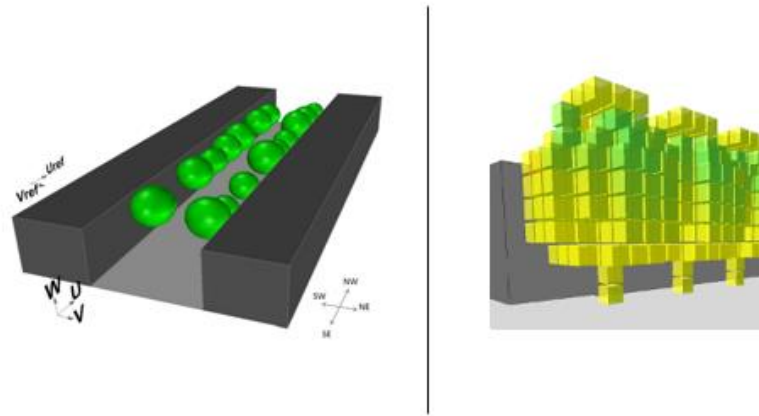
Fig.50 – Tree 3D plan geometry and foliage representation in Ansys Fluent (right) (Glover, 2015) and ENVI-met (Left).

Table 10 summarises the technical comparison of ENVI-met and ANSYS Fluent based on the literature review (Albdour and Baranyai, 2019; Ansys, 2020; Bruse, 2014; Naboni et al., 2017) and the author's experience of working with the tools.

Criteria	ENVI-met	ANSYS Fluent
License cost	Low	Very high
Computational cost	High	Very high
Reliability & Accuracy	High	High
User interface	User friendly	Extremely Complex
Fluid flow	Yes	Yes
Turbulence	Yes	Yes
Solar load model	Yes	Yes
Heat transfer	Yes	Yes
Radiation	Yes	Yes
Convection	Yes	Yes
Pollutant dispersion	Yes	Yes
Evapotranspiration	Yes	Yes
Air temperature	Yes	Yes
Wind velocity	Yes	Yes
Wind Direction	Yes	Yes
Relative humidity	Yes	Yes
MRT	Yes	Yes
CO_2	Yes	Yes
Air pollutants ($PM_{2.5}$, PM_{10}, NO_2, NO, O_3, user defined)	Yes	Limited
Plant library (catalogue)	Yes	No
Background air pollution	Yes	No

Pollution level calculation based on traffic count	Yes	No
Surface temperature	Yes	Yes
Shading effect	Yes	Yes
Solar heat flux	Yes	Yes
Turbulent kinetic energy	Yes	Yes
Heat Sinks	Yes	Yes
Comfort Prediction Index (PET, SET, UTCI, PDD)	Yes	No
Sky-view Factor	Yes	Yes
Natural ventilation	Outdoor	Indoor & Outdoor
Building geometry	Limited	Yes
Street orientation	Yes	Yes
Urban aspect ratio	Yes	Yes
Building arrangement	Yes	Yes
Building envelope	Yes	Yes
Building Roof Shape	Limited	Yes
Green Roofs	Comprehensive	Limited
Green Walls	Comprehensive	Limited
Streets Canyon Geometry	Yes	Yes
Materials and Albedo	Yes	Yes
Green blue infrastructures (e.g., park, waterbody)	Yes	Yes
Site topography	Yes	Yes

Table.10 – Detailed comparison between ENVI-met and Ansys Fluent CFD software. The green highlighted labels represent the advantages of one software over another.

Based on the above studies and presented table, it can be concluded that ENVI-met is capable of analysing micro scale interactions between urban form and microclimate. With a fine resolution between half a metre and 10 metres, a typical time frame of 24-48 hours, and a time step of 1-5 seconds, the model can simulate complex scenarios and graphically display the interactions between solid and porous barriers at varying levels and resolutions. In view of the above evaluation and comparison, and due to its proven reliable outcomes examined by previous researchers (Berardi and Wang, 2016; Jin et al., 2017; Peter E.J Vos, 2013; Tsoka, 2017; Bruse, 2012; Wang et al., 2005), the ENVI-met application is recommended for microclimate studies with focus on vegetation and multiple pollutants sources like this thesis study.

4.4 Statistical model and correlation analysis

The statistical models are seldom as detailed as the deterministic models but can be more efficient and are still able to address very important research questions. In general, statistical models are methods that are based on statistical data analysis of previously recorded ambient pollution concentrations. These models use less input and are more straightforward than deterministic models. They don't establish or simulate a cause-and-effect, physical relationship between emissions and ambient concentrations in the same way as deterministic models (Daly and Zannetti, 2007).

There are several approaches and techniques developed based on this model to analyse and measure ambient air pollution concentration. Out of which, two types are being used more than the others. The empirical model is mostly used for practical applications. One of the good examples of this model is the box model (Lyons et al., 2003; Sportisse, 2001). Another popular statistic model is regression-based models, particularly linear models.

Regression analysis is a basic technique in air pollution forecasting and investigates relationships between variables. In this model, gathered datasets are used as input of the regression model to predict continues valued output. For example, extracted data from web traffic monitoring will enable us to create a model that reasonably correlates traffic congestion with air pollution. The accuracy and reliability of the regression model output ultimately depend on validity and resolution of the input dataset. These models have been used to predict air pollution trends a few hours in advance for the purpose of alerting urban residents and to propose mitigation strategies to reduce or control the air pollution levels, for example, diverting vehicle traffic or closing down schools etc (Aarthi et al., 2020; Aditya et al., 2018; McKendry, 2002; Zhang et al., 2015; Gardner and Dorling, 2000).

Apart from prediction of air pollution, another common use of linear regression is for co-location exercise. According to the Local Air Quality Management Technical Guidance (DEFRA, 2018) air quality devices, whether portable, fixed or nitrogen dioxide diffusion tubes, should be verified and if needed calibrated by co-locating them with an automatic monitor.

Based on DEFRA's air quality assessment, it is a requirement to co-locate a non-reference monitor, under real-world conditions for a defined evaluation period alongside a reference monitor. This will minimise the uncertainty associated with air quality devices and any adjustment factor can be identified prior to the start of the project. In this process both data collected from the device and from the monitoring station are compared using a linear regression model and analysis to demonstrate the close relationship between the portable, fixed, or nitrogen dioxide diffusion tubes and reference air quality station; any adjustment for future measurements is explained by the linear regression equation i.e. Y=mx+b (Department for Environment Food and Rural Affairs, 2018; Williams et al., 2014; Hongyong Li, 2020). In the study carried out by A. Ripoll et. al (2019), a number of air quality O_3 sensors are compared against referenced air quality station with the aim of validating the portable sensors as well as to suggest further adjustment to calibrate the sensors. Fig.51 indicate the data collected by the portable O_3 sensor and reference air quality station plotted on a linear regression model.
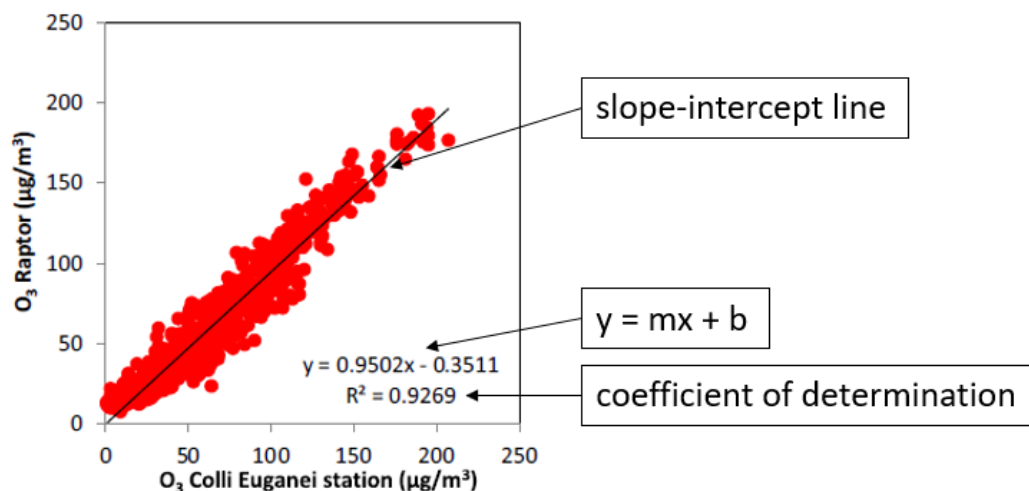
Fig.51 - Scatter plots of the ozone sensors raw data vs. ozone reference concentrations.

In a number of studies (Li et al., 2020; Oxford City Council, 2021; Chatzidiakou et al., 2019; Nowack et al., 2020) both portable device and monitoring station data were compared using a linear model and linear regression analysis, and the correlation of determination (R^2) and correlation coefficient were calculated to demonstrate the close relationship between the

portable air quality device and the reference air quality station. The R-squared (R^2) coefficient of determination measures how close the data are to the slope-intercept line.

The correlation coefficient (r) is also supplied to help comprehend the best fit of the data and to show how closely the points in a scatter plot are related to a linear regression line. The R-squared is a statistical measure that shows how much of a dependent variable's variance is explained by independent variables in a regression model. It also shows how much the variance of one variable explains the variance of the second variable.

The correlation coefficient (r), on the other hand, expresses the strength of the association between an independent and dependent variable. It has a range of values between +1 and -1, with +1 signifying perfect positive correlation and -1 denoting perfect negative correlation. Any adjustment factor for future measurements is explained by the linear regression equation (Y=mx+b), where 'Y' represents the dependent variables and 'm' represents the slope, the independent variables are denoted by 'x' (extracted from the reference station), and the Y-intercept is denoted by 'b'. This equation provides a statistically sound method for comparing sensor data to reference data. Moreover it will make it possible to take the portable device away from the reference location and still extract data which represent true values to reference station values (AQMesh, 2019). This can be done by using the value from (slope) and b (intercept) which were computed during the co-location exercise and apply these to the new sensor data and adjust the second data to be close to reference data. Therefore, the equation becomes:

$$Adjusted\ sensor\ concentration = \frac{Measured\ sensor\ concentration - b}{m}$$

It is important to take into account the R2 value as the farther R2 is from 1 the less useful this adjustment will be (DEFRA, 2021; Kalenderski, 2009; Conner et al., 2018). As part of the co-location exercise, it is important to check the accuracy, bias and precision of the devices (Fig.52). The accuracy is how close a measured value is to the actual reference (true) value. Bias is a systematic (built-in) error which makes all measurements wrong by a certain amount either higher or lower than the true reference value. In other words, this is the

intercept value in the slope-intercept equation y=mx+b. Precision is how close the measured values are to each other and being able to consistently predict the same concentration (Fig.53).
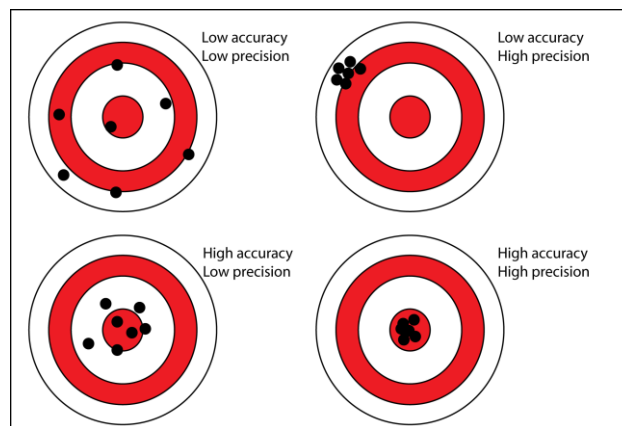
Fig.52 - Picture showing the most accepted definitions of accuracy and precision.
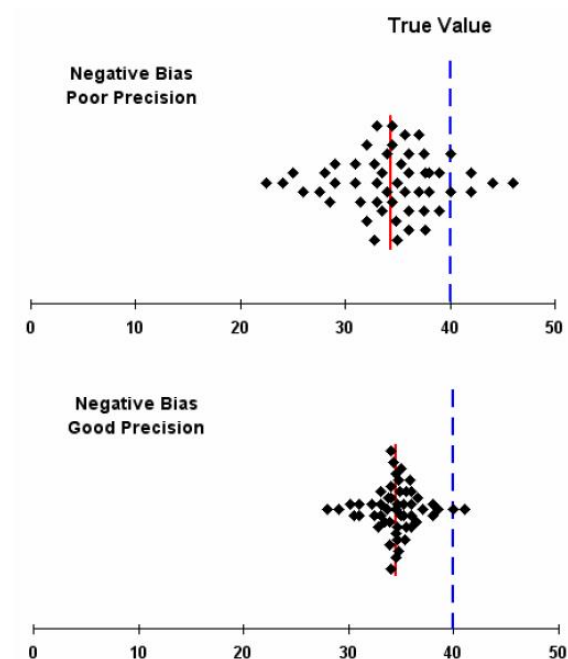
Fig.53 - Accuracy is the degree of veracity (truth) while precision is the degree of reproducibility.

In the figure (above) both sets of results have the same calculated negative bias, shown by the vertical red line, compared with the true value. However, those in the top part of the

figure have poor precision, whereas those in the lower part have good precision (DEFRA, 2021b). In the UK, statistical evaluation of the meteorological and air pollution data used for the UK-AQF (UK-Air Quality Forecast) is achieved by comparing the modelled or forecast meteorological and pollutant parameters to the UK ground-based meteorological and air quality station observations of ambient temperature, wind speed, wind direction and six major air pollutants via Pearson and scatter plots (Lingard et al., 2013).

The Pearson correlation coefficient is capable to summarise the strength and direction (negative or positive) of relationships between variables. Statistical significance was defined as $p \leq 0.05$ to identify associations between various method of measurement. This can be between the portable device and the reference station or between real-word measurements and computational model measurements. This is to ascertain if any adjustments are necessary to calibrate the computational simulation values and improve its accuracy while also matching its outputs to real-world measurements. Table 11 explains the strength of association according to Raithel (2008). Depending on whether the relationship is positive or negative, the Pearson correlation coefficient, r, will be closer to +1 or -1. A value of +1 or -1 indicates that all data points are on the line of best fit.

Strength of association, according to Cohen (1988,1992)	Coefficient, r
A perfect positive relationship	0.5 to 1.0
A fairly strong positive relationship	0.3 to 0.5
A moderate positive relationship	0.1 to 0.3
No relationship /Equal to 0	0
A moderate negative relationship	-0.1 to -0.3
A fairly strong negative relationship	-0.3 to -0.5
A perfect negative relationship	-0.5 to -1.0

Table.11 - Interpretation of the correlation coefficient and strength of association according to Raithel (2008).

It is worth noting that, in establishing a relationship between two methods of measurement, a small p-value, in addition to the strength of the Pearson correlation coefficient, is an important factor (0.05 or less). P-values are determined as part of a statistical test procedure to determine whether the results are significant as an indicator of whether or not the variables are correlated. The null hypothesis is rejected if there is strong evidence for it,

and an alternative hypothesis must be considered. The p-values, as well as the significance levels associated with them, are listed in Table 12 (Bühl 2012).

Significance level		Specification
P>0.05		Not significant
P≤0.05	(5%)	Significant
P≤0.01	(1%)	Very significant
P≤0.001	(0.1%)	Highly significant

Table.12 - P-values and the related significance levels

4.5 Conclusion

To meet a variety of requirements, various organisations and disciplines employ a range of air quality modelling techniques to measure and assess a variety of pollutants at various spatial scales ranging from meso to micro scale. Based on the preceding literature review, it was determined that there are three major types of air quality models used in environmental studies conducted within the urban canopy layer (micro-scale), namely physical, deterministic, and statistical models. Each has advantages and disadvantages and provides outputs that can aid in the investigation of air quality and microclimatic issues.

Combining outputs from various air pollution models is a common practice that can reduce errors and compensate for the shortcomings of each model. For example, the advantage of a full scale physical model experiment, is that it is carried out in a real and existing context, accurately depicting urban conditions as well as the true complexity of the problem under investigation. However, field measurements can only be conducted on existing sites, therefore, making a prior assessment of new urban developments is impossible. This motivates the use of additional computational models. The advantage of using computational models is that it can be calibrated/verified based on field measurements and then used to provide information beyond the point measurements made in the field. In the case of deterministic models, authoritative organisations such as DEFRA (Department for Environment, Food, and Rural Affairs) have shown a strong preference in recent years for using more sophisticated and flexible models such as Eulerian models, which is a multi-scale,

multi-pollutant model framework that can offer a way to quantify the influence of different policy scenarios on a variety of pollutants with a single high-resolution model run. In this regard, a number of deterministic models were reviewed, and it was discovered that Ansys fluent, a CFD simulation software used by previous researchers, has limitation in the calculation of vegetation and multiple pollutants. ENVI-met, on the other hand, allows researchers to investigate the impact of foliage interaction on microclimate by calculating the interaction of leaf surface with respect to the actual meteorological, pollutants, and plant physiological conditions for each grid box of the plant canopy.

It was also discovered that statistical models can often be used to supplement deterministic and full scale experiments when scientific understanding of physical and chemical processes is lacking. Although statistical models are not as detailed as deterministic models, they can be more efficient and still address important research questions. It is common practise to combine and complement linear regression models with additional statistical and correlation analysis, such as Pearson correlation analysis, which can summarise the strength and direction (negative or positive) of relationships between variables to produce probabilistic forecasts and explicitly account for uncertainty in general, which is an additional desirable feature of such model.

Fig.54 depicts a summary of the recommendations based on the above literature review, as well as models that should be considered for micro scale environmental and air quality investigation in particular urban street canyon, which is also the focus of this thesis.
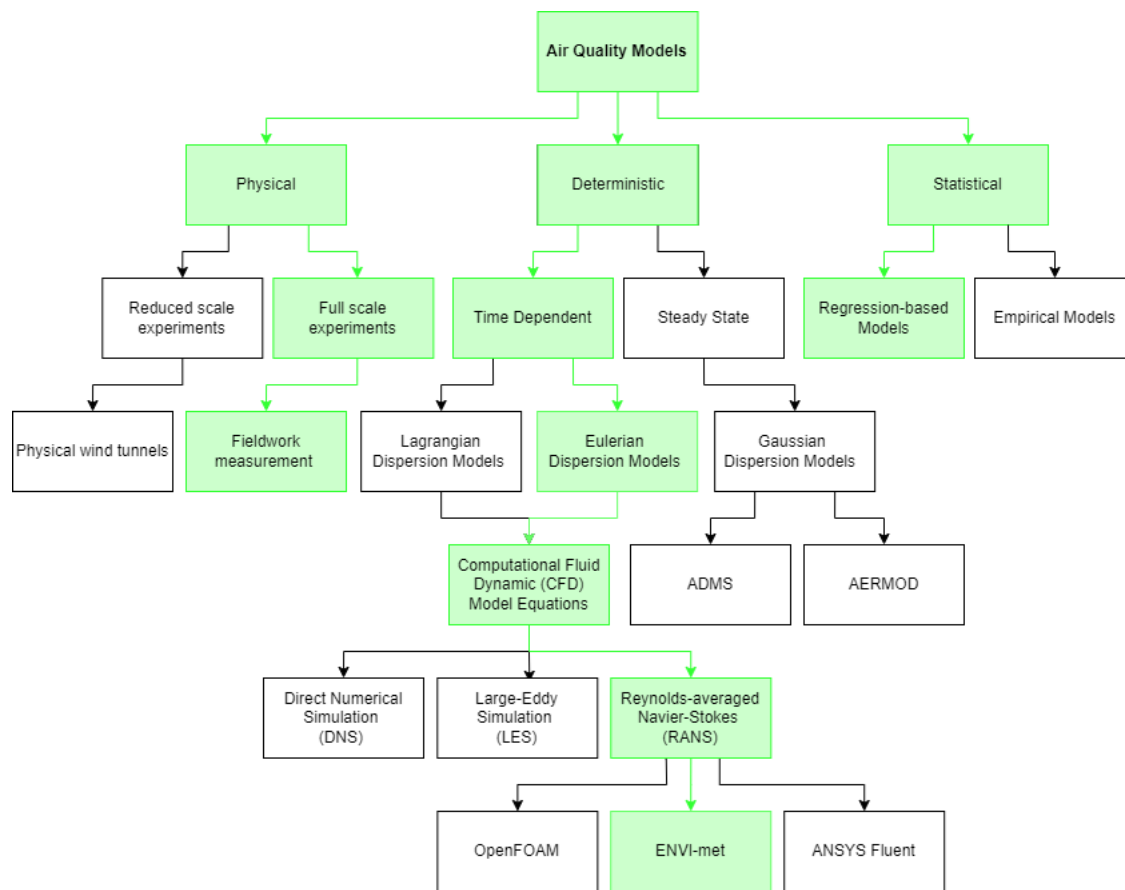
Fig.54 – Types of air quality models, the light green boxes are the models and methods which should be considered further for micro scale environmental and air quality investigation.

Part 2

Fieldwork & calibration study

Chapter 5

Chapter 5

Fieldwork and calibration study

This chapter summarises the methodology and findings of the full-scale experiment (fieldwork study) that were used to calibrate the computational modelling software (ENVI-met) outputs. The purpose of this fieldwork study was first to identify any limitations or discrepancies between the computational model outputs and fieldwork spot measurements and then apply any adjustments to calibrate the computational model to represent real-world measurements. Second, the fieldwork study offered an opportunity for a deeper understanding of pollution dispersion within various urban street canyon types, as well as the real-time measurement of microclimate parameters such as wind behaviour and flow structure between buildings. The rationale for the fieldwork and calibration exercise was that many studies used computational modellings such as ENVI-met in isolation and either ignored fieldwork measurement (Maerschalck & Janssen, 2010; Rui et al., 2019; Arapakis, 2019; Sharmin and Steemers, 2017; Chatzinikolaou et al., 2017; Tsoka, Tsikaloudaki and Theodosiou, 2017; Gaspari and Fabbri, 2017; Wania et al., 2012) or used fieldwork measurement to only compare and validate the software rather than providing a formula for adjusting and calibrating the output of the computational model (Bande and Manandhar, 2019; (Bande et al., 2019; Tumini, 2015; Glover, 2015). The calibration of computational models is critical for their effectiveness as a tool for assessing and accurately predicting air pollution concentrations and other microclimate parameters within the urban environment. Due to the nature of the study and the assumption of a linear relationship, the Pearson correlation coefficient was chosen to summarise the strength and direction (negative or positive) of relationships between variables. Statistical significance was defined as $p \leq 0.05$ to identify associations between fieldwork spot measurement and ENVI-met modelling output values. The knowledge from this chapter informs the steps that must be taken to model and calibrate the ENVI-met outputs and allow the study to model and simulate idealised and future scenarios across a variety of urban settings in various seasons while ensuring that the results are reliable and accurate predictions of real-world scenarios.

5.1 Methodology of the fieldwork

To ensure that the fieldwork study's findings are more broadly applicable, the study was conducted on a typical London urban block, which largely represents the configurations, conditions, and characteristics of many existing built environments throughout the inner part of London and many other large European city centres with high, medium, and low densities. When choosing a location for the fieldwork study, care was taken to choose a location with a variety of aspect ratios and sky view factors to represent the five urban street canyon classifications which was derived from Manual for Street (2007 & 2010) and highlighted in Chapter 3 namely mews, residential streets, high streets, narrow high streets, and boulevards (Davis and Huxford, 2007; Young et al., 2010). Another criterion for choosing these locations was varying levels of vegetation volume and vehicle traffic flow, all of which have the potential to influence air pollution levels. As a result, the area around Regent's Place Plaza, known as 'Triton Square', was chosen as it contains a variety of building typologies ranging from mid-rise to high-rise and fine to coarse grain. More importantly, according to a number of reports published pre and during COVID-19 indicates that Marylebone Road and Euston Road are the two most polluted roads in London (DEFRA, 2015; Camden Council, 2017 and 2021). Moreover, apart from being partially within the Congestion Charge zone, a portion of the site is also within Ultra Low Emission Zone (ULEZ), which came into effect in April 2019 and replaced the less stringent T-charge. The combination of the above factors made the Regent's Place neighbourhood the ideal location to conduct the fieldwork study. The location of the fieldwork study is depicted in Figure 55.
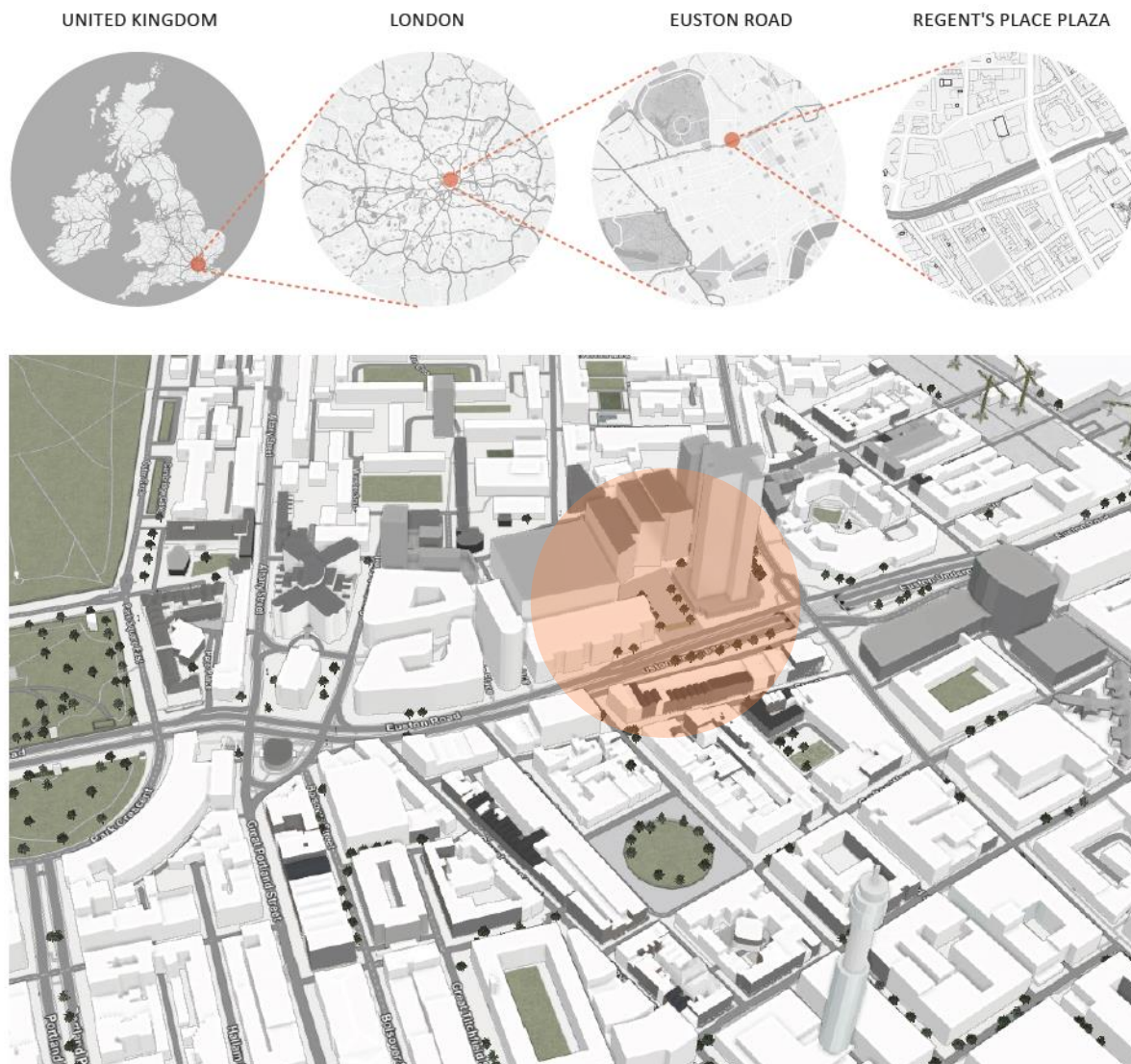
Fig.55 – Regent's Place plaza, Euston Road, London, United Kingdom.

5.1.1 Scale of the study area

Previous research on urban studies defined the study area's boundaries using a specific scale range, such as a 1km x 1km urban grid (Theurer, 1999) or a 500m X 500m urban grid (Rode et al., 2014). The majority of these ranges are purely speculative and difficult to apply to measure air pollution at street level in urban fabrics such as that around the Euston Road. In comparison to the above urban grids, and as it was concluded in chapter 3, the Urban Canopy Layer (UCL) and the microscale unit introduced by Oke (1984, 1989 and 2017) are the most relevant level and scale for the study of wind and air pollution behaviour within urban street canyons.

Considering the above, and in order to gain a better understanding of the effect of immediate urban morphological indicators on air pollution concentrations, the study site was restricted to the microscale boundaries of Drummond Street from the north, Triton Square and Fitzroy Street from the west, Warren Street from the south, and Hampstead Road from the east. Figure 56 depicts the boundary of the fieldwork investigation, in which all relevant morphological, meteorological, and pollutant variables were obtained. Another advantage of collecting data on a smaller scale urban site is that various air pollution and meteorological parameters can be measured at short intervals in multiple locations, allowing measurements to be taken under similar microclimate and air pollution conditions.
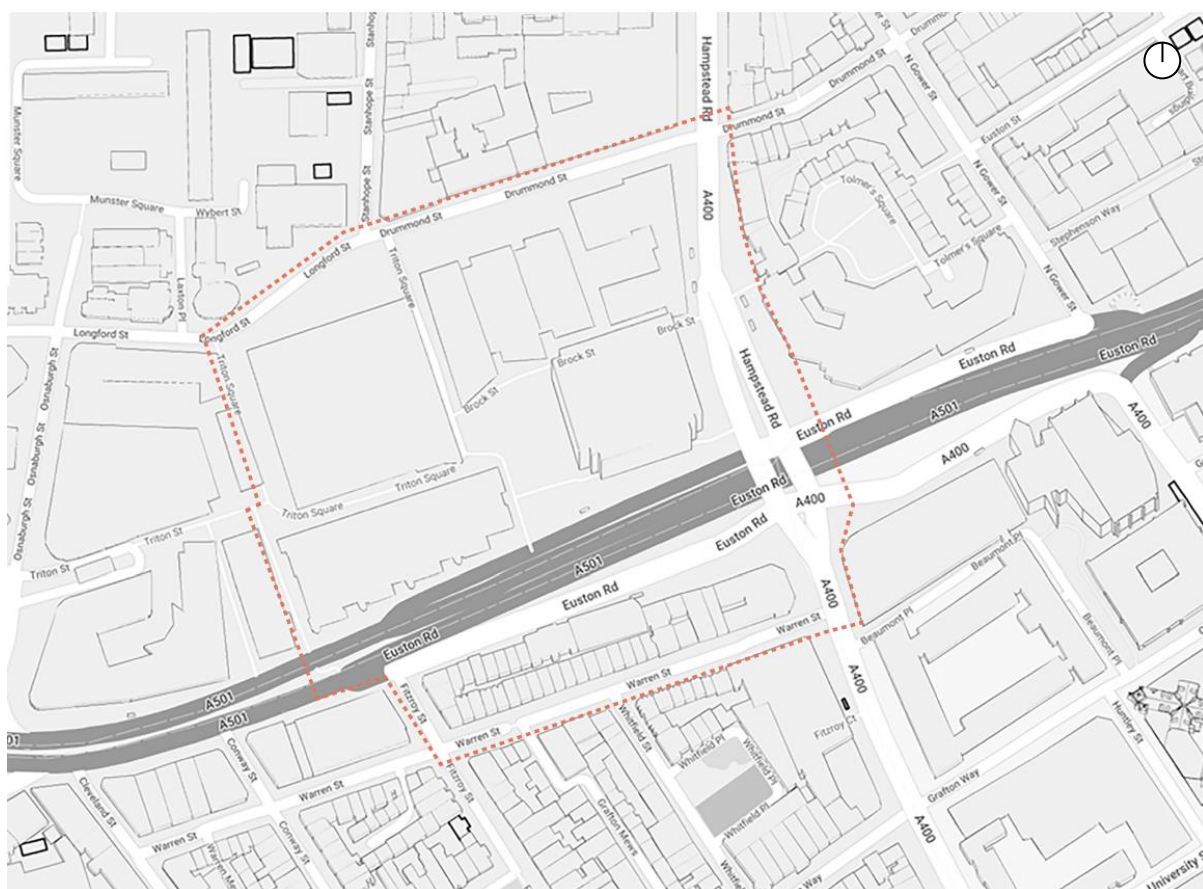
Fig.56 – The orange dashed line indicates the extent and boundary of the fieldwork study area

5.1.2 Description of site

The fieldwork study site located in Regent's Place Plaza in London, UK. Generally, and based on the Köppen-Geiger climate classification the UK climate is characterised by oceanic

climate due to the warmth provided by the Gulf Stream (Kottek et al., 2006). Temperatures do not typically fluctuate to great extremes annually features warm summers and cool winters. There is precipitation through the year with higher rainfall during the winter season. London is located on 51°N latitude and 0.12° W longitude. The warmest season usually lasts for 2.7 months between June to September, with an average daily high temperature above 20°C. The hottest month of the year is end of July and beginning of the August with an average high of 23°C and low of 15°C. However, due to the increasing frequency of extreme weather events such as heat waves, daytime temperatures can exceed 30°C. The cool season lasts for 4 months, between November and March, with an average daily high temperature below 11°C. The coldest month of the year is February, with an average low of 4°C and high of 9°C (Fig.57).

The humidity stays quite stable throughout the year. It peaks at around 80% during night-time and drops to about 50% during daytime. The highest average relative humidity is between December to mid February and the lowest average relative humidity would between May to August (Fig.57b). The average percentage of the sky covered by clouds is varied through the year but generally London is predominately cloudy for a large percentage of the year (68%). Between April and October, the sky is clearer than the rest of the year with the August as the clearest month of the year. The cloudiest is December during which the sky is overcast or mostly cloudy 72% of the time (Fig.57c) (weather spark, 2022). Rain is quite frequent and unpredictable, and London experiences some seasonal variation in monthly rainfall. According to the Met Office Climate data (2020), in 30 years (1991 – 2020) there was an average of 111 days of rainfall per year with an annual rainfall of below 70mm, going against the common knowledge that London is a rainy city (Fig.57d).

The wind experienced at any given location is highly dependent on local topography and other factors such as urban fabric. Generally, windiest month of the year is January with monthly wind speed of 4.3 m/s and the calmest time of the year is July with an average monthly wind speed of 3.2 m/s (from Meteonorm v.8.0) (Fig.57a). Prevailing wind direction in London is from west or south-west (Fig.57e)

The sun hour in London varies extremely over the course of the year. The shortest daily sun hour is 21 December (Winter solstice) with just under 8 hours of daylight; and the longest sun hour is 21 June Summer solstice, with around 16 hours of daylight (Fig.57f). The East side receives the highest global vertical radiation of 3.29 kWh/m² in May. The same trend follows for the west side too with the highest global vertical radiation of 3.2 in July. The south side receives a relatively constant radiation of over 2.2kWh/m² throughout the year (Fig.57g). The annual average global diffused horizontal radiation is also 2.6 kWh/m² with the highest value in July 4.79 kWh/m² and the lowest in December with 0.51 kWh/m² (Fig.57a).
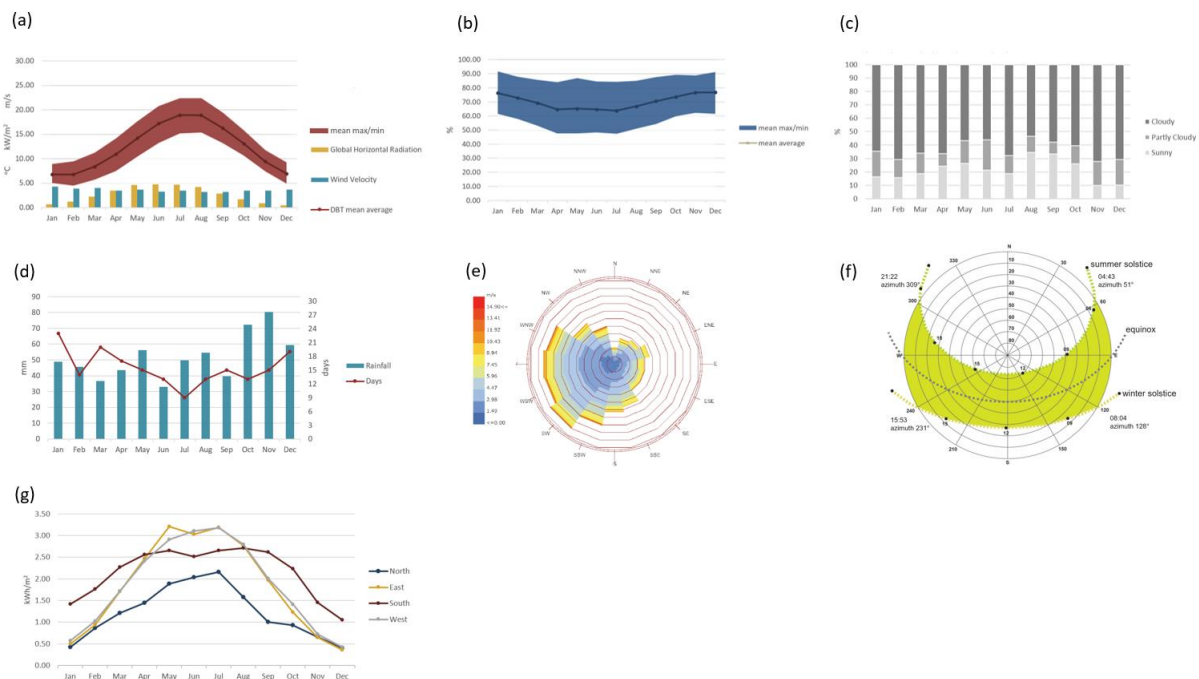
Fig.57 – London climate analysis. (a) Monthly average climate data including temperature, wind velocity and global horizontal radiation (b) Monthly average relative humidity (c) Frequency of sky types (8am – 6pm) (d) Cumulative rainfall (e) wind rose plot showing the annual wind direction and speed (f) Sun path diagram (g) Monthly average global vertical radiation

As it was mentioned, the study site is located at the Regent's Place Plaza in London which is adjacent to Euston Road, where NO_2 pollution levels exceed the annual mean of 40 µgm^{-3} set by national air quality objectives and the air quality standard. Furthermore, between 2012 and 2022, Euston Road exceeded the NO_2 short term air quality objective of 200 µgm^{-3}

1059 times over the permitted 18 days per year (Air Quality England, 2022; London Borough of Camden Air Quality Annual Status Report, 2022).

Particulate matter exceedances are not as high as NO_2 exceedances, but as discussed in Chapter 1, even moderate to low levels of particulate pollution are associated with a short-term increase in mortality and morbidity, making Euston Road one of the UK's most polluted roads. The study site includes a variety of building typologies ranging from mid-rise to high-rise and fine to coarse volume, as well as reasonable access to green infrastructure and scattered trees. The urban form and building arrangements within this site created a variety of urban street canyon types, each with a different sky view factor and aspect ratio as defined in chapter 3 (Fig.37).

Overall, the Regent's Park neighbourhood is a reasonably accurate representation of many city centres in the United Kingdom and many European cities, allowing the findings of this study to have broader applicability. Figure 58 highlights the sky view factor and aspect ratio of various street canyons with associated street canyon types.
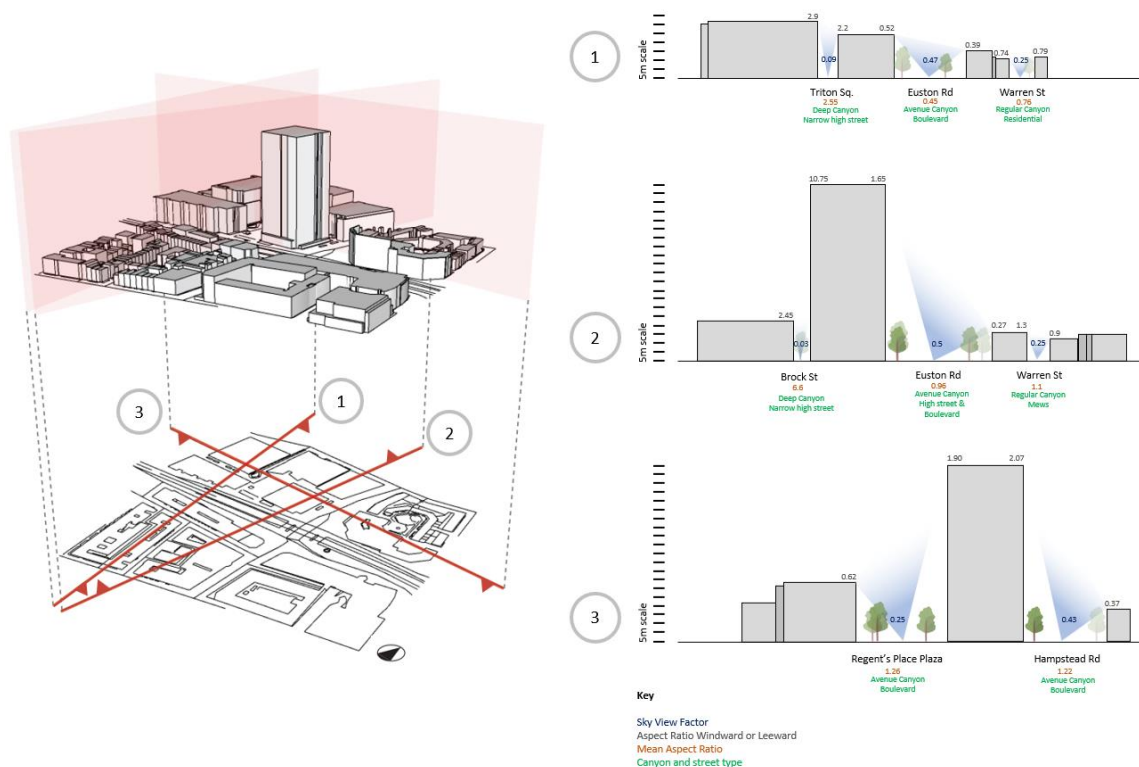
Fig.58 – Sections 1, 2 and 3 highlight various sky view factors, aspect ratios and canyon and street types within Regent's Place Plaza neighbourhood.

Information related to vegetation characteristics such as species name, height, crown shape/size, clear stem height, and Leaf Area Density (LAD), leaf persistence and surface cover has been described in Table 13 and Figure 59. The greenery properties and associated details were obtained from a number of previous studies (Buccolieri et al., 2011; Buccolieri et al., 2009; Amorim et al., 2013; Gromke, 2011; Wania et al., 2012; Ng and Chau, 2012; Ruck, 2007; Johnson and More, 2004) and cross checked by fieldwork observation.

Location & Vegetation Image number	Vegetation Scientific name	Vegetation Common name	Vegetation Height (top of vegetation from ground) (meter)	LAD (High/Low – Dense/Sparse)	Leaf Surface		Evergreen /Deciduous	Trunk Size (Small/Medium/Large)	Crown shape/Size (Cylindrical/Heart-shape/Spherical)	Clear Stem height (meter)
					Hairiness 0 (Smooth) – 10 (silky)	Stickiness 0 (Leathery) – 10 (highly viscid)				
1	Buxus	Box Hedging	1	High	0	1	Evergreen	N/A	Hedge	0
2	Hedera helix	English Ivy	0.30	High	0	1	Evergreen	N/A	N/A	0
3	Platanus × acerifolia	London Plane	10	Low	5	3	Deciduous	Medium	Broadly Oval (Heart-Shaped)	2.5
4	Platanus × acerifolia	London Plane	10	Low	5	3	Deciduous	Medium	Broadly Oval (Heart-Shaped)	2.5
5	Prunus	Cherry Tree	4	Low	3	2	Deciduous	Small	Irregular (Heart-Shaped)	2
6	Tilia	Lime Tree	8	High	4	6	Deciduous	Medium	Broadly Round (Spherical)	2.5
7	Tilia	Lime Tree	8	High	4	6	Deciduous	Medium	Broadly Round (Spherical)	2.5
8	Platanus × acerifolia	London Plane	4	Low	5	3	Deciduous	Small	Irregular (Heart-Shaped)	2
9	Platanus × acerifolia	London Plane	10	Low	5	3	Deciduous	Medium	Broadly Oval (Heart-Shaped)	2
10	Quercus cerris	Turkey Oak	15	Low	2	2	Deciduous	Medium	Broadly Oval (Heart-Shaped)	4
11	Buxus	Box Hedging	2	High	2	1	Evergreen	N/A	Hedge	0

Table.13 – description of the main vegetation characteristics of the study site

1. Buxus

2. Hedera helix

3. Platanus × acerifolia

4. Platanus × acerifolia

5. Prunus

6. Tilia

7. Tilia

8. Platanus × acerifolia

9. Platanus × acerifolia

10. Quercus cerris

11. Buxus

Fig.59 - Location and vegetation image number

5.1.3 Choice of Equipment

The sampling and measurement of meteorological conditions and air pollutants were carried out with portable data loggers, allowing for short-term monitoring. The portability of these data loggers enables them to locate pollution hotspots, identify pollution sources, and measure meteorological parameters in additional locations, supplementing data from fixed-site monitoring. Due to the high cost of air quality devices, only two devices were used simultaneously, and staggered measurements were implemented to minimise the time and changes in meteorological conditions and air pollution levels between each set of measurements at various locations. The findings of Chapter 1 have led to the selection of only three key urban pollutants to be measured and evaluated for this study; these are nitrogen dioxide (NO_2), particulate matter with a diameter of 10 microns (PM_{10}), and particulate matter with a diameter of 2.5 microns ($PM_{2.5}$). Similarly, the findings of chapter 3 led to the selection of the most influential meteorological indicators on air pollution levels, such as temperature, relative humidity, wind speed and direction. Furthermore, and according to World Meteorological Organization (WMO) guidelines published by Tim R. Oke (2004), site-specific microclimatic conditions and air quality levels were measured for 10 minutes at each point of interest, with readings taken every minute and average values logged in for further computational analysis on computational modelling stage. Spot measurements have been logged for a variety of high and medium pedestrian traffic locations within various street canyons, such as outside cafés, bus stops, streets with high and low vehicle traffic flows, at the entrance and middle section of the street canyon, and places designed to encourage people to stay for longer periods of time, such as public seating areas or under large trees. Figure 60 shows the location of the spot measurement in the sequence of measurements.
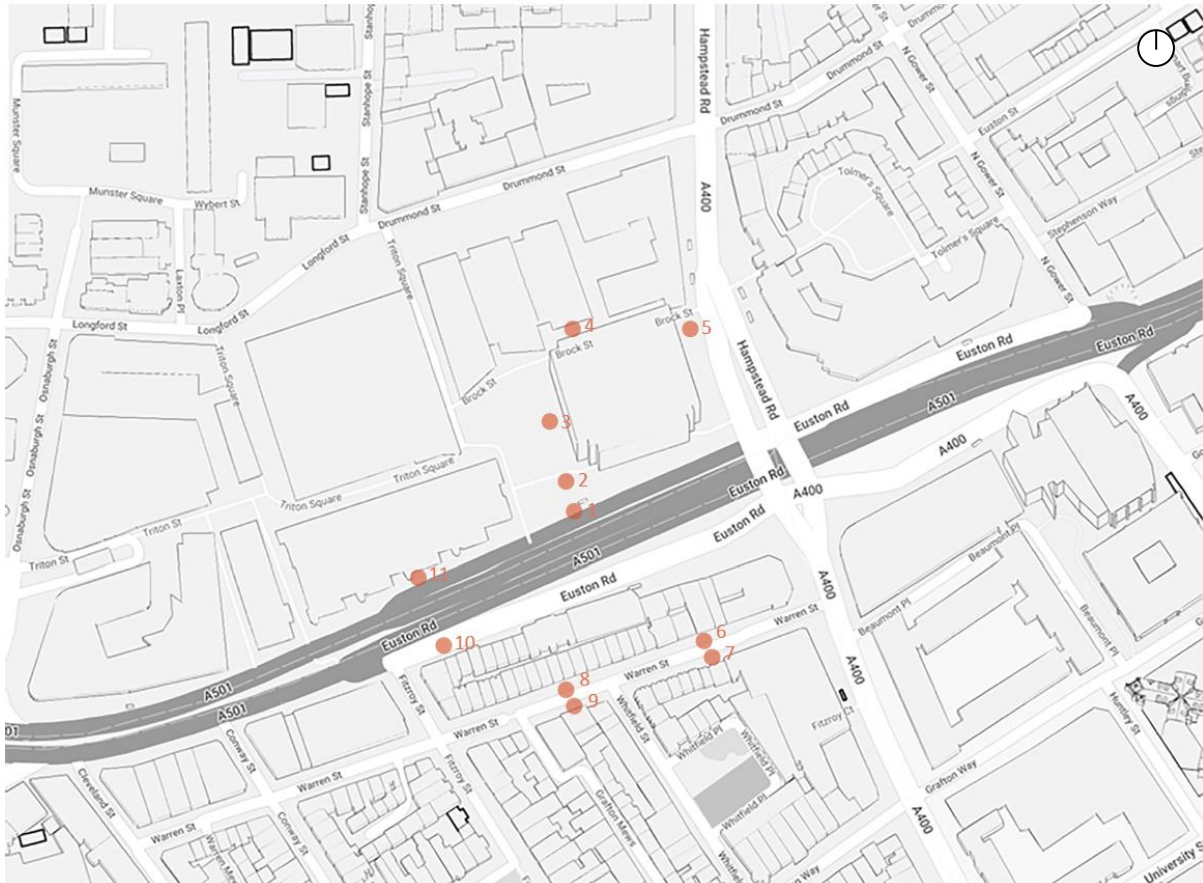
Fig.60 – Location of the spot measurement in the sequence of measurements. Starts from location 1 and ends at location 11. site-specific microclimatic conditions and air quality levels were measured for 10 minutes at each point of interest, with readings taken every minute and average values logged in for further computational analysis on computational modelling stage.

Three portable real-time monitoring devices were used during the fieldwork study. Portable air quality monitors Aeroqual series 200 and 500, which can measure PM_{10}, $PM_{2.5}$, and NO_2; and a Vane anemometer and Thermo hygrometer, Testo 410-2, which can measure airflow velocity, air temperature, and relative humidity (Fig.61). It is worth noting that, all the parameters were measured under the same environmental conditions at each location.

Fig.61 - Portable air quality monitors Aeroqual series 200 (left), series 500 (middle) & Vane anemometer + Thermo hygrometer (right).

The Testo 410-2 vane anemometer is ideal for rapid measurement of meteorological parameters such as relative humidity, air velocity, and air temperature. The permanently installed vane (30 mm in diameter) enabled accurate measurement of low air velocities ranging from 0.4 to 20 m/s. The anemometer is equipped with a humidity sensor that maintains its accuracy over time and a Negative Temperature Coefficient (NTC) temperature sensor that measures between -10 and +50 °C. The readings can be viewed on the digital display, which also features single-point averaging, max/min, and a Hold function for manually taking readings. The Aeroqual 200 and 500 are portable air quality monitors designed to collect data in real time in outdoor and indoor environments. These lightweight portable monitors (460g with sensor head and battery) can be carried around a large area to identify and measure air pollution concentration and levels. Various pollutants, such as gaseous or particulate matter, can be measured using special sensor heads. Active fan sampling is used in the sensor heads to ensure that a representative sample is taken, providing the highest possible measurement accuracy. Changing the sensors is simple, requires no configuration or re-calibration, and can be performed anywhere, allowing for continuous monitoring throughout the monitoring period. The Aeroqual series 200 and 500 series have a large LCD display that shows minimum, maximum, and average values. The only drawback is that the Aeroqual series 200 does not permit storage or connection to a PC and the user must manually record readings while on site and monitoring. In contrast, the Aeroqual series 500 can store up to 8,188 data points and connects to a computer via USB,

allowing data to be downloaded and viewed in Microsoft Excel. A location ID and a monitor ID are also included in the Series 500. Monitor ID is a number that uniquely identifies a location and ensures that all data from that location is linked to it. When sampling at several places throughout the day or week, Monitor ID can be used to correlate measurements with a specific location. Both series work with a number of head sensors which can measure up to 16 different pollutants with the addition of swappable sensor heads. The NO_2 sensor (Fig.62) has a resolution of 0.001 parts per million and stores data every 30 seconds with a detection limit of 0.005 parts per million. The PM_{10} & $PM_{2.5}$ sensor (Fig.63), with a resolution of 0.001 mg/m^3, can simultaneously measure and store particulate matter with diameters of 2.5 and 10 microns. The simultaneous measurement of NO_2 and $PM_{10/2.5}$ was enabled by the use of both Aeroqual devices at the same time. The 200 series was used to measure PM_{10}

and $PM_{2.5}$, while the 500 series was used to measure NO_2.

Nitrogen Dioxide Sensor Head 0-1PPM	
Range	0-1ppm
Sensor Type	GSE
Minimum Detection Limit	0.005ppm
Accuracy of Factory Calibration	<±0.02ppm 0-0.2ppm <±10% 0.2-1ppm
Resolution	0.001ppm
Response Time	30 Seconds

Fig.62 – Nitrogen Dioxide sensor head - NO_2

Particulate Matter Sensor Head PM_{10}/$PM_{2.5}$	
Range	0 to 1 mg/m^3
Sensor Type	Laser particle counter
Minimum Detection Limit	0.001 mg/m^3
Accuracy of Factory Calibration	±(0.002 mg/m^3 + 15% of reading)
Resolution	0.001 mg/m^3
Response Time	5 Seconds

Fig.63 – Particulate matter sensor head PM_{10} & $PM_{2.5}$

As it was mentioned in chapter 4 and in order to minimise errors and improve the accuracy of collected data, prior to the start of the project and field measurements, all sensor heads, including NO_2, PM_{10}, and $PM_{2.5}$, were co-located through a series of comparison trials. Therefore, both data collected from the device and monitoring station were compared using a linear model with linear regression analysis to demonstrate the close relationship between the portable air quality and reference air quality station; any adjustment for future measurements explained by the linear regression equation (Y=mx+b). The co-location measurement took place over four days and each day for four hours. As with numerous previous studies (Spagnolo and de Dear, 2003; Ng and Cheng, 2012), the equipment sets are positioned 1.5 metres above ground level and within the range of average pedestrian height. After the co-location phase, the study then collected data on a variety of days and weather conditions, including dry and rainy days, throughout the Spring (4th and 24th April 2019), Summer (16th and 26th August 2019), Autumn (24th and 26th November 2019), and Winter (14th and 28th February 2020) seasons. When selecting these dates, consideration was given to wind directions that corresponded to the London prevailing wind directions of West to South-Westerly (SSW), SW, and WSW (Fig.57e) as this would make the study more comparable to other studies (Glover, 2015; Jeanjean et al., 2017) and any future studies within the same context.

The measurements were taken in different seasons to ensure that seasonal changes in deciduous trees were accounted for in the calibration process, providing finer data to be compared with the output of computational modelling (ENVI-met). Between April 2019 and February 2020, a total of 616 measurements were made, 264 of which were for the three air pollutants and the remainder for meteorological parameters. It is worth noting that the measurements have taken into account the background concentration caused by Deepawali (27th October) and Bonfire Night (5th November), and no measurements have been taken in the days preceding or following the above events. The reason for this is that when fireworks explode, they emit very fine dust particles rich in toxic metals. As a result, these have frequently resulted in elevated particle levels, with local concentrations exceeding the 'very high' pollution threshold. People traditionally begin to celebrate these events a few days before the actual event dates and if the weather is with little or no wind, the pollution can

last for several days and thus any measurement within these periods does not accurately reflect traffic-related pollution (London Air, 2017).

5.1.4 Choice of morphological indicators to measure

The spatial dimension of the site is fundamental for monitoring air pollution concentrations at street level. Based on chapter 3 and the extensive exploration and review of respected literatures, it was ascertained that not all morphological indicators are appropriate for the study of microclimate and air pollution within street canyons and only a handful of indicators that influence the wind and air circulation in and around the buildings should be considered. As a result, only the parameters highlighted in Table 14 were taken into account for this thesis. The justification for using these parameters has been explained in detail in Chapter 3.

Urban Form Attributes			
	Building Site Coverage (%)	Surface-to-volume ratios [sqm/cbm]	Sky View Factor (SVF)
	Floor Area Ratio (%)	Mean Canyon Aspect Ratio	Frontal area index (λf)
	Building Height Differentials	Street Canyon Type	Average building height (m)
Street Network	Street & Building Orientation	Road Coverage %	Impervious surface fraction (%)
	Mean Street Width [m]	Street Length [m]	Pedestrian Area Coverage %
Greenery	Green Cover Ratio %	Average Tree Heights [m]	Type of trees and specious

Table.14 – Morphological indicators that impact the air pollution concentration within urban street canyons and have been used in this study.

Data on the aforementioned morphological indicators were collected using both conventional field measurements and satellite-based measurements. Official GIS documents and Ordnance Survey maps were used to determine the footprint and height of the building

(Ordnance Digimap Survey Collection, 2019). Data collected from official GIS were checked and verified against conventional field measurement data, and in some cases, aerial perspectives published by Bing Maps and Google Maps were used to minimise possible errors.

5.2 Device calibration

According to the Local Air Quality Management Technical Guidance (DEFRA, 2018) air quality devices, whether portable or fixed or nitrogen dioxide diffusion tubes, must be verified by co-locating the devices with an automatic air pollution monitor. It is common practice in air quality measurement to co-locate a non-reference monitor, in this case Aeroqual, under real-world conditions for a defined evaluation period alongside a reference monitor, i.e. Marylebone Road air quality station. This will minimise the uncertainty associated with air quality devices and any adjustment factor can be identified prior to the start of the project. For that reason, both Aeroqual devices were kept next to the 'Westminster - Marylebone Road – kerbside' meteorological and air quality monitoring station and faced towards the incoming traffic (Fig.64). The Marylebone air quality station was chosen as the co-location site because it is less than a kilometre from the fieldwork study site and its urban form is very similar to that of the study site.
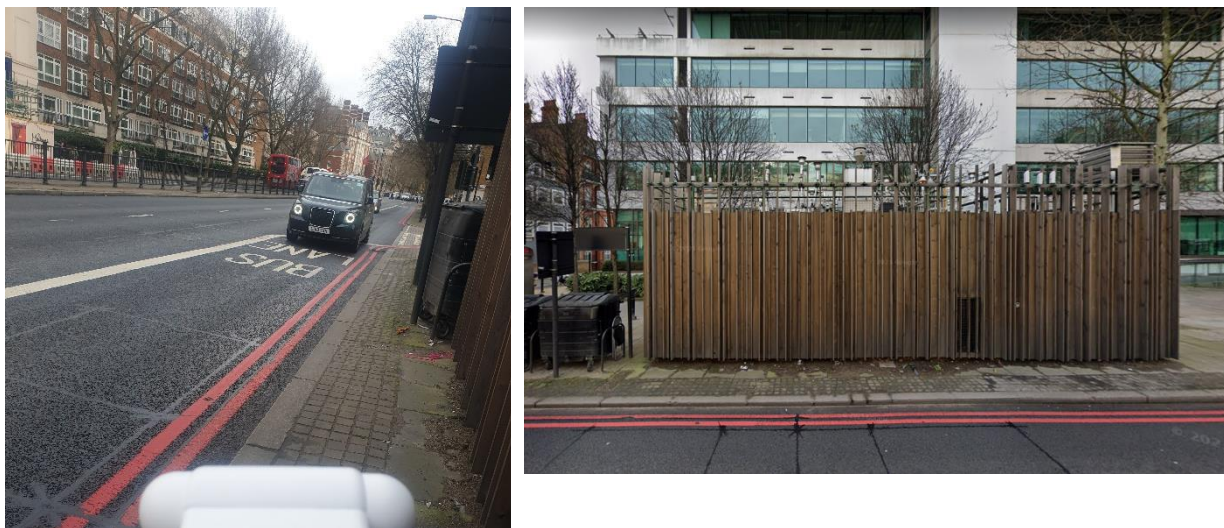
Fig.64 - Aeroqual facing towards the incoming traffic and next to Marylebone meteorological and air quality monitoring station.

Both portable devices' data were compared against the reference monitoring station data by employing a linear model and linear regression analysis. The correlation of determination (R^2) and correlation coefficient were calculated to demonstrate the close relationship between the portable air quality device and the reference air quality station. The coefficient of determination R-squared (R^2) indicates how close the data are to the slope-intercept line. The correlation coefficient (r) is also included to aid in understanding the best fit of the data and to demonstrate how closely the points in a scatter plot are associated with a linear regression line. The R-squared is a statistical measure that shows how much of a dependent variable's variance is explained by independent variables in a regression model. It also shows how much the variance of one variable explains the variance of the second variable. The correlation coefficient (r), on the other hand, expresses the strength of the association between an independent and dependent variable. It has a range of values between +1 and -1, with +1 signifying perfect positive correlation and -1 denoting perfect negative correlation. Any adjustment factor for future measurements is explained by the linear regression equation (Y=mx+b), where 'Y' represents the dependent variables (Aeroqual data) and 'm' represents the slope, and the independent variables are denoted by 'x' (extracted from the reference station), and the Y-intercept is denoted by 'b' (Fig.65). This equation provides a statistically sound method for comparing sensor data to reference data. Scatter plots were used in this study to determine the regression equation and the equations for NO_2, PM_{10}, and $PM_{2.5}$. The co-location measurement took place over the course of four days, each day lasting four hours between 11:00 am and 3:00 pm. The NO_2 sensor head measurements were taken on 7th and 9th February 2019, as were the PM_{10} & $PM_{2.5}$ data measurements were taken on February 15th and 16th, 2019. The measurements for the reference air quality station were obtained from www.londonair.org.uk and are summarised in table 15. It is worth mentioning that the analysis is based on ratified data that was extracted one month after the initial measurement. This procedure was repeated during the fieldwork study and Aeroqual sensors heads were always compared to the reference station prior to and following each field measurement.

NO2 Sensor head co-location comparison against certified reference station

y = 1.78x - 36.25
$R^2 = 0.89$

PM10 Sensor head co-location comparison against certified reference equipment

y = 0.91x + 10.61
$R^2 = 0.9144$

PM2.5 Sensor head co-location comparison against certified reference equipment

y = 0.62x + 0.77
$R^2 = 0.7294$
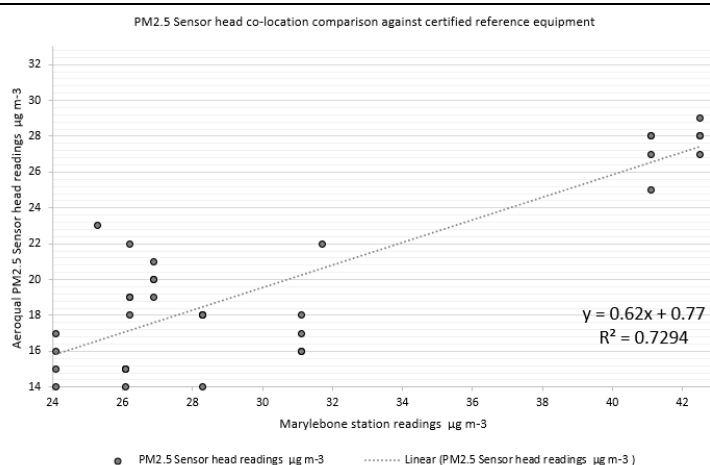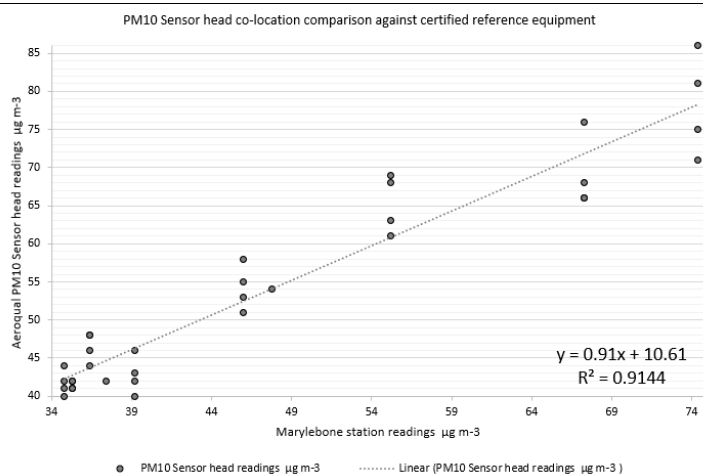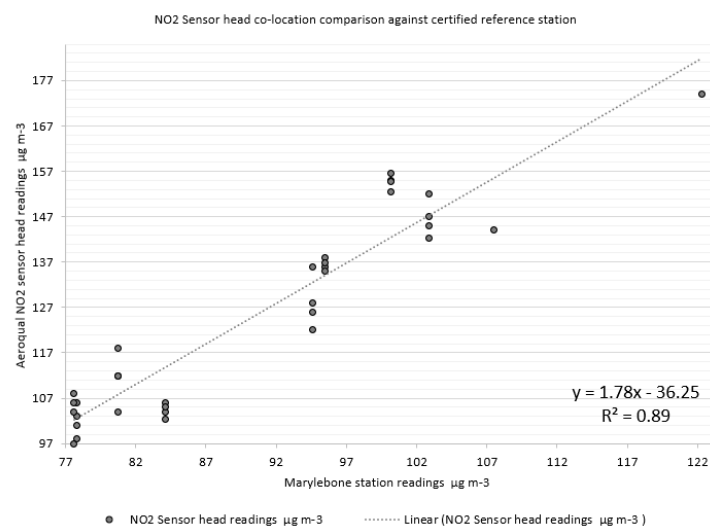
Fig.65 - Scatterplots of Marylebone reference Air quality station versus Aeroqual portable air quality device, NO_2 values (left) PM_{10} (centre) and $PM_{2.5}$ (right), with simple regression lines to indicate the trend and correlation co-efficient (R^2).

7th Feb 2019	NO$_2$ Marylebone station readings µg m^{-3}	NO$_2$ Sensor head readings µg m^{-3}
11:00 AM	84.1	104
11:15 AM	84.1	102.3
11:30 AM	84.1	106
11:45 AM	84.1	105
12:00 PM	102.9	152
12:15 PM	102.9	144.9
12:30 PM	102.9	142.2
12:45 PM	102.9	147
1:00 PM	95.5	136
1:15 PM	95.5	138
1:30 PM	95.5	135
1:45 PM	95.5	136.8
2:00 PM	100.2	155
2:15 PM	100.2	156.5
2:30 PM	100.2	154.7
2:45 PM	100.2	152.5
3:00 PM	122.3	174

9th Feb 2019	NO$_2$ Marylebone station readings µg m^{-3}	NO$_2$ Sensor head readings µg m^{-3}
11:00 AM	77.8	106
11:15 AM	77.8	98
11:30 AM	77.8	103
11:45 AM	77.8	101
12:00 PM	80.7	112
12:15 PM	80.7	112
12:30 PM	80.7	104
12:45 PM	80.7	118
1:00 PM	94.6	126
1:15 PM	94.6	128
1:30 PM	94.6	136
1:45 PM	94.6	122
2:00 PM	77.6	97
2:15 PM	77.6	106
2:30 PM	77.6	108
2:45 PM	77.6	104
3:00 PM	107.5	144

15th Feb 2019	PM$_{10}$ Marylebone station readings µg m^{-3}	PM$_{10}$ Sensor head readings µg m^{-3}	PM$_{2.5}$ Marylebone station readings µg m^{-3}	PM$_{2.5}$ Sensor head readings µg m^{-3}
11:00 AM	74.4	81	42.5	29
11:15 AM	74.4	86	42.5	27
11:30 AM	74.4	75	42.5	28
11:45 AM	74.4	71	42.5	28
12:00 PM	67.3	76	41.1	28
12:15 PM	67.3	66	41.1	28
12:30 PM	67.3	66	41.1	27
12:45 PM	67.3	68	41.1	25
1:00 PM	55.2	63	31.1	16
1:15 PM	55.2	68	31.1	16
1:30 PM	55.2	69	31.1	18
1:45 PM	55.2	61	31.1	17
2:00 PM	46	53	26.1	15
2:15 PM	46	58	26.1	14
2:30 PM	46	55	26.1	15
2:45 PM	46	51	26.1	15
3:00 PM	47.8	54	31.7	22

16th Feb 2019	PM$_{10}$ Marylebone station readings µg m^{-3}	PM$_{10}$ Sensor head readings µg m^{-3}	PM$_{2.5}$ Marylebone station readings µg m^{-3}	PM$_{2.5}$ Sensor head readings µg m^{-3}
11:00 AM	34.8	42	28.3	18
11:15 AM	34.8	44	28.3	18
11:30 AM	34.8	41	28.3	14
11:45 AM	34.8	40	28.3	18
12:00 PM	36.4	46	26.9	19
12:15 PM	36.4	48	26.9	21
12:30 PM	36.4	48	26.9	20
12:45 PM	36.4	44	26.9	20
1:00 PM	35.3	41	24.1	16
1:15 PM	35.3	42	24.1	15
1:30 PM	35.3	41	24.1	14
1:45 PM	35.3	42	24.1	17
2:00 PM	39.2	40	26.2	19
2:15 PM	39.2	43	26.2	19
2:30 PM	39.2	46	26.2	18
2:45 PM	39.2	42	26.2	22
3:00 PM	37.4	42	25.3	23

Table.15 – air quality data extracted from Westminster - Marylebone Road – kerbside station and measurements were taken over four days of co-location exercise with different Aeroqual sensor heads, i.e. NO$_2$ and PM$_{10}$&PM$_{2.5}$

According to Figure 65 and Table 15, the Aeroqual $PM_{2.5}$ head sensor consistently reports values that are 21% lower than the reference station, while the PM_{10} and NO_2 head sensors consistently report values that are 6% and 16% higher than the reference station, respectively. In other words, the data quality is biased, implying that there is a systematic (built-in) error that caused all measurement values to be higher or in the case of $PM_{2.5}$, lower (Fig.66). While it is common practice to send the sensor heads to the factory for re-calibration, however, due to the cost and time involved, it was decided to use the regression equation to match any future measurements to the reference station. Interestingly and as it can be seen in figure 66, this error is constant, indicating that the device is in good working order and that only the values should be adjusted after each measurement.
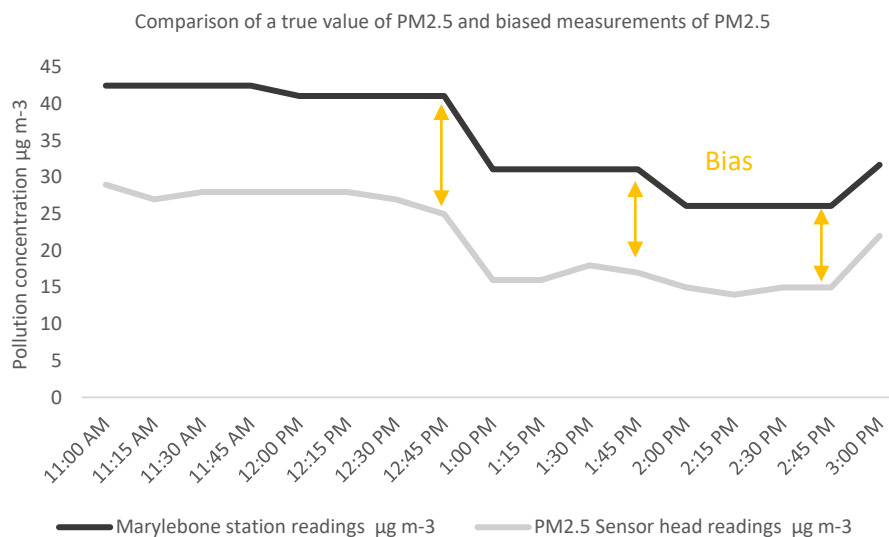
Fig.66 – Comparison of reference values of $PM_{2.5}$ and Aeroqual portable air quality device. The portable device data is constantly lower than the reference air quality station.

Another reason for a difference in measurement is that the device was co-located two metres below the reference station's height, making it more exposed to the turbulence created by the vehicles. As a result, the measurements are different, but as can be seen, the correlation coefficient and R-squared are extremely high, indicating that the correlation is strong and that makes the device a good fit to carry out the fieldwork. In light of the above, the following equations were derived from the aforementioned graphs and will be used throughout the fieldwork measurement process to adjust and correct the measurement

values to bring them closer to the reference data and thus into better agreement with it. The equation is as follows:

$$x = \frac{Y - b}{m}$$

x = Adjusted sensor concentration

Y = Measured sensor concentration

Therefore:

$$Adjusted\ sensor\ concentration = \frac{Measured\ sensor\ concentration - b}{m}$$

Adjusted NO2 (X) = $\frac{(Y-b)}{m}$ where Y is any future measured data minus (b) which is -36.25 divided by (m) which is 1.78

Adjusted PM10 (X) = $\frac{(Y-b)}{m}$ where Y is any future measured data minus (b) which is 10.61 divided by (m) which is 0.91

Adjusted PM2.5 (X) = $\frac{(Y-b)}{m}$ where Y is any future measured data minus (b) which is 0.77 divided by (m) which is 0.62

5.3 Result of the fieldwork measurement

The co-location practice confirmed that the portable air quality devices are suitable for this study and can be used for future measurements as long as the measured values are adjusted according to the previously stated equations. Accordingly, for the fieldwork study, in total eight days equal to 88 spot measurements taken and included in this section, the measurement dates are April 4th and 24th 2019 for Spring season, August 16th and 26th 2019 for Summer season, November 24th and 26th 2019 for the Autumn season and for Winter season Feb 14th and 28th 2020. To better understand the effect of weather conditions on measurement values and to verify the ENVI-met's accuracy, measurements were taken on dry day and rainy days within each season.

Sky condition	Rainy day	Meteorological conditions on Thursday 4th April 2019				Street-level air pollutant concentration		
Location	Time (hrs:mins)	Air temperature	Relative Humidity	Wind Velocity	Wind Direction	NO_2 ($\mu g/m^3$)	PM_{10} ($\mu g/m^3$)	$PM_{2.5}$ ($\mu g/m^3$)
1	11:20 - 11:30	8.1	83	2.9	202	78	14	9
2	11:30 - 11:40	7.3	82	1.37	180	63	11	7
3	11:40 - 11:50	7.6	79.9	1.7	180	48	8	7
4	11:50 - 12:00	7.9	83	2.1	202	45	8	8
5	12:00 - 12:10	7.6	84	1.9	157	48	9	8
6	12:10 - 12:20	8.3	84.3	1.9	270	42	8	9
7	12:20 - 12:30	8.1	84.7	1.8	270	43	10	10
8	12:30- 12:40	8.1	84.5	1.1	270	47	10	9
9	12:40 - 12:50	7.9	84.8	0	270	51	12	9
10	12:50 - 13:00	7.1	85.9	1.3	252	65	11	9
11	13:10 - 13:20	6.8	83.3	0.92	180	71	7	7

Table.16 - Meteorological and air pollution data for 4th April 2019. Spot measurement is taken during the fieldworks done by the author.

Sky condition	Dry day	Meteorological conditions on Wednesday 24th April 2019				Street-level air pollutant concentration		
Location	Time (hrs:mins)	Air temperature	Relative Humidity	Wind Velocity	Wind Direction	NO_2 ($\mu g/m^3$)	PM_{10} ($\mu g/m^3$)	$PM_{2.5}$ ($\mu g/m^3$)
1	14:50 - 15:00	17.3	64.3	1.6	247	102	21	12
2	15:00 - 15:10	16.3	65.8	0.6	180	83	11	7
3	15:10 - 15:20	16.2	65.3	0.3	157	61	13	7
4	15:20 - 15:30	16.2	65.1	1.3	202	56	10	7
5	15:30 - 15-40	15.8	66.3	1	157	82	11	8
6	15:40 - 15:50	17.6	62.9	2.1	247	68	12	3
7	15:50 - 16:00	17.3	62.7	2.1	270	72	15	8
8	16:00 - 16:10	17.3	62.5	1.5	247	63	11	10
9	16:10 - 16:20	17.5	62.7	0.8	270	71	15	8
10	16:20 - 16:30	17	61.2	2.1	292	113	17	11
11	16:30 - 16:40	16.2	64.3	0.9	225	74	13	8

Table.17 - Meteorological and air pollution data for 24th April 2019. Spot measurement is taken during the fieldworks done by the author.

Sky condition	Rainy day	Meteorological conditions on Friday 16th August 2019				Street-level air pollutant concentration		
Location	Time (hrs:mins)	Air temperature	Relative Humidity	Wind Velocity	Wind Direction	NO_2 ($\mu g/m^3$)	PM_{10} ($\mu g/m^3$)	$PM_{2.5}$ ($\mu g/m^3$)
1	17:10 - 17:20	17.5	86.5	1.2	202	86	16	11
2	17:20 - 17:30	17	87	0.7	135	52	11	7
3	17:30 - 17:40	16.3	88	0.6	202	48	7	3
4	17:40 - 17:50	16.7	88	1.3	225	43	6	3
5	17:50 - 18:00	16.1	91	1.5	157	56	11	5
6	18:00 - 18:10	16.5	89.9	2	247	52	12	6
7	18:10 - 18:20	16.8	88	1.6	247	53	11	7
8	18:20 - 18:30	16.5	88.4	1.9	247	52	11	5
9	18:30 - 18:40	16.5	88.1	1.3	247	53	11	7
10	18:40 - 18:50	16.9	85.1	1.6	270	81	14	8
11	18:50 - 19:00	16.1	92.6	0.8	202	65	8	4

Table 18 - Meteorological and air pollution data for 16th August 2019. Spot measurement is taken during the fieldworks done by the author.

Sky condition	Dry day	Meteorological conditions on Monday 26th August 2019				Street-level air pollutant concentration		
Location	Time (hrs:mins)	Air temperature	Relative Humidity	Wind Velocity	Wind Direction	NO_2 ($\mu g/m^3$)	PM_{10} ($\mu g/m^3$)	$PM_{2.5}$ ($\mu g/m^3$)
1	15:30 - 15:40	33.8	48	0.8	225	161	27	14
2	15:40 - 15:50	33.1	48.6	0.6	112	124	19	9
3	15:50 - 16:00	32.6	48.9	0.4	112	112	16	11
4	16:00 - 16:10	32.1	49.8	1	202	115	14	7
5	16:10 - 16:20	32.3	49.2	1.2	157	102	19	7
6	16:20 - 16:30	32.1	48.2	1.1	247	96	18	9
7	16:30 - 16:40	32.2	48.6	0.9	247	102	20	10
8	16:40 - 16:50	32.1	47.8	1	247	92	18	10
9	16:50 - 17:00	32.3	47.6	0.6	247	106	21	12
10	17:00 - 17:10	33.6	47.1	1.1	247	112	19	9
11	17:10 - 17:20	33.1	47.3	0.7	202	116	23	9

Table 19 - Meteorological and air pollution data for 26th August 2019. Spot measurement is taken during the fieldworks done by the author.

Sky condition	Dry day	Meteorological conditions on Sunday 24th November 2019				Street-level air pollutant concentration		
Location	Time (hrs:mins)	Air temperature	Relative Humidity	Wind Velocity	Wind Direction	NO_2 ($\mu g/m^3$)	PM_{10} ($\mu g/m^3$)	$PM_{2.5}$ ($\mu g/m^3$)
1	10:30 - 10:40	11.6	96.3	1.2	180	92	32	19
2	10:40 - 10:50	10.2	96.4	0.2	180	52	19	8
3	10:50 - 11:00	11.5	95.8	0	180	59	19	6
4	11:00 - 11:10	11.3	95.3	0.6	202	36	16	6
5	11:10 - 11:20	12.3	94.3	0.5	180	55	22	8
6	11:20 - 11:30	12.6	95	0.9	247	69	23	10
7	11:30 - 11:40	12.2	95	0.7	247	63	21	11
8	11:40 - 11:50	12.8	96	0.9	247	68	22	10
9	11:50 - 12:00	12.3	96	0.5	247	64	19	8
10	12:00 - 12:10	10.4	98	1.3	225	86	23	12
11	12:10 - 12:20	10	96	0.6	225	55	21	9

Table 20 - Meteorological and air pollution data for 24th November 2019. Spot measurement is taken during the fieldworks done by the author.

Sky condition	Rainy day	Meteorological conditions on Tuesday 26th November 2019				Street-level air pollutant concentration		
Location	Time (hrs:mins)	Air temperature	Relative Humidity	Wind Velocity	Wind Direction	NO_2 ($\mu g/m^3$)	PM_{10} ($\mu g/m^3$)	$PM_{2.5}$ ($\mu g/m^3$)
1	11:50 - 12:00	13.2	93	0.7	180	98	16	10
2	12:00 - 12:10	13.3	93.5	0	90	74	9	8
3	12:10 - 12:20	13.1	92.9	0.2	225	67	10	7
4	12:20 - 12:30	12.9	93	1.6	202	63	10	5
5	12:30 - 12:40	12.4	93.5	0.9	135	89	10	8
6	12:40 - 12:50	13.8	92.3	1.4	270	71	11	8
7	12:50 -13:00	13.6	92.3	1.1	270	72	12	8
8	13:00 - 13:10	13.4	93.1	1	270	71	12	7
9	13:10 - 13:20	13.3	93.2	0.5	270	75	14	8
10	13:20 - 13:30	12.6	94.3	1.1	292	96	15	9
11	13:30 - 13:40	13.4	94	1	225	89	11	8

Table 21 - Meteorological and air pollution data for 26th November 2019. Spot measurement is taken during the fieldworks done by the author.

Sky condition	Dry day	Meteorological conditions on Friday 14th February 2020				Street-level air pollutant concentration		
Location	Time (hrs:mins)	Air temperature	Relative Humidity	Wind Velocity	Wind Direction	NO_2 ($\mu g/m^3$)	PM_{10} ($\mu g/m^3$)	$PM_{2.5}$ ($\mu g/m^3$)
1	11:00 - 11:10	9.2	86.4	2.1	225	105	21	11
2	11:10 - 11:20	9	87.7	0.2	135	58	14	8
3	11:20 - 11:30	7.9	87.2	0.1	180	49	16	9
4	11:30 - 11:40	8	86.4	1.8	202	42	13	8
5	11:40 - 11:50	8.1	86.5	0.6	180	65	15	8
6	11:50 - 12:00	9.7	86.8	1.7	270	62	18	9
7	12:00 - 12:10	9.8	86.8	1.8	270	68	20	9
8	12:10 - 12:20	9.3	87	1.3	270	63	20	9
9	12:20 - 12:30	9.4	87.2	1	270	68	20	9
10	12:30- 12:40	8	88.6	2.3	252	87	23	10
11	12:40 - 12:50	9.3	86.2	1.4	202	65	21	9

Table 22 - Meteorological and air pollution data for 14th February 2020. Spot measurement is taken during the fieldworks done by the author.

Sky condition	Rainy day	Meteorological conditions on Friday 28th February 2020				Street-level air pollutant concentration		
Location	Time (hrs:mins)	Air temperature	Relative Humidity	Wind Velocity	Wind Direction	NO_2 ($\mu g/m^3$)	PM_{10} ($\mu g/m^3$)	$PM_{2.5}$ ($\mu g/m^3$)
1	13:50 - 14:00	10.4	98	1.14	180	81	11	12
2	14:00 - 14:10	10.1	99	0.8	112	64	8	6
3	14:10 - 14:20	11	100	0.6	180	56	8	5
4	14:20 - 14:30	12	98	1.2	202	48	8	6
5	14:30 - 14:40	10.3	100	0.6	202	61	10	5
6	14:40 - 14:50	10.6	97	2.1	270	63	11	7
7	14:50 - 15:00	10.5	98	1.6	270	68	12	8
8	15:00 - 15:10	10.9	98	1.1	270	66	11	6
9	15:10 - 15:20	10.7	98	0.2	270	66	11	7
10	15:20 - 15:30	10.4	100	1	247	73	12	9
11	15:30 - 15:40	10.6	98	1	202	78	9	6

Table 23 - Meteorological and air pollution data for 25th February 2020. Spot measurement is taken during the fieldworks done by the author.

When comparing measurements taken during different weather conditions and seasons, it can be seen that the levels of pollutants, such as NO_2 and PM_{10} & $PM_{2.5}$, were the highest on dry days and mostly during the Summer and Autumn seasons, respectively. The increase in the particulate matter can be explained by the fact that it is expected that on a rainy day, most of the common airborne particles such as smoke, dust, and soot will be washed away to the ground, thereby improving the quality of the air. The increase in nitrogen dioxide in summer requires further investigation, but it is possible that it is due to a decrease in wind velocity and airflow caused by an increase in the volume of vegetation in and around the fieldwork site. The highest NO_2 was measured at location 1 on August 26th, 2019 at 161 $\mu g/m^3$, and the highest PM_{10} and $PM_{2.5}$ were measured at the same location on November 24th, 2019 at 32 $\mu g/m^3$ and 19 $\mu g/m^3$, respectively.

Having said that, when only locations are considered, it can be seen that Location 1, which is close to Euston Road on average, has the highest pollution level throughout the year, while Location 4, which is more than 100 metres away from the roadside and is protected by rows of trees and tall buildings, has the lowest. If we divide the 88 measurements taken from 11 locations into four equal quarters, the top 22 measurements (Fig.67) standing in the upper quarter (Q1) have 10 locations in which the measurements were taken under tree and when we compare this to the lower quarter (Q4) this number reduced to only 4 locations; a decrease of 60% in locations with trees and in average an increase of 60% in PM_{10} concentration and 50% of $PM_{2.5}$. Interestingly Q1 has only one dry day in comparison to Q4 which has no rainy day and all measurements were taken place under dry weather conditions. As it was mentioned in chapter 3, this shows the importance of trees and their ability to deposit and absorb pollution on their leaves through dry and wet deposition which, based on the result, on rainy days can be extremely effective under and around the vicinity of mature trees and can slows down the transportation of particulate matter in the environment. Contrary to the particulate matter concentration, the NO_2 concentration and level were observed the highest on 26th August 2019 at locations 1 which is without trees and location 11 which is with tree, and in August, when the trees are fully foliaged. On 24th November, 14th February, and 4th April, the lowest NO_2 concentrations were measured at locations 4, 6, 7, and 8, where none of the locations had trees and the weather was sunny. It's worth noting that even if these locations have had trees, they would likely have no or

few leaves due to the early spring and winter season and the typical type of trees used within this site, i.e. deciduous trees. Another reason for this, as it was mentioned in chapter 2, is that NO_2 concentration is affected by more local air pollution and the distance between the source of emission and the receptor.
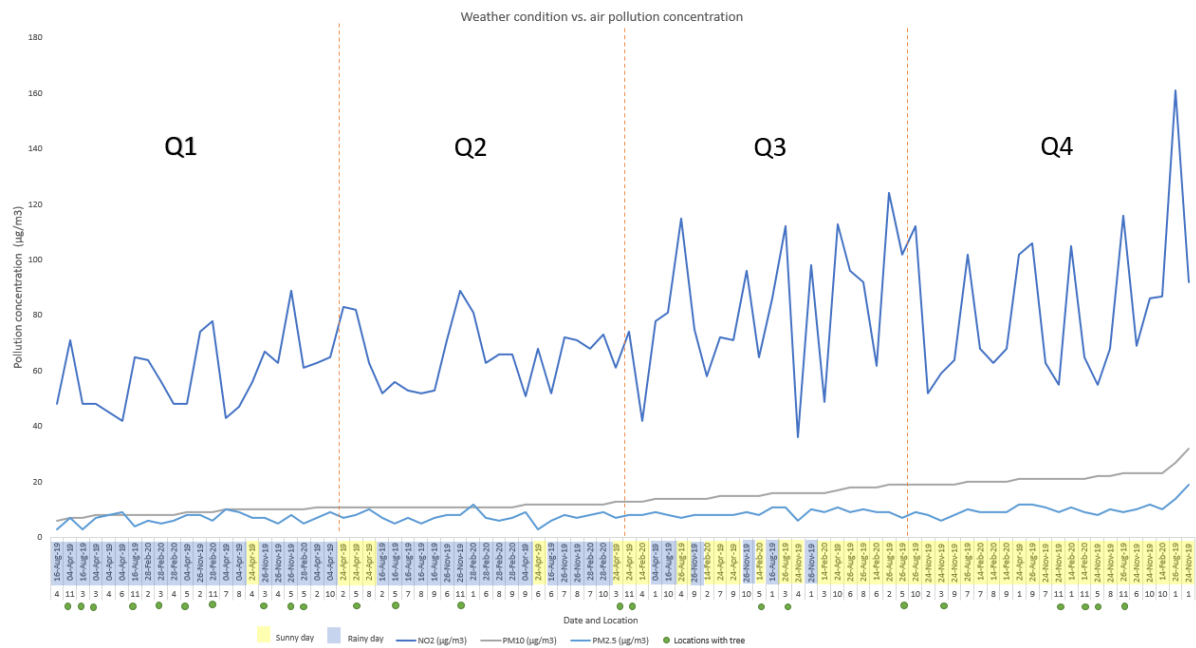
Fig.67 – Weather condition vs. pollution concentration. To understand the relationship between weather conditions and air pollution the graph has been sorted (ordered) based on PM_{10} from lowest to highest levels.
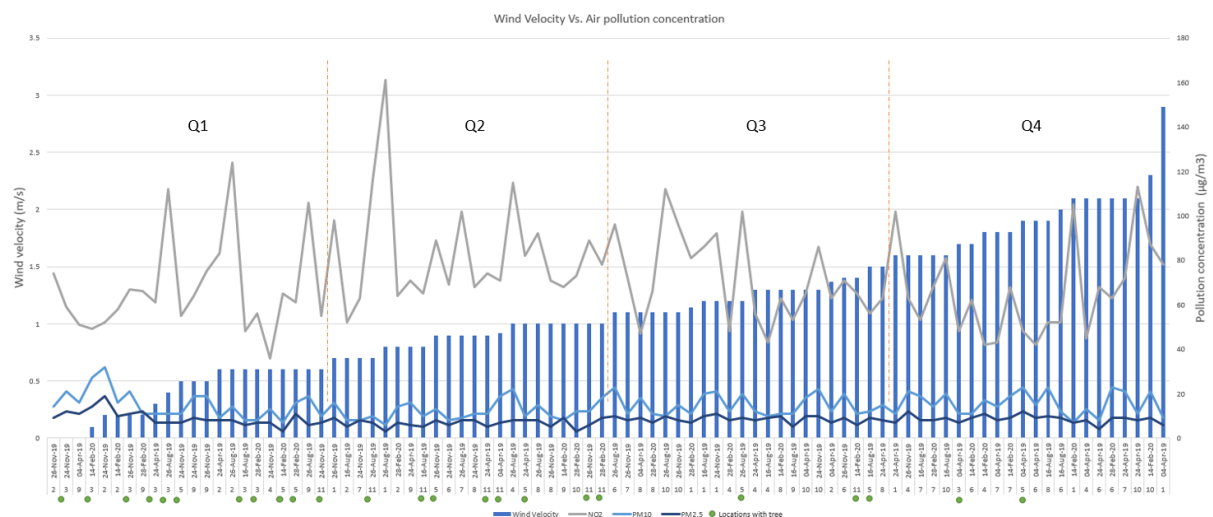
Fig.68 – Wind velocity vs. air pollution concentration. To understand the relationship between weather conditions and air pollution the graph has been sorted (ordered) based on wind velocity from lowest to highest speed (m/s).

Further to the above, the wind velocity pattern as it can be seen in figure 68, the upper quarter Q1, which has 11 locations with trees has the lowest wind speed. In comparison to Q1, the lower quarter Q4 has only two locations with trees and the wind speed reaches its maximum velocity among the 88 measurements. There is undoubtedly a pattern here that corresponds to previous research that was mentioned in chapter 3 at length. Having said that, it's surprising that pollution levels on various days do not follow a consistent pattern, and the presented graph shows no discernible trend. One reason for this is that the time of collection varied between the days; for example, some days measurements were taken in the morning, while others were taken in the afternoon or late afternoon. Furthermore, and perhaps most importantly, variables like traffic flow and weather conditions were varied across the study site and between locations.

To gain a better understanding of how wind velocity affects air pollution, it is ideal to conduct long-term and continuous measurements at a single location, as this minimises the number of dependent variations and makes it easier to observe and spot a trend between wind velocity and air pollution levels. Another important reason is the impact of urban form attributes on wind velocity and air pollution. For example, Location 1, which is adjacent to the street and close to the source of pollution, is innately more polluted; however, Location 2, based on the data collected has demonstrated that the hedgerows placed between the street and the plaza effectively deposit and deflect air pollution away from the plaza, resulting in significant reductions in both air pollution and wind speed and as a result, even though the wind speed is reduced but that didn't necessarily increase the pollutants concentration.

This exploration and realisation brought to light the critical role of urban morphological indicators in influencing microclimate and air pollution, which will be discussed in greater depth in Chapter 6. Figure 69 highlights the different pollution levels between two sides of the hedgerow during the fieldwork measurement on April 24th 2019.
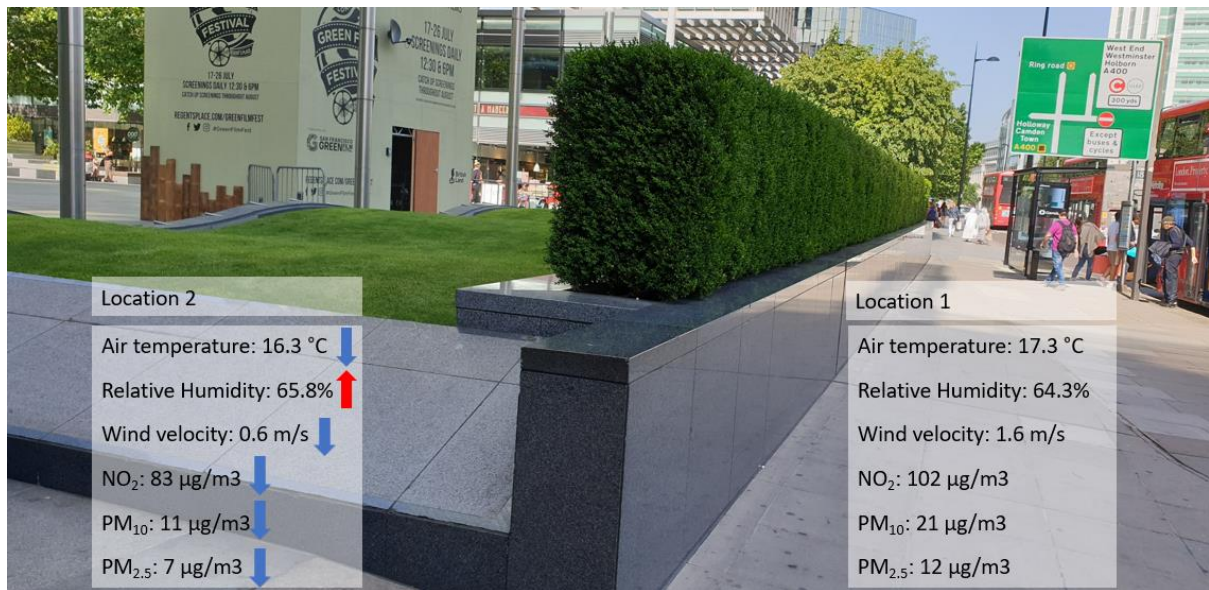
Fig.69 - Meteorological and air pollution data for 24th April 2019 in locations 1 and 2 (top). View from location 2 to location 1 and Euston Road which has been blocked by a hedgerow (bottom).

Air temperature and relative humidity seem to be less influenced by urban morphological indicators, with a more consistent pattern across locations and seasons, and more influenced by seasonal weather change. However, a closer look at the data collected each day and at different locations (Fig.70) reveals that the average air temperature is lowest in location 5, which was shaded by trees and tall buildings with a limited sky view factor of 0.03, and it was the highest in location 1, which is mostly exposed to direct sunlight with the sky view factor of 0.67 which is almost twenty times greater than location 5. The relative

128

humidity was the lowest in location 1 and the highest in location 5. As a result, it is possible to assume that there is an indirect and negative relationship between air temperature and relative humidity at the study site.
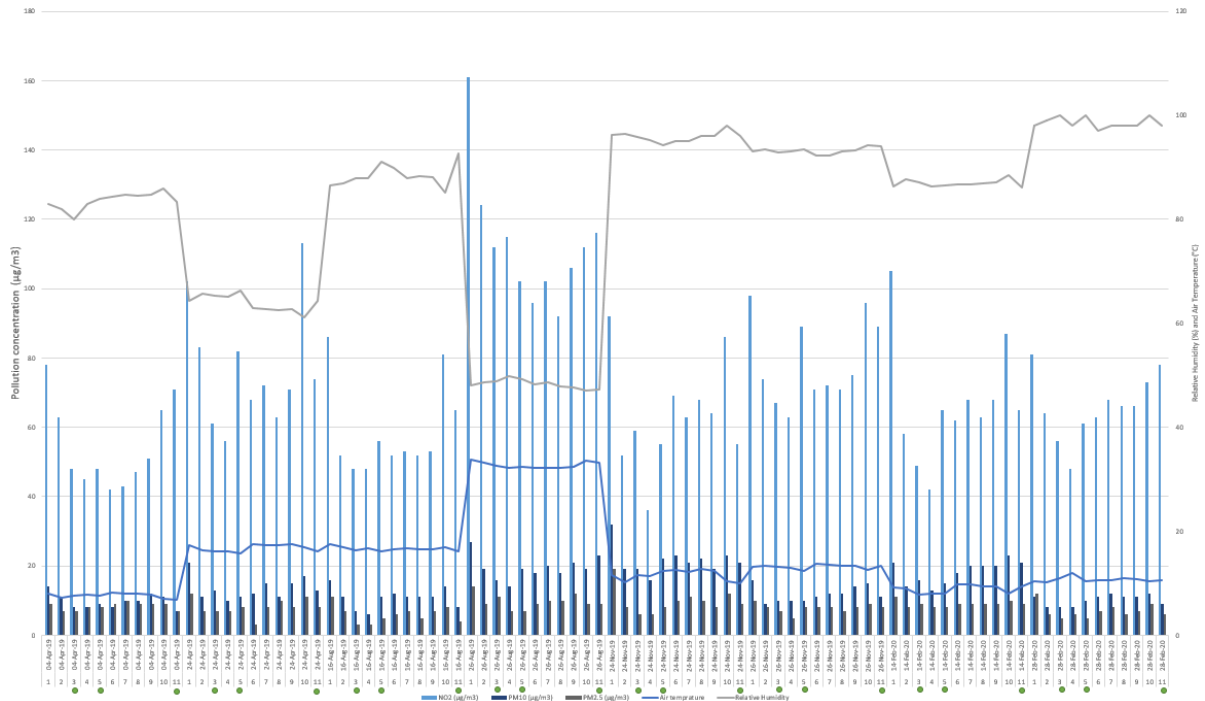
Fig.70 - To understand the relationship between air temperature, relative humidity and air pollution the graph has been sorted (ordered) based on locations and seasons starting from Spring and ending with Winter.

In the following section, the procedures and methods used for computational modelling software (ENVI-met) will be described, as well as the results and findings. Following that, there will be a discussion based on the comparison of spot measurement and ENVI-met results to determine any adjustment needed to be applied to the result of the computational modelling output. This is when any additional calibration will be introduced and applied to computational modelling to provide a much more accurate representation of real-world conditions.

5.4 Methodology of computational simulation and calibration

As mentioned in Chapter 4, the ENVI-met version 4.4.6 application which is a 3D CFD application, was chosen as the computational modelling software for this study because of its proven capability in simulating complex microclimate and air pollution conditions. There

are five main parts in modelling a site in ENVI-met which is illustrated in Figure 71 and explained in the next section.
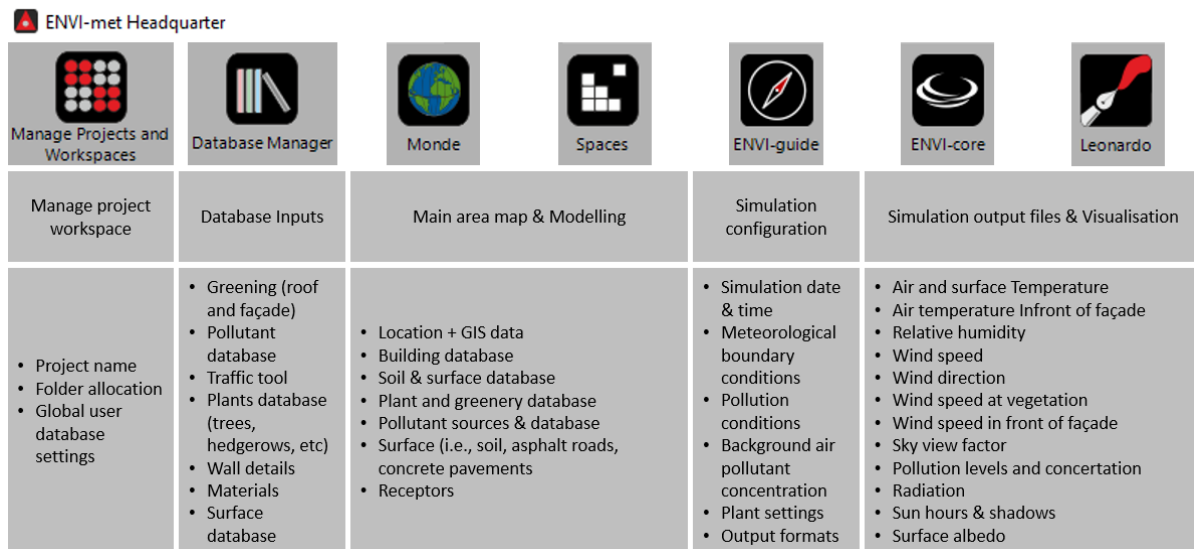
Fig.71 – ENVI-met 4.4.6 Setting and structure

5.4.1 ENVI-met modelling and pollution data settings

The first step is to create the project and populate it with air pollutants data in sources via the 'Manage Database' tab of ENVI-met. It is common practice to extract air pollution data from the co-located air monitoring device or from the nearest air quality station, for example, 'Westminster - Marylebone Road – kerbside' monitoring station operated by King's College London, which sits within a kilometre distance from the study site. However, because the purpose of this study is to establish and understand ENVI-met's accuracy and precision, it was decided to use ENVI-met's 'Traffic Tools,' which is an expert tool for calculating air pollutants values based on traffic counts for each street (Fig.72). The traffic tool is a key feature of air pollution modelling software and an efficient way to model air pollution in the absence of real-time data. In this study, the data related to traffic flow and traffic count was extracted from Department for Transport (Department for Transport, 2019). The street-level road traffic estimates show the number of cars passing through the 'Count Point' location in both directions on an average day of the year. It's worth mentioning that the Department for Transport's traffic count is done over a twelve-hour period on a weekday by a trained enumerator (7 am to 7 pm) (Department for Transport, 2019). However, as illustrated in figure 72, the ENVI-met Traffic Tools require a daily traffic

value of 24 hours. As a result, the missing pollution data for off-peak hours (7 pm–7 am) was calculated using the ENVI-met 'distribution traffic flow tool' (Fig.72a). The off-peak hours were estimated to be 25% of total peak hours (7am -7pm). For example, the traffic count number for Tottenham Court Road extracted from Dft for 12 peak hours was 17012, and by adding 25% to this number, the 24 hour traffic count has increased or adjusted to 21288, with 4274 for off peak hours (7 pm – 7 am).

The percentage of each vehicle category has been entered in the Traffic Tool's traffic composition section. Table 24 shows traffic counts for various vehicle types extracted from the Department for Transport, including taxis, cars, buses, coaches, heavy goods vehicles, light vans and motorcycles. It's worth noting that pedal cyclists are more active on the road early in the morning and late in the afternoon; for cars, this is during lunchtime when most office workers are outside their office to buy or eat lunch. The HDV early morning and LDV are almost constant similar to Bus and Coaches. The data extracted from DfT was used to determine the percentage of vehicles in each category that should be included in the ENVI-met Traffic Tools. Since each vehicle category is associated with a specific level of pollution, it is critical that the vehicle category percentages are accurate, as any discrepancies will have an impact on the emission rate and pollution level. Prior to generating output, one final step is to add the emission factors for the given traffic scenario for each vehicle category. This information should be entered for a single vehicle in the form of [g] per [km]. In this thesis, the Emission Factors Toolkit (EFT) V.10 (DEFRA, 2019) was used to calculate the emission factor for each vehicle category in accordance with the recommendation of Technical Guidance (Department for Environment Food and Rural Affairs, 2018). The EFT is a Defra-published spreadsheet tool that allows calculating NOx, PM_{10}, and $PM_{2.5}$ vehicle emissions factors for a range of vehicle classifications and splits, at a variety of speeds, and on a variety of road conditions. The NO_X and PM Emission Factors were calculated from the Air Pollutant Emission Inventory Guidebook 2019 by the European Environment Agency (EEA) and the European Monitoring and Evaluation Programme (EMEP) (European Environment Agency, 2019). To calculate the total emission from a specific road, the Emissions Factors were combined with newly collected data on fleet composition on various road types as part of the National Atmospheric Emissions Inventory (NAEI, 2019).

Annual Average daily flow								
Year	Count method	Pedal Cycles	Two wheeled motor vehicles	Cars and taxis	Buses and coaches	Light goods vehicles	Heavy goods vehicles	All motor vehicles
2019	Estimated using previous year's AADF on this link	1943	2316	31084	1047	7902	7071	43420

Table.24 – Annual average daily flow divided by vehicle type (Department for Transport, 2019)

As previously stated, the output of EFT would be NOx, PM_{10}, and $PM_{2.5}$, therefore after entering NOx values into ENVI-met, NO and NO_2 values must be generated using the ENVI-met NO/NO_2 generator, which requires the fraction of primary NO_2 emissions (f-NO_2) in the NOx value, which for this study has been extracted from the EMEP/EEA Emissions Inventory Guidebook (EEA, 2013) for the various vehicle type. Once all of these data have been entered into the Traffic Tools, ENVI-met will be able to calculate the emissions associated with these data, which can then be used in the modelling stage for further computation.
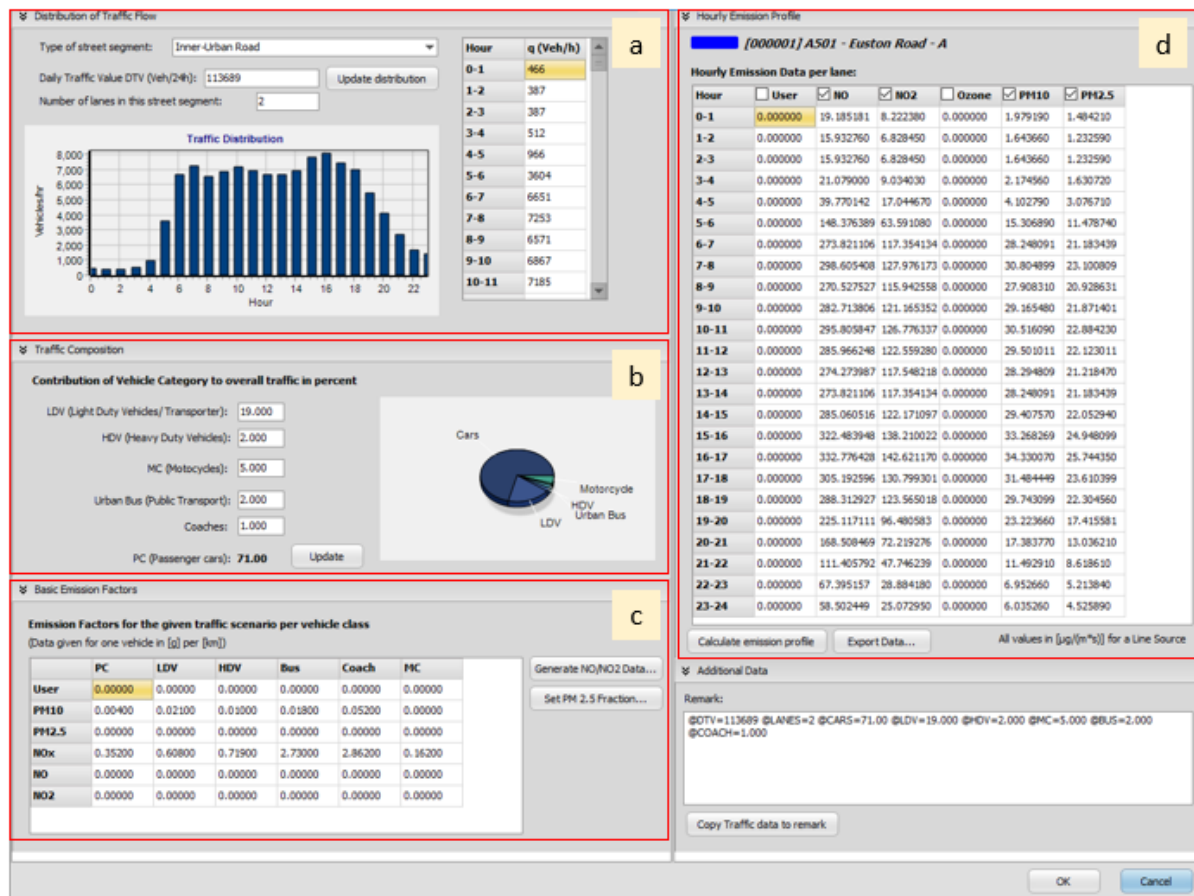
Fig.72 - ENVI-met Traffic Tools interface a) data related to Traffic count b) Traffic composition c) data related to emission factors, data given for one vehicle in [g] per [km] d) Hourly emission profile for NO, NO_2, PM_{10} and $PM_{2.5}$

The next step in ENVI-met air quality modelling is to use 'Spaces' application in ENVI-met which allows digitising a raster-based model area directly in the ENVI-met software. Data from the fieldwork, such as road length and width, building heights and forms, vegetation species and sizes, and surface material, can be added and modelled in Spaces, and pollution data can be added over the roads with various traffic volumes. In this study, the urban form is modelled via 'Monde' tool of the ENVI-met which allows importing an accurate GIS shapefile (Ordnance Digimap Survey Collection, 2019) straight into Spaces. GIS shapefiles are a non-topological vector data storage format used to store the shape, geometric location and attributes of geographic features (Fig.73).

Fig.73 – ENVI-met's Monde interface
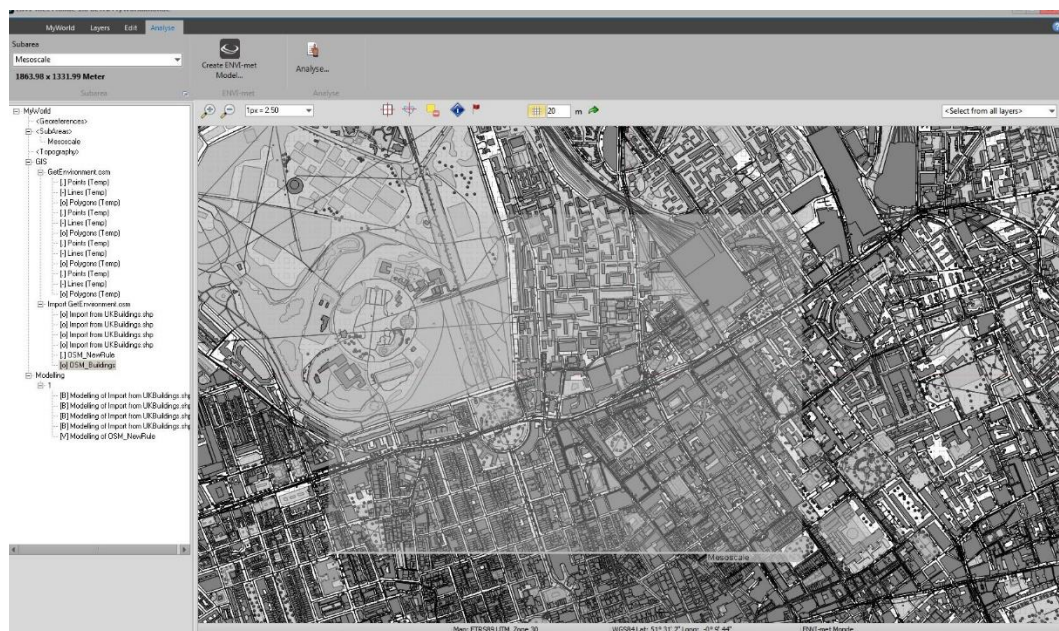
The data from Monde can be opened in Spaces, but further refinement may be necessary to clean up the model and prepare it for simulation processes. Figure 74 illustrates the final model in the local scale, complete with all physical and nonphysical features including buildings, vegetation (trees, hedges, green surfaces), pollution sources, roads, and surface materials such as concrete paving, soil, and asphalt.
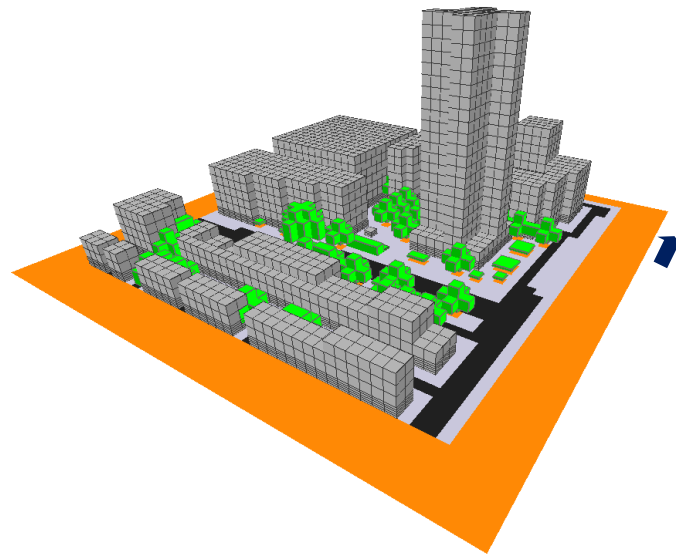
Fig.74 – completed model with all physical and nonphysical features including buildings, vegetation (trees, hedges, green surfaces), pollution sources, roads, and surface materials such as concrete paving, soil, and asphalt.

It's worth noting that the ENVI-met model does not work reliably at model edges or grids that are very close to the model area borders (ENVI-met, 2018b). As a result and based on the ENVI-met guide, all simulation scenarios' nesting areas (grid cells at the borders of the model) were chosen to be sufficiently large in order to improve the simulation result's accuracy and computational stability. For that reason and based on ENVI-met guide (ENVI-met, 2018a), five nesting grid cells (five grid cells at the borders of the model) were set on each side of the model, and the z-grid was set to three times higher than the tallest building in the model site based on Erell E., et al. (2011) guidelines. The resolution was reduced to 6 for all axes (dx, dy, and dz), and the grid dimension was reduced to 50X50X70 (x-Grid, y-Grid and z-Grid) to minimise the simulation's computational (rendering) time. Additional setting and configuration considerations are summarised in Table 25.

Modelling area file (.inx) settings	
Model Location	
Localisation	Euston Road, London, UK
Latitude (deg,+N,-S)	51.52
Longitude (deg,-W,+E)	-0.14
Model Geometry	
Grid dimension (x, y, z)	50 x 50 x 70
Grid cells size (dx; dy; dz)	6m; 6m; 6m
Model rotation out of grid north	-20.00
Nesting Grids	5
Number of nesting grids	

Table.25 - Study site input setting in ENVI-met 4.4.6.

To improve accuracy and mitigate the effects of initialisation and convergence error, the simulation had to run for six hours prior to and following the sampling period (Salata et al., 2015; NG et al., 2012). Due to the fact that the fieldwork involved a two-hour spot measurement period, the total simulation time was set to 14 hours (6 hours prior to interested hours plus 2 hours during interested hours and additional 6 hours after interested hours). The simulation dates are identical to the spot measurements, and the meteorological conditions for the reference meteorological station were obtained from the Met Office (www.metoffice.gov.uk). Accordingly, the minimum and maximum temperatures, relative humidity as well as wind speeds in m/s at ten-meter heights and wind direction were added to ENVI-met. It is important to mention that ENVI-met software accepts wind velocity measurements only at a height of 10 meters. If the wind speed is measured at a different height, the measurement must be adjusted using the formula provided by Mansoureh Tahbaz in her 2009 study titled "Estimation of Wind Speed in Urban Areas with Heights Less than 10 Meters". The correct roughness length at the measurement site was determined using the Davenport roughness terrain classification adapted by Wieringa (1993) (Table.26)

Class	Short terrain description	Z_0 (m)
1	Open sea, fetch at least 5 km	0.0002
2	Mud flats, snow; no vegetation, no obstacles	0.005
3	Open flat terrain; grass, few isolated obstacles	0.03
4	Low crops; occasional large obstacles x/H>20	0.10
5	High crops; scattered obstacles, 15<x/H<20	0.25
6	Parkland bushes; numerous obstacles, x/H≈10	0.5
7	Regular large obstacle coverage (suburb, forest)	1.0
8	City centre with high and low rise buildings	≥2

Table.26 – Aerodynamic roughness length Z0 and terrain classification from Davenport's (1960) adapted by Wieringa (1993)

The concentrations of NO, NO_2, O_3, PM_{10}, and $PM_{2.5}$ in urban background pollution are another important parameter to consider which often it has been ignored in similar studies (Wen, 2017; Glover, 2015). Even though O_3 and NO were not the focus of this study, still these pollutants are required to be included to make up the real-world background air pollution composition. This is because ENVI-met is capable of calculating the effect of chemical reactions between NO, NO_2, and O_3 on the total concentration of each of the pollutants. Needless to say, the pollution levels produced by this process are significantly closer to what is occurring in the real world and one of the advantages of the ENVI-met is that it can account for this in its calculation. Table 27 shows the data related to urban background concentration which were taken from DEFRA air quality statistics (Department Environment For Affairs Food & Rural, 2020). The output from the preceding procedure was saved in a SIM format file for simulation proposes.

Urban Background Concentration	
NO	7.2 µg/m^3
NO_2	15.1 µg/m^3
O_3	64.4 µg/m^3
PM_{10}	13.2 µg/m^3
$PM_{2.5}$	9.8 µg/m^3

Table.27 – Urban background concentration extracted from DEFRA air quality statistics and added in ENVI-met simulation file.

The output of the simulation process can be viewed by the Leonardo tool of ENVI-met. Leonardo tool allows generating a graphical representation of output parameters at one hour time steps and at a specified height which for this study height of 1.50 meter was chosen to match the values with the fieldwork spot measurement. The Leonardo results will then be compared to the spot measurement results to ascertain if any adjustments are necessary to calibrate the ENVI-met and improve its accuracy while also matching its outputs to real-world measurements. As it was mentioned in chapter 4, Pearson correlation analysis was employed to find correlations between two sets of data extracted from the ENVI-met and fieldwork measurement. Furthermore, all correlational analyses, including the creation of graphs and heatmaps, were performed using Microsoft Excel and GraphPad Prism version 9.

5.5 Result of computational simulation and calibration analysis

A total of 8 simulations and 616 simulation outputs were taken from the Leonardo. As previously stated, the locations, dates, and times are identical to those used in fieldwork spot measurement. This has allowed for a like-for-like comparison of variables, culminating in a conclusive result. To avoid repetition, in this section, it was decided to explore and investigate the ENVI-met result through the analysis of the Pearson correlation result and only comment and investigate further if any differences or anomalies appear. To conduct the Pearson correlation between all variables, including temperature, relative humidity, wind velocity, wind direction, NO_2, PM_{10}, and $PM_{2.5}$, a total of 1232 data points were entered into GraphPad (Fig.75). This is the data gathered and extracted from fieldwork spot measurement and ENVI-met results combined. When the ENVI-met result was compared to the spot measurement, it was discovered that the ENVI-met result in most of the variables showed a significant correlation with fieldwork measurement, with temperature (r=+0.98, P≤0.001) and relative humidity (r=+0.96, P≤0.001) being the most noticeable. The Pearson correlation coefficient of r=+0.98 and r=+0.96 for temperature and relative humidity is surprisingly high and shows perfect positive correlation as well as strong significance. Similarly, wind velocity and wind direction show a perfect positive correlation of r=+0.75 and r=+0.79, respectively, with a highly significant p-value greater than 0.001 for both variables. According to these findings, the ENVI-met results are consistent with those

observed in the real world and during the fieldwork spot measurement, making it an excellent software for microclimate analysis.
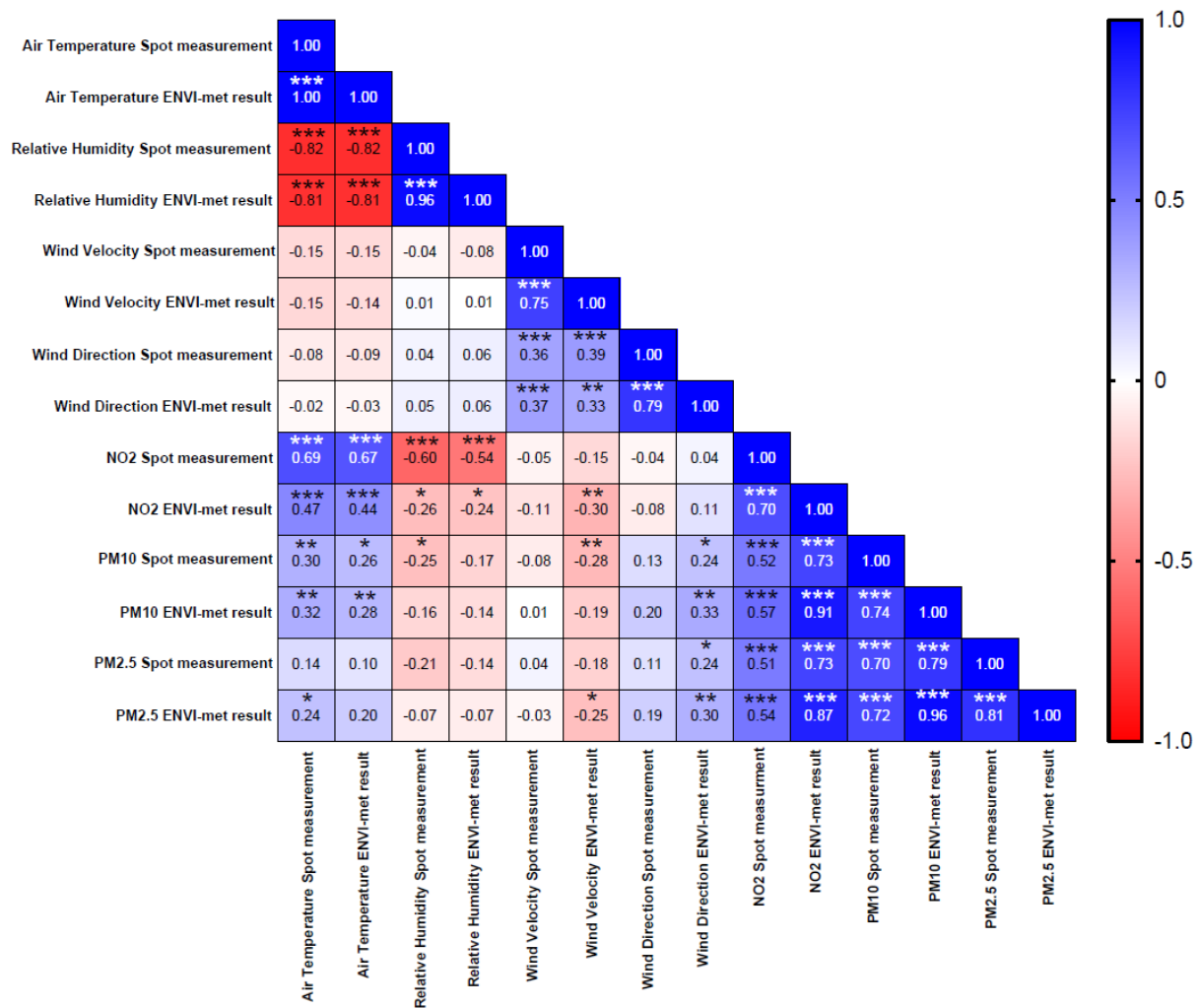
Fig.75 - Heatmap displaying Pearson correlation analysis, R values and p-values between ENVI-met and spot measurement results *(p*≤0.05, **≤0.01, ***≤0.001).*

In terms of air pollutants, $PM_{2.5}$ had the highest correlation coefficient (r=0.81, P≤0.001), followed by PM_{10} (r=+0.74, P≤0.001), and NO_2 had the lowest correlation coefficient (r=+0.70), with a p-value greater than 0.001. The above results were obtained by comparing both dry and rainy day measurements; however, in order to better understand the impact of weather conditions on the correlations, the Pearson correlation was divided based on weather conditions, i.e. dry and rainy days (Fig.76 and Fig.77). The extracted coefficients are compiled in table 28. These results show that ENVI-met is less accurate when accounting for wet deposition, but the correlation coefficient of +0.60 and P-value greater than 0.001

demonstrate that ENVI-met still is a reliable and good fit for future simulations. Furthermore and except for NO2, all of the other correlation coefficients are higher in dry weather conditions, indicating that, for an idealised scenario or any future simulation, dry weather should be considered because the outcomes are more in line with real-world measurements.
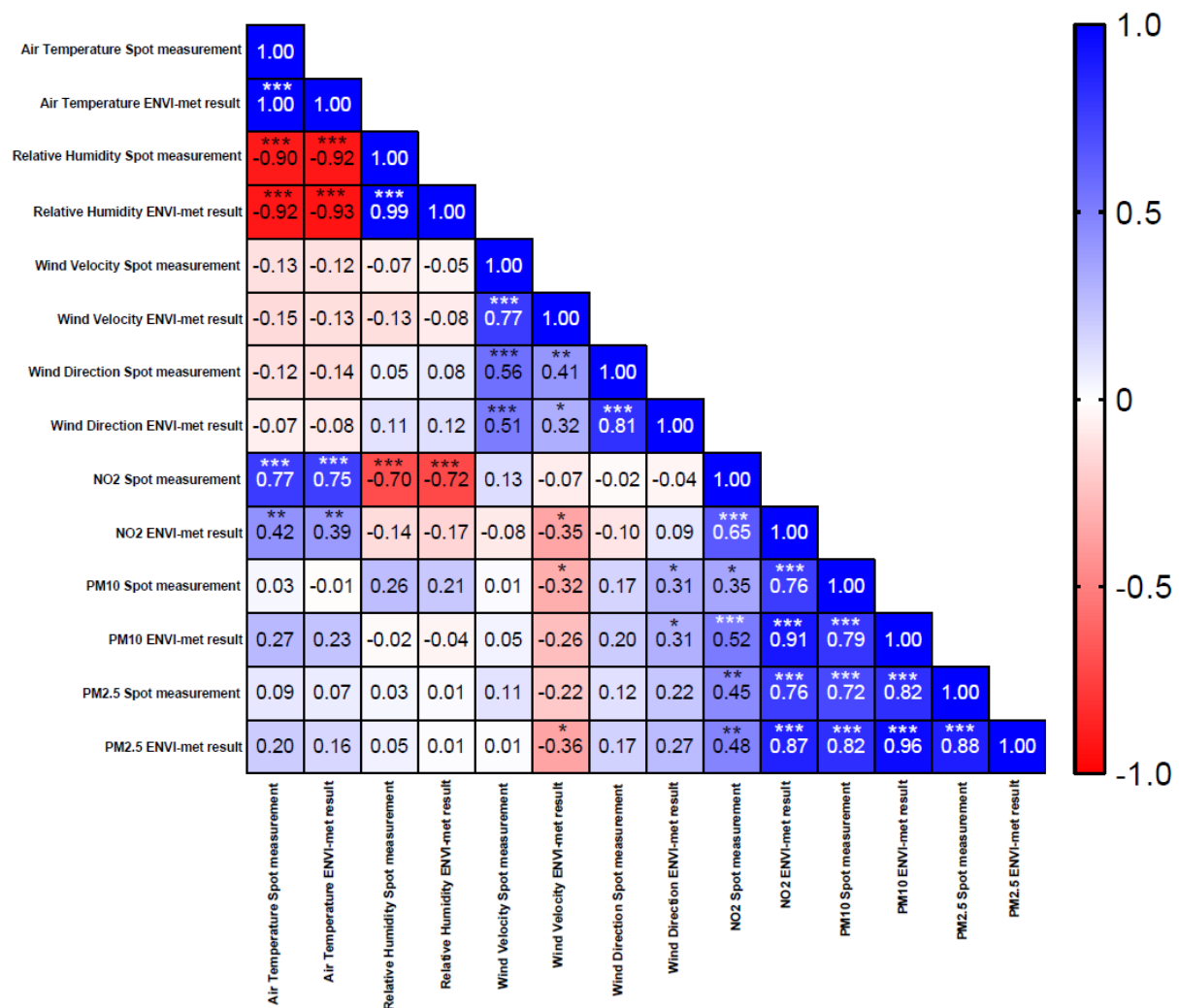
Fig.76 - Heatmap displaying Pearson correlation analysis, R values and p-values between ENVI-met and spot measurement results, representing dry day (p*≤0.05, **≤0.01, ***≤0.001).
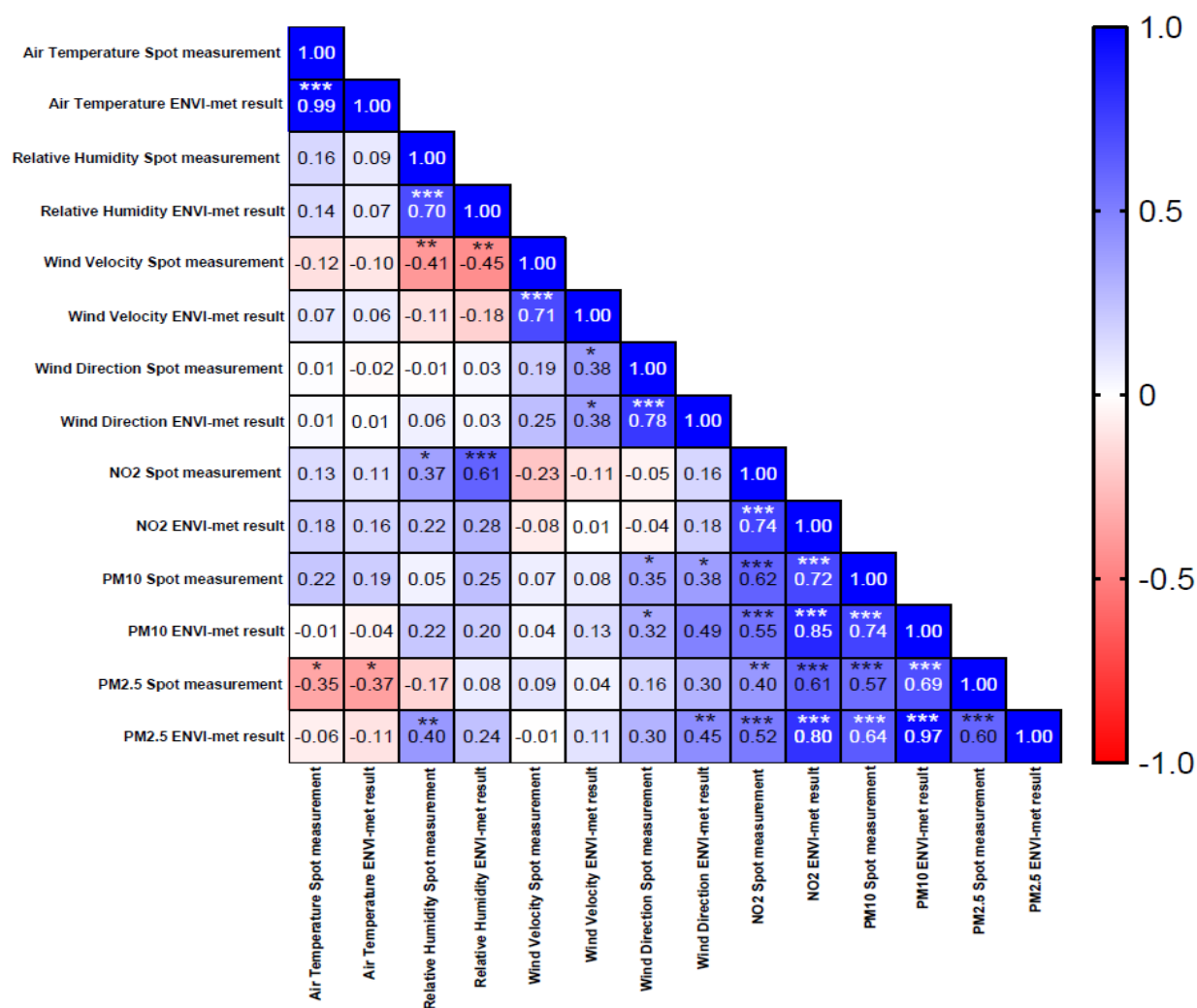
Fig.77 - Heatmap displaying Pearson correlation analysis, R values and p-values between ENVI-met and spot measurement results, representing rainy day *(p*≤0.05, **≤0.01, ***≤0.001)*.

Parameters	Dry days	Rainy days	Dry & Rainy days
Temperature	+0.99	+0.98	+0.98
Relative Humidity	+0.99	+0.70	+0.96
Wind velocity	+0.77	+0.71	+0.75
Wind Direction	+0.81	+0.78	+0.79
NO_2	+0.65	+0.74	+0.70
PM_{10}	+0.79	+0.74	+0.74
$PM_{2.5}$	+0.88	+0.60	+0.81

Table.28 – Pearson correlation coefficient of all parameters for dry, rainy and combined days.

A closer look at the data revealed that the mean percentage difference between spot measurement and ENVI-met for temperature and relative humidity is 7% and 9%, respectively. The wind velocity is the opposite, which means that the ENVI-met values on average have a higher wind velocity than spot measurements (the mean percentage difference of 45%). One reason for this difference is that the ENVI-met model did not have all of the details as the real world scenario, and there are many urban form attributes that could have impacted wind velocity that were not modelled in ENV-met, resulting in the outcomes being different and with higher wind velocity. The same exploration into air pollutants revealed that NO_2 levels in the real world are on average 32% higher than the ENVI-met. As previously stated, NO_2 is a gaseous pollutant that is expected to be more dynamic and local than particulate matter. In contrast to NO_2, the level of PMs measured by ENVI-met is higher than the level measured during the spot measurement. The mean percentage difference is 32% and 43% higher in PM_{10} and $PM_{2.5}$, respectively. It is worth noting that the concentration of pollution pattern between spot measurement and ENVI-met was the same even if the levels were generally lower (for NO_2) or higher (for PMs). As it can be seen in figure 78, the same pattern of pollution reduction similar to the fieldwork measurement can be observed behind the hedgerow (Location 2 of the fieldwork spot measurement). The ENVI-met vegetation module similar to fieldwork study effectively deposits and deflects air pollution away from the plaza.
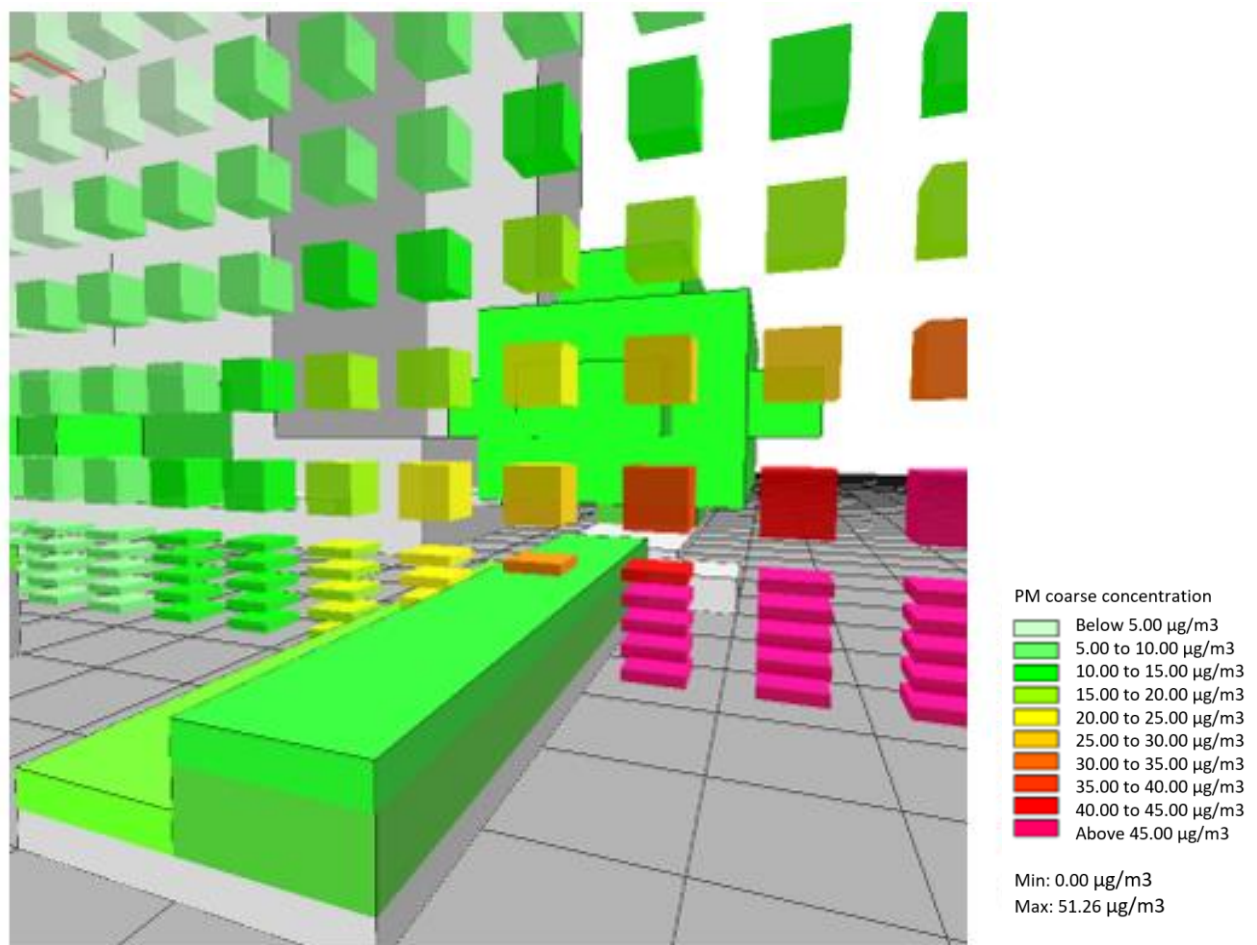
Fig.78 - Snapshot of PM$_{10}$ concentration levels around hedgerow at the south side of the Regent Place Plaza (Location 1 & 2 of the spot measurement)

As a result, and as shown by the Pearson correlation, the ENVI-met and spot measurement values are highly correlated, making the ENVI-met software a reliable software to use for microclimate and air pollution studies. However, it has been discovered that the levels are somewhat different, either being higher or lower than the spot measurement value, necessitating the calibration of the ENVI-met application. Therefore, the same procedure used for head sensor calibration was used here, with the results shown in table 29. With the exception of temperature and relative humidity which have $R^2 = 0.99$, Y=1.00x-1.06 and $R^2=$ 0.91, Y=0.81x+8.42 respectively the rest of the variables were indicated lower R-square. For that reason, in order to offer a higher R-square, it was decided to run the scatter plot for rainy, dry and different seasons separately. Table 29, therefore, presents the R-square and respective calibration equations that were taken into account in the above decision.

	Spring dry day	Spring rainy day	Summer dry day	Summer rainy day	Autumn dry day	Autumn rainy day	Winter dry day	Winter rainy day	Total dry day	total rainy day	
PM$_{2.5}$	0.87	0.48	0.78	0.75	0.86	0.64	0.77	0.84	0.77	0.36	R-square
	$x=(y-1.58)/1.05$	$x=(y-5.35)/0.66$	$x=(y-2.73)/1.34$	$x=(y-6.56)/0.73$	$x=(y-1.01)/1.50$	$x=(y-0.5)/1.42$	$x=(y+3.17)/1.81$	$x=(y-6.91)/0.93$	$x=(y+0.34)/1.53$	$x=(y-6.95)/0.65$	Calibration equation
PM$_{10}$	0.66	0.68	0.6	0.76	0.75	0.79	0.5	0.51	0.62	0.54	R-square
	$x=(y-9.19)/0.62$	$x=(y-12.77)/0.51$	$x=(y-6.03)/0.94$	$x=(y-9.24)/0.81$	$x=(y+11.75)/1.67$	$x=(y-5.27)/1.14$	$x=(y-9.48)/0.52$	$x=(y-6.86)/1.25$	$x=(y-3.85)/0.96$	$x=(y-10.04)/0.80$	Calibration equation
NO$_2$	0.67	0.71	0.93	0.75	0.74	0.59	0.91	0.51	0.42	0.54	R-square
	$x=(y+4.85)/0.53$	$x=(y-17.26)/0.40$	$x=(y+50.97)/01.24$	$x=(y+7.87)/0.86$	$x=(y+71.78)/2.36$	$x=(y+29.40)/0.97$	$x=(y+5.38)/0.70$	$x=(y+23.19)/1.03$	$x=(y+6.91)/0.85$	$x=(y-1.65)/0.64$	Calibration equation
Wind velocity	0.7	0.52	0.2	0.46	0.56	0.75	0.5	0.7	0.59	0.5	R-square
	$x=(y-0.37)/1.54$	$x=(y-0.72)/0.81$	$x=(y-0.56)/0.68$	$x=(y-0.10)/1.54$	$x=(y-0.49)/0.64$	$x=(y-0.71)/1.14$	$x=(y-0.97)/0.66$	$x=(y-0.67)/1.19$	$x=(y-0.35)/1.18$	$x=(y-0.79)/0.95$	Calibration equation

Table.29 – Equation to convert the output from ENVI-met to real-world spot measurement. In this formula (y) is the measurement from ENVI-met and (x) is the spot measurement value.

In this way, any future simulation depending on their weather condition and season can be calibrated to real world measurement. Needless to say that the more scatter in the data the farther R-square is from 1 and the less useful the calibration. It is worth mentioning that, the R-square presented in the above table can still be used for any future calibration, however this is less useful for matching with the real world measurement. Having said that, one can still generate many data with the low R-square because it is not expected from the current model with high variability to include all the relevant predictors to explain the outcome variable. After all, the R-square is a measure of explanatory power and not fit. For that reason, in the next chapter, only dry day and summer and winter seasons will be used for further computational simulation.

5.6 Conclusion

This chapter carried out a full-scale experiment (fieldwork study) to gain a better understanding of pollution dispersion within different real-world urban street canyon types with varying sky view factors and aspect ratios. The fieldwork study was carried out in Regent's Place Plaza, on Euston Road, one of London's most polluted roads. As part of this fieldwork study, 88 spot measurements (from 11 locations) were collected over the course

of eight days. The eight days were chosen from four seasons to provide more coverage and to address some of the knowledge gaps identified in chapter 4, where many studies did not consider seasonality in their research. Importantly, all portable air quality monitors were co-located and calibrated next to a continuously monitored reference station.

According to the findings of the fieldwork, the concentrations of air pollutants such as NO_2, PM_{10}, and $PM_{2.5}$ were highest on dry days and primarily during the summer and autumn seasons. On average, the location which had the shortest distance to Euston Road had the highest pollution level throughout the year. Most notably, locations with trees and vegetation were found to have the highest levels of pollution. The same locations also had the lowest wind speed, indicating the role of green infrastructure in influencing the microclimate and thus the concentration of air pollution. In contrast to this understanding, the fieldwork made an interesting discovery; the results of the measurements on different days and weather conditions indicated that a 2-metre hedgerow placed between the roadside and the Regent's Place plaza effectively deposited and deflected air pollution away from the plaza, resulting in significant reductions in both air pollution and wind speed, and as a result, even though the wind speed is reduced, it did not necessarily increase the pollution levels. This is a discovery that can be used as an effective mitigation strategy in the following chapters.

This chapter also compared the results of the fieldwork with the outputs of computational simulation (ENVI-met) of the same study site. All the locations, dates, and times were identical to those used in fieldwork spot measurement. This has offered a like-for-like comparison and an opportunity to calibrate the ENVI-met and improve its accuracy while also matching its outputs to real-world measurements. In total, eight simulations and 616 simulation outputs were extracted from the ENVI-met.

The correlation analysis revealed that the ENVI-met and spot measurement values are highly correlated, indicating that the ENVI-met software is a reliable tool for microclimate and air pollution research. However, the correlation analysis revealed a much stronger correlation with dry day measurements, so in the following chapter, only dry days and

summer and winter seasons will be used for further computational simulation. Furthermore, it was discovered that the levels were slightly different, being either higher or lower than the spot measurement value, necessitating the calibration of the ENVI-met application outputs. As a result, this chapter provided an equation for converting ENVI-met outputs to real-world spot measurement. Table 29 shows these equations which can be used for any future study.

As a result, for the first time, this thesis enabled any future simulation to be calibrated to real-world measurements based on weather conditions and seasons. The knowledge gained in this chapter will be applied to the design of idealised street canyons in chapter 6, which will investigate the impact of microclimate and urban form on the concentration of air pollution in a variety of idealised urban street canyons. Furthermore, additional discussion on the findings of this chapter is provided in Chapter 7 to inform the development of the set of recommendations for influencing the microclimate and reducing air pollution concentrations within street canyons.

Part 2

Computational model and analysis of pollutant dispersion in idealised urban street canyons

Chapter 6

Chapter 6

Computational model and analysis of pollutant dispersion in idealised urban street canyons

One of the key objectives of this study, as stated in the introduction to this thesis in chapter 1, is to identify those urban form attributes that have the greatest impact on air pollution concentrations within urban street canyons. As a result, by using the knowledge gained in chapter 5, this chapter investigates the behaviour of air pollutants within the idealised urban street canyons identified in Chapter 3, i.e. mews, residential, high street, narrow high street, and boulevard street canyons. The advantage of using computational simulation models, as mentioned in chapter 4, is that they can be calibrated and adjusted based on fieldwork measurements and then used to provide information beyond the point measurements made in the field. Another advantage of computational simulations such as ENVI-met application is that every single pixel in the model site can be modified, and its impact can be calculated in understanding their effect on microclimate and specially air pollution dispersion or concentration.

In order to ensure broader applicability for future studies, each urban street canyon is divided into three main configurations. The symmetric urban canyon (H1=H2), the asymmetric step-up canyon (H1≤H2), and the asymmetric step-down canyon (H1≥H2) are the main configurations used for this exploration. With the exception of mews street canyon, all other canyon configurations were simulated once with and once without trees. The result of this investigation is presented and discussed in this chapter and will be complemented by correlation analyses in chapter 7 to develop a comprehensive set of recommendations to improve dispersion rate and air quality levels within various urban canyon configurations.

6.1 Methodology

The findings of chapter 5 demonstrated that dry weather conditions provide the most accurate inputs for ENVI-met to generate a representation of real-world conditions. The ENVI-met analysis showed to be less accurate when accounting for wet deposition whereas the correlation coefficient is higher in dry conditions and the outcomes are more in line with real-world measurements. In light of the climate analysis presented in Chapter 5, and in order to clearly identify the impact of meteorological conditions such as temperature and relative humidity on air pollution concentration, two dry days with extremely opposite meteorological

conditions were chosen, one in the warmest month of the year (August) and the other in the coldest month of the year (February).

Due to ENVI-met's input data requirements, information relating to air pollution, air temperature, and relative humidity must be entered for a 24-hour period, while wind speed and wind direction are averaged. For that reason and in order to make the results of this study more applicable to London meteorological conditions, summer and winter dates were carefully selected to ensure that the wind velocity corresponds to the annual mean velocity of 2 to 3m/s in London and follows the prevailing wind direction of London, i.e. west to east (Fig.57a). As a result, the 3rd August 2018 were chosen for the summer period and 11th February 2019 were chosen for the winter period. The wind direction on both days was from west to east, with the average wind speed of 2.5m/s. It is worth noting that, the wind is perpendicular to the canyon axis of idealised street canyons as this is the most polluting condition, as determined by the findings of Chapter 3.

In terms of air pollution data, in order to gain a better understanding of how different urban canyon configurations and vegetation affect air pollution concentrations, it was decided to keep the pollution levels the same for both summer and winter days. Furthermore, in order to broaden the applicability of the study's findings, a date with air pollution levels closer to London's mean annual pollution levels was chosen for the two nominated days. Accordingly, the pollution data related to 3rd August 2018 was used for both the winter and summer days, as its air pollution levels were nearly similar to the London's annual mean pollution levels presented in Chapter 5, making this day a good representation of pollution levels on many other days throughout the year (Fig.79). The values for NO_2, PM_{10}, and $PM_{2.5}$ are shown in Table 30. The only variables that differ between the winter and summer periods are the air temperature and relative humidity levels. Table 31 summarises these values, which were obtained from www.metoffice.gov.uk (Met Office, 2021) and the monitoring station 'Westminster - Marylebone Road - kerbside' (London Air, 2019).
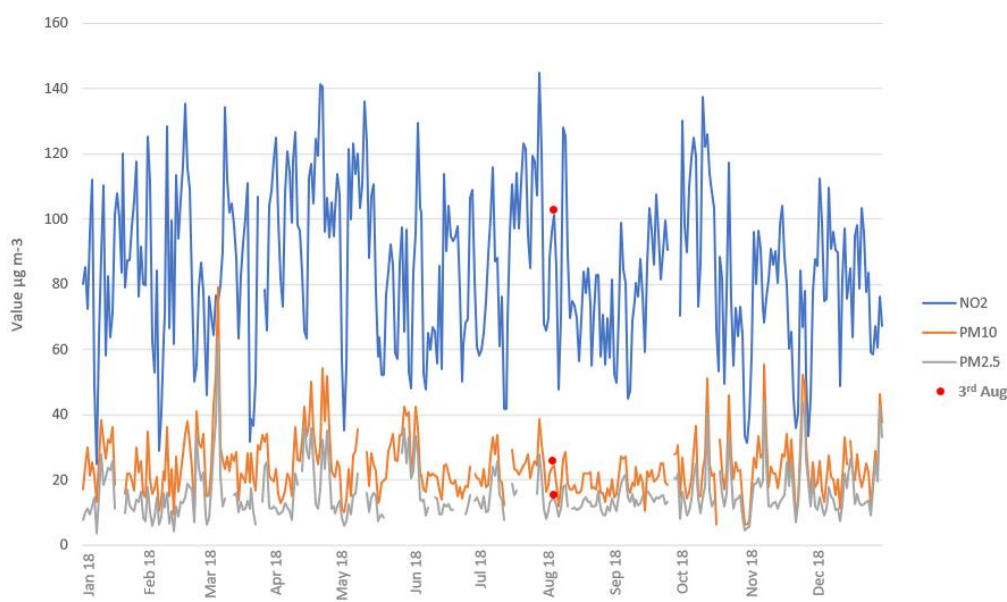
Fig.79 – Daily mean reading from 1st Jan 2018 to 31st Dec 2018, with the indication of pollution level on 3rd August 2018 which is nearly the same as the mean annual pollution levels. Data were extracted from 'Westminster - Marylebone Road – kerbside' monitoring station (London Air, 2019).

Time	NO_2 µg m^{-3}	PM_{10} µg m^{-3}	$PM_{2.5}$ µg m^{-3}
1:00 AM	61.1	15.7	8.5
2:00 AM	50.1	13.6	8.6
3:00 AM	49.2	13.6	9.3
4:00 AM	48.2	13.7	8.3
5:00 AM	55.8	18.3	9.3
6:00 AM	59.9	12.4	9
7:00 AM	56.2	18.8	12.5
8:00 AM	68.2	20.7	13.2
9:00 AM	112.2	26.2	13.7
10:00 AM	129.7	16.6	16.7
11:00 AM	127.6	23	14
12:00 PM	147.39	21.3	18.1
13:00 PM	159.3	24.6	19.3
14:00 PM	155.6	30.4	16.3
15:00 PM	131	23.1	18.4
16:00 PM	180.1	25.9	15.2
17:00 PM	90.8	30.2	13.7
18:00 PM	52.8	35	8.7
19:00 PM	54.9	23.2	11.1
20:00 PM	51.6	18.7	9.2
21:00 PM	42.9	17.9	10
22:00 PM	46.9	17.9	10.8
23:00 PM	46.2	16.5	8.4
24:00 PM	79.9	20.7	15.1

Table.30 - Air pollution data for summer and winter simulation. 3rd August 2018 data were extracted from 'Westminster - Marylebone Road – kerbside' monitoring station.

Time	Temperature 3rd August	Temperature 11th February	Relative Humidity 3rd August	Relative Humidity 11th February
1:00 AM	20	3	83%	87%
2:00 AM	19	4	83%	87%
3:00 AM	18	3	88%	87%
4:00 AM	18	1	88%	93%
5:00 AM	17	0	94%	93%
6:00 AM	17	0	94%	93%
7:00 AM	18	0	94%	93%
8:00 AM	21	1	78%	93%
9:00 AM	23	4	69%	87%
10:00 AM	25	6	61%	81%
11:00 AM	27	7	54%	76%
12:00 PM	28	8	51%	71%
13:00 PM	29	8	43%	66%
14:00 PM	30	8	38%	66%
15:00 PM	31	8	38%	66%
16:00 PM	32	8	38%	66%
17:00 PM	31	8	43%	66%
18:00 PM	30	6	49%	76%
19:00 PM	28	7	55%	71%
20:00 PM	26	8	61%	66%
21:00 PM	25	7	61%	71%
22:00 PM	25	6	61%	71%
23:00 PM	23	2	69%	81%
24:00 PM	22	1	73%	81%

Table.31 – Temperature and relative humidity for 3rd August 2018 and 11th February 2019. Meteorological values extracted from www.metoffice.gov.uk

Due to the fact that this study was piloted on an idealised street canyon configuration and the data was extracted from a reference air quality monitoring station, no background concentrations were added to the simulations, and thus the values are absolute and serve only to demonstrate the difference in air pollution levels between various locations inside the urban street canyon. The receptors were placed based on the Local Air Quality Management Technical Guidance 16 published by DEFRA (2018) and located in potential 'hot spots' within the canyon's middle section (Fig.80).
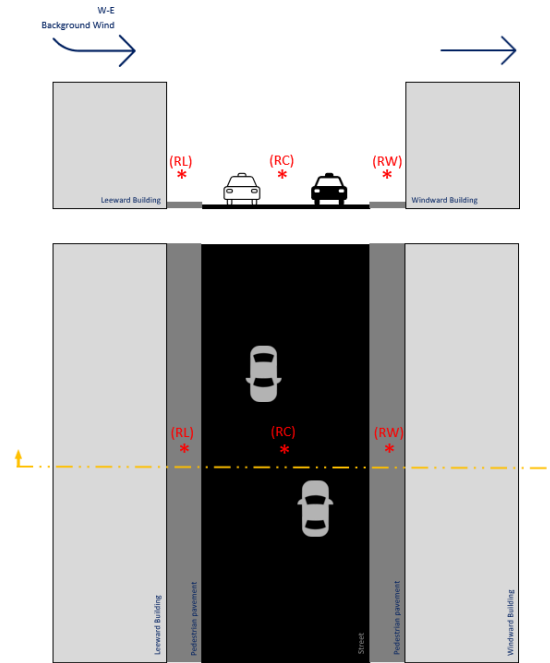
Fig.80 – Schematic diagram of a typical street canyon showcasing the location of the receptors. Receptors were placed at the exact height of the fieldwork study, which was 1.5 metre above the ground. (RL) Receptor located at the leeward side (RC) Receptor located in the centre and (RW) Receptor locate at the windward side of the canyon.

As a result, one receptor has been located on each side of the urban canyon, i.e. leeward and windward sides, to represent the locations of maximum pedestrian exposure, and one has been located in the canyon's centre to represent the pollution level close to the source of pollution. It is worth noting that the receptors were placed at the exact height of the fieldwork study, which was 1.5 metre above the ground. This enables a more precise comparison of the simulation result and the data extracted from the fieldwork study. The data from the leeward and windward receptors were then compared to the data from the receptor located in the centre and expressed as a percentage change between the two locations. The percent change was calculated using the below formula:

$$\frac{(\text{leeward or windward value } - \text{ centre value})}{|\text{centre value}|} \times 100$$

Similar to the fieldwork study, the tree species selected as Platanus × acerifolia (London Plane) tree which is a deciduous tree with large maple-like leaves during the summer and loses its leaves during the colder months of the year, leaving the bare canopy shape with exposed

152

empty branches and trunk. The tree arrangement in configurations with tree scenario followed spacing guidance specified by Manual for Street (2007 & 2010) and Urban tree manual version 15 (2018). As a result, trees were spaced apart based on their mature canopy spread, allowing for the development of the tree's open grown form and to retain their individual identity when investigating their role in impacting the microclimate and air pollution concentration. In addition to that, this spacing arrangement in real-world scenario protects the foundations, sewers and drains and maintains a safe distance from buildings.

To calculate the green cover ratio, the area of the canopy of the fully matured tree was calculated and multiplied by the number of trees within each canyon configuration and divided by the total area of the site and indicated as a percentage. To calculate the percentage of impervious surfaces, the total impervious surfaces in square metre are divided by the total area plane and then multiplied by 100. Based on the Tree Council tree planting guide (The Tree Council, 2012), one square meter around the tree must be filled with soil or pervious material. The building width and height, together with street and pedestrian area width were taken from Street Manual (2007) and inclusive mobility (2005)(Kelly, 2012) published by Department for Transport.

The sub-classification introduced by Oke (1988) which was highlighted in chapter 3 led to the selection of a 62-metre-long buildings on each side of the canyon for this study. This number is based on the average building height of all street canyon types multiplied by five to represent the dimensions of a medium urban canyon. It is important to note that the length and width of buildings were kept the same across all the canyon types and configurations to gain a better understanding of the impact of building height variation on air pollution concentration. Other settings and configurations of ENVI-met software and morphological indicators used in this chapter have been summarised in Table 32 of this chapter and Table 09 of chapter 3.

Modelling area file (.inx) settings		Simulation file (.sim) settings	
Model Location		**Start and duration of model run**	
Localisation	London, UK	Start Date (DD.MM.YYYY)	Variable
Latitude (deg, +N, -S)	51.51	Start time (HH:MM)	10:00
Longitude (deg, -W, +E)	-0.13	Total simulation time (h)	14
Model Geometry		**Initial meteorological conditions**	
Grid dimension (x, y, z)	50 x 55 x 30	Wind speed at 10m height (m/s)	2.5
Grid cells size (dx; dy; dz)	2m; 2m; 2m (different in	Wind direction (deg)	270
Model rotation out of grid		Air Temperature (°C)	17 (min.) – 32 (max.) Summer
north	0.0		0.0 (min.) – 8.0 (max.) Winter
Nesting Grids		Relative Humidity in 2m (%)	38 (min.) – 94 (max.) Summer
Number of nesting grids	5		66 (min.) – 93 (max.) Winter
		Pollution Dispersion	
		Operation mode	Multi Pollutant
		Chemistry (NO-O3-NO2)	Dispersion & Action Chemistry

Table.32 - ENVI-met 4.4.6 input data and settings (summer and winter periods)

6.2 Result and discussion of computational modelling of urban street canyons

This section presents the five studied idealised urban street canyons with a total of 30 configuration variations. In all configurations, the street and building orientations are identical and perpendicular to the upwind of westerly wind direction. As it was mentioned in chapter 3, the perpendicular wind direction is considered the worst case scenario in terms of air pollution concentration for any urban canyon configuration. The following results include only the Leeward Receptors (LR) and Windward Receptors (WR) values, firstly, because the areas of interest are the sides of the canyon where higher pedestrian activities are taking place. Secondly, the receptor in the centre of the canyon was too close to the main source of pollution to be included in this study and was only used to calculate the leeward and windward percentage change from the source of pollution.

6.2.1 Mews street canyon

The mews street canyon has a width of 10 metre and a street length of 62 metre for both symmetric and asymmetric canyons. Road covers 33.33 percent of the site's total area, with no designated pedestrian area or planting trees. In symmetric and asymmetric canyons, the mean height of buildings are 10 and 8 metre, respectively, with building height differentials (ΔH) of 4 metre. The upwind of west wind blowing toward the east resulted in the creation of

a skimming flow regime in the symmetric and asymmetric step-down canyon (Fig.81 a & c) and wake interference flow regime in the asymmetric step-up canyon configuration ((Fig.81 b).
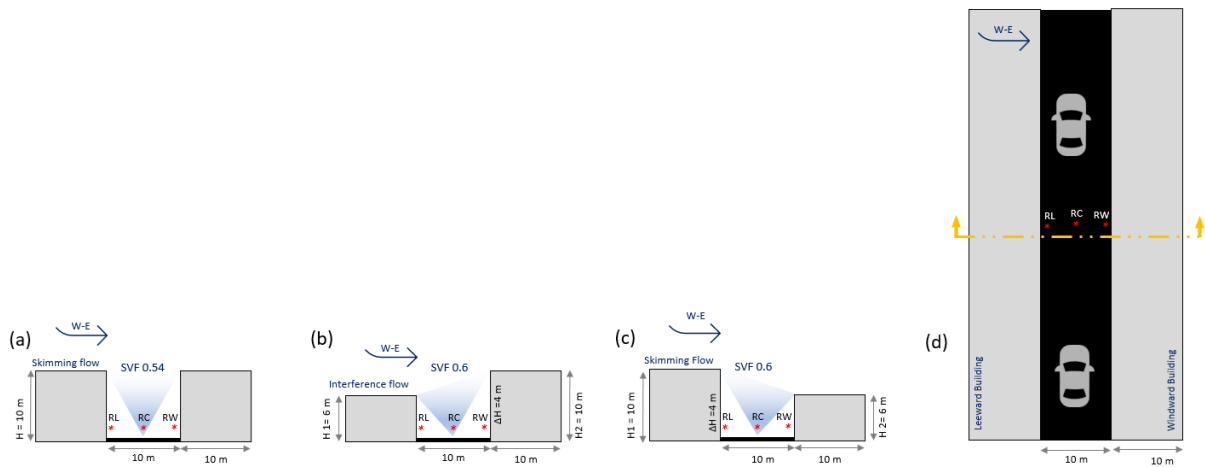
Fig.81 – Schematic plan and section view of mews street canyon. (a) Symmetric, (b) Step-up asymmetric, (c) Step-down asymmetric and (d) plan view with section line.

The windward side of the asymmetric step-up canyon had the highest reduction in pollutants, followed by the leeward side of the same configuration in both summer and winter periods. The highest level of pollution was recorded on the leeward and windward sides of the symmetric street canyon during both summer and winter periods. One explanation is that the low winter air temperature or high summer air temperature and heating that occurred on various surfaces, such as the road surface and building roofs and facades, as well as overall buoyancy due to temperature stratification, complicated and exacerbated skimming flow regime and influenced the wind flow pattern and pollutant dispersion behaviour (Esch, 2015; Ng, 2012; Kim and Baik, 1999; Xie, Liu and Leung, 2007).

This is an interesting finding and will be discussed and investigated further in the next section. When the pollution levels on the leeward and windward sides are compared, it can be observed that the pollution levels at the leeward sides were always higher than the windward sides, regardless of canyon type or building heights (Fig.82).
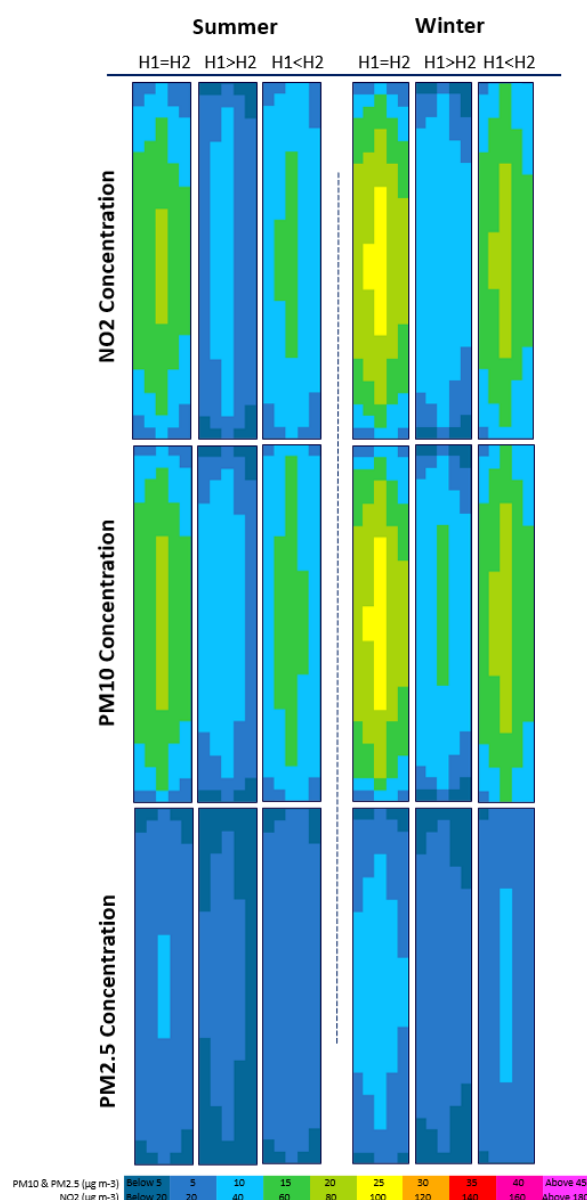
Fig.82 – Pollution levels within various mews street canyon configurations with west to east wind direction. Only the pollution levels between two buildings at a height of 1.5 metres above the ground are illustrated in the graph.

On average, NO₂, PM₁₀ and PM₂.₅ were reduced by 30% when compared to the receptor located in the centre of the canyon. The lowest reduction is at the leeward side of the symmetric canyon with only 15% reduction in all pollutants and in both summer and winter periods. Interestingly, the step-down asymmetric with sky view factor (SVF) of 0.6 showed to have the highest dispersion rate of 30% across all pollutants, i.e., NO₂, PM₁₀ and PM₂.₅ during the summer period but this is not the case in the winter period but still one of the highest reductions between other canyon configurations (Fig.83 and Fig.84).
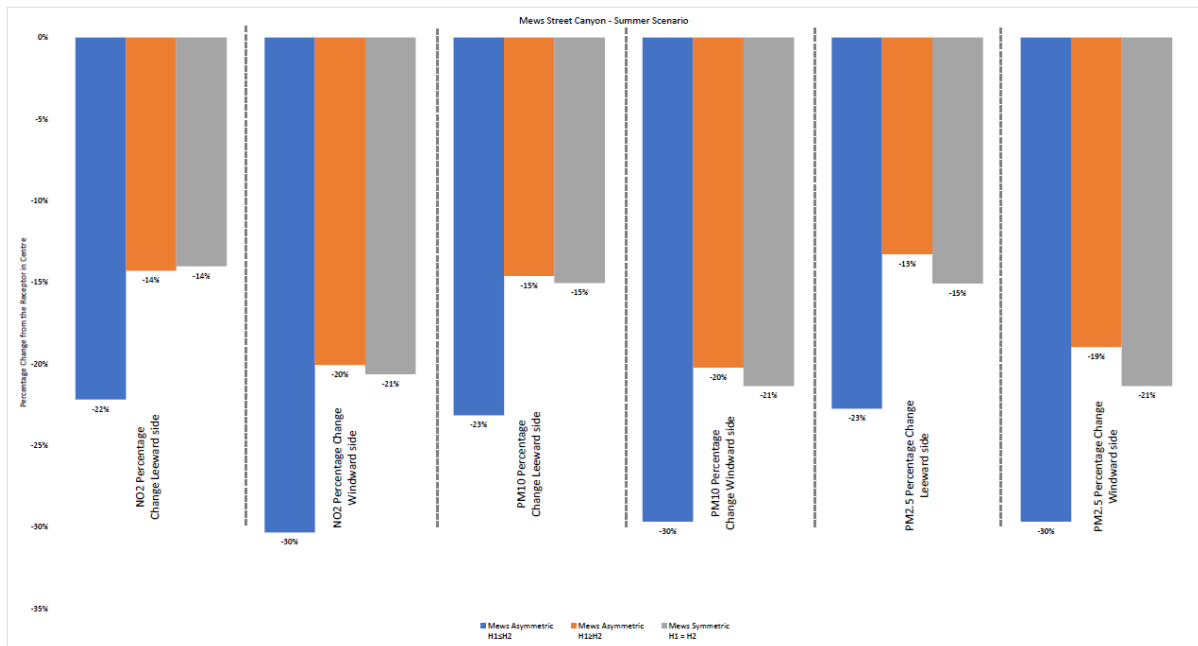
Fig.83 – Mews street canyon dispersion rate in percentage. The higher the negative percentage, the more effective in dispersing air pollution (at pedestrian level). This figure was obtained by calculating the percentage change between the source of pollution (centre receptor) and leeward or windward receptors. (Summer period)
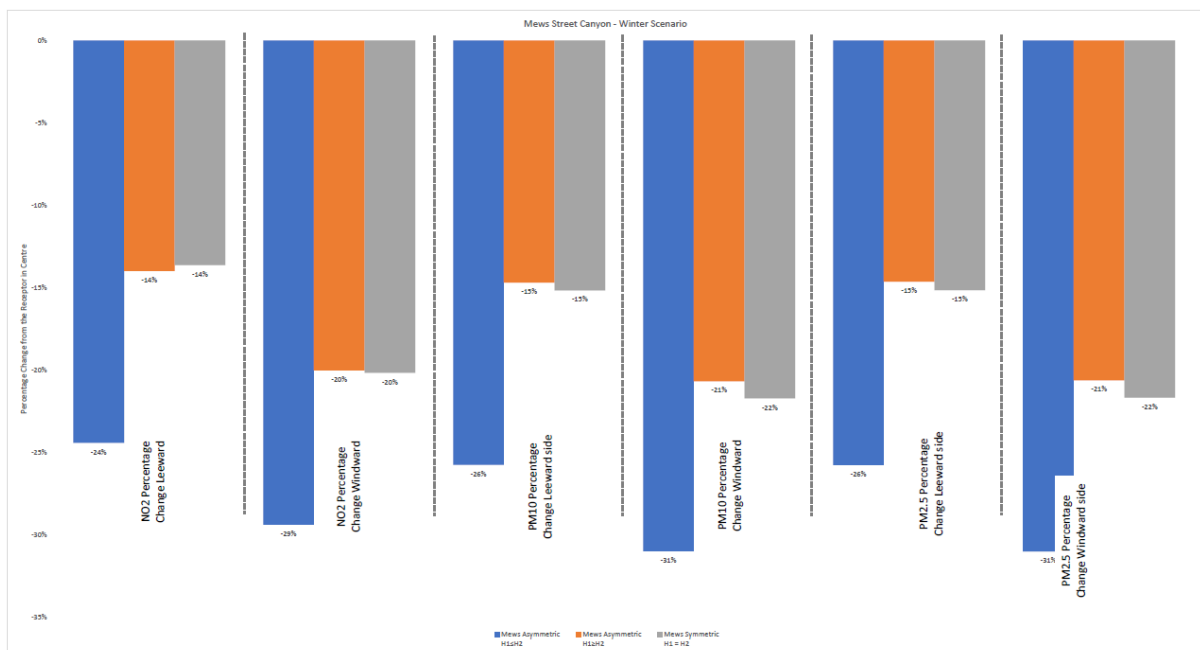
Fig.84 – Mews street canyon dispersion rate in percentage. The higher the negative percentage, the more effective in dispersing air pollution (at pedestrian level). This figure was obtained by calculating the percentage change between the source of pollution (centre receptor) and leeward or windward receptors. (Winter period)

The air temperature and relative humidity remained relatively constant in all configurations. Wind velocity was marginally higher within the windward side of the asymmetric step-up

157

canyon during summer and the leeward side of the asymmetric step-down canyon during the winter period, but was generally less than 0.1 m/s. The lowest wind velocity of 0.03 m/s was measured at the leeward side of the asymmetric step-down canyon configuration during the summer period (Fig.85 and Fig.86).
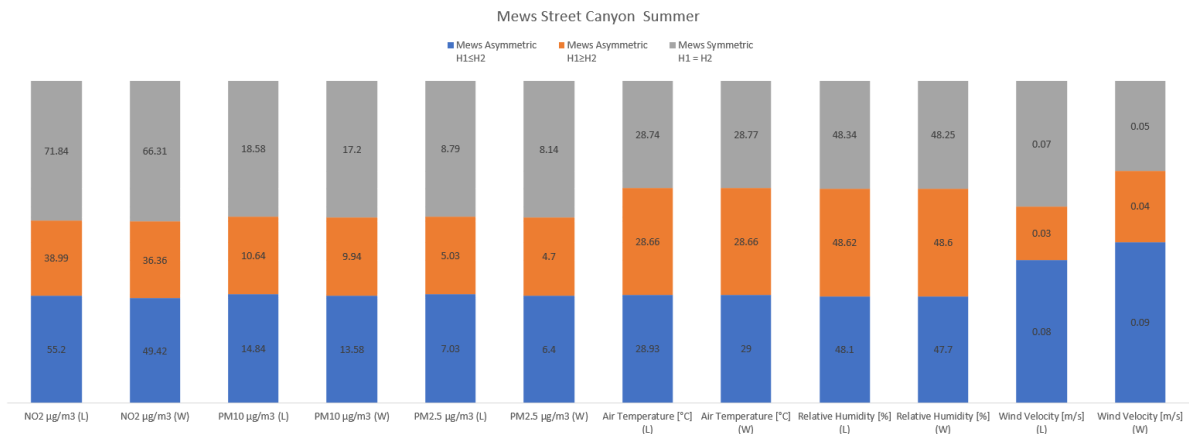
Fig.85– Mews street canyon air pollution and meteorological parameters values – Summer period
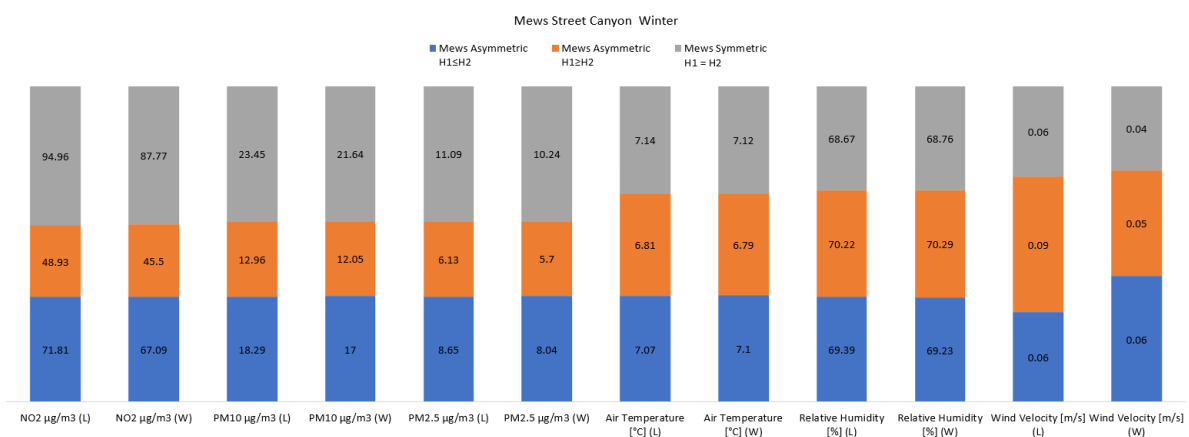
Fig.86 – Mews street canyon air pollution and meteorological parameters values – Winter period

6.2.1.1 Discussion - Mews street canyon

As it can be seen from the preceding graphs and results, in both the summer and winter seasons, mews street canyon showed the same pattern of change; the step-up canyon had the highest pollution percentage change (high dispersion rate), but the step-down canyon had the lowest measured pollution level. This demonstrates that the canyon side with the greatest percentage change does not always imply the least amount of pollution.

As a result, it's critical to consider the mean pollution concentration in the canyon when deciding on the best configuration with the lowest pollution levels. Further investigation into the step-up canyon configuration revealed that the windward building in the step-up canyon blocked the perpendicular wind stream, causing stagnation and deflecting the wind stream into updraught and downdraught in both summer and winter periods (Fig.87).
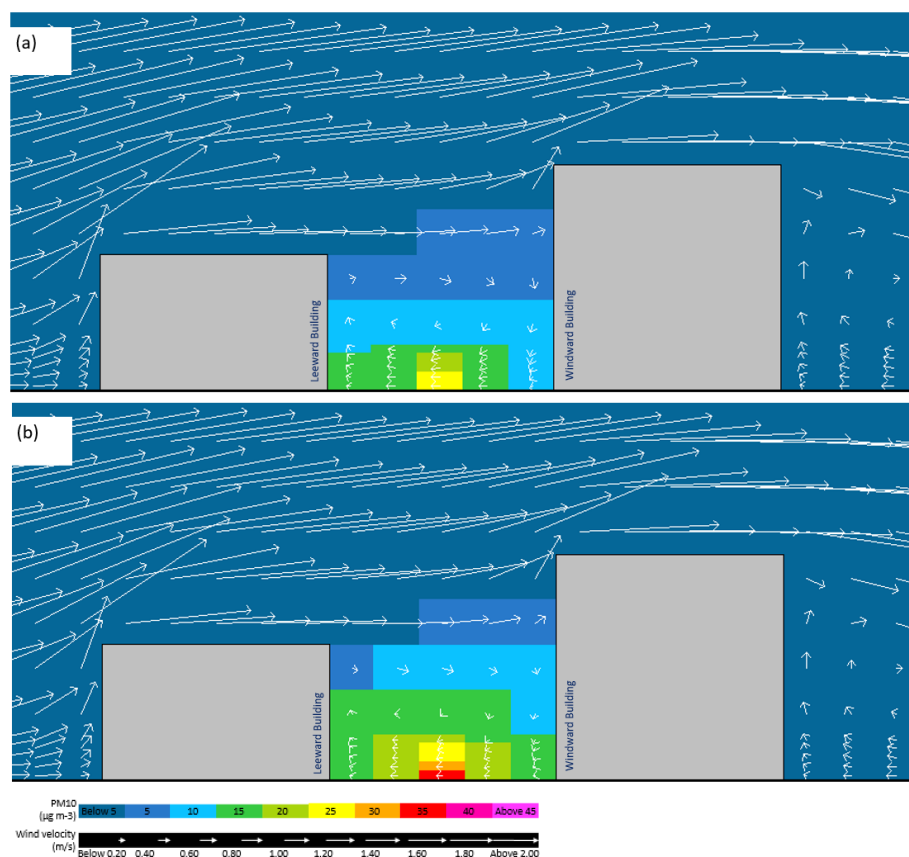
Fig.87 – Step-up mews canyon configuration indicating PM10 concentration inside the canyon for (a) summer period and (b) winter period. Section line is the same as Fig.81 (d).

The downdraught carries the pollution downwards to the leeward side, where it is flushed out of the canyon by the leeward updraught (Edward NG, 2005). With the incoming wind, the pollution is partially removed from the canyon but partially forced back into the canyon, increasing the mean pollution level within the canyon. This is consistent with the theories introduced by Johnson et al. (1973), Oke (1988), Gromke and Ruck (2012) and Gromke et al. (2008). The symmetric configuration indicated a uniformed distribution of pollutants at both sides of the canyon with a slight increase at the leeward side (Fig.88 c and d).
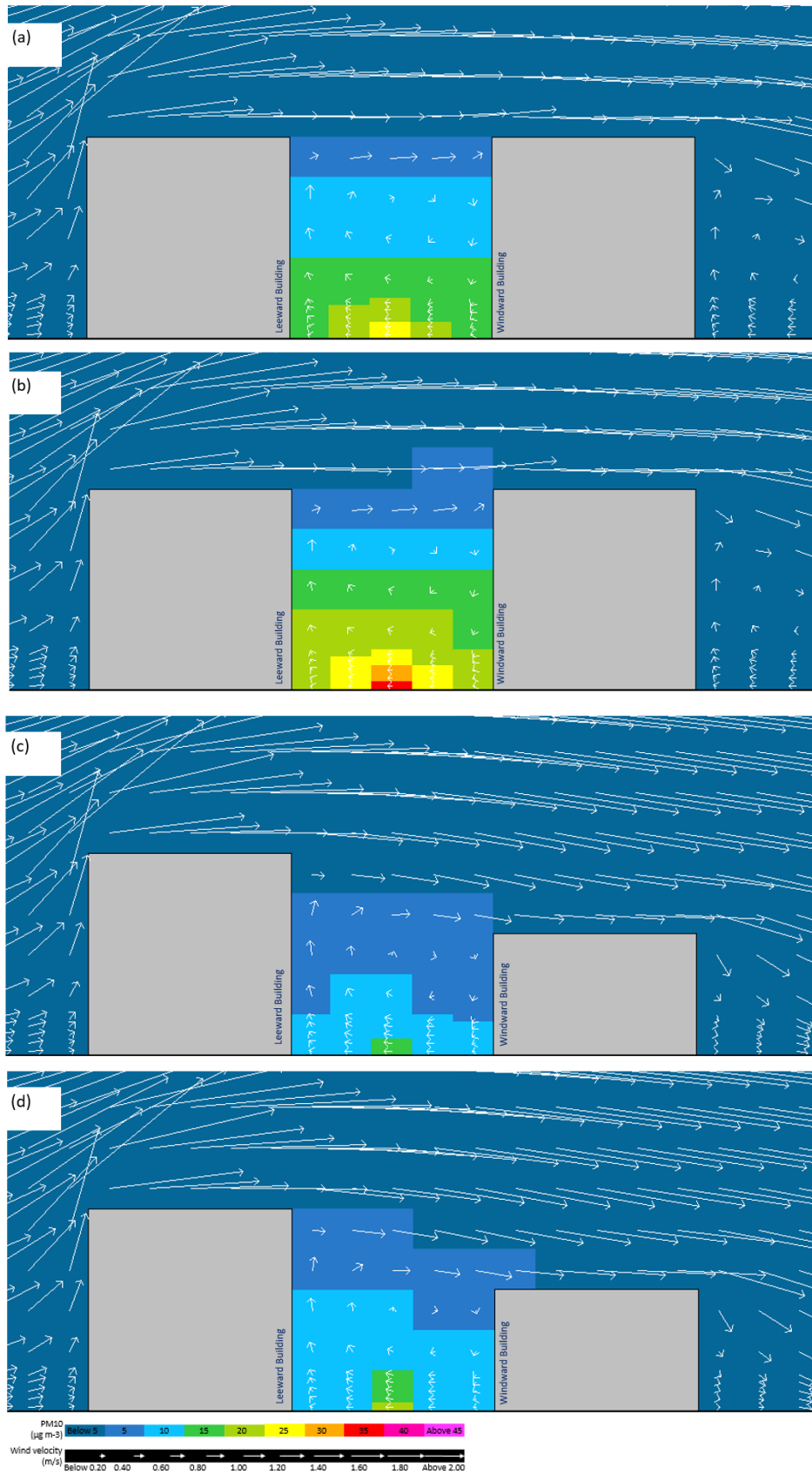
Fig.88 – Step-down and symmetric mews canyon configuration indicating PM10 concentration inside the canyon for (a) symmetric summer period, (b) symmetric winter period (c) step-down summer period and (d) step-down winter period. Section line is the same as Fig.81 (d).

As it can be seen from fig.88 c and d and Fig.82 amongst all mews canyon type step-down configurations exhibited the lowest air pollution levels due to the formation of primary vortex in the middle of the street canyon which has encouraged pollutants to dilute with the above-the-roof incoming airflow and be carried out of the canyon, resulting in significantly lower mean pollution levels than in step-up and symmetric canyon configurations. This finding is consistent with that of Li et al. (2020), who discovered the same association in asymmetric canyons with low incoming wind speeds. In their study, they considered the temperature of the wall (façade) and discovered a correlation between the temperature of the wall and its effect on natural convection within each side of the canyon, as well as an increase in air movement.

Interestingly and based on the result of the computational modelling when summer and winter wind velocity and pollution levels are compared against each pair of street canyons, a similar phenomenon is observed. Accordingly, summer configurations are always 1.2 times less pollutant than their winter counterparts. As it was highlighted in chapter 3 and illustrated in figure 42, this is primarily because of the wind and thermal environments, which have an effect on pollutant dispersion in street canyons due to thermal buoyancy force effects. As a result, the typical wind flow is altered by this buoyancy effect at low wind speeds, and due to higher summer temperature than the winter, the wind velocity and flow structure at the pedestrian level is increased more effectively, thereby increasing the updraught and dispersion rate.

Evidently, and as a result of this study's findings, this updraught effect increased the rate of pollution dispersion in the step-down canyon, making it one of the best configurations within this canyon type in terms of air quality level in comparison to other mew street canyon configurations. **Therefore, to improve air quality within mews canyon type, step-down configuration is more effective and at the same time the symmetric canyon configuration is the canyon configuration to avoid** as it has demonstrated to have the lowest dispersion rate while also having the highest pollution levels within the canyon and at the pedestrian level. As a general rule, the **pedestrian activity and traffic movement should be designed to occur on the windward side of the mews canyon**, which has a lower concentration than the leeward side.

6.2.2 Residential street canyon

The idealised residential street canyon or regular canyon has a width of 14 metre with a street length of 62 for both symmetric and asymmetric configurations. The road coverage is 41.14 percent, and pedestrian areas cover 11.7 percent of the site's total area. In symmetric and asymmetric canyons, the mean height of buildings are 10 and 8 metre, respectively, with building height differentials (ΔH) of 4 metre (Fig.89).
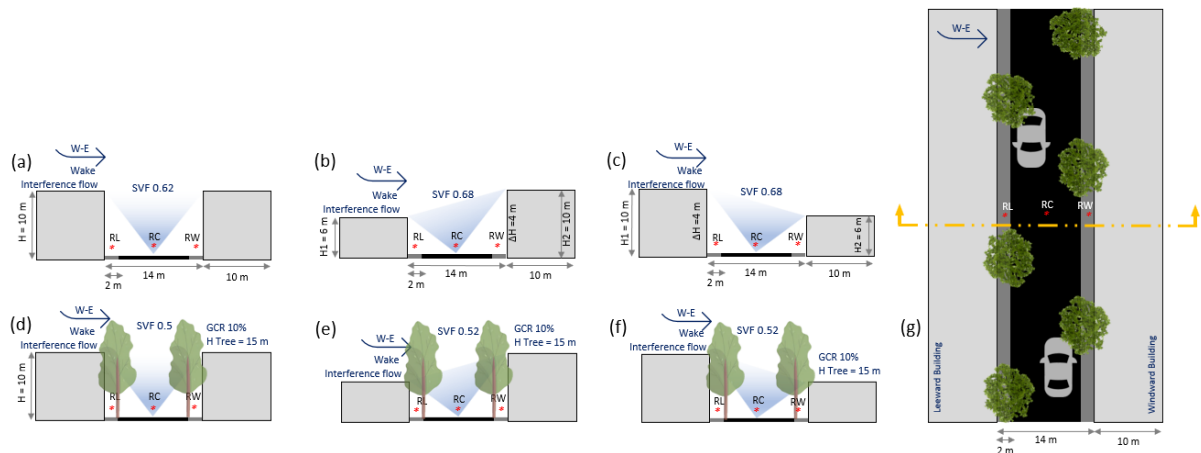
Fig.89 - Schematic section and plan view of 62 meter longitudinal length street canyon layout with the indication of monitoring receptors (*). (a) Symmetric (b) step-up asymmetric (c) step-down asymmetric (d) symmetric + trees (e) step-up asymmetric + trees (f) step-down asymmetric + trees (g) plan view with section line

Within green configurations, the average tree height is 15 metre, which is equivalent to a mature Platanus × acerifolia (London Plane) tree with a canopy diameter of 9 metre, which adds up to 10% green cover ratio of the total area. The upwind of west wind blowing toward the east resulted in induced wake interference flow regimes across all configurations. Overall, the windward side of the canyon exhibited less pollution levels than the leeward side of the canyon with the exception of the step-up canyon configuration which showed the opposite pattern and the pollution levels are measured higher on the windward side of the canyon (Fig.90). It is worth mentioning that this increase in pollution is marginal and in most cases it is less than 3% increased.
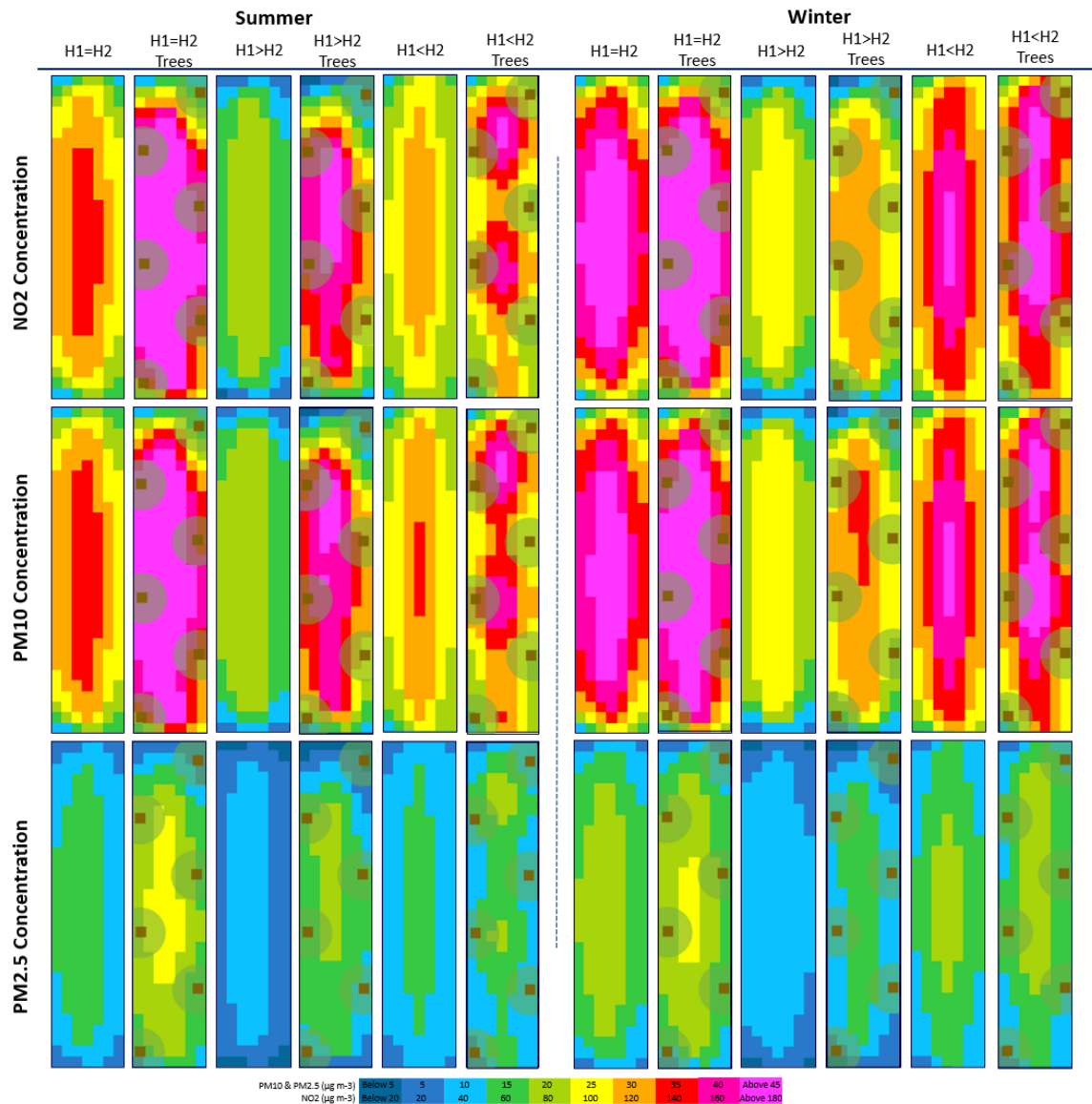
Fig.90 - Pollution levels within various residential street canyon configurations

The highest reduction in pollutants between all configurations was recorded at the leeward side of the asymmetric step-up canyon with trees in the winter period. The levels recorded are 30% for NO_2 and 32% for both PM_{10} and $PM_{2.5}$ less than the measurement taken from the receptor located in the centre of the canyon (source of pollution). Interestingly, the mean wind velocity in this configuration is also showing the highest speed in comparison to the rest of the residential street canyon configurations. It is believed that the combination of high wind velocity and lack of leaves on the trees during the winter period and most importantly the step-up urban form are the reason for this reduction. The minimum reduction between all configurations was recorded at the leeward side of the symmetric street canyon with trees during the summer period. The NO_2 is only reduced by 9% and PM_{10} and $PM_{2.5}$ are reduced

164

by 12%. The windward side presented a more constant pattern of change between various configurations and the difference between the highest reduction and lowest reduction was only 6%. The highest reduction in pollutants on the windward side was the asymmetric step-up canyon with trees in the summer period. It is believed that in this configuration the volume of vegetation which has covered 10% of the total area, succeeded in blocking pollutants from entering or concentrating on the windward side. In general, the top two configurations with the highest reduction on the leeward side belong to the winter period and for the windward side this will shift to the summer period. This is a common pattern between all measured pollutants i.e. NO_2, PM_{10} and $PM_{2.5}$. Remarkably, the step-up canyon with and without trees showed the highest reduction on both sides of the canyon. On the contrary, the lowest reduction is within symmetric street canyons and unsurprisingly, these are also the ones with the highest pollution levels (Fig.91and Fig.92).
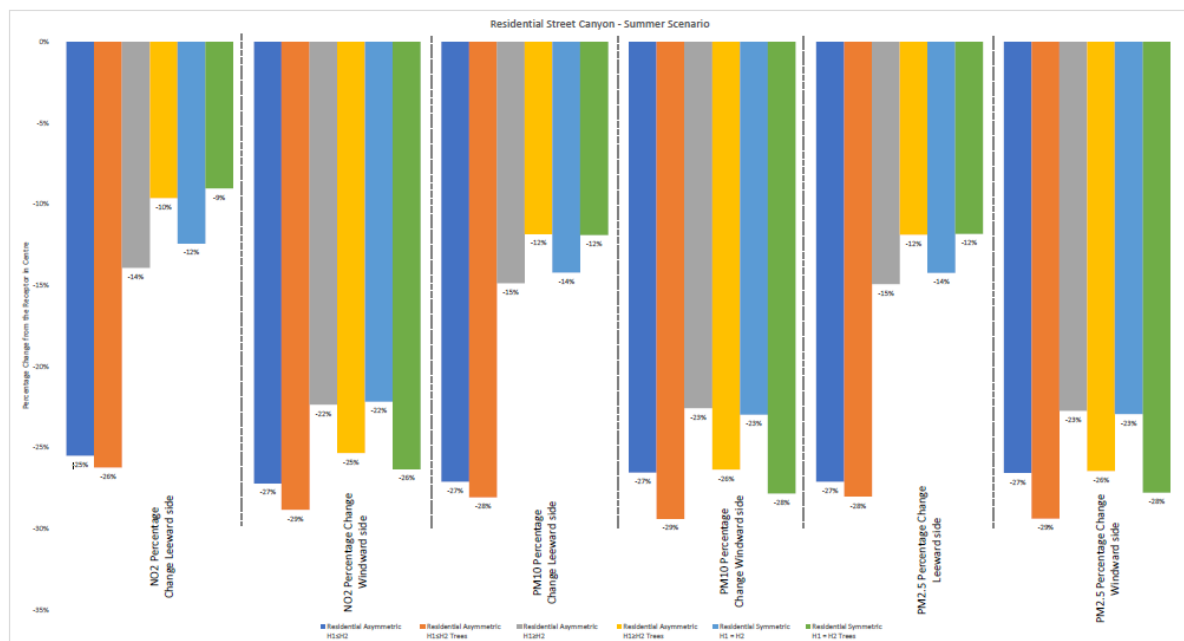
Fig.91 – Residential street canyon dispersion rate in percentage. The higher the negative percentage, the more effective in dispersing air pollution (at pedestrian level). This figure was obtained by calculating the percentage change between the source of pollution (centre receptor) and leeward or windward receptors. (Summer period)

Fig.92 – Residential street canyon dispersion rate in percentage. The higher the negative percentage, the more effective in dispersing air pollution (at pedestrian level). This figure was obtained by calculating the percentage change between the source of pollution (centre receptor) and leeward or windward receptors. (Winter period)

Air temperature remained relatively constant, with only a slight increase in relative humidity within the canyons with tree configuration. Wind velocity was highest within the windward side of the asymmetric step-up canyon (with trees) but was generally less than 0.3 m/s. Notably, this location with a sky view factor of 0.52, the third best SVF among all configurations, also demonstrated the greatest dispersion and dilution capability. The lowest wind velocity was measured within four similar urban street canyons, namely symmetric with and without trees in winter and the same configuration for summer. Indicating that the wake interference regime didn't allow the wind flow enters the canyon as freely as asymmetric urban configurations, resulting in less wind exchange and inevitably an increase in pollution concentration at windward and leeward sides (Fig.93 and Fig.94).
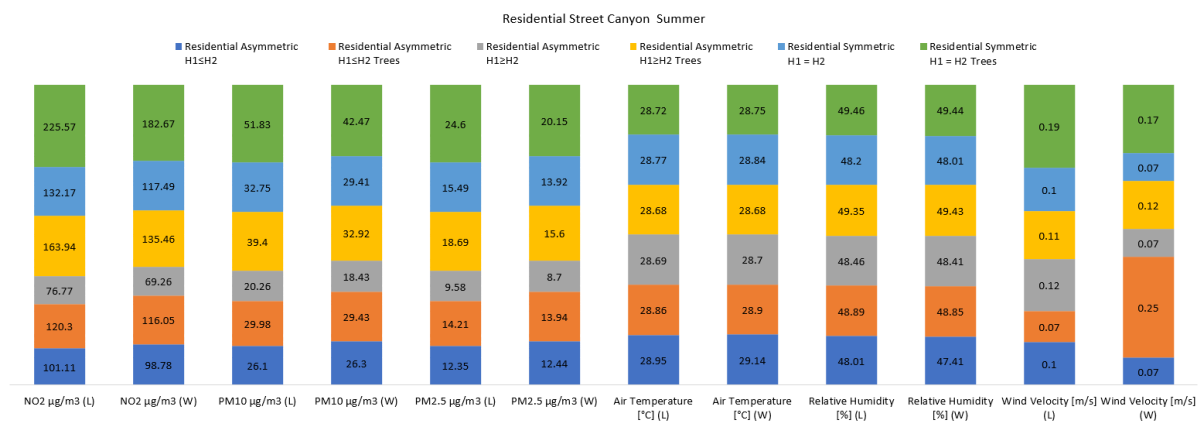
Residential Street Canyon Summer

Fig.93 – Residential street canyon air pollution and meteorological parameters values – Summer period

Residential Street Canyon Winter
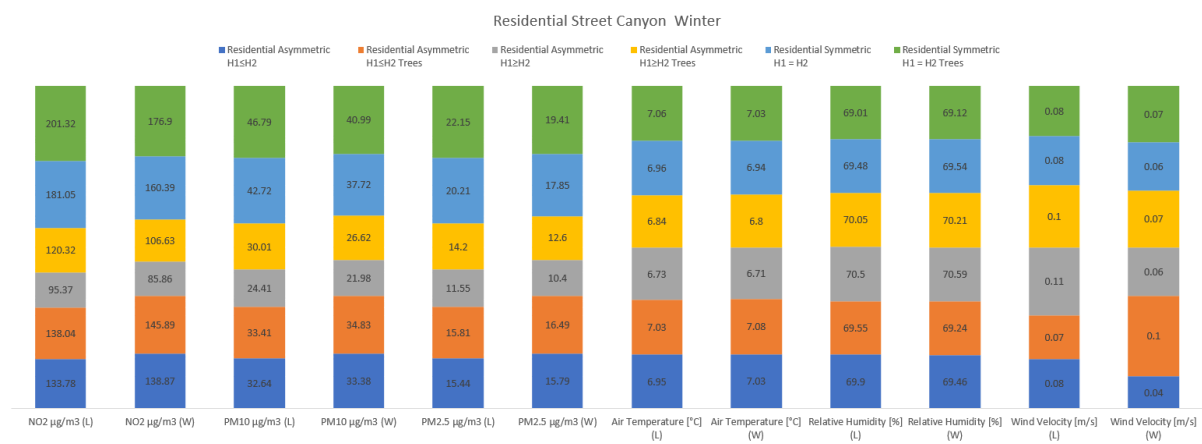
Fig.94 – Residential street canyon air pollution and meteorological parameters values – Winter period

6.2.2.1 Discussion - Residential street canyon

According to the results of computational modelling, the asymmetric step-up canyon configuration with and without trees (Fig.91 and 92) has the highest pollution percentage change with a reduction in pollution in both summer and winter, as well as at the leeward and windward side of the canyon. Additionally, it can be seen that the windward side of the residential street canyon consistently performed better and recorded a greater percentage change, therefore lower pollution level than the leeward side. This is due to a greater distance between buildings in the residential canyon in comparison to the mews canyon type, where the wake interference flow is induced (Oke, 1980). As a result of the washdown (downdraught) effect, the incoming perpendicular wind increases air flow at the windward side and transports pollution to the centre and leeward side of the canyon. However, as it was observed with the mews street canyon, the canyon with the highest percentage change

167

is not always the least polluted canyon, at least when the configurations with and without trees are compared. In terms of pollution, the least polluted canyon is the asymmetric step-down canyon (H1>H2) in summer, which performed similarly to the asymmetric mews step-down canyon (Fig.88 c and d). When only tree configuration is compared, the similar configuration exhibited less pollution but only during the winter period. Given that deciduous trees were used in this study, it was expected that a summer configuration with no trees would perform the same as their winter period counterpart with and without trees. However, based on the results, it is clear that the no tree summer period configuration is always less polluted than the winter with and without tree configuration (Fig 93 and 94).

This is due to the same phenomenon that was explained in the previous section, and it is caused by solar and thermal radiation that heats the building facades and surfaces, resulting in a buoyancy-driven flow that affects the flow field inside the urban canyon. Therefore, heating a surface in a street canyon changes the vortex flow characteristics i.e. heating of upwind, downwind, and canyon walls in this case alter the vortex flow and pollution concentration (Kim and Baik, 1999). This is in line with the findings of Xie, Liu and Leung (2007), who used CFD to explore the impact of building facades and ground heating on wind flow and pollution dispersion in street canyons. Their study discovered that increased surface temperature of facades had a significant impact on air motions and wind structure. Their CFD results revealed that buoyancy complicated pollutant dispersion and wind flow under temperature stratification. It's worth noting that, unlike the current thesis, Xie, Liu and Leung didn't model trees, or vegetation in their modelling. Furthermore, the surfaces were heated numerically rather than by solar radiation. As a result, the current thesis is thought to be a more accurate representation of the real scenario. As shown in Fig.95 a,b and c, during the summer, the wall surfaces on the windward and leeward sides are heated differently and with variation, with the windward side being primarily warmer. In the winter, because of the sun's angle and reduced solar radiation, windward and leeward temperatures are relatively equal. As a result, there are greater surface temperature differences between each side of the canyon in the summer than in the winter, causing the summer period to generate a greater amount of buoyancy Fig.96 d,e and f.
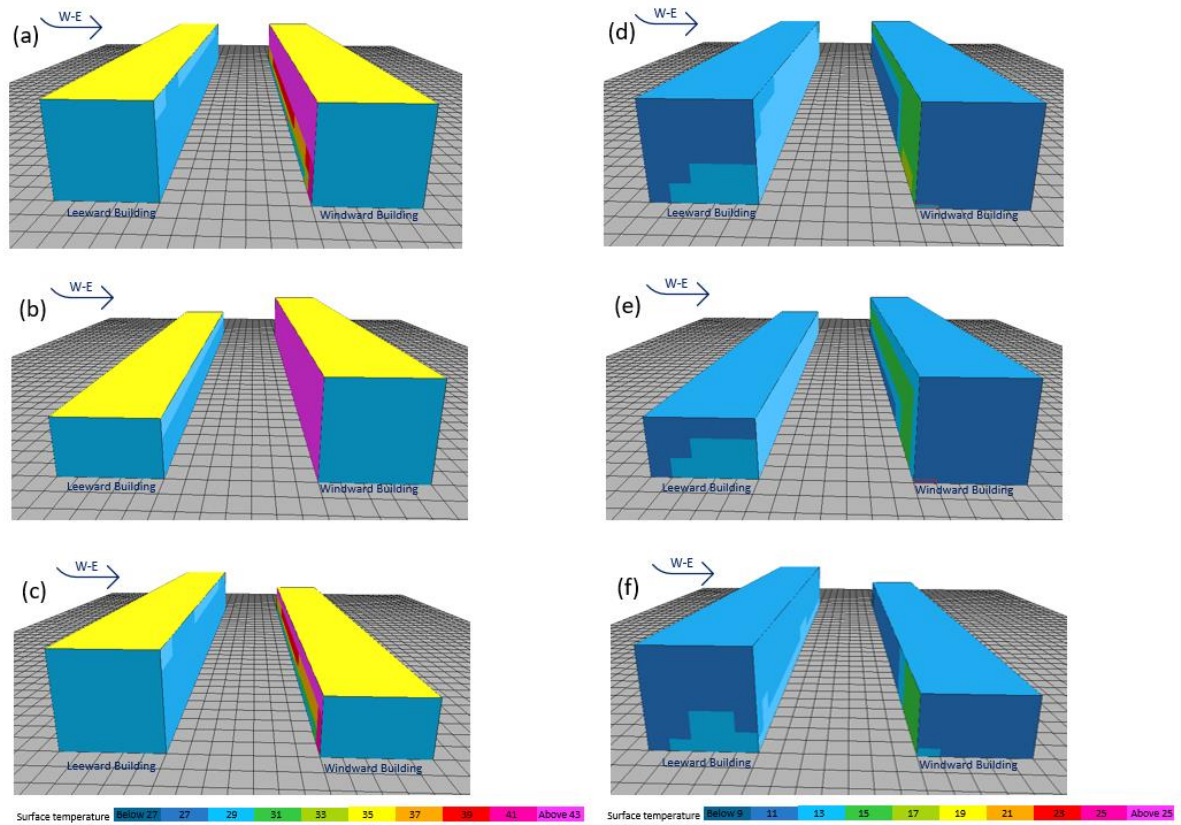
Fig.95 – façade temperature difference between leeward and windward side of various residential canyon configurations. (a) symmetric summer period (b) step-up summer period (c) step-down summer period (d) symmetric winter period (e) step-up winter period (f) step-down winter period

The buoyancy-driven flow caused by differential wall heating affects the flow field inside the urban street canyon. Accordingly, a stronger wind flow was generated on the canyon's windward side, pushing the pollution emitted in the canyon's centre upwards, where it dispersed quickly and was removed from the street canyon before it was transported to either side of the canyon Fig.96.
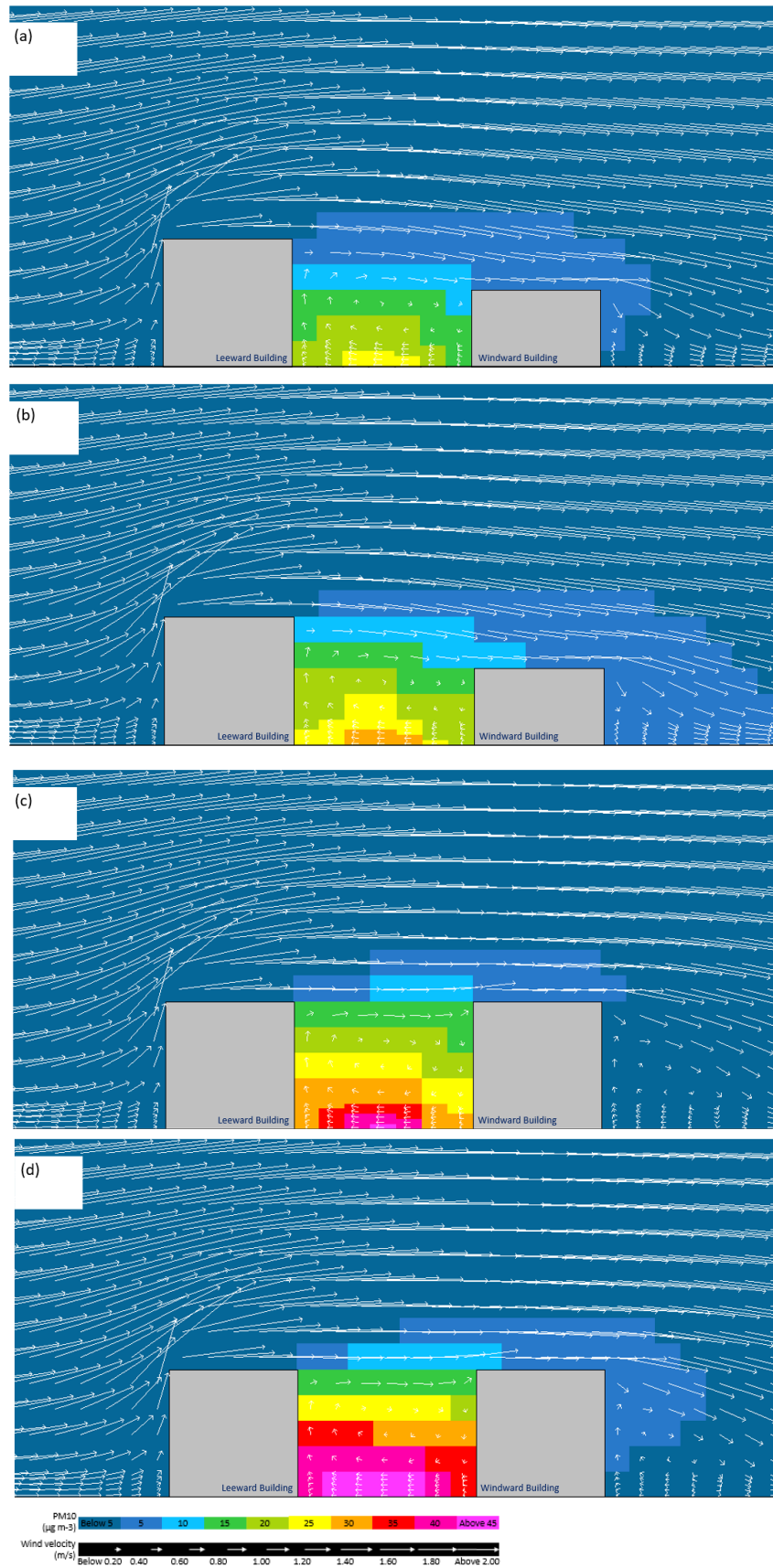
Fig.96 – Various residential canyon configuration indicating PM$_{10}$ concentration inside the canyon for (a) step-down summer period, (b) step-down winter period (c) symmetric summer period and (d) symmetric winter period. Section line is the same as Fig.81 (d)

The above findings highlight the importance of urban morphological indicators and even the materiality of our built environment, which by correct selection can manipulate the microclimate and increase the air pollution dispersion. It is interesting to note that the addition of trees significantly altered the above effect, and it can be seen that almost all **configurations of canyons with trees have a higher pollution level**. For instance, while the step-down canyon configuration without tree was previously identified as the least polluted, the tree configuration of the same canyon type exhibited an 82% increase in mean NO_2 and a 68% increase in mean PM_{10} and $PM_{2.5}$ levels.

6.2.3 High street canyon

High street canyon has a width of 22 metre and a street length of 62 metre for both symmetric and asymmetric canyons. The total road cover percentage is 23.8 percent of the site's total area, while pedestrian areas cover 28.57 percent. In symmetric and asymmetric canyons, the mean height of buildings are 12 and 9 metre, respectively, with building height differentials (ΔH) of 6 metre (Fig.97).

Fig.97 - Schematic section and plan view of 62 meter longitudinal length street canyon layout with indication of monitoring receptors (*). (a) Symmetric (b) step-up asymmetric (c) step-down asymmetric (d) symmetric + trees (e) step-up asymmetric + trees (f) step-down asymmetric + trees (g) plan view with section line

Within green configurations, the average tree height is 15 metre, which is equivalent to a mature Platanus × acerifolia (London Plane) tree with a canopy diameter of 9 metre, which adds up to 30 percent green cover ratio of the total area. The upwind of west wind blowing toward the east, resulted in wake interference flow regimes within the symmetric and isolated roughness flow regime within the asymmetric canyons with and without tree configurations. The highest reduction of pollutants i.e. NO_2, PM_{10} and $PM_{2.5}$ observed on the leeward side of the asymmetric step-up canyon with trees in both the summer and winter periods. Surprisingly, the same canyon configuration recorded the lowest reduction at its windward side in both seasons (Fig.98).
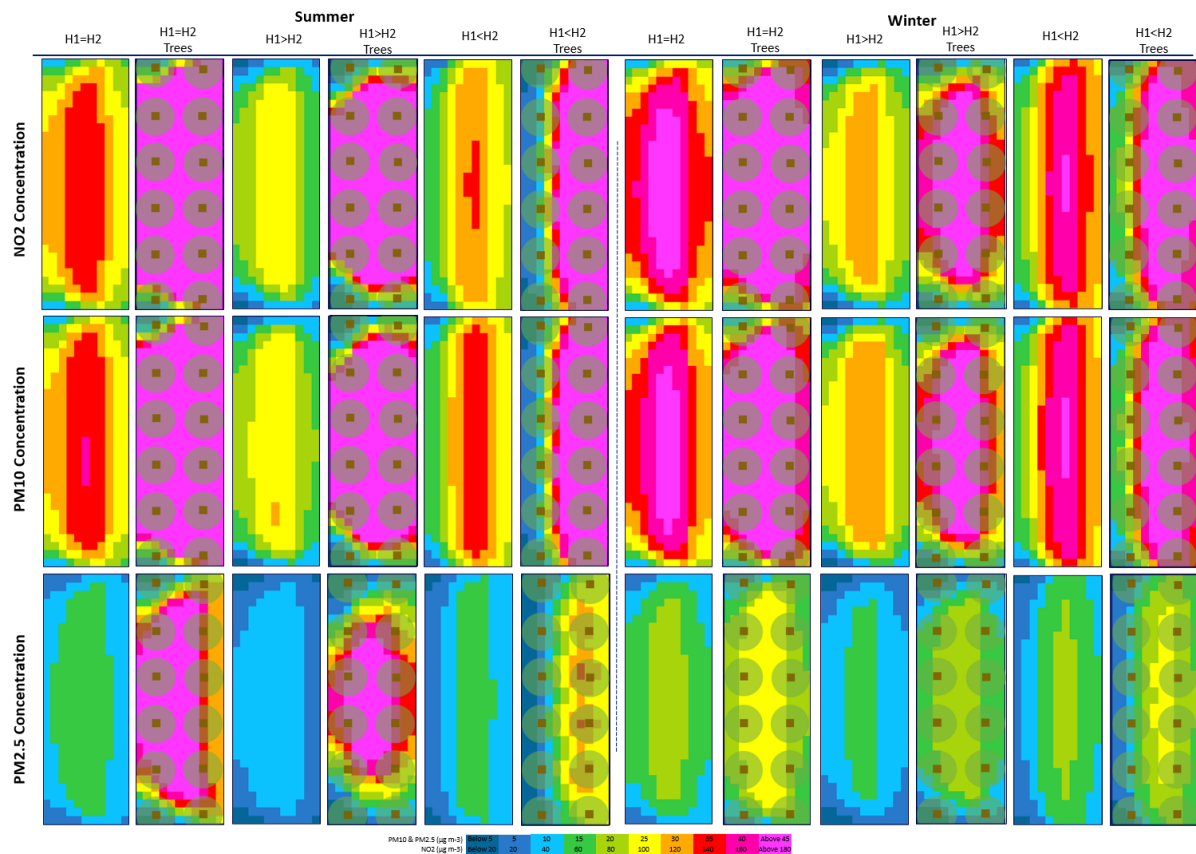
Fig.98 - Pollution levels within various high street canyon configurations

In the case of NO_2, the concentration of this gaseous pollutant increased by 4% on the windward side of the asymmetric step-up with trees configuration during the summer. This could be due to the impact of trees with dense foliage on wind behaviour, which reduces wind velocity. However, when the wind velocity is compared to other configurations, it is discovered that the wind velocity is one of the highest, with a mean wind velocity of 0.35m/s. This indicates that higher wind velocity does not always imply higher dispersion and that other factors such as vegetation density and urban form are far more important in increasing or decreasing pollution concentrations, especially for gaseous pollutants like NO_2. In general, the windward side of the step-up and symmetric canyon configuration showed to have less pollution than the leeward side and centre of the canyon. In a similar vein, the leeward side of the step-up canyon showed to have less pollution than the centre and windward side of the canyon. Across all the configurations and in terms of average air pollution levels, the leeward side of the symmetric canyon with trees in the summer period was recorded as the highest; this canyon also has one of the lowest sky view factors (0.41) (Fig 99 and Fig.100).

Fig.99 – High street canyon dispersion rate in percentage. The higher the negative percentage, the more effective in dispersing air pollution (at pedestrian level). This figure was obtained by calculating the percentage change between the source of pollution (centre receptor) and leeward or windward receptors. (Summer period)
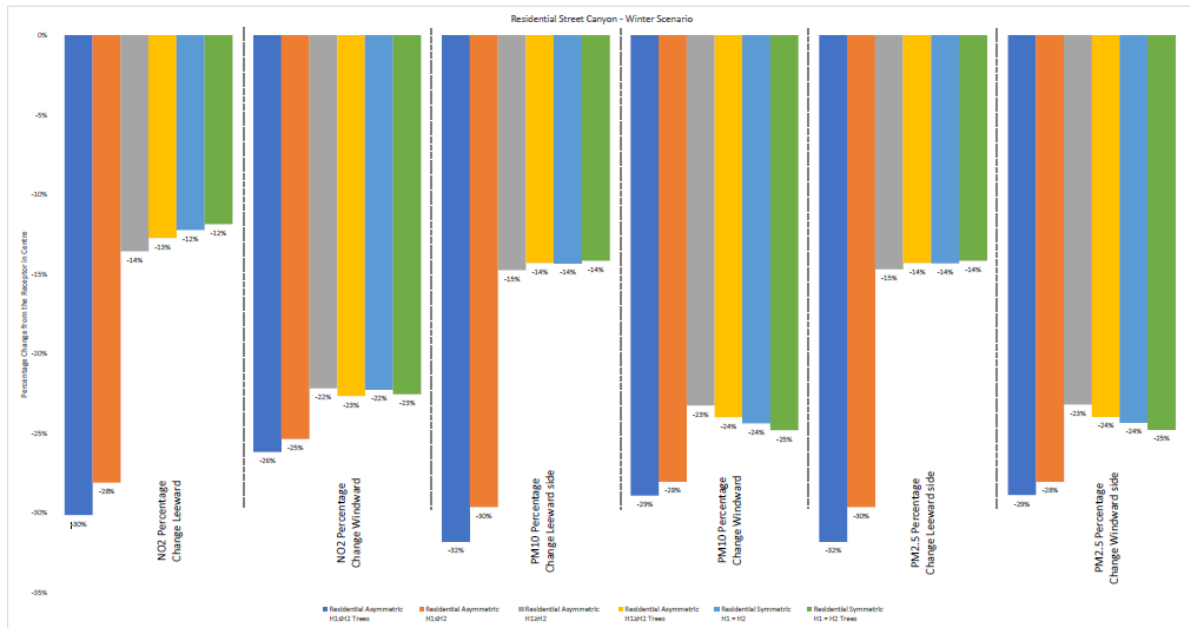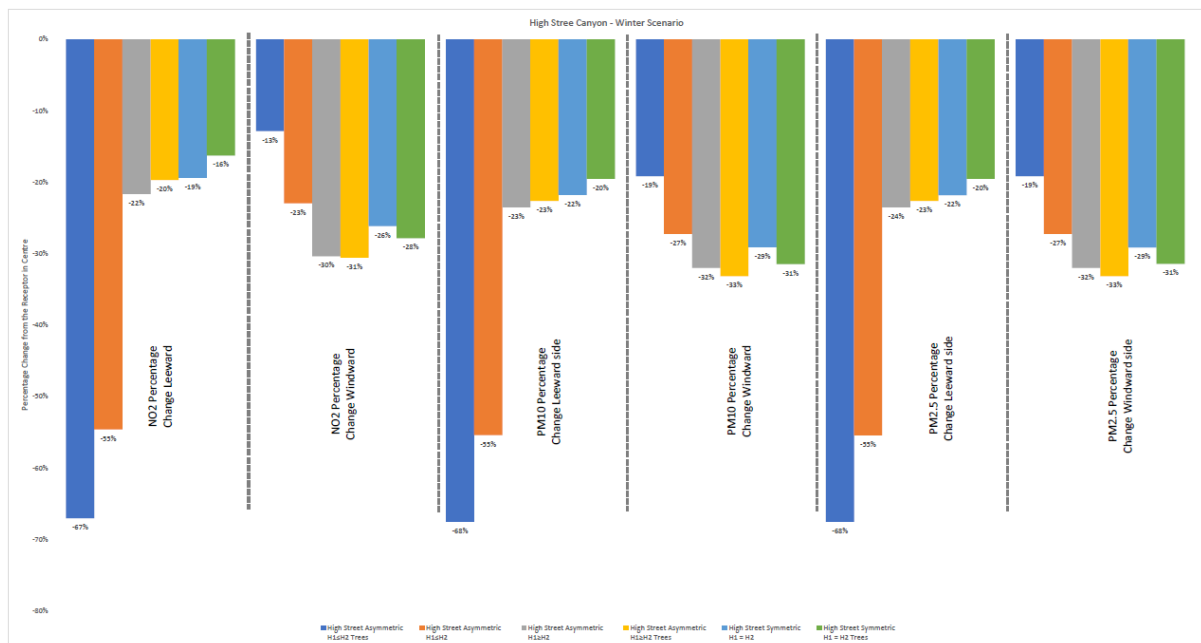

Fig.100– High street canyon dispersion rate in percentage. The higher the negative percentage, the more effective in dispersing air pollution (at pedestrian level). This figure was obtained by calculating the percentage change between the source of pollution (centre receptor) and leeward or windward receptors. (Winter period)

Air temperature remained relatively constant, with only a slight increase in relative humidity within the canyons with tree configuration during the summer period. The Winter period

showed the opposite and the canyon with trees had on average 2% less relative humidity value in comparison to without tree configurations. As it was mentioned, the wind velocity was the highest within the leeward side of the asymmetric step-up canyon (with trees) during the summer period. The lowest wind velocity was measured within three locations, namely the windward of the asymmetric step-down canyon in the winter period with almost 0 m/s wind velocity and the symmetric canyon with trees in summer with 0.01 m/s and again in the same season and with the same wind velocity at the asymmetric canyon step-up without trees (Fig.101 and Fig.102).

Fig.101 – High Street canyon air pollution and meteorological parameters values – Summer period

Fig.102 – High street canyon air pollution and meteorological parameters values – Winter period

6.2.3.1 Discussion – High street canyon

In contrast to mews and residential canyons, the high street canyon type did not exhibit a consistent pattern of change in leeward and windward air pollution levels or mean air pollution levels between various configurations. These changes were relatively homogeneous in mews and residential canyons, making it simpler to compare and identify the best and

worst case scenarios. As the leeward and windward pollution levels have not changed uniformly, the highest percentage change at leeward is recorded at the step-up canyon with trees, but at the same time the windward side of this configuration has the least percentage change among the rest of the configurations, with -4 percent for particulate matter and NO_2 levels.

When measured pollution levels are considered, it can be seen that the step-down configuration with no trees in both seasons and the step-up configuration with no trees in the summer season had the lowest pollution levels, whereas the symmetric configuration with trees in both seasons and the step-down configuration with trees in the summer season had the highest pollution levels and should be avoided in urban settings. It's worth noting that when trees are added, the least polluted canyon (step-down configuration) becomes the worst case with the highest pollution level.

According to the ENVI-met outputs, the no tree scenario (Fig.103 a) created isolated roughness flow and removed pollution from the canyon. However, as shown in Fig.103 b, trees disrupt the flow structure and two horizontal clockwise and counter-clockwise vortexes push the pollution from the emission source to the sides, and the tree canopy decelerates the dispersion, resulting in an excessive increase in pollution levels. As previously stated, low height and fewer trees on the windward side of the canyon increases wind velocity and dispersion rate to encourage more mixing of lower level air volume with above the building roof airflow.
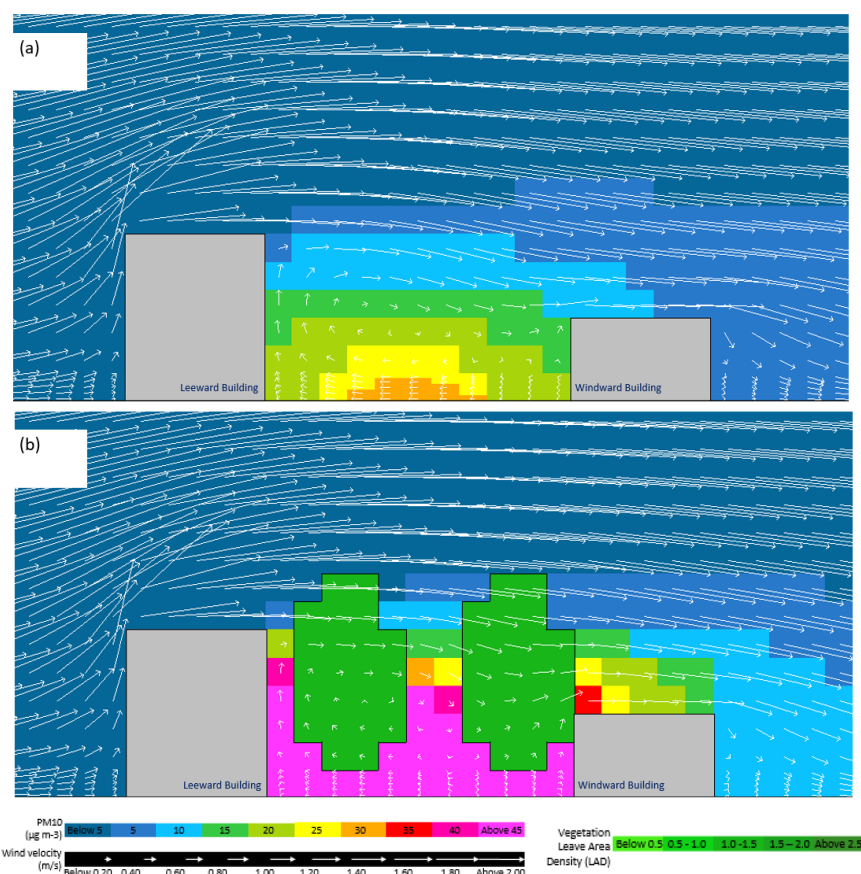
Fig.103 – Step-down high street canyon configurations indicating PM$_{10}$ concentration inside the canyon for (a) step-down summer period, (b) step-down with trees summer period. Section line is the same as Fig.81 (d)

Another interesting configuration in this canyon type is the step-up with trees during the summer period (Fig.104). The leeward configuration had the least amount of pollution, 4whereas the windward configuration had one of the three highest levels of pollution.

This is because the tall tree on the leeward side blocked the incoming wind and redirected it downwards alongside the leeward building and tree. This has pushed pollution to the canyon's centre and under the trees on the windward side, and pollution has been trapped within the windward side due to the tree canopy and height of the windward building, increasing pollution to as much as 8 times higher than the leeward side. Again, based on what has been discussed, to encourage greater pollution dispersion from the canyon, less trees with low heights must be planted on the windward side of the canyon.
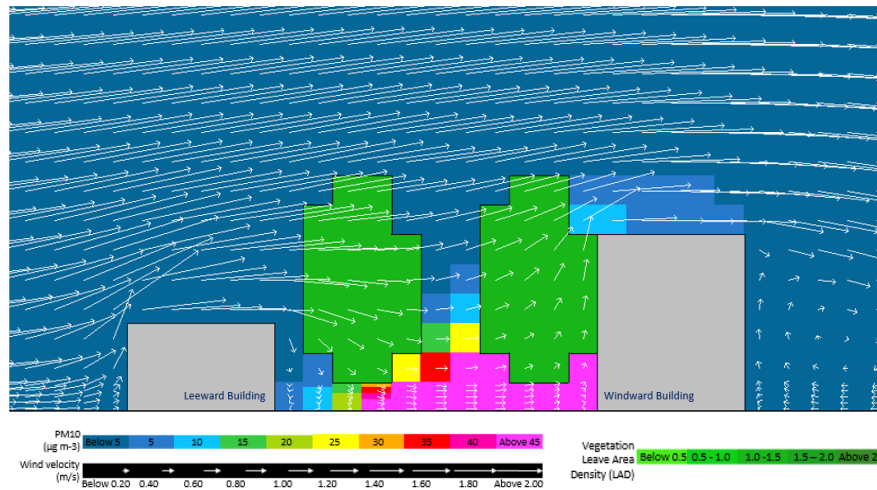
Fig.104 – Step-up high street canyon configuration indicating PM$_{10}$ concentration inside the canyon for summer period. Section line is the same as Fig.81 (d)

It is worth mention that the buoyancy effect can still be seen when comparing summer and winter period in no tree configurations, which always show lower pollution levels in leeward, windward, and mean pollution levels in summer periods.

6.2.4 Narrow high street canyon

A narrow high street or deep canyon street has a width of 22 metre and a street length of 62 metre for both symmetric and asymmetric canyons. Road covers 23.8 percent and pedestrian areas cover 28.57 percent of the site's total area. In symmetric and asymmetric canyons, the mean height of buildings are 50 and 37.5 metre, respectively, with building height differentials (ΔH) of 25 metre. Within green configurations, the average tree height is 15 metre, which is equivalent to a mature Platanus × acerifolia (London Plane) tree with a canopy diameter of 9 metre, which adds up to 30% green cover ratio of the total area. The upwind of west wind blowing toward the east, resulted in the creation of a skimming flow regime across all configurations except asymmetric step-up canyon, which induces a wake interference flow regime (Fig.105).
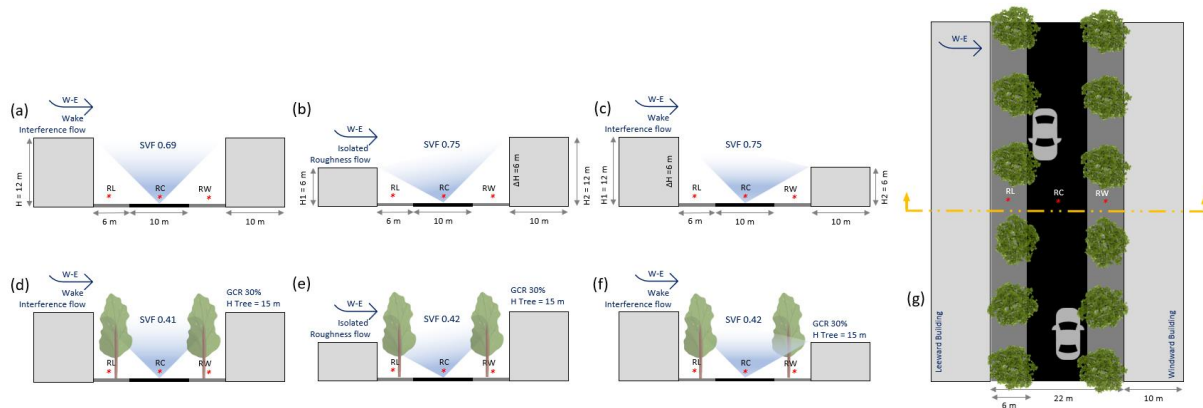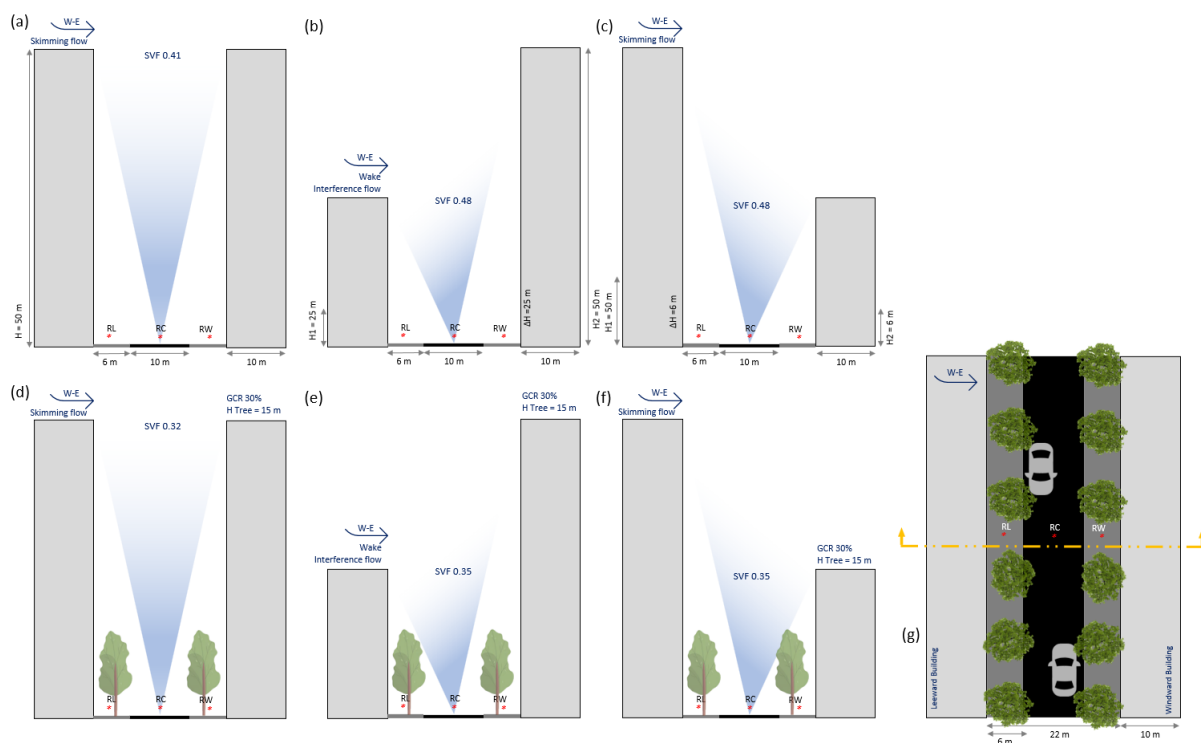

Fig.105 - Schematic section and plan view of 62 meter longitudinal length street canyon layout with indication of monitoring receptors (*). (a)Symmetric (b) step-up asymmetric (c) step-down asymmetric (d) symmetric + trees (e) step-up asymmetric + trees (f) step-down asymmetric + trees (g) plan view with section line

Similar to mews street canyon, this canyon also exhibited the same pattern of pollution levels difference between the leeward and windward sides of the canyon and regardless of the canyon configuration the leeward side was always more pollutant than the windward side of

the canyon (Fig.106). This indicates that mitigation strategies must be considered to reduce pedestrian exposure to air pollutants and if possible, public activities such as sitting areas or outside cafés/restaurants should be limited and avoided within the leeward side of deep canyons.
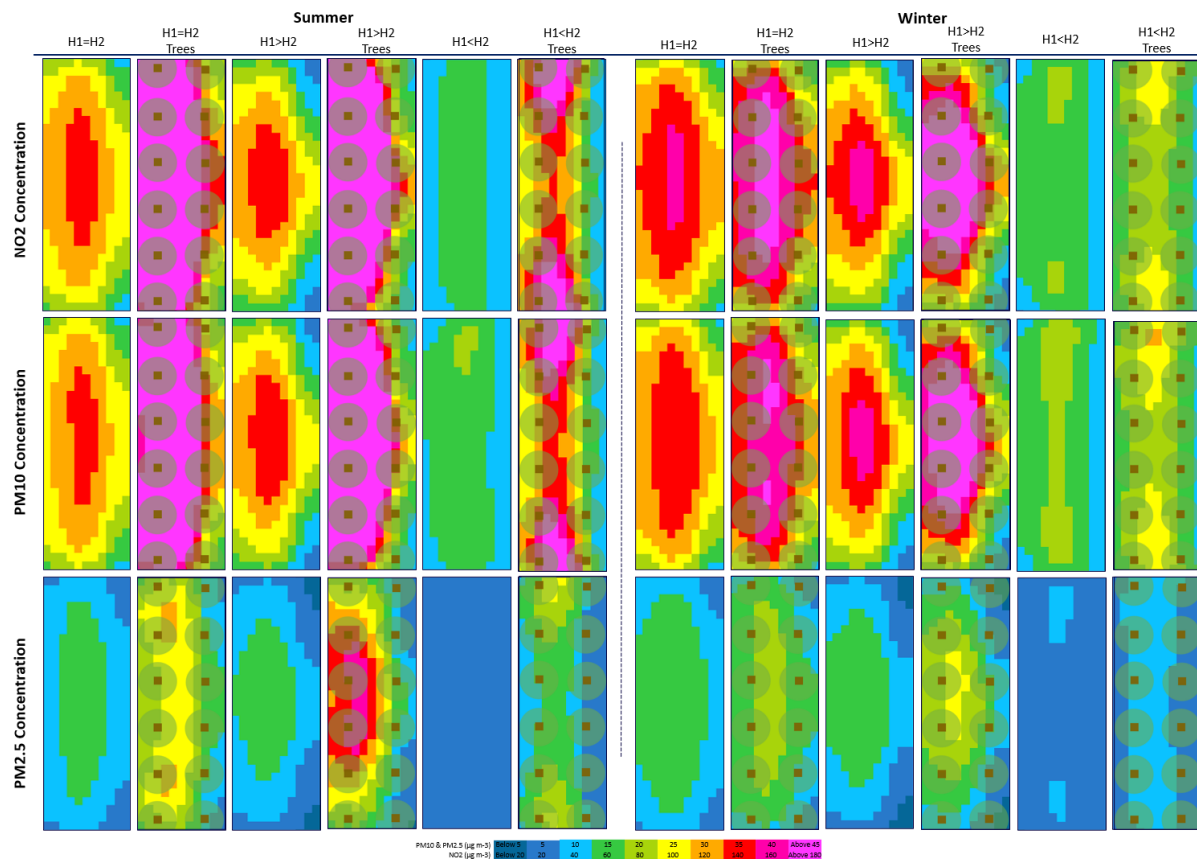
Fig.106 - Pollution levels within various narrow high street canyon configurations

The highest reduction in pollution was recorded at two canyon configurations, both in the summer period and on the windward side of the step-up and step-down with trees. The NO_2 was reduced by 60% and PM_{10} and $PM_{2.5}$ were reduced by 61%. It is interesting that both configurations are included trees and it is indicting their role in effectively protecting the space beneath their canopy.

The above findings demonstrate the significance of the downdraught effect, which has pushed wind downward and towards the street, which has accelerated due to the limited space between row of buildings. This is the same within the winter period and the highest reductions were recorded on the windward side of the same urban canyon configurations. The lowest reductions were recorded on the leeward side of asymmetric step-down with

trees in both seasons. In the winter period, the reduction for NO_2 is only 12% and for PM_{10} and $PM_{2.5}$ is 16%. The summer period which has trees with full foliage is worse than the winter period and the reduction for NO_2 is only 2% and for particulate matter 10 and 2.5 is 4%; the pollution levels are almost the same as levels at the centre of the canyon (Fig.107 and Fig.108).

Fig.107– Narrow high street canyon dispersion rate in percentage. The higher the negative percentage, the more effective in dispersing air pollution (at pedestrian level). This figure was obtained by calculating the percentage change between the source of pollution (centre receptor) and leeward or windward receptors. (Summer period)
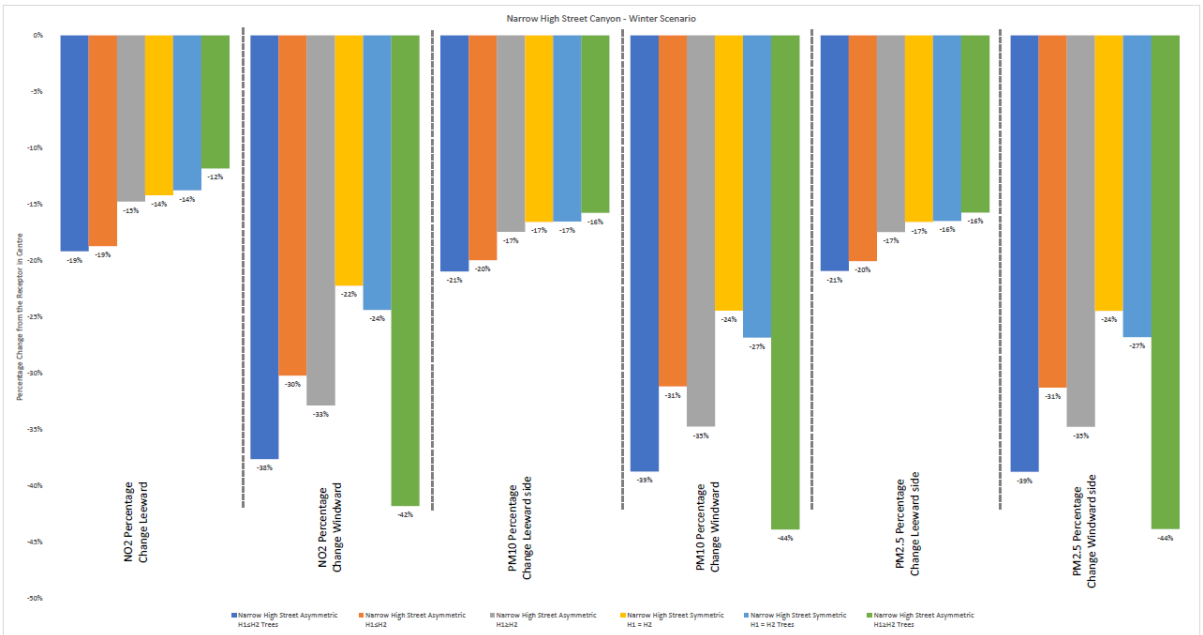
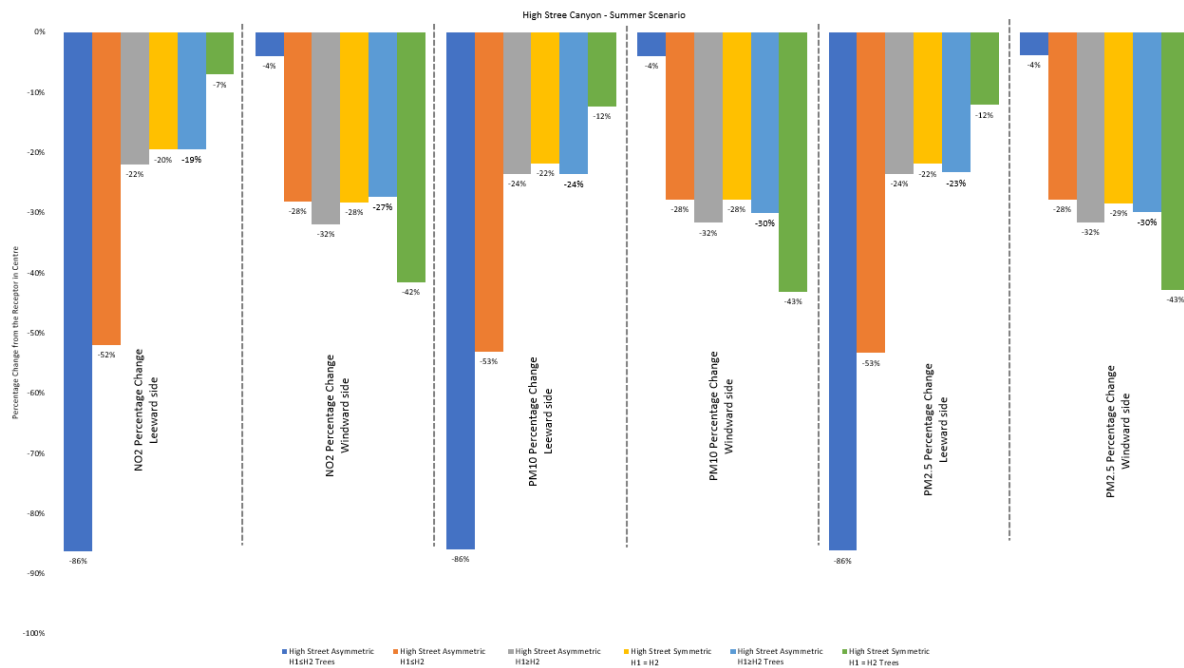Fig.108 – Narrow high street canyon dispersion rate in percentage. The higher the negative percentage, the more effective in dispersing air pollution (at pedestrian level). This figure was obtained by calculating the percentage change between the source of pollution (centre receptor) and leeward or windward receptors. (Winter period)

The highest wind velocity is related to the summer and winter periods of the asymmetric step-up canyon with and without trees configurations. Interestingly the other configuration (asymmetric step-down with and without trees) which jointly demonstrated the highest reduction on the windward side of its canyon has the second-highest wind velocity but not on its windward side but on its leeward side. Meaning that the pollution is constantly pushing upwards, where it can be easily diluted into the new upwind flow and disperse from the site.

The air temperature remained relatively constant, with a slight decrease in the symmetric canyon with trees in the summer period and the asymmetric step-up canyon in the winter, which also had a 0.32 and 0.35 sky view factors respectively, the lowest of SVF among all canyons in each season. In addition, canyons with trees had slightly higher relative humidity i.e. 2% in the summer period than configurations without trees. The winter period showed relatively constant relative humidity across various configurations (Fig.109 and Fig.110).
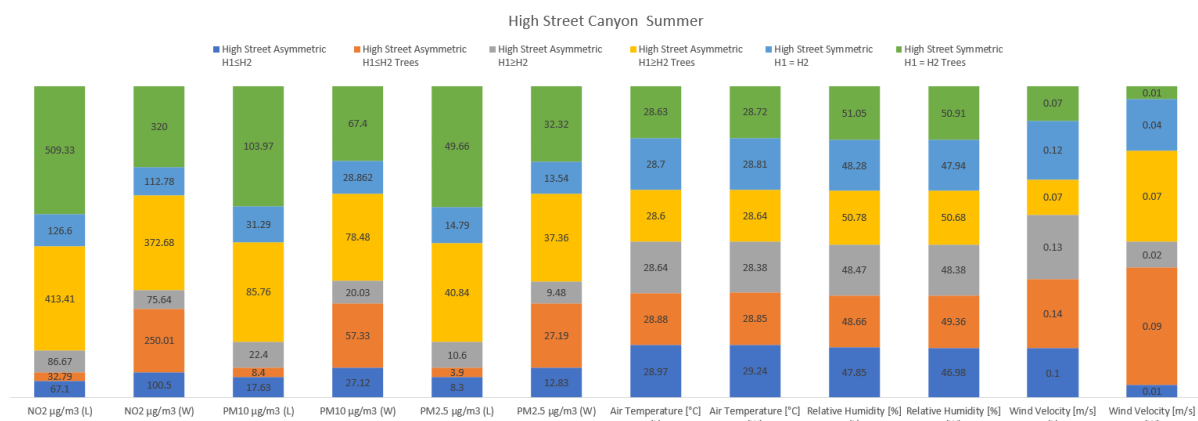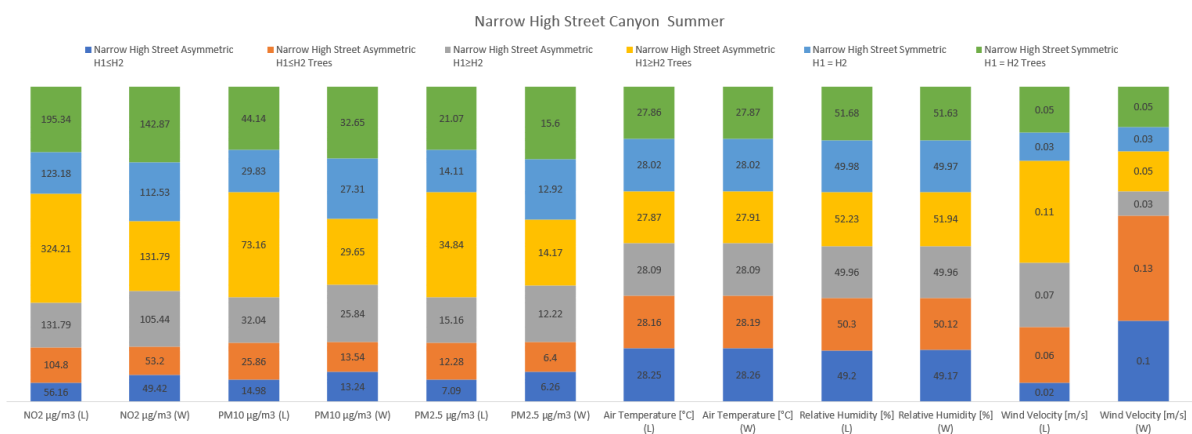

Fig.109 – Narrow high street canyon air pollution and meteorological parameters values – Summer period
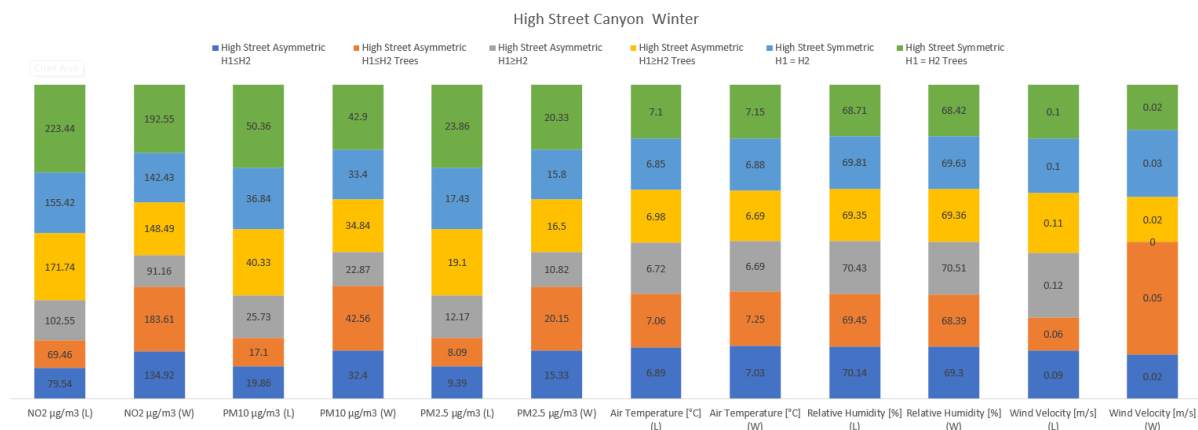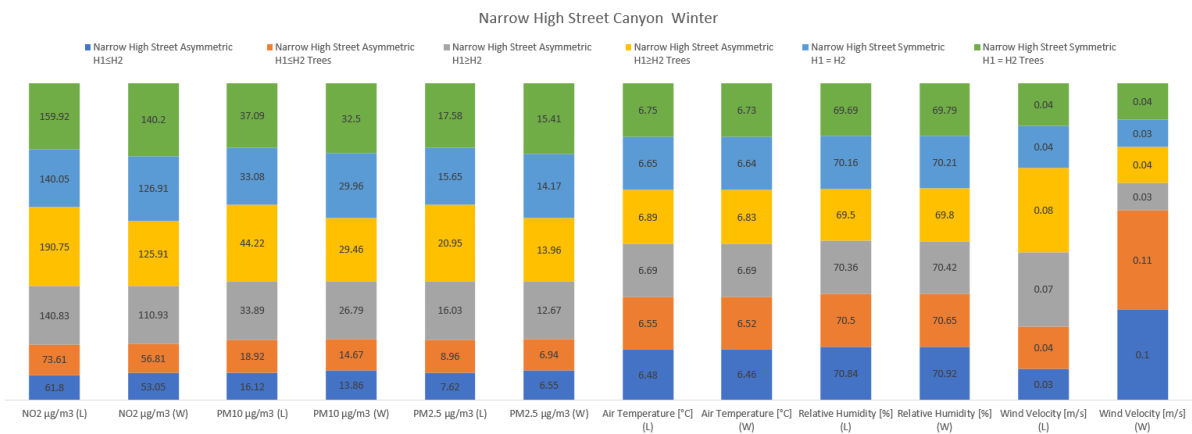
Fig.110 – Narrow high street canyon air pollution and meteorological parameters values – Winter period

6.2.4.1 Discussion - Narrow High Street canyon

Similar to the results of the previous canyon types, the canyon with the greatest percentage change did not necessarily have lower pollution levels. The asymmetric step-up with trees has the highest percentage change among narrow high street canyons, and its average pollution level is 1.9 times greater than the canyon with the lowest average pollution level. The canyon with the **lowest pollution levels is the step-up canyon configuration without trees** (Fig.111 a). it is worth noting that, the winter period of step-up without tree is 9 percent more polluted than its summer counterpart due to the previously mentioned buoyancy effect (Fig.111 b).
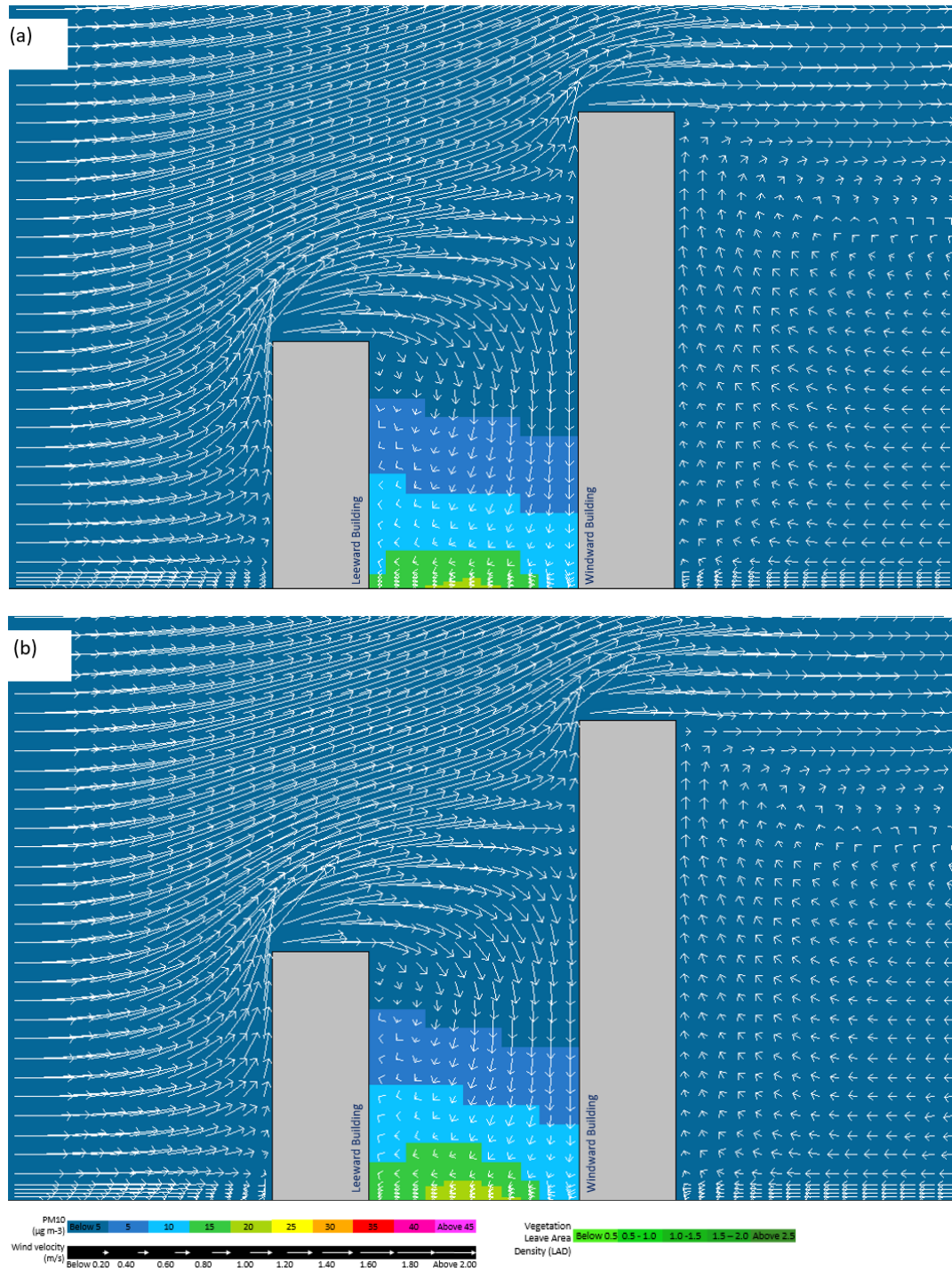
Fig.111 – Step-up narrow high street canyon configurations with no trees indicating PM$_{10}$ concentration inside the canyon for (a) step-up summer period, (b) step-up winter period. Section line is the same as Fig.81 (d)

Interestingly, the same canyon configuration (step-up) with trees demonstrated a lower pollution level than step-down and symmetric with and without trees configurations. That means the placement of trees under tall buildings should be encouraged because the

184

downdraught effect can still effectively disperse the pollution back to the centre and leeward side of the canyon (Fig.112).
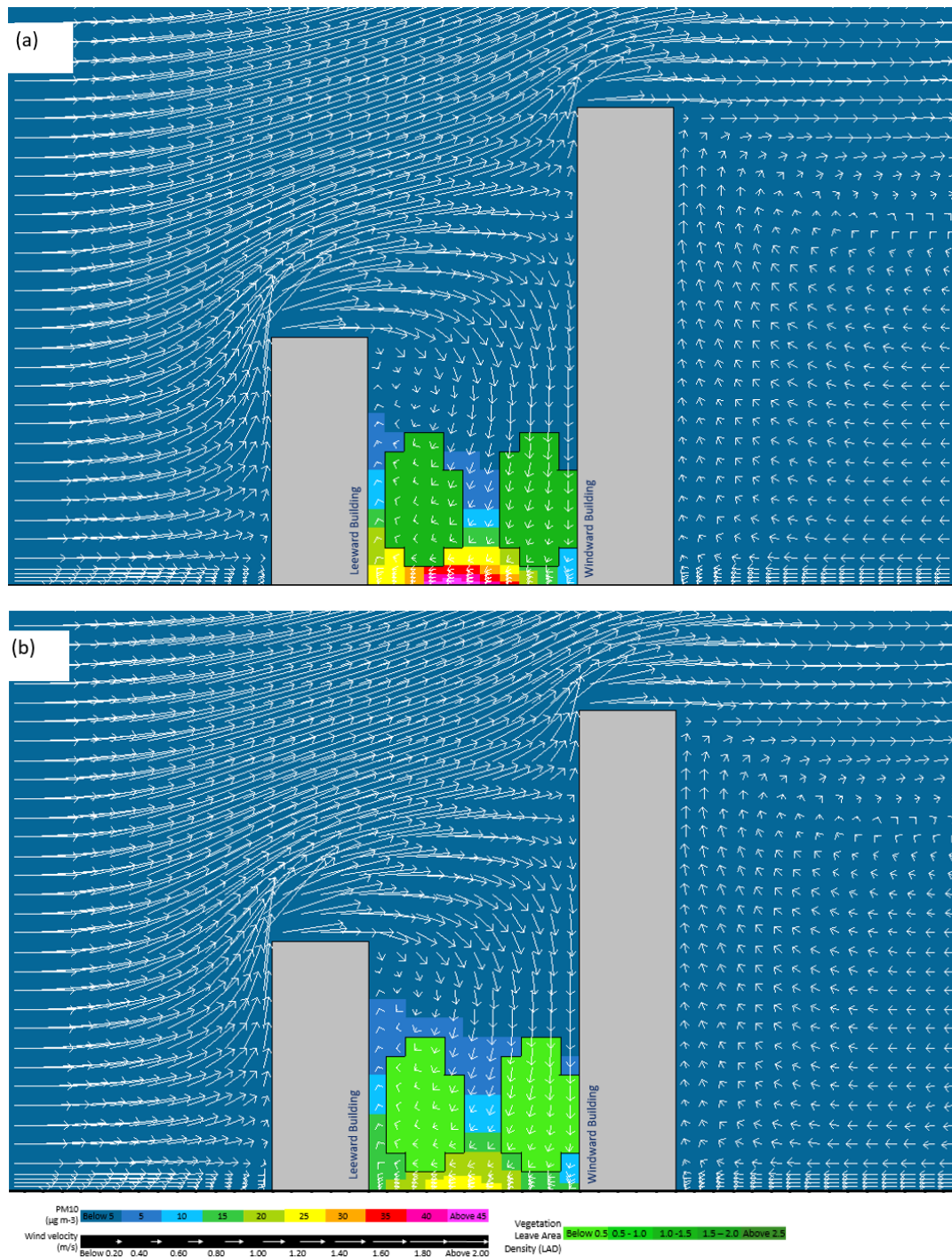
Fig.112 – Step-up narrow high street canyon configurations with trees indicating PM$_{10}$ concentration inside the canyon for (a) step-up summer period, (b) step-up winter period. Section line is the same as Fig.81 (d)

configurations, respectively (Fig.113). This is explained by the fact that when the perpendicular wind direction blows against the leeward building, its velocity decreases significantly, and because of the narrow distance between canyon building rows, the skimming flow regime lacks the necessary force to disperse pollution out of the canyon, instead pushing it from the windward side to the centre and leeward side. As a result, the pollution level at the windward side was lower than the leeward side. One solution to reduce pollution concentrations at pedestrian heights on the leeward side is to place a two-meter hedge row similar to those observed during fieldwork (Fig.69) beneath the tree canopy, where they can protect the public from high air pollution concentration. The author expanded on this idea in a separate study, and the results of fieldwork and computational modelling suggested that combining hedgerows beneath tall trees can slow downwind pollution travel and maximise protection in terms of air pollution concentration at pedestrian height (Borna and Schiano-phan, 2020).
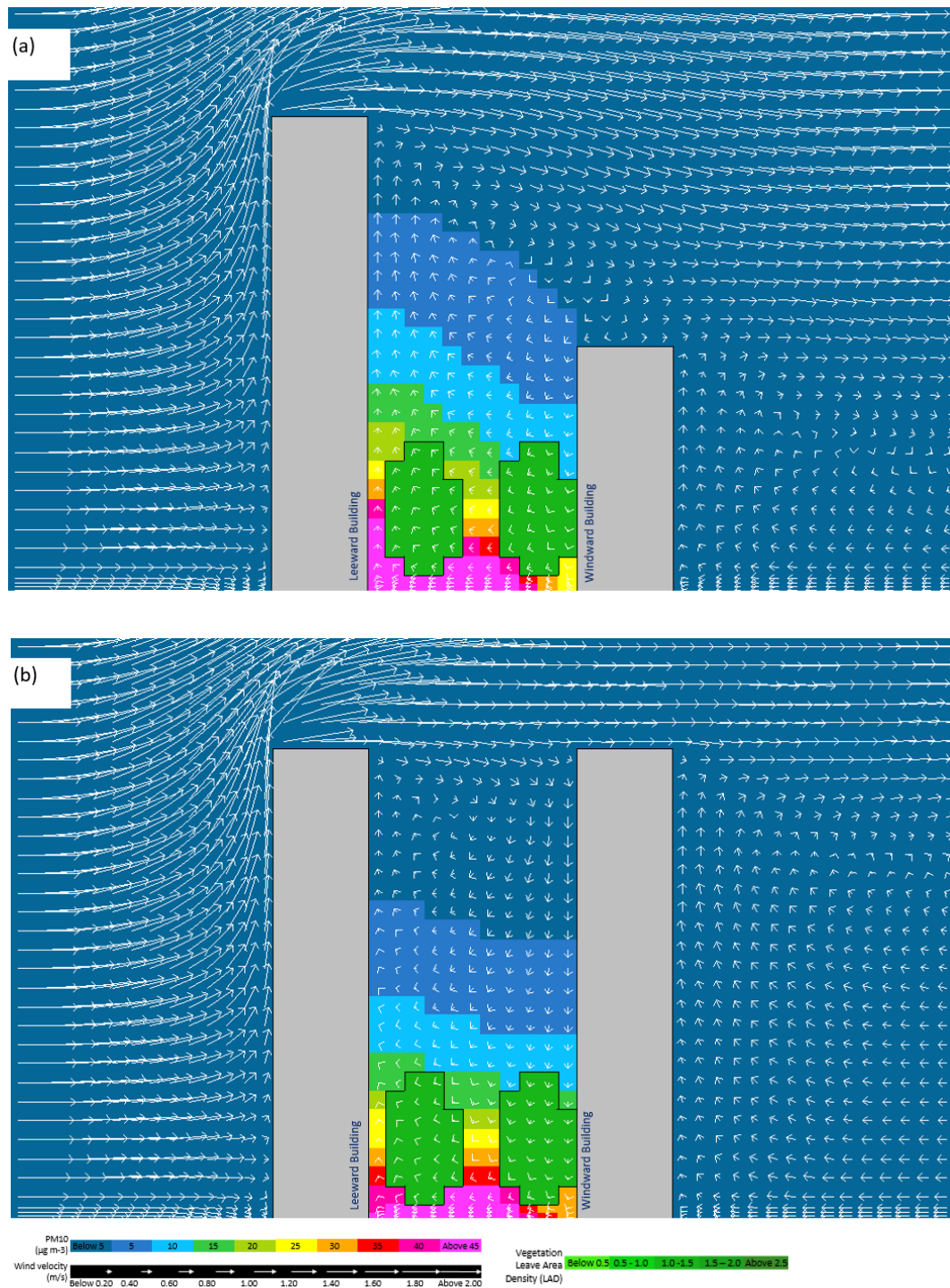
Fig.113 – Step-down and symmetric narrow high street canyon configurations with trees indicating PM$_{10}$ concentration inside the canyon for (a) step-down summer period, (b) symmetric summer period. Section line is the same as Fig.81 (d)

6.2.5 Boulevard street canyon

Boulevard street canyon or avenue canyon has a width of 30 metre with two street widths of 8 metre separated by a pedestrian island in the middle with a street length of 62 metre for both symmetric and asymmetric canyons. The road coverage is 32 percent of the site's total area, while pedestrian areas cover 16 percent. In symmetric and asymmetric canyons, the mean height of roughness elements is 12 and 9 metre, respectively, with building height differentials (ΔH) of 6 metre (Fig.114).
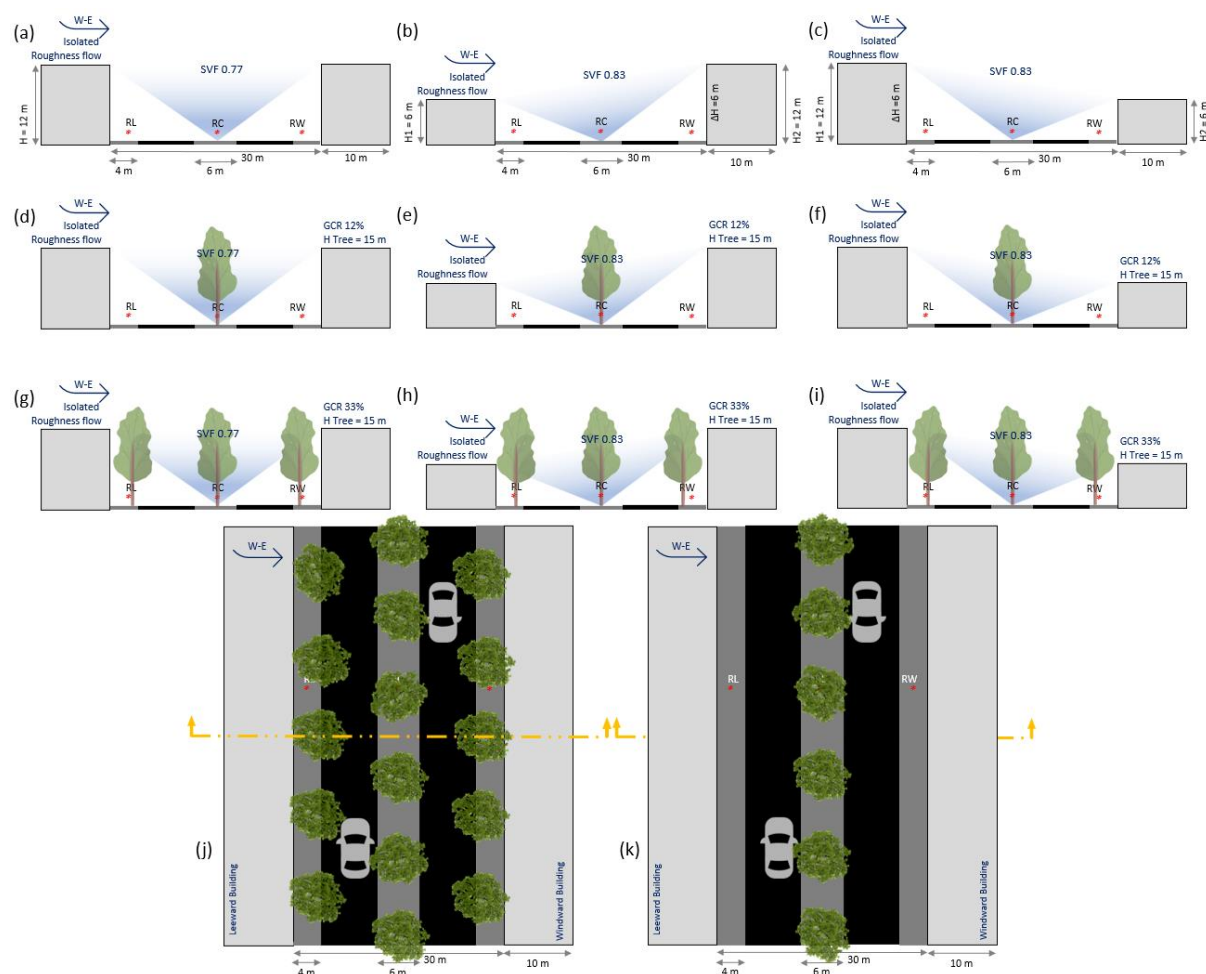
Fig.114 - Schematic section and plan view of 62 meter longitudinal length street canyon layout with the indication of monitoring receptors (*). (a) Symmetric (b) step-up asymmetric (c) step-down asymmetric (d) symmetric + trees in the middle (e) step-up asymmetric + trees in the middle (f) step-down asymmetric + trees in the middle (g) symmetric + trees in 3 sides (h) step-up asymmetric + trees in 3 sides (i) step-down asymmetric + trees in 3 sides (j) & (k) plan views with section line

Within green configurations, the average tree height is 15 metre, which is equivalent to a mature Platanus × acerifolia (London Plane) tree with a canopy diameter of 9 metre, which adds up to 12% green cover ratio of the total area for configurations with one row of trees in the middle of the canyon and 33% for configuration of three rows of trees in the leeward, middle and windward side of the canyon. The upwind of west wind blowing toward the east, resulted in isolated roughness flow regimes across all configurations. In previous canyon configurations i.e. mews, residential, high street and narrow high street, the leeward tend to have the highest pollution levels but as it can be seen from (Fig.115) this pattern has shifted and the windward side constantly exhibited higher pollution level than the leeward side (Fig.115).
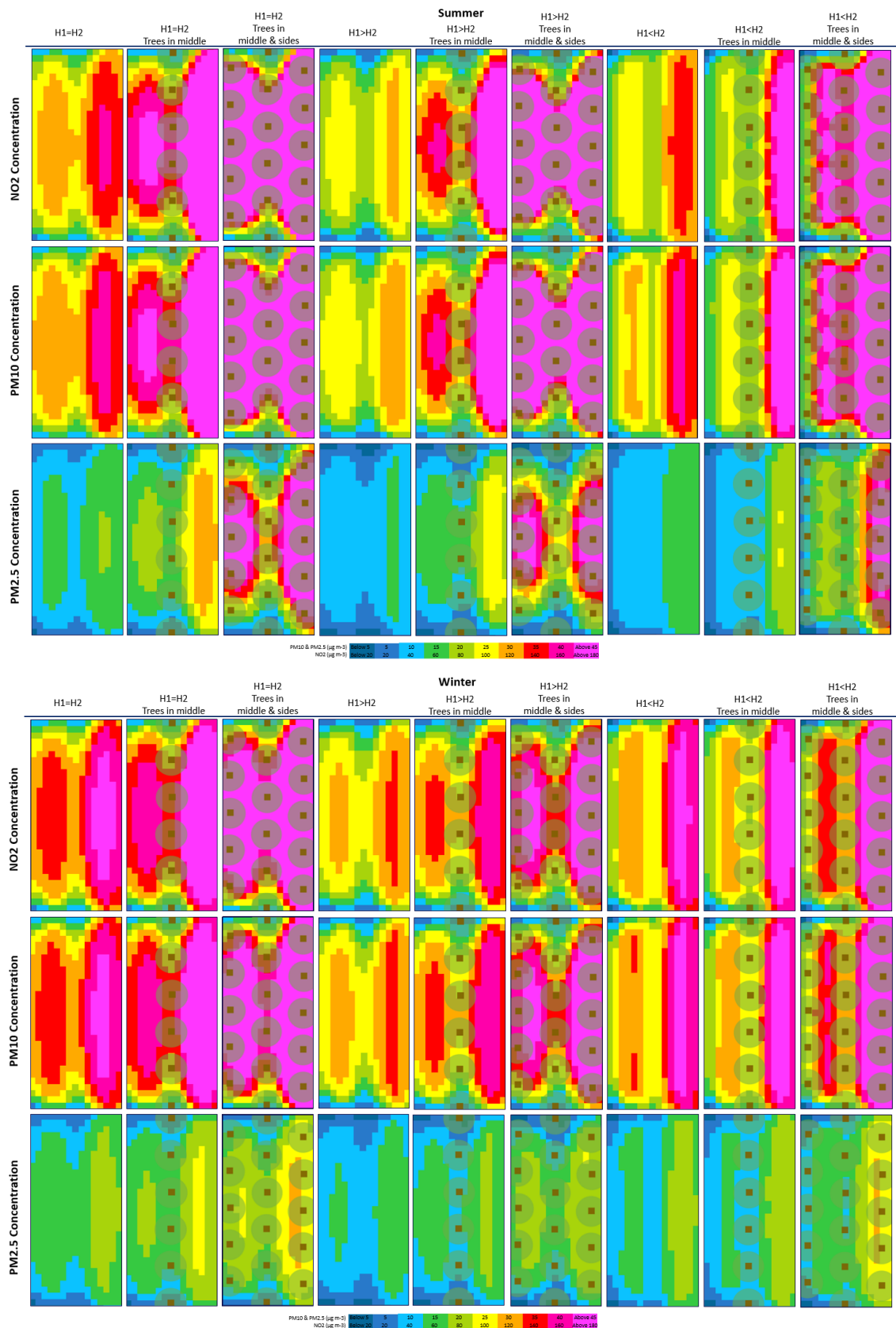
Fig.115 - Pollution levels within various boulevard street canyon configurations. Top (summer), Bottom (winter)

Overall, and among the five urban street canyon types studied, this urban canyon has displayed some of the most controversial results. The pollutant at leeward and windward has increased in most configurations, and in some cases, such as the asymmetric step-up canyon with three rows of trees, NO_2 levels increased by 170 percent, PM_{10} and $PM_{2.5}$ increased by 140 percent in the summer period which is well over the measurement of the receptor located in the middle of the canyon which is relatively closer to the source of pollution. The same configuration ranks second most polluted in the winter period, in comparison to other configurations.

Surprisingly, the highest reduction in pollution was observed at the leeward of the same canyon configuration i.e., step-up canyon with three rows of trees in both summer and winter periods. This is due to the step-up canyon formation and aspect ratio of 0.3, which indicates the large distance between two rows of buildings which induced isolated roughness wind regime in which the pollution has pushed to the windward side of the canyon and accordingly increased the pollution levels at the windward side and reduced the pollution at the leeward side of the canyon. The same pattern can be observed with the rest of the step-up canyon configurations i.e. step-up with trees in the middle and step-up without trees. All these configurations demonstrated a reduction of pollution at their leeward side and a significant increase at their windward side (Fig.116 and Fig.117).
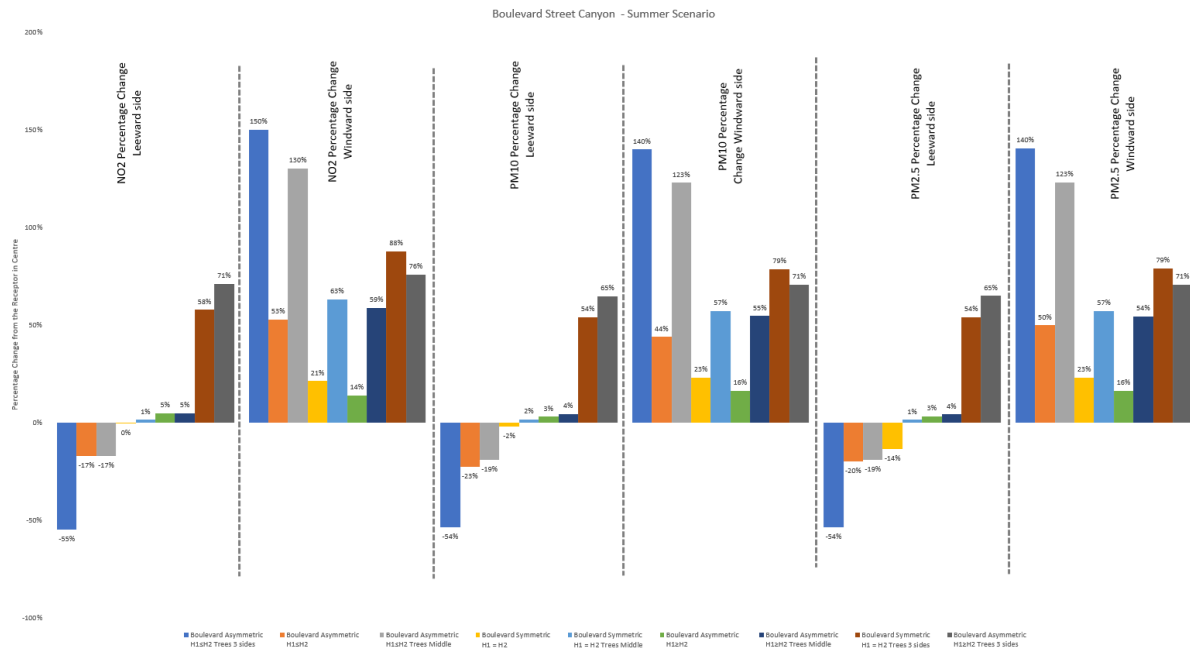
Fig.116 – Boulevard street canyon dispersion rate in percentage. The higher the negative percentage, the more effective in dispersing air pollution (at pedestrian level). This figure was obtained by calculating the percentage change between the source of pollution (centre receptor) and leeward or windward receptors. (Summer period)
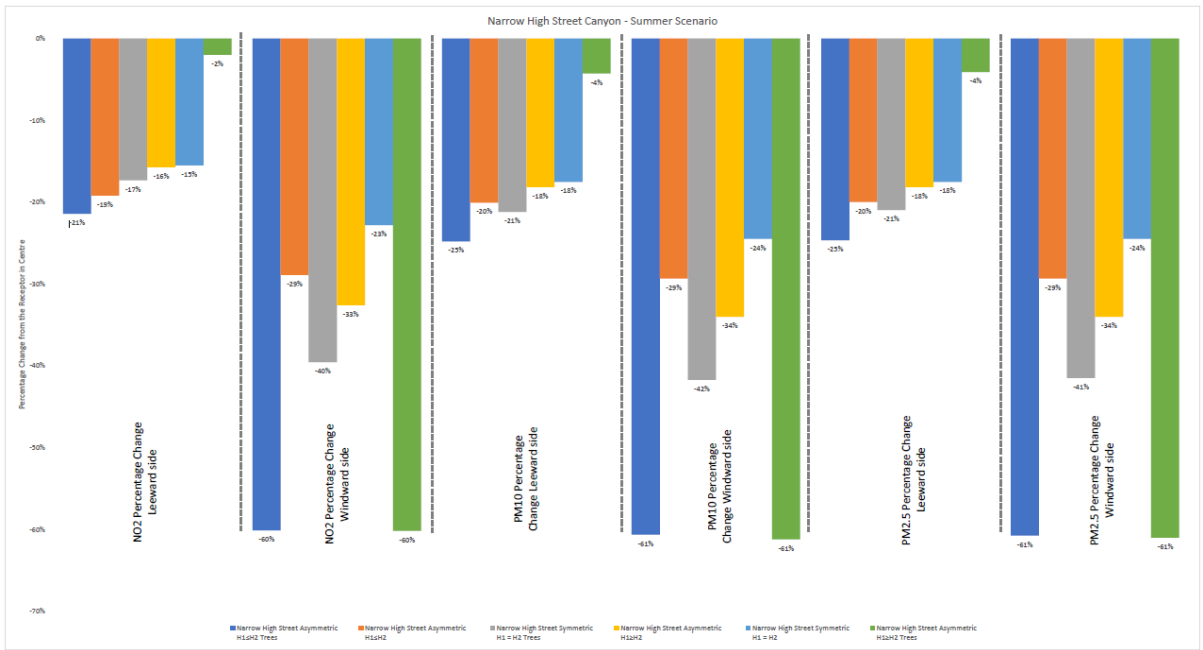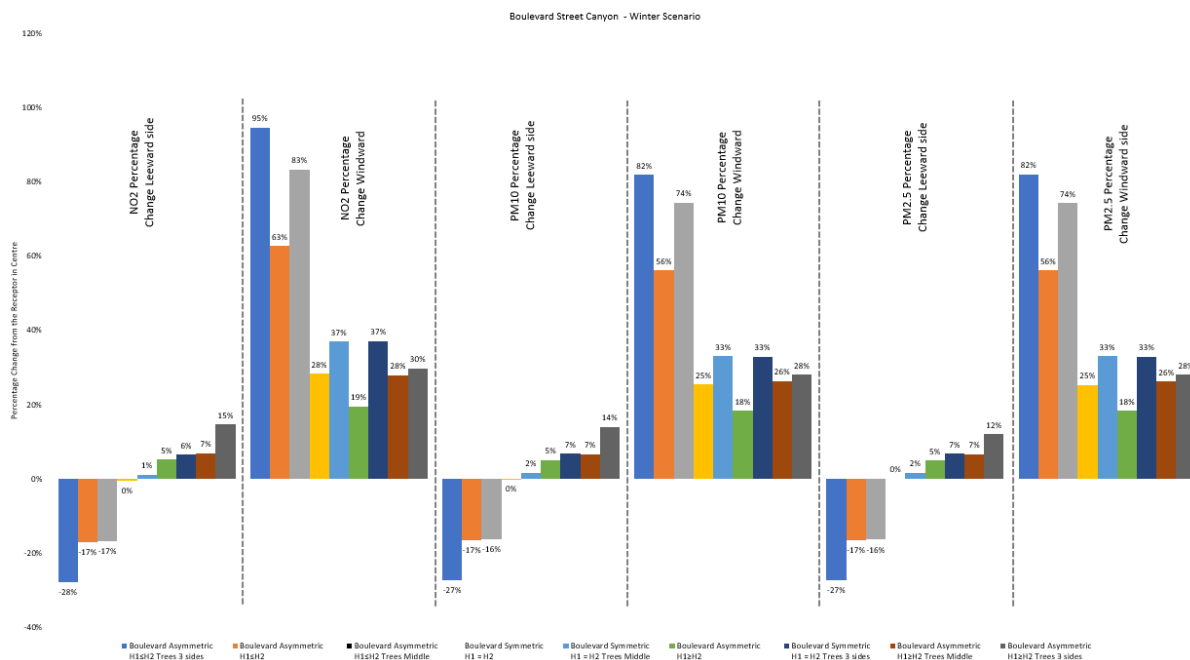

Fig.117 – Boulevard street canyon dispersion rate in percentage. The higher the negative percentage, the more effective in dispersing air pollution (at pedestrian level). This figure was obtained by calculating the percentage change between the source of pollution (centre receptor) and leeward or windward receptors. (Winter period)

Air temperature remained relatively constant, with only a slight increase in relative humidity within the canyons with tree configuration during the summer and the change wasn't noticeable during the winter period. The highest wind velocity was recorded within

192

windward of two canyons, asymmetric step-down and step-up with a row of trees in the middle. Interestingly, the lowest wind velocity observed was 0.01 m/s within the leeward of the asymmetric step-up canyon with three rows of trees during the summer period; this is precisely where the highest dispersion percentage was observed among other canyons. Notably, this location has a sky view factor of 0.37, which is the second-lowest among the other locations, but the pollution dispersion percentage is still significantly higher than, for example, asymmetric step-up or down with a 0.83 SVF (Fig.118 and Fig.119)
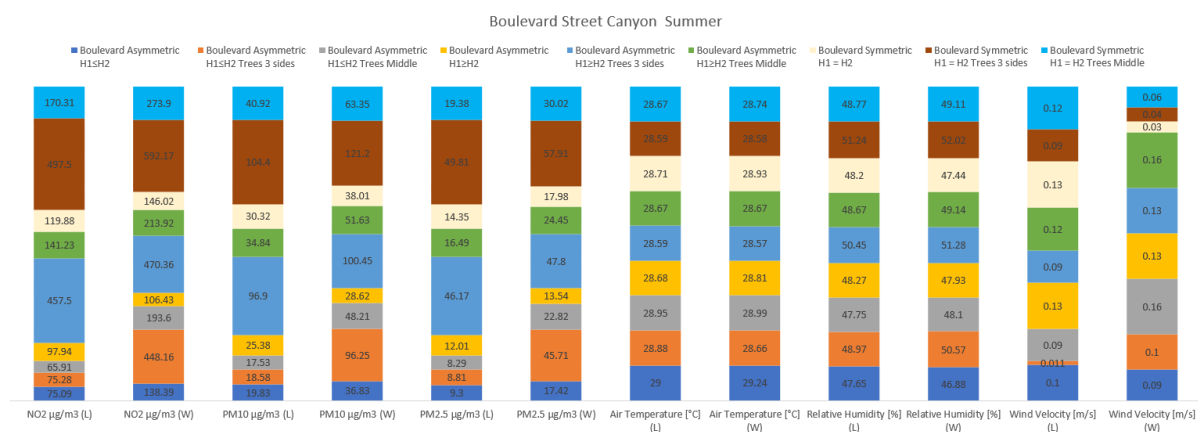
Fig.118 – Boulevard street canyon air pollution and meteorological parameters values – Summer period
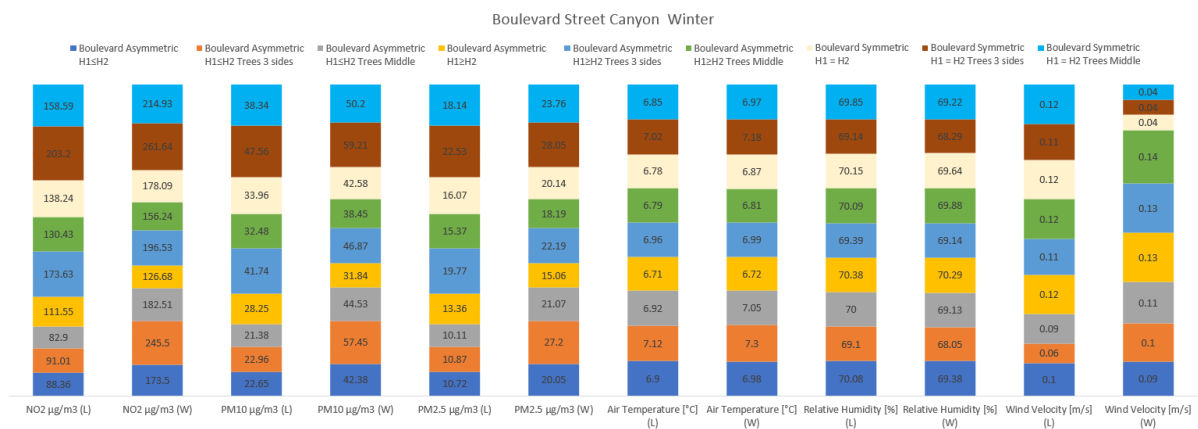
Fig.119 –Boulevard street canyon air pollution and meteorological parameters values – Winter period

6.2.5.1 Discussion – Boulevard street canyon

Based on the results, some of the Boulevard street canyon configurations were found to be the worst case among other canyon types in terms of increasing the concentration of pollution on either side of the canyon. In all configurations, the windward side of the boulevard street canyon increased pollution concentrations to levels that exceeded the levels

measured at the centre of the canyon. The most interesting configuration is the step-up canyon with trees in three sides of the boulevard which exhibited the greatest reduction on its leeward side and the greatest increase on its windward side in both summer and winter (Fig.120).

Fig.120 – Step-up boulevard street canyon configurations with trees indicating PM_{10} concentration inside the canyon for (a) step-up summer period, (b) step-up winter period. Section line is the same as Fig.81 (d)

As it can be seen from the above figure, the lower height leeward building enabled the upwind flow to enter the canyon and pushed pollution to the canyon's centre and under the trees on the windward side. Due to the height of the windward buildings and tree canopy the pollution

is trapped for a longer time and increases the concentration. That means, if there is a choice to limit the pedestrian activities to only one side, it is better to divert the pedestrian flow to the leeward side as people will be exposed to less amount of pollution in comparison to the windward side.

Another interesting finding is the leeward side that demonstrated to have less pollution than the windward side regardless of canyon configurations. For example as it can be seen from Fig.120 the wind rushes downward after being blocked by the row of trees at the leeward side and middle of the canyon and creates a clockwise air recirculation within the leeward side which encouraged partly for the air to mix with the above the roof air volume and partly pushed to the windward side and inevitably reduced the pollution levels at the leeward side and due to the tree canopy and higher building height on the windward side, pollution remained suspended within the pedestrian level for a longer period of time, increasing the pollution concentration. The same pattern of change in pollution levels can be observed in step-down configurations in both seasons (Fig.121). That means, it is crucial to mitigate and reduce pedestrian exposure to pollutants on the windward side. Based on the result of the fieldwork findings and similar to the narrow high street, it is more effective to have a two-meter hedgerow at the windward side adjacent to the street kerbside and under the trees (in canyons with tree configuration) to block pollution and recirculate them upwards and reduce pedestrian exposure.
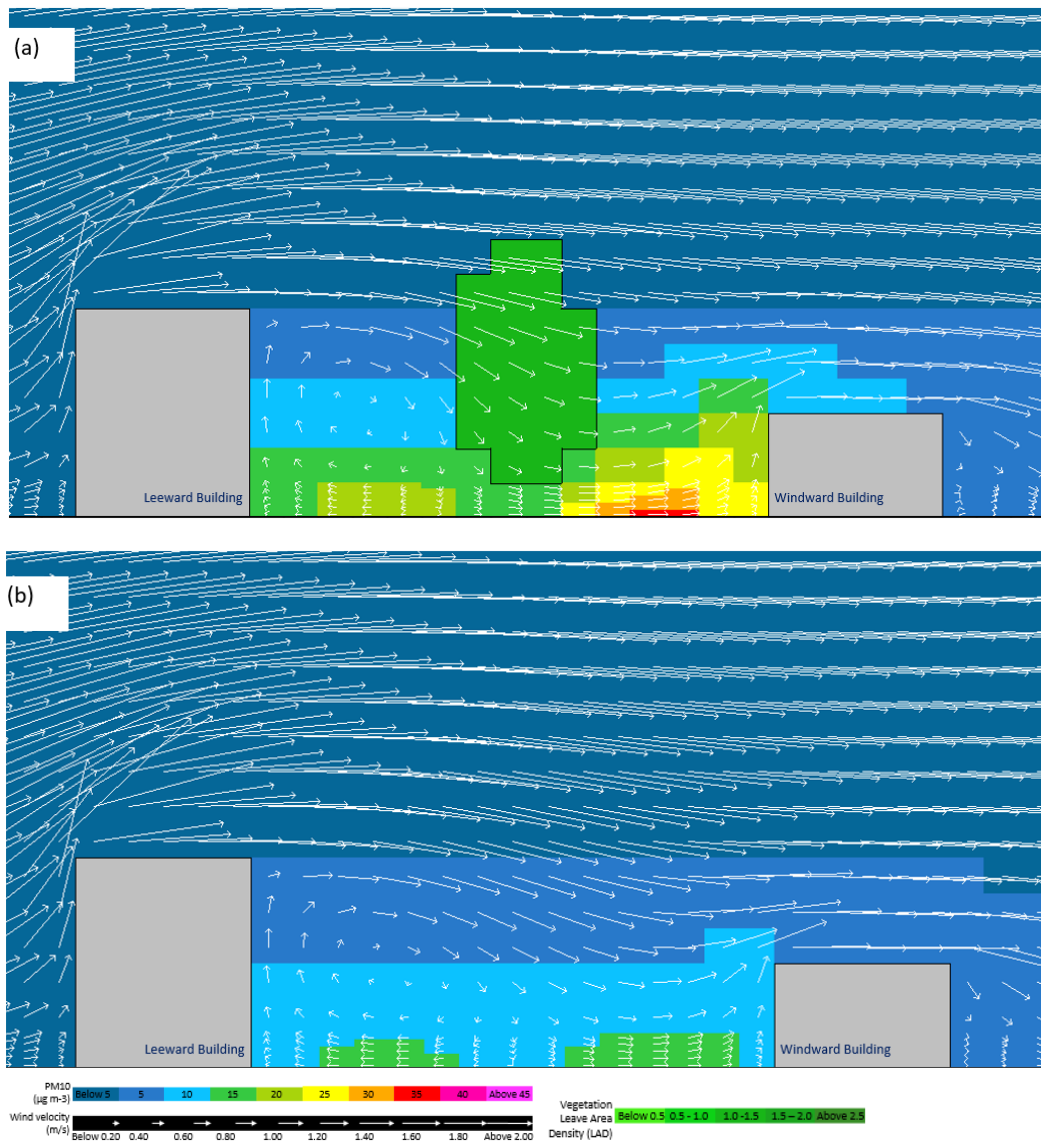
Fig.121 – Step-down boulevard street canyon configurations with trees indicating PM$_{10}$ concentration inside the canyon for (a) step-down with trees in middle summer period, (b) step-down with no tree summer period. Section line is the same as Fig.81 (d)

Interestingly, similar to the other canyon types, the winter period of the no tree configuration is more polluted than the summer period. This demonstrates that the buoyancy effect continues to influence wind behaviour even when the distance between buildings is increased.

6.3 Conclusion

This chapter modelled and compared five major urban street canyons with ENVI-met and to investigate and identify those meteorological and urban morphological indicators that can have the potential to influence the concentration or dispersion of the air pollutants in various street canyons. The street canyons used in this study were mews, residential, high street, narrow high street, and boulevard street canyons. Each urban street canyon was divided into six variations, each with a different aspect ratio (H/W) and tree arrangement. The symmetric urban canyon (H1=H2), asymmetric step-up canyon (H1≤H2), and asymmetric step-down canyon (H1≥H2) were the three variations used for this exploration. With the exception of mews street canyon, all other canyon configurations were simulated once with and once without trees.

Overall, the air temperature and relative humidity remained relatively constant within various canyon types and configurations. The highest relative humidity was recorded as 70.92% on the windward side of asymmetric step-down in residential canyon type in the winter period and the lowest of 46.88% on the windward side of the boulevard step-up street canyon type in the summer period. The highest temperature of 29.24 °C was recorded on the windward side of the boulevard step-up canyon type in summer and the lowest temperature of 6.46 °C was recorded on the windward side of the narrow high street step-up canyon type in the winter period.

In terms of pollution levels and within the mews canyon type, the step-up canyon had the highest pollution percentage change (high dispersion rate), but the step-down canyon with SVF of 0.6 had the lowest measured pollution level. This demonstrates that the canyon side with the greatest percentage change does not always imply to have the least amount of pollution. As a result, it's critical to consider the mean pollution concentration in the canyon when deciding on the best configuration with the lowest pollution levels. Generally, the summer configurations were 1.2 times less polluted than their winter counterparts. This is primarily because of the wind and thermal environments, which have an effect on pollutant dispersion in street canyons due to thermal buoyancy force effects. As a result of this phenomenon the rate of pollution dispersion in step-down canyon has increased, making it one of the best configurations within this canyon type in terms of air quality level in

comparison to other mews street canyon configurations, particularly symmetric canyon configurations which should be avoided.

The residential canyon at the windward side of the canyon side exhibited less pollution levels than the leeward side. This is due to a greater distance between buildings in the residential canyon where the wake interference flow is induced. Moreover, the buoyancy-driven flow caused by differential wall heating affects the flow field inside the urban street canyon. Accordingly, a stronger wind flow was generated on the canyon's windward side, pushing the pollution emitted in the canyon's centre upwards, where it dispersed quickly and was removed from the street canyon before it was transported to either side of the canyon. Surprisingly, the step-up canyon configurations showed the opposite pattern and pollution levels were measured higher at the leeward side of the canyon. As a result of the washdown (downdraught) effect, the incoming perpendicular wind increases airflow at the windward side and transports pollution to the centre and leeward side of the canyon.

Within the high street canyon type and across all the configurations the highest air pollution levels were recorded at the leeward side of the symmetric canyon with trees in the summer period; this canyon also has one of the lowest sky view factors. The concentration of NO_2 increased on the windward side of the asymmetric step-up with trees configuration during the summer. This could be due to the impact of trees with dense foliage on wind behaviour, which reduces wind velocity. However, when the wind velocity was compared to other configurations, it was discovered that the wind velocity was one of the highest, with a mean wind velocity of 0.35m/s. This indicates that higher wind velocity does not always imply higher dispersion and that other factors such as vegetation density and urban form are far more important in increasing or decreasing pollution concentrations, especially for gaseous pollutants like NO_2.

The narrow high street canyon type showed a similar pattern of pollution levels change between the leeward and windward sides as the mews street canyon. Regardless of the canyon configuration, the leeward side was always more polluted than the windward side of the canyon. The highest reduction in pollution was recorded at two canyon configurations, both in the summer period and on the windward side of the step-up and step-down with

trees. It is interesting that both configurations are included trees and it is an indication of their role in effectively protecting the space beneath their canopy. Furthermore, this demonstrates the significance of the downdraught effect, which has pushed wind downward and towards the street, which has accelerated due to the limited space between buildings. The worst case scenarios, according to the results, are for symmetric and step-down canyon configurations, respectively. This is explained by the fact that when the perpendicular wind direction blows against the leeward building, its velocity decreases significantly, and because of the narrow distance between canyon building rows, the skimming flow regime lacks the necessary force to disperse pollution out of the canyon, instead pushing it from the windward side to the centre and leeward side. One solution for reducing pollution concentrations at pedestrian heights on the leeward side is to place a two-meter hedge row similar to those observed during fieldwork (Fig.69) beneath the tree canopy, where they can protect the public from high air pollution concentration.

The boulevard street canyon showed the most controversial results among the five urban street canyons studied. In previous canyon configurations the leeward side of the canyon showed to have the highest pollution levels but this pattern has shifted within the boulevard canyon type and the windward side constantly exhibited higher pollution levels than the leeward side. The most interesting configuration is the step-up canyon with trees in three sides of the boulevard which exhibited the greatest reduction on its leeward side and the greatest increase on its windward side in both summer an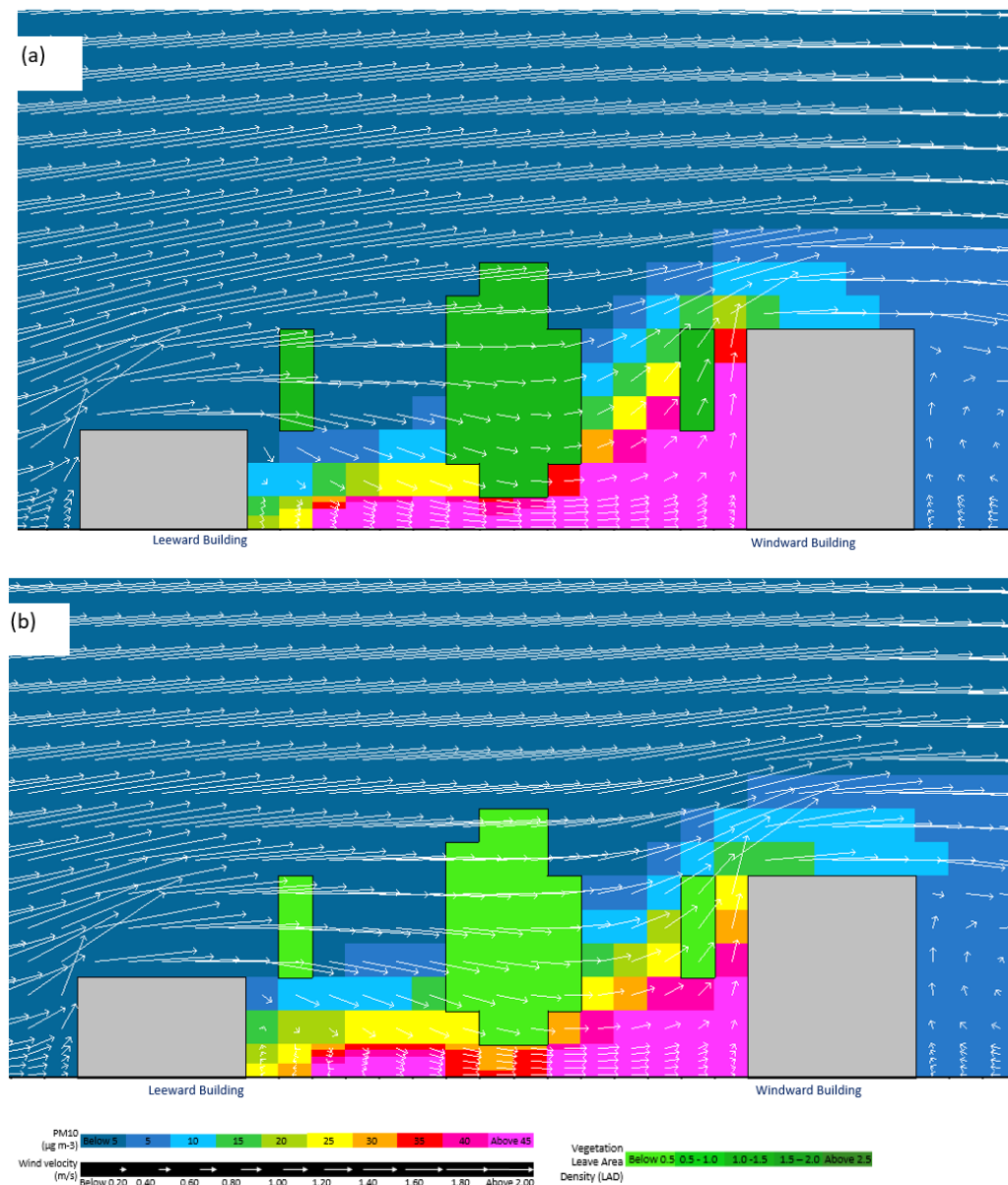d winter. This is because the lower height leeward building enabled the upwind flow to enter the canyon and pushed pollution to the canyon's centre and under the trees at the windward side. Due to the height of the windward buildings and tree canopy the pollution is trapped for a longer time and increases the concentration. That means, if there is a choice to limit the pedestrian activities to only one side, it is better to divert the pedestrian flow to the leeward side as people will be exposed to less amount of pollution in comparison to the windward side.

These are interesting findings that require further investigation and discussion to reveal interdependencies and identify relationships between various parameters in order to determine which parameters can be manipulated to affect the microclimate and reduce air pollution concentration in various urban canyons. For that reason, the next chapter builds on

the findings of this chapter by analysing the results of the computational modelling with the Pearson correlation to highlight the strength and direction (negative or positive) of relationships between variables and to identify associations between air pollution concentration and meteorological parameters and morphological indicators within each canyon type and configuration. The following chapter will also outline a set of recommendations for the most favourable urban street canyon configuration(s) capable of improving urban microclimate and air pollution concentration at pedestrian height.

Part 3

Correlation analysis and recommendations

Chapter 7

Chapter 7

Correlation analysis and recommendations

Similar to the fieldwork study (chapter 5), to analyse the result of the computational modelling (chapter 6), this chapter uses the Pearson correlation coefficient to summarise the strength and direction (negative or positive) of relationships between variables. As it was explained in chapter 5, correlation analysis can identify meaningful relationships between various metrics and parameters to offer new insights and reveal direct and indirect interdependencies to explain phenomena and complement the results from the computational modelling. Accordingly, statistical significance was defined as $p \leq 0.05$ to identify associations between the level of change in one variable due to the change in the other.

In addition to the above, this chapter provides a greater discussion on the findings of the fieldwork (chapter 5), computational modelling (chapter 6) and correlation analysis to signify the impact of urban form on microclimate and concentration of air pollution within various urban street canyons. Based on this discussion, it then provides a set of recommendations on the most effective urban street canyon configuration(s) capable of eliminating or reducing undesirable microclimate conditions in urban outdoor spaces, thereby reducing air pollution concentrations. This will assist urban planners and designers in considering their design implications in advance and making informed design decisions to encourage greater dispersion of air pollution within various urban street canyons, particularly in areas with high pedestrian traffic.

7.1 Result and discussion of correlation analysis

This section presents the results and discussion of the Pearson correlation analysis performed on the five urban street canyons. The Pearson correlation data was extracted from the computational modelling results presented in chapter 6. Each canyon type's data is analysed three times, once with summer data and once with winter data and once with data from both seasons combined. The latter analysis provides a deeper understanding of the dominant seasonal and annual parameters that influence the microclimate and air pollution concentration. The parameters that had the same value within each urban canyon were omitted from the analysis because the Pearson correlation does not calculate parameters with similar values in a similar set; therefore, no values will be assigned.

7.1.1 Mews street canyon

Pearson correlation analysis was applied to all mews street canyons to investigate possible relationships between air pollutants, meteorological conditions and urban morphological indicators. The Pearson correlation analysis of the summer period identified that the p-values of all the air pollution correlations are greater than 0.05 and therefore, none of the parameters are taken forward for further discussion or exploration. However, non-air pollution parameters such as air temperature on the windward side of the canyon showed a significant positive correlation with the air temperature of the leeward side and a negative correlation with the relative humidity of the opposite side (windward side). The sky view factor showed a significant negative correlation with floor area ratio and mean canyon aspect ratio and showed a positive correlation with building height differentials (Fig.122).

Fig.122 – Heatmap displaying Pearson correlation analysis r values and p-values between mews street canyon summer period

The winter period Pearson correlation analysis identified that there is a statistically significant negative correlation between pollution levels on the leeward and windward sides of the mews street canyon and relative humidity on the leeward side of the canyon. The relative humidity of the windward side of the canyon showed a significant negative correlation with mean pollution levels (Fig.123).

Fig.123 – Heatmap displaying Pearson correlation analysis r values and p-values between mews street canyon Winter period

When both summer and winter data were compared the Pearson correlation analysis identified that there is a statistically significant negative correlation between pollution levels on the leeward and windward sides and mean pollution levels with wind velocity at the centre of the canyon and mean wind velocity (Fig.124).

Fig.124 – Heatmap displaying Pearson correlation analysis R values and p-values between mews street canyon Summer and Winter period

7.1.1.1 Discussion - Mews street canyon

In addition to the above and in order to further reduce the pollution levels in various configurations, it is critical to consider the correlation of mean wind velocity with other parameters. For example, in addition to its negative correlation with all pollutants, mean wind velocity was found to have a negative correlation with floor area ratio, mean aspect ratio, and average building heights. It also showed a positive correlation between the sky view factor and the building height differentials. **That means, if possible asymmetric canyons should be encouraged otherwise in the case of symmetric canyons the floor area ratio, mean canyon aspect ratio, and average building heights must be kept as low as possible while in asymmetric canyons the building height differentials must be increased to their maximum, which will effectively increase the sky view factor and will increase the mean wind velocity, thereby reducing pollution level within the canyon.**

In the similar vein and based on the preceding argument, **it is recommended to keep the leeward side higher than the windward side in order to maximise wind flow within the canyon's central section and dilute more pollutants with incoming air.** Having said that, it is not recommended to alter the street width or building heights in canyon type, as this may result in the canyon transforming to a residential or high street urban street canyon type. As previously stated, the street width and building heights are taken from the street manual guideline, and for the sake of consistency, it was decided to disregard changes in floor area ratio or mean canyon aspect ratio and instead focus on average building heights and differentials. **Overall, and based on the result, in symmetric canyon type the greater the average building height, the lower the dilution rate and consequently higher concentration of air pollution within the canyon.** Based on the result of the correlation analysis the lower the height of the windward side building the lower air pollution levels at the leeward, centre, and windward side of the canyon and overall mean pollution levels.

7.1.2 Residential street canyon

Similar to the mews street canyon the Pearson correlation analysis was applied to all residential street canyons to investigate possible relationships between air pollutants, meteorological conditions and urban morphological indicators. The result of the summer period Pearson correlation analysis identified that there is a statistically significant negative correlation between pollution levels on the windward side of the residential street canyon and the sky view factor ($p \leq 0.05$). Although the heatmap indicated a greater number of correlations with high strength of associations (r-value) however, the p-value was greater than 0.05; therefore, these correlations weren't taken forward. A similar pattern can be observed with mean NO_2 and $PM_{2.5}$ and the sky view factor but not with mean PM_{10} (Fig.125).

Fig.125 – Heatmap displaying Pearson correlation analysis R values and p-values between residential street canyon Summer period

The winter period Pearson correlation analysis identified that there is a statistically significant positive correlation between pollution levels and air temperature levels on both sides of the canyon (leeward & windward). The same parameters showed a significant negative correlation between relative humidity on both sides of the canyon and mean relative humidity and wind velocity on the leeward side of the canyon. The pollution levels on the leeward side of the canyon were also negatively correlated with relative humidity on the leeward side and mean relative humidity, surface-to-volume ratio, building height differentials and positively correlated with floor area ratio, mean canyon aspect ratio and average building heights. The heatmap also demonstrated that there is a significant negative correlation between pollution levels on the leeward and windward sides of the residential street canyon and surface to volume ratio, Sky view factor and Building height differentials (Fig.126).

Fig.126 – Heatmap displaying Pearson correlation analysis R values and p-values between residential street canyon Winter period

When both summer and winter data were compared the Pearson correlation analysis identified that there is a statistically significant positive correlation between pollution levels on the leeward and windward sides and mean pollution levels of the residential street canyon and floor area ratio, mean canyon aspect ratio and average building heights. The heatmap also demonstrated that there is a significant negative correlation between pollution levels on the leeward and windward sides and mean pollution levels of the residential street canyon and surface to volume ratios, sky view factor and building height differentials. At the same time, no significant correlation was found between air pollution concentration and meteorological parameters such as wind, temperature or relative humidity (Fig.127).

Fig.127 – Heatmap displaying Pearson correlation analysis r values and p-values between residential street canyon Summer and Winter period

7.1.2.1 Discussion - Residential Street canyon

The correlation analysis revealed that trees reduce the sky view factor and slow down the wind velocity and movement, resulting in an increase in the concentration of pollutants due to a negative correlation between trees and air pollution levels. This is consistent with fieldwork and computational modelling results presented in chapter 5 and 6 and it indicates that in this configuration, increasing the number of trees results in an increase in pollution levels.

A closer look at the correlation analysis reveals that wind velocity on the windward side of the canyon is positively correlated with the green cover ratio and average tree heights, demonstrating the critical importance of reducing obstacles and greenery on the leeward side to increase wind velocity and promote greater air movement within the canyon, resulting in

increased pollution removal. **Therefore, it is recommended to have a limited number of trees and, if possible, trees of lower height on the canyon's leeward side.**

Additionally, and perhaps most importantly, the green cover ratio and average tree heights exhibited a negative correlation with the sky view factor, implying that generally a lower height and fewer trees within the canyon will result in a higher dispersion rate and improved air quality in the canyon, which should be encouraged. **The negative correlation between building height differentials and air pollutants demonstrates the critical nature of height variation within this canyon configuration**. **That means the lower the building height differentials, the higher the pollution levels** and the symmetric canyon configuration is strong evidence for this outcome and should be avoided on busy roads with high pedestrian traffic. Alternatively, any high pedestrian activities must be located on the windward side of the canyon, so that public exposure is minimised.

Based on the results, the best case scenario for tree configurations is step-up canyon, while the best case scenario for no tree configurations is the asymmetric step-down, which should be encouraged. **The symmetric canyon, whether with or without trees, increased mean pollution levels and should be avoided entirely.** Based on the result of the correlation analysis the lower the height of the windward side building the lower the air pollution levels at centre, windward and overall mean pollution levels.

7.1.3 High street canyon

Based on the result of the Pearson correlation analysis it has been identified that there is a statistically significant positive correlation between pollution levels on the windward side and mean pollution levels with mean relative humidity, relative humidity at both sides of the canyon, green cover ratio and average tree heights. The same parameters showed a negative correlation with the sky view factor and impervious surface fraction. The pollution levels on the leeward side of the canyon showed a negative correlation with wind velocity on the leeward side and a positive correlation with mean relative humidity and relative humidity on both sides of the canyon (Fig.128).
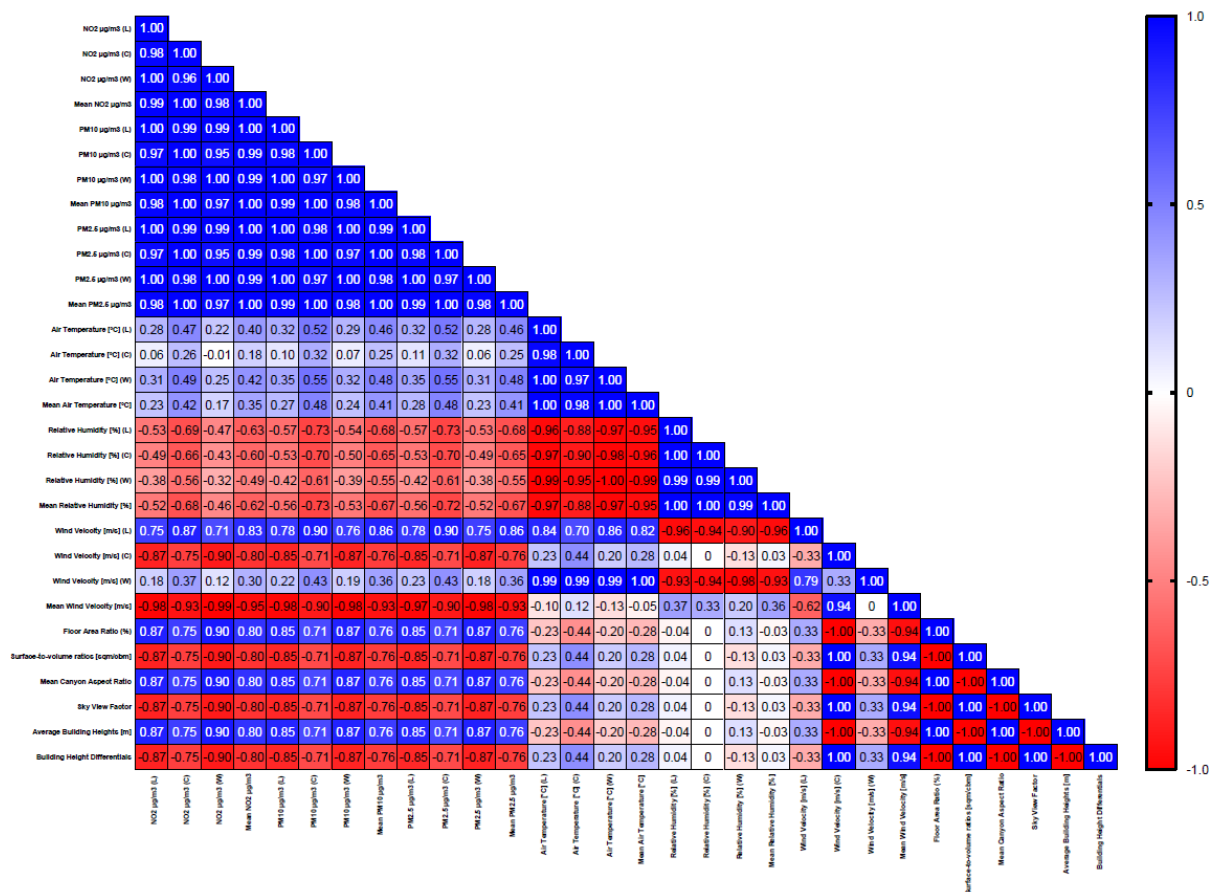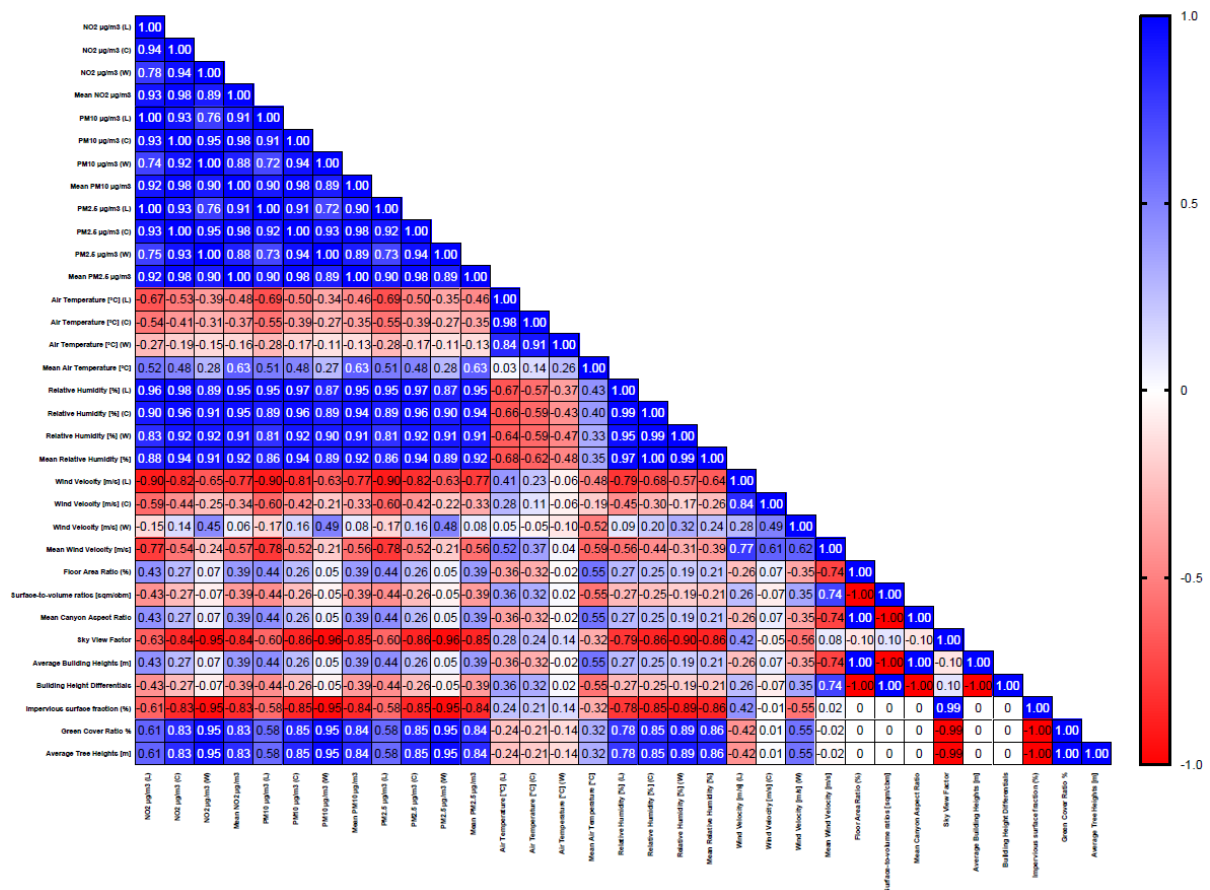
Fig.128 – Heatmap displaying Pearson correlation analysis r values and p-values between high street canyon Summer period

The winter period Pearson correlation analysis identified that there is a statistically significant negative correlation between pollution levels on the windward side and mean pollution levels with mean relative humidity, relative humidity at both sides of the canyon and a positive correlation with mean air temperature and air temperature measured on the leeward side of the canyon. The leeward side air pollution levels only showed a significant negative correlation with mean wind velocity. The sky view factor showed a negative correlation with windward air pollution levels and no significant correlation was identified with leeward side or mean air pollution levels (Fig.129).
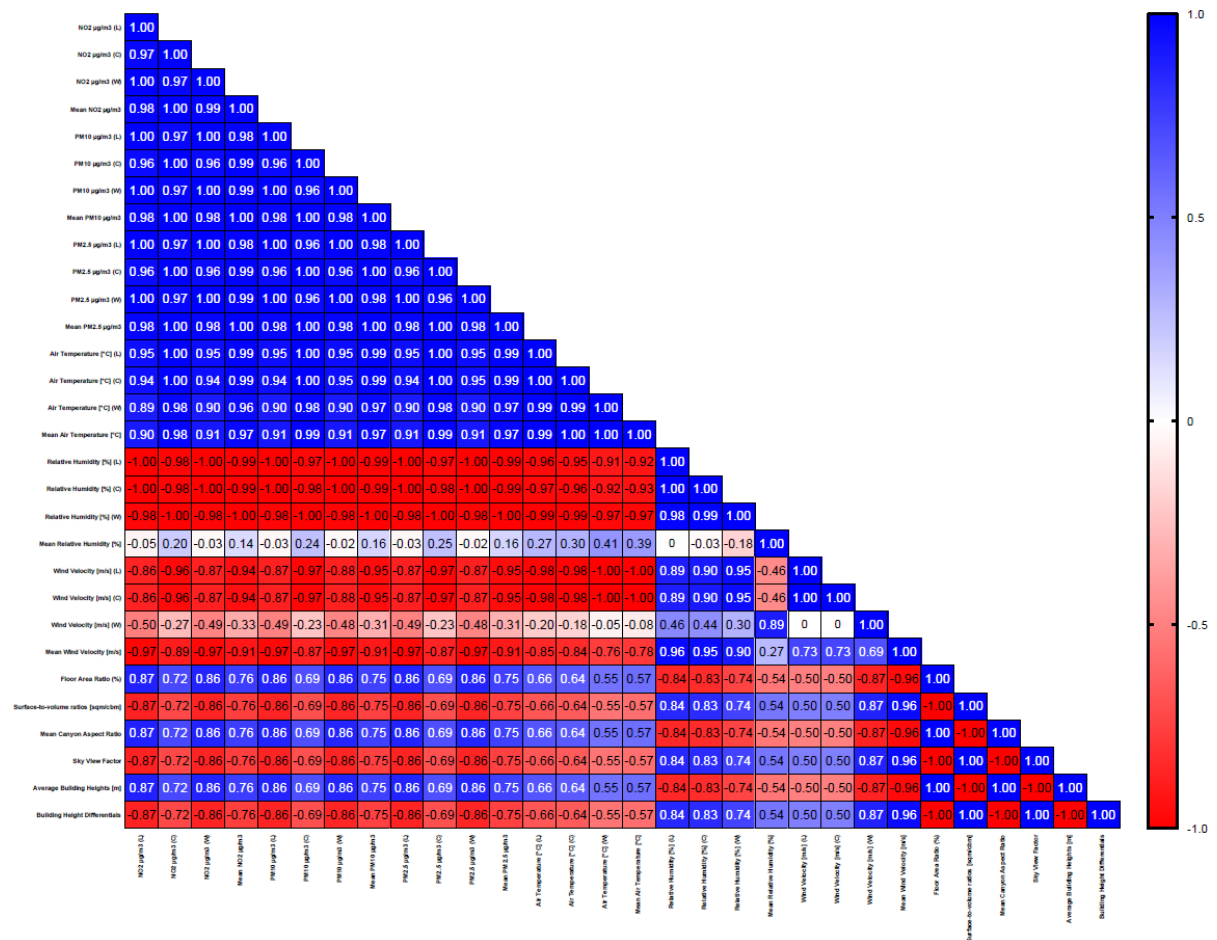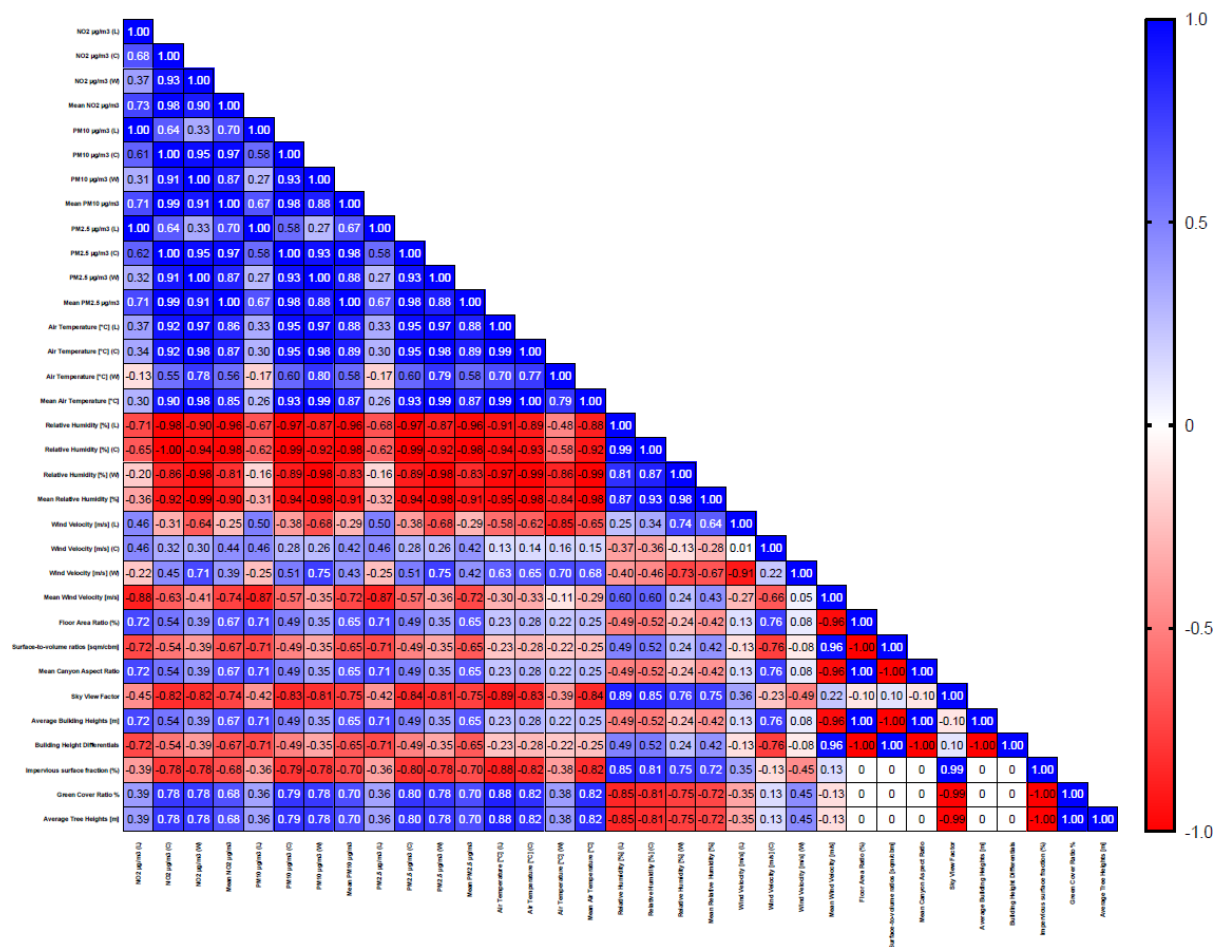
Fig.129 – Heatmap displaying Pearson correlation analysis r values and p-values between high street canyon Winter period

The result of the Pearson correlation analysis for both summer and winter identified that there is a statistically significant negative correlation between pollution levels on the leeward side of the high street canyon and mean wind velocity. The heatmap also demonstrated that there is a significant negative correlation between pollution levels on the windward and mean air pollution levels with the sky view factor and impervious surface fraction. The same parameters showed a significant positive correlation with the green cover ratio and average tree heights. Surprisingly, no significant correlation was found between air pollution concentration and urban form parameters on the leeward side of the high street canyon (Fig.130).
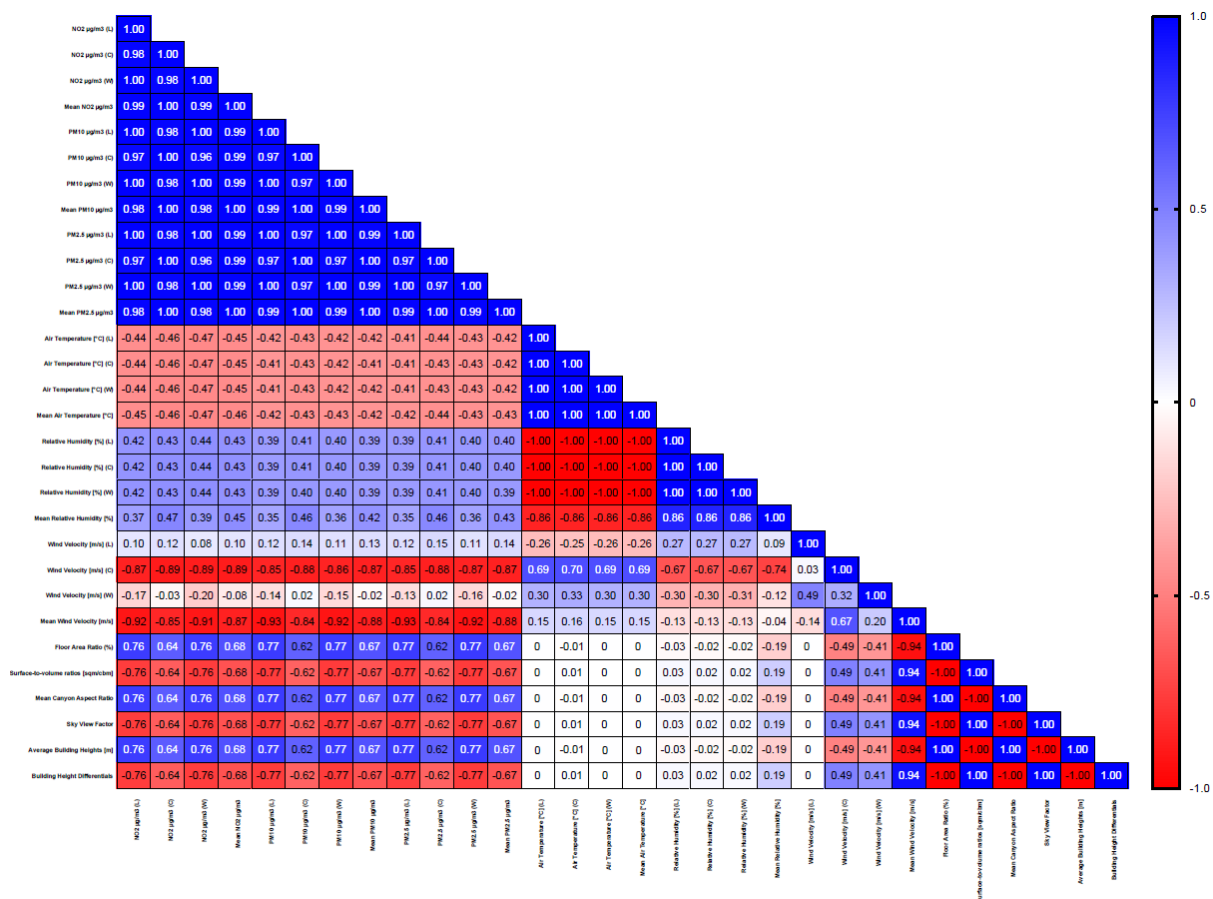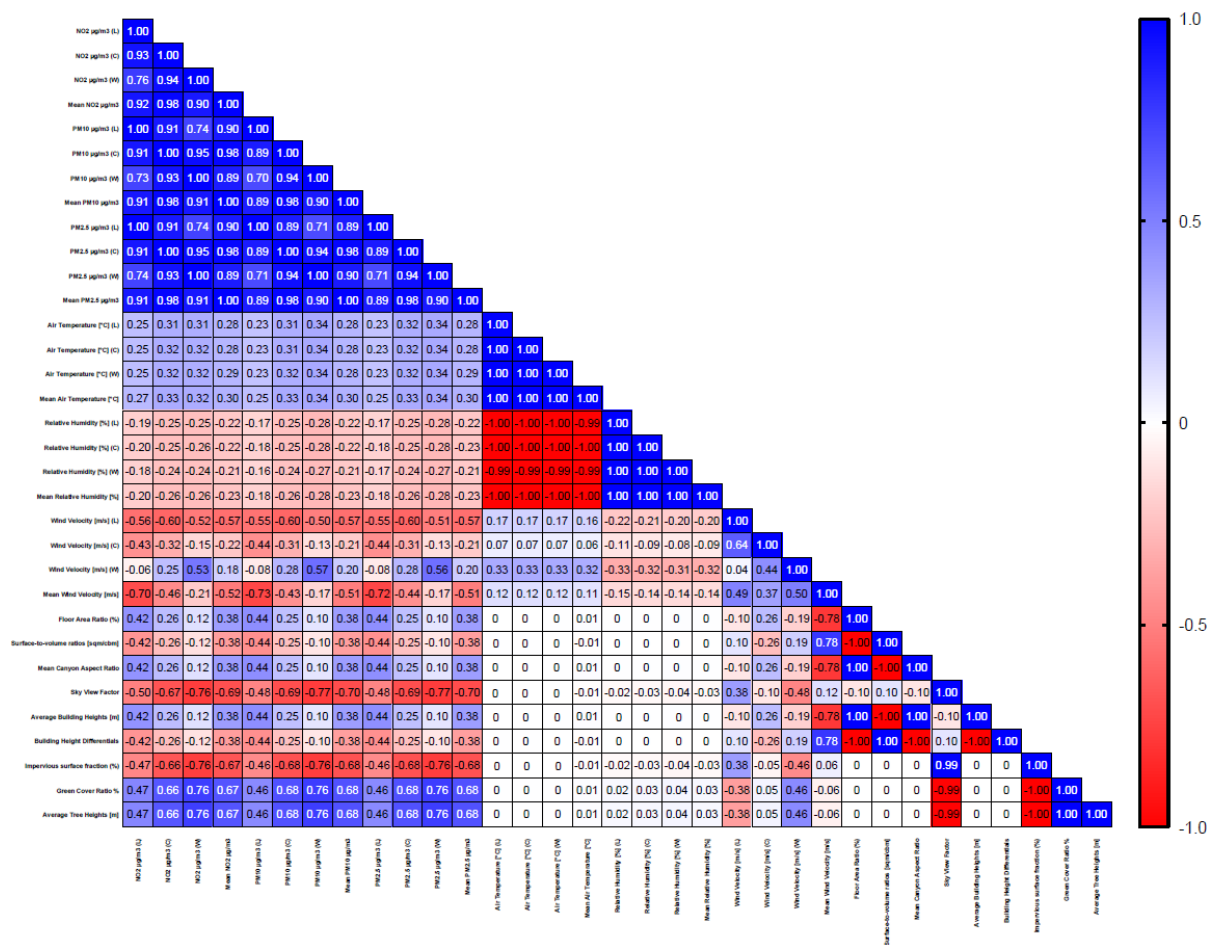
Fig.130 – Heatmap displaying Pearson correlation analysis r values and p-values between high street canyon Summer and Winter period

7.1.3.1 Discussion – High street canyon

In contrast to mews and residential canyons and as it was mentioned in chapter 6, the high street canyon type **did not exhibit a consistent pattern of change in leeward and windward air pollution levels or mean air pollution levels.** These changes were relatively homogeneous in mews and residential canyons, making it simpler to compare and identify the best and worst case scenarios. As a result, the correlation coefficient r between pollution levels on the leeward and windward sides is lower than in mews and residential canyons. For example, the r value of NO_2 at leeward and windward is 0.76 with a p-value of less than 0.01 in comparison to the same pair in residential, which is 0.96 with a p-value of less than 0.001, and this is the same and even stronger within mews canyon, with an r value of 1.00 and a p-value of less than 0.001.

The only parameter with a high potential to reduce pollution concentrations on the leeward side of the canyon is mean wind velocity, which has a negative correlation with leeward pollution levels but no correlation with windward or mean air pollution levels. That means, the mean wind velocity must be increased to provide a higher dispersion rate and better air quality on the leeward side.

Given that the mean wind velocity has a positive correlation with building height differentials (r-value = -0.78 and p-value 0.01), a larger difference between leeward and windward building heights will cause more wind flow and velocity inside the canyon. The pollution level on the leeward side also exhibited a correlation with other urban morphological indicators such as floor area ratio and mean canyon aspect ratio; however, as previously stated, it was decided not to manipulate these parameters because doing so would change the fundamental of the canyon configuration and its classification.

To influence change and reduction in pollution levels on the windward side, the green cover ratio and average tree heights showed a positive correlation with pollution levels on the windward side and overall within the canyon (mean pollution level), while the sky view factor has a negative correlation, implying that having shorter heights and fewer trees at windward side will increase the sky view factor, and the overall result of this manipulation will be a microclimate capable of dispersing greater pollution from the canyon. Furthermore, because mean pollutant levels have a positive correlation with leeward and windward pollution levels, the leeward side is expected to be less polluted as a result of changes in tree allocation and height.

7.1.4 Narrow high street canyon

Based on the result of the Pearson correlation analysis it has been identified that the leeward side of the canyon has a significant negative correlation with the air temperature on both sides of the canyon and a positive correlation with mean relative humidity and relative humidity at both sides of the narrow high street canyon. The mean pollution levels showed a highly significant positive correlation with mean relative humidity and relative humidity on both sides of the canyon and a significant negative correlation with mean air temperature and air temperature on both sides of the canyon and wind velocity on the windward side of

215

the canyon. The sky view factor only showed to have a significant negative correlation with mean air pollution levels (Fig.131).
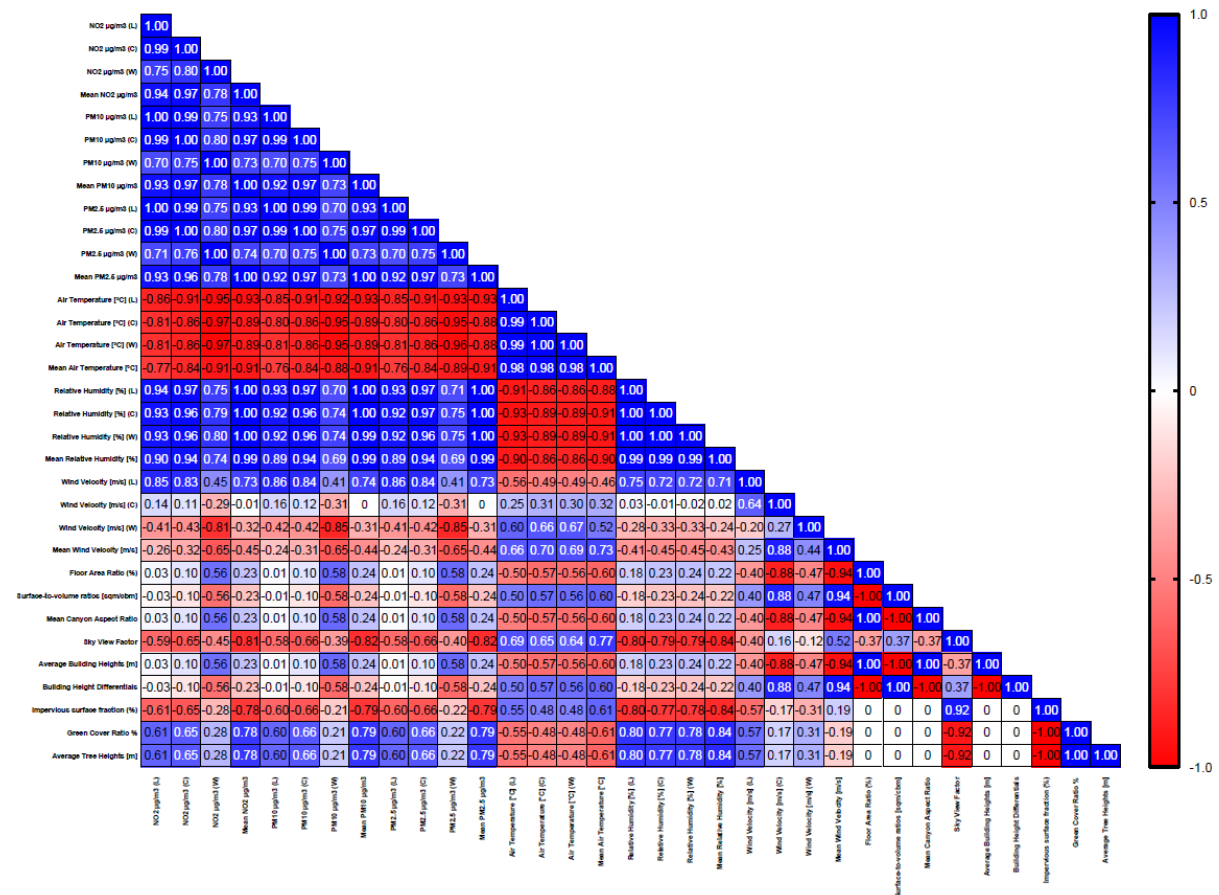
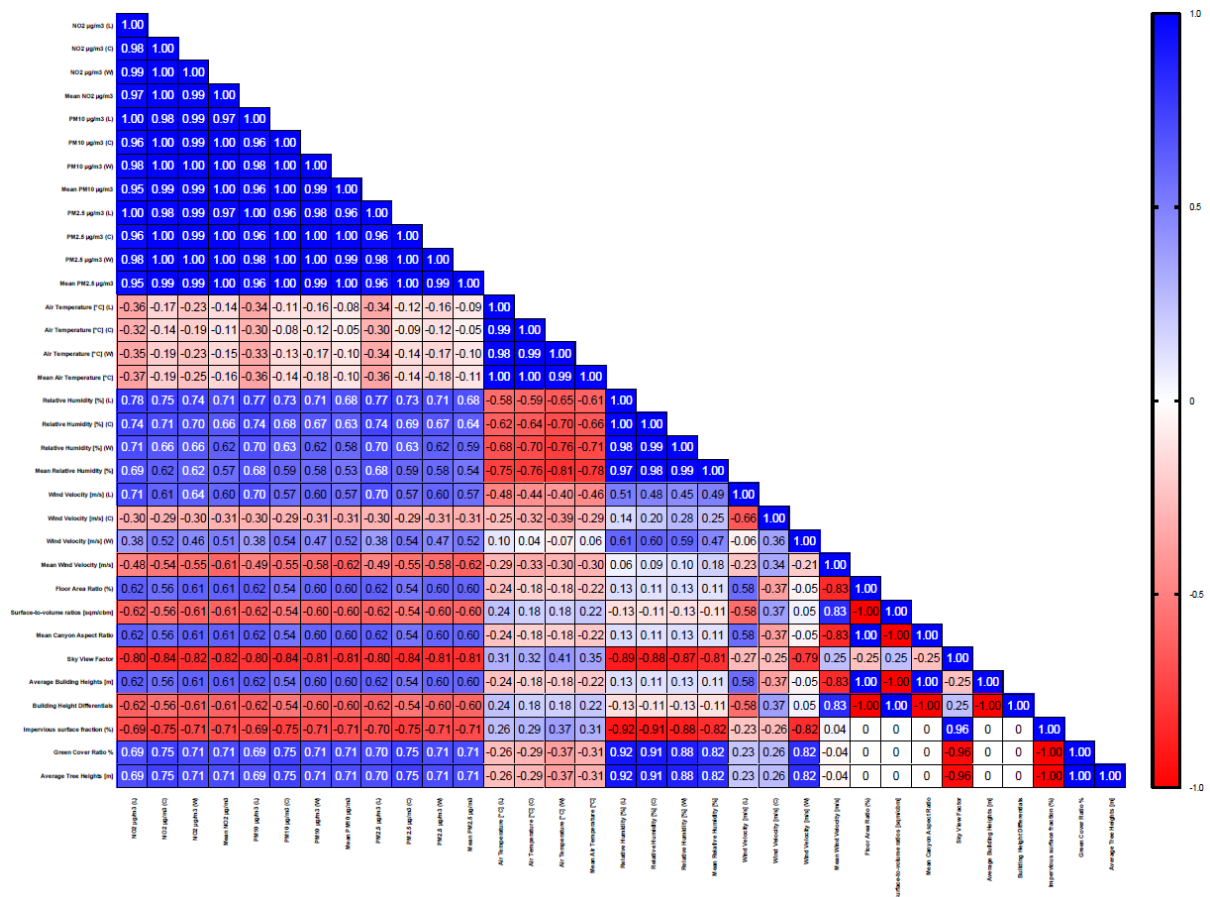Fig.131 – Heatmap displaying Pearson correlation analysis r values and p-values between narrow high street canyon Summer period

The winter period correlation analysis showed a unified pattern of correlation between air pollution levels on both sides of the canyon and mean air pollution levels. All these parameters showed a significant positive correlation with the air temperature on both sides of the canyon and a negative correlation with relative humidity on both sides of the canyon and wind velocity on the windward side of the canyon (Fig.132).
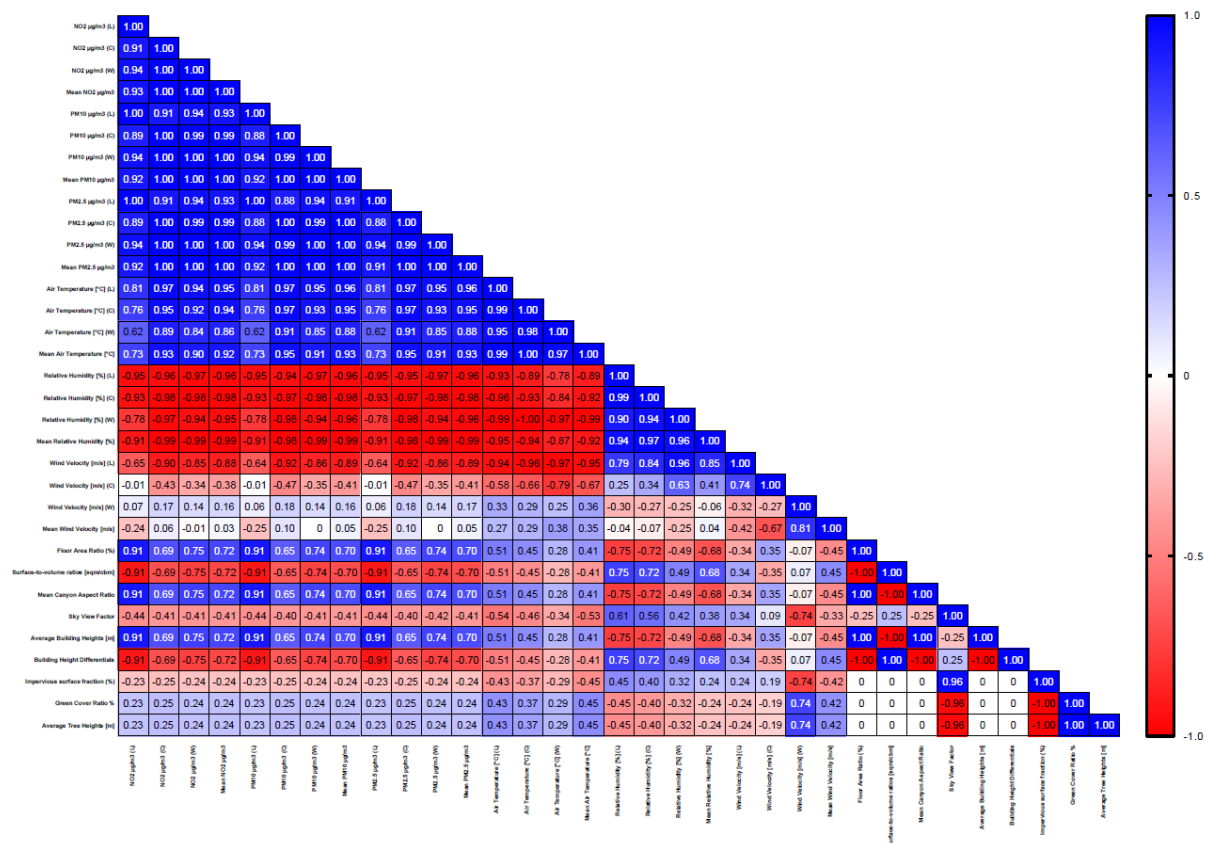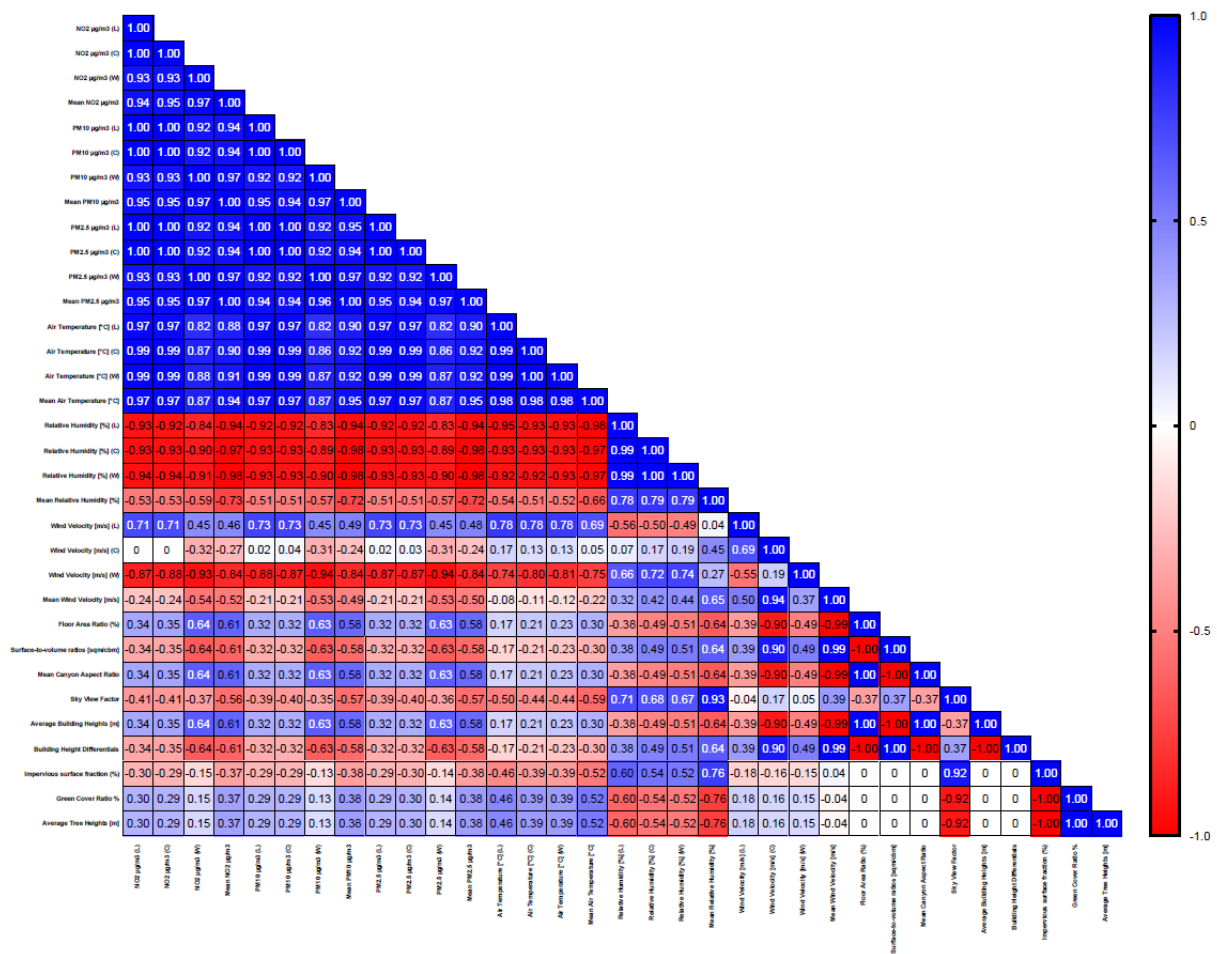
Fig.132 – Heatmap displaying Pearson correlation analysis R values and p-values between narrow high street canyon Winter period

When both summer and winter seasons are considered in the correlation analysis, it can be seen that there is a highly statistically significant negative correlation between pollution levels on the windward side of the narrow high street canyon and windward wind velocity (p≤0.001) and significant negative correlation with mean wind velocity (p≤0.05). The heatmap also demonstrated that there is a significant positive correlation between pollution levels on the leeward side of the narrow high street canyon and leeward wind velocity (p≤0.01). None of the urban form parameters had a significant correlation with leeward but had a significant positive correlation with windward side and floor area ratio, mean canyon aspect ratio and average building heights and a negative correlation were observed with the surface to volume ratio and building heights differentials. The mean air pollution levels showed to have a significant positive correlation with wind velocity on the leeward side, green cover ratio and

average tree heights. It is also identified that the same parameters have a significant negative correlation with the sky view factor and impervious surface fraction (Fig.133)
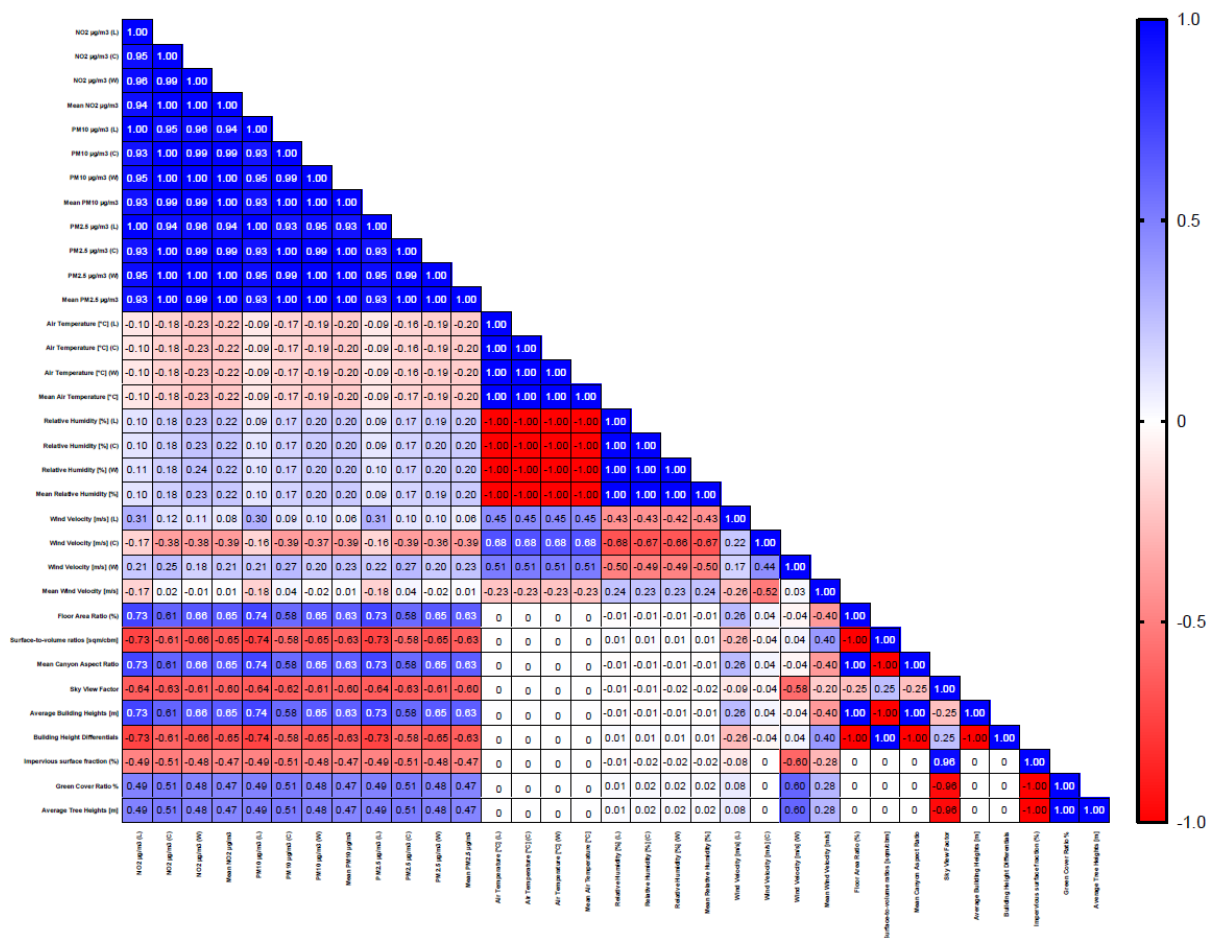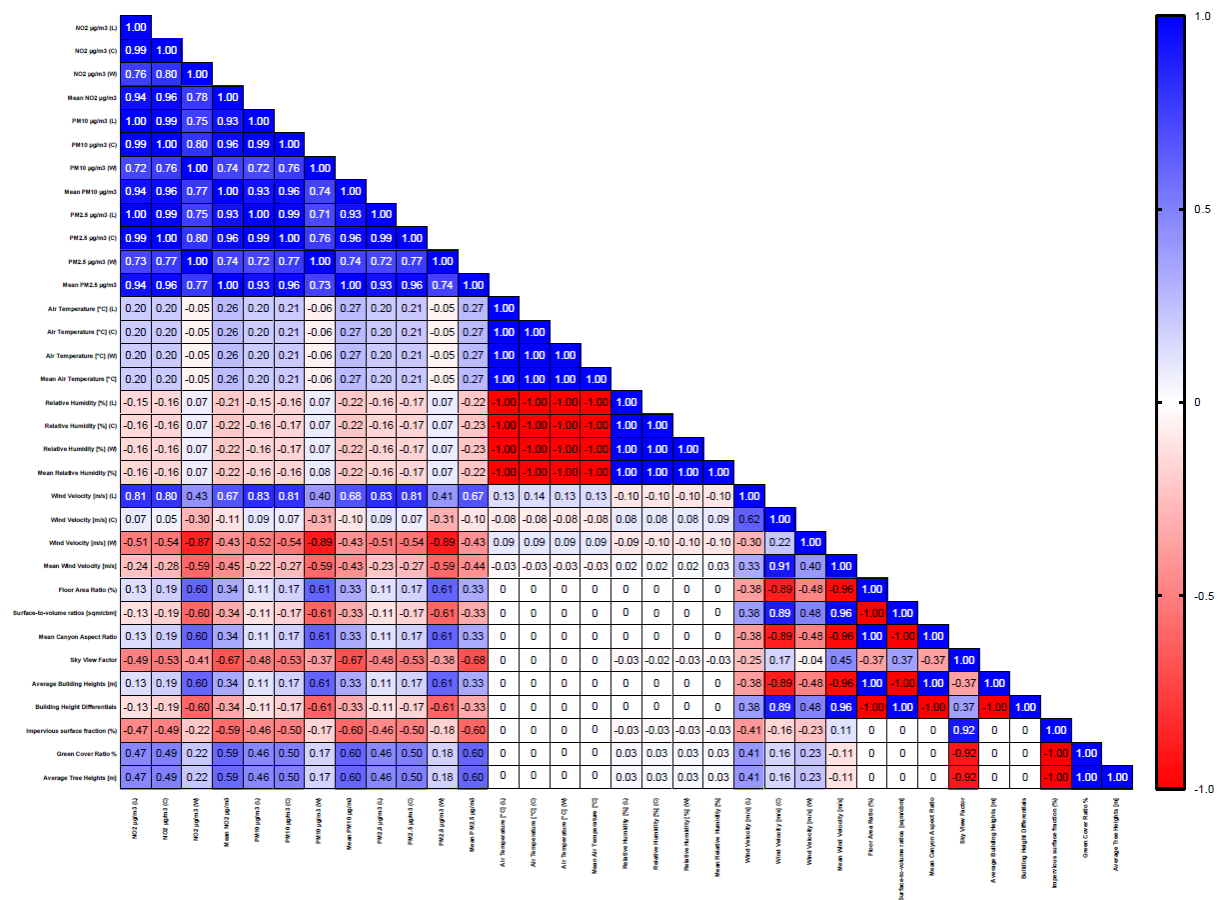

Fig.133 – Heatmap displaying Pearson correlation analysis R values and p-values between narrow high street canyon Summer and Winter period

7.1.4.1 Discussion – Narrow high street canyon

In contrast to the leeward side, the windward side showed a negative correlation between windward side wind velocity and pollution levels; as highlighted by Edward NG in the book Designing High-Density Cities (2009), the downdraught effect improves ventilation in street canyons as well as improving human thermal comfort and lowering energy consumption. Other **urban morphological indicators that can be manipulated to increase dispersion and decrease mean pollution levels are the green cover ratio and average tree heights, both of which have a positive correlation with mean pollution levels.** This means that trees' heights should be reduced and their spacing increased. As with the other canyons, this canyon demonstrated a negative correlation between building height differentials and pollution levels, particularly windward pollution levels. **According to the correlation analysis, the**

differential in building heights is positively correlated with mean wind velocity and negatively correlated with windward pollution levels. This means that by increasing the height differentials between buildings, the mean wind velocity will increase and windward pollution levels will decrease. As previously stated in chapter 6, this pollution can be pushed to the centre and leeward side of the canyon, and **it is recommended to either have fewer trees at the leeward side to allow the wind to freely circulate and disperse the pollution out of the canyon, or to add two-meter hedgerow at the leeward side to protect pedestrians from exposure to air pollution.**

Based on the result, **it is clear that the step-up configuration of each set of canyons performed better and resulted in lower pollution concentrations. Therefore, it is recommended to encourage more narrow high street step-up canyons in urban areas, as the downdraught effect caused by the perpendicular wind direction effectively increases airflow and mixing within the urban canyon, as well as dispersed pollution.** It is worth noting that when comparing the pollution concentration within the high street canyon and narrow high street canyon, as essentially all of their urban forms are the same except for the height of the buildings, it can be seen (Fig.134) that within the top two quartiles least polluted canyons, 8 out of 12 configurations are narrow high street canyons and within the two bottom quartiles (most polluted) only 4 out of 12 configurations are narrow high street canyons and the rest are high street configurations.

This is very significant findings which indicate that a greater number of tall buildings adjacent to lower or medium-rise buildings will be more effective at removing pollution from urban areas. According to correlation analysis, the lower the leeward side buildings, the lower the pollution level on the leeward, centre, and windward sides of the canyon, as well as the overall mean pollution level.
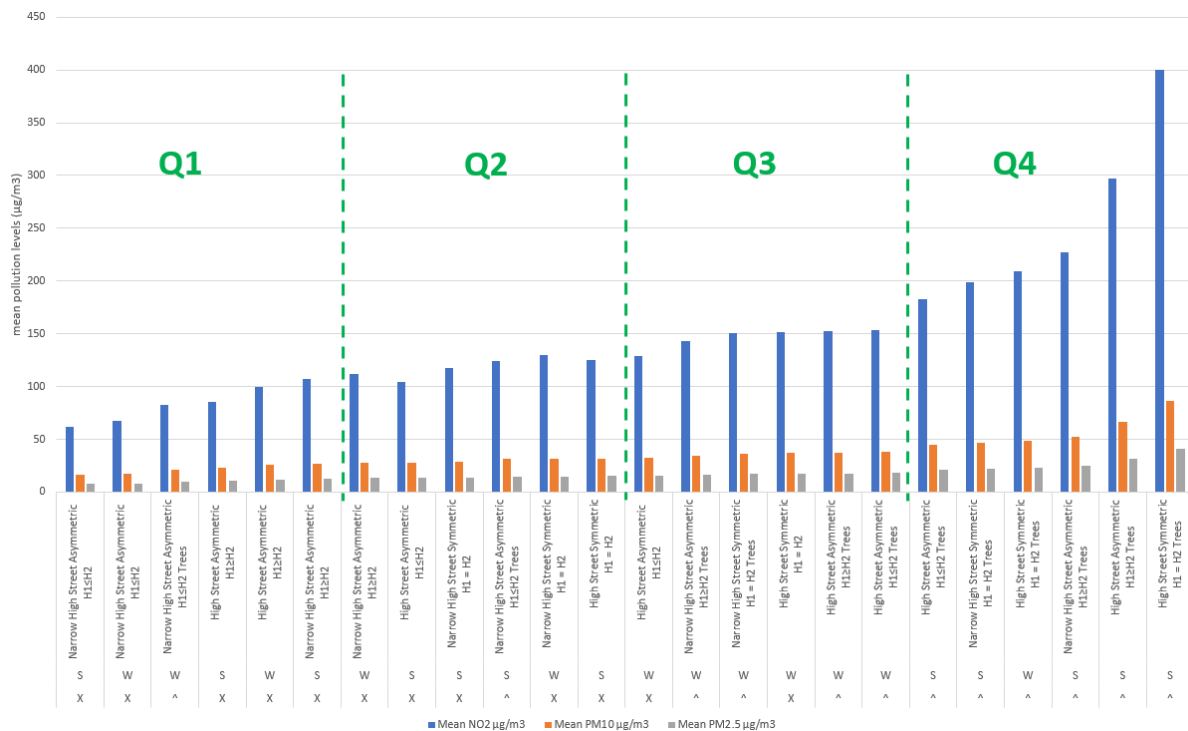
Fig.134 – Indicating the least and most polluted configurations between the high street canyon and narrow high street canyon configurations. (W=Winter, S=Summer, X=no tree configuration and ^=with tree configuration canyon)

7.1.5 Boulevard street canyon

Pearson correlation analysis was applied to all boulevard street canyons to investigate possible relationships between air pollutants, meteorological conditions and urban form parameters. Based on the result of the Pearson correlation analysis, it has been identified that there is a statistically significant negative correlation between pollution levels on the leeward side and air temperature on the leeward side and impervious surface fraction. The same side showed a significant positive correlation with mean relative humidity and relative humidity at both sides of the canyon and the green cover ratio. The windward and mean pollution levels showed almost the same pattern of correlation with a significant negative correlation with the air temperature on the windward side, sky view factor and impervious surface fraction. It has also shown a significant positive correlation with mean relative humidity and relative humidity at both sides of the canyon and the green cover ratio (Fig.136)
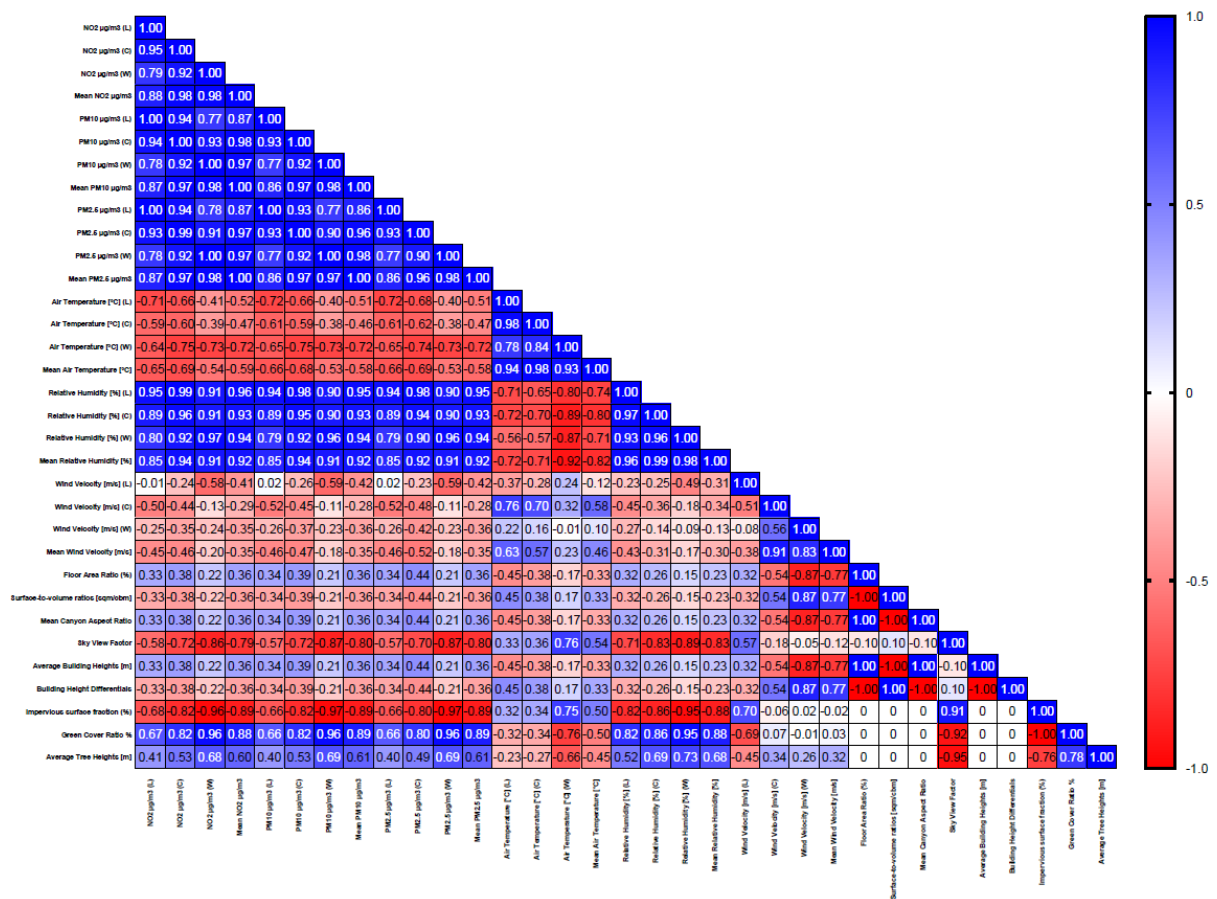
Fig.135 – Heatmap displaying Pearson correlation analysis R values and p-values between Boulevard street canyon Summer period

The winter season Pearson correlation analysis showed that there is a statistically significant negative correlation between pollution levels on the windward side and mean pollution levels with relative humidity at both sides, mean relative humidity, sky view factor and impervious surface fraction. It has been identified that the same parameters have a highly significant positive correlation with the air temperature at both sides, mean air temperature and green cover ratio. The air pollution on the leeward side only showed to have a significant negative correlation with mean wind velocity (Fig.136).
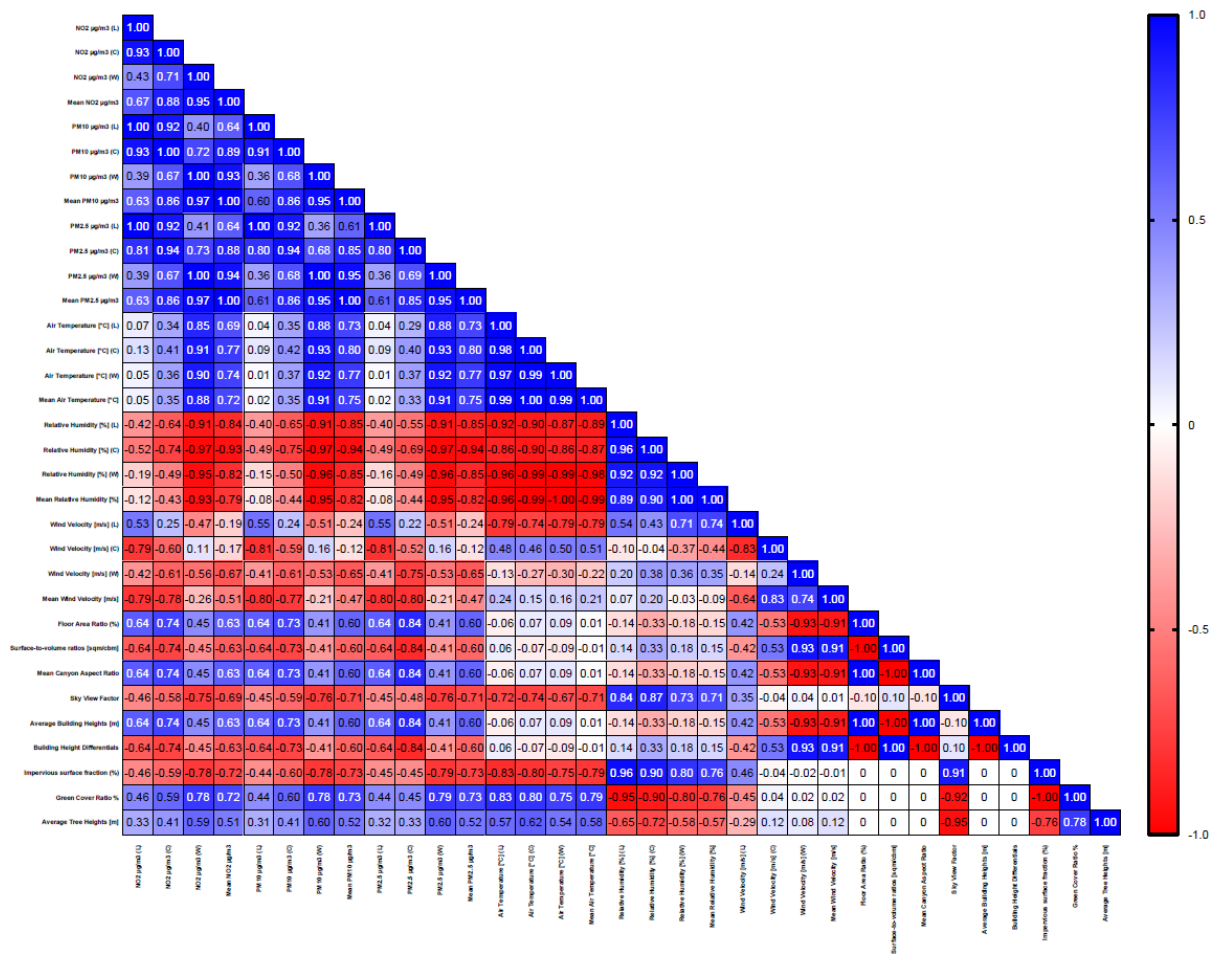
Fig.136 – Heatmap displaying Pearson correlation analysis R values and p-values between Boulevard street canyon Winter period

Pearson correlation analysis of both seasons has identified that there is a statistically significant negative correlation between pollution levels on the windward side of the boulevard street canyon with the impervious surface fraction (p≤0.001). This is the same when we look at the leeward but with a lower p-value of less than and equal to 0.05. The green cover ratio indicated a significant positive correlation with both leeward and windward and mean pollution levels again are highly significant on the windward side of the boulevard street canyon (p≤0.001). Another parameter that jointly indicated a negative correlation between windward and mean pollution levels is the sky view factor. The windward side also showed a negative correlation with wind velocity on the leeward side and a positive correlation with average tree heights (Fig.137).
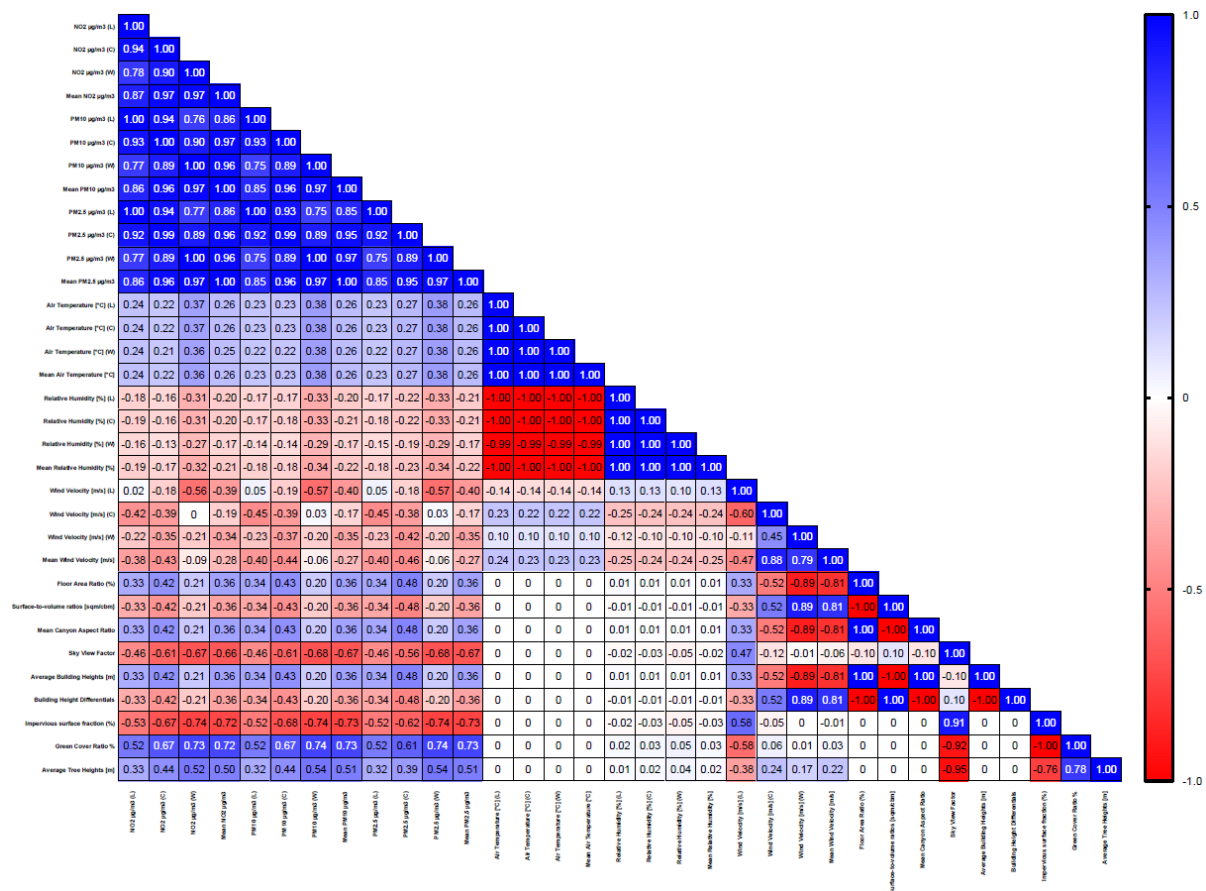
Fig.137 – Heatmap displaying Pearson correlation analysis R values and p-values between Boulevard street canyon Summer and Winter period

7.1.5.1 Discussion – Boulevard street canyon

Further analysis of the data gathered through **correlation analysis indicates that the leeward side, windward side, mean pollutants, and even the canyon's centre are all positively correlated with the green cover ratio, implying that fewer trees in the canyon will result in better air quality.** Having said that, the configuration with trees in the canyon's middle part resulted in generally better air quality and a lower concentration of air pollution on either side of the canyon in comparison to the tree arrangement on three sides of the canyon. Furthermore, because the windward side of the canyon demonstrated a significant degradation of air quality and a negative correlation with the leeward side wind velocity, increasing the leeward side wind velocity has the potential to reduce pollution on the windward side.

Interestingly, the leeward wind velocity had a negative correlation with the green cover ratio (p = 1.02 and r = -0.58), which means that the less green cover on the leeward side of the canyon, the greater the leeward wind velocity and thus the lower the concentration on the windward side. **Therefore, it is recommended to reduce greenery on the leeward side, which benefits both the leeward and windward sides and will help reduce pollution levels. It is also recommended to have shorter tree heights on windward sides to increase the pollution dispersion rate.** This may result in smaller canopy size, and the smaller tree will be more effective at protecting pedestrians from pollution exposure. This will work well because the sky view factor has a negative correlation with both windward and mean pollution levels; thus, fewer trees with shorter height will result in a higher sky view factor and more open space for pollution to disperse from the site, resulting in a lower mean pollution level.

The height differentials and building heights did not correlate in this scenario, as the greenery and tree configuration had a substantial influence on the air pollution concentration, and due to the large distance between the row of buildings in this canyon, leeward and windward concentrations varied between various configurations. Having said that, and based on the correlation analysis, **the only correlation that can be seen is with leeward building height which the higher the leeward side building, the more pollutant can accumulate on the leeward side, affecting primarily particulate matter and having a negligible effect on NO_2 concentration.** This is due to the fact that one of these pollutants is a gas, while the other is a solid particle and as it was discussed in chapter 2 these pollutants behave differently in the environment.

The following section will summarise the major findings, followed by a table outlining the benefits and drawbacks of each canyon, as well as a set of recommendations and mitigation strategies based on the findings of fieldwork, computational modelling and correlation analysis.

7.2 Summary of correlation analysis findings

The correlation analysis revealed a number of interesting correlations between urban form, microclimate, and air pollution. In another words, these findings confirm the hypotheses stated in the introduction of this thesis and provide strong evidence that manipulation of urban form can create a desirable microclimate capable of mitigating air pollution concentrations and respectively reduce its adverse impact on human health.

In chapter 3 of this thesis, a handful of morphological and meteorological indicators were identified and proposed for use in studying air pollution and wind behaviour in urban street canyons. However, based on the results of the correlation analysis, it appears that four of the parameters listed in table.09 of chapter 3 have a greater influence on wind behaviour and the dispersion or concentration of air pollution. These are building height differentials, average building heights, the green cover ratio and the sky view factor.

Mews street canyon, for example, demonstrated that air pollution has a direct correlation with mean wind velocity and an indirect interdependency with average building heights, sky view factor, and building height differentials. That means, by manipulation of these morphological indicators, the mean wind velocity can be increased or decreased, affecting air pollution dispersion effectively. Based on the correlation analysis, average building heights must be kept low while building height differentials are increased to their maximum, which will effectively increase the sky view factor and mean wind velocity, reducing pollution levels within the canyon.

As a result of a negative correlation between trees and air pollution levels, the presence of trees in canyons reduces the sky view factor and slows wind velocity and movement, resulting in an increase in the concentration of pollutants. This is clearly displayed in all canyons with tree configurations. Consistent with previous authoritative researches discussed in chapters 3 and 4, as well as fieldwork and computational simulation results presented in chapters 5 and 6, these findings reconfirmed that, in general, increasing the number of trees increases pollution levels within street canyon.

The correlation between high street canyon and narrow high street canyon types reveals the most interesting results. The correlation between air pollution and building height differentials suggests that a greater number of tall buildings adjacent to low-rise or medium-rise buildings will be more effective at removing pollution from urban canyons. According to correlation analysis, the lower the buildings on the leeward side, the lower the pollution levels on the leeward, centre, and windward sides of the canyon, as well as the overall mean pollution level. The green cover ratio which has a positive correlation with average pollution levels, exhibited the same pattern. Therefore, in order to increase dispersion and decrease mean pollution levels, the green cover ratio must either be decreased or its arrangement must be altered in order to increase dispersion or block pollution from the street side in order to protect pedestrians from exposure to harmful pollutants. Table 33 provides additional information on the optimal tree locations and recommendations on urban form manipulation.

Interestingly, the boulevard canyon type did not exhibit the same correlation strength as other canyon types in terms of building heights and height differentials. Due to the large distance between the rows of buildings in this canyon, the leeward and windward concentrations varied in different configurations. The only common correlation observed is between leeward building height and pollutant concentration on the leeward side. That means, the taller the leeward building, the more pollutant concentrate on the leeward side. Based on the results, it is clear that the green cover ratio and tree heights and their configurations are the most influential factors on air pollution behaviour in this canyon type.

Although it was decided during the discussion of the results to disregard recommendations for changes in the floor area ratio and building site coverage, a closer look at the summer and winter correlation analysis of all canyon types reveals that floor area ratio has a strong negative correlation with mean wind velocity. That means, changes in the number of floors or width of the canyon can affect wind velocity within the urban canyon. This reinforces the guidelines and standards proposed by Oke (1987 and 1988), the Manual for Streets (2007 and 2010), and the Department for Transport's inclusive mobility (2005).

In the following section and in the recommendation matrix (Table.33), a more detailed manipulation of urban form parameters for each canyon configuration is presented. The table provided recommendations for both existing contexts/scenarios and for new urban areas/streets.

7.3 Recommendations

The concentration of air pollution, as expected, is influenced by a variety of factors such as urban form, tree arrangements, and meteorological conditions. In some urban street canyons, the three mentioned factors increased the dispersion of air pollution from the canyon, while in others, these factors were less successful, and in some cases, the condition resulted in the formation of hotspots with high air pollution concentrations and reduced air movement. As it was mentioned in chapter 2, on days when pollution levels are high, these hotspots can even go beyond the ambient pollution levels and harm the environment, biodiversity, and pose significant health risks to humans.

As a result, it is critical and highly recommended that urban street canyons be oriented parallel to or 30 degrees to the prevailing wind (see section 3.4 of chapter 3) in order to maximise air path/breezeways and thus influence air flow and increase air pollution dispersion. However, as discussed in chapter 5, urban spaces are made up of very complex building arrangements, and it is not always possible to align the canyon orientation with the prevailing wind. As a result, the findings of this thesis can help urban planners and designers implement the following recommendations to reduce and limit public exposure to air pollution when the wind direction is perpendicular to the canyon axis, which is the most polluting condition. Additionally, it is worth noting that the application of these considerations is dependent on the type of urban canyon, tree arrangements, source of pollution, and volume of vehicle traffic.

One of the study's key findings is that trees, regardless of canyon type, unplanned tree arrangement, may result in significantly higher pollution concentrations within urban canyons. According to the current study, urban trees obstruct wind flow and reduce air exchange between the air above the roof (urban canopy layer) and polluted air within the canyon, thereby reducing ventilation and increasing air pollution concentration within the

urban street canyon. This decrease in wind velocity and change in wind structure appears to outweigh trees' capacity to filter air pollution. Thus, increasing tree cover does not always equate to decreased pollution, at least locally. Rather than that, more attention should be paid to the type, scale, and, most importantly, the locations and distributions of trees within a given urban canyon in order to alleviate air quality problems. At the same time, we cannot overlook the benefits of trees in our urban spaces, including their capacity to store and absorb CO_2, their ability to reduce temperature and mitigate the urban heat island effect, their ability to provide shade, reduce noise, and enhance biodiversity, not to mention their aesthetic and emotional value.

In light of the above understanding, and based on the findings of this study, trees can contribute to a higher concentration of pollution in a variety of ways, but they can also block or redirect wind, directing it away from the canyon and protecting pedestrians from excessive exposure as it was observed with the hedgerows in Regent's place plaza during the fieldwork study. According to the findings, a canyon with dense trees may be recommended if vehicle traffic and pollution levels are extremely low within the canyon, as the tree canopy can help block incoming pollutants from above the rooftop (urban canopy layer) and keep the canyon's air pollution levels low, encouraging more active travel. In other words, if the air quality at the street level is better than the air quality above the building rooftop (urban canopy layer), trees should be encouraged; if the air quality at the street level is worse than the urban canopy layer, trees should be limited.

This especially works in canyons with an aspect ratio greater than 0.5, such as mews, residential streets, and narrow and high streets. Additionally, it is recommended to plant deciduous trees rather than evergreen trees within urban canyons with a high pollution source. This is to ensure that at the very least during the winter period, when pollution levels may be even higher than during the summer, there is a greater sky view factor provided by the lack of foliage, resulting in increased wind velocity and air pollution dispersion.

Alternatively, relocating trees to one side of the urban canyon or planting trees with a lower tree height was found to be more beneficial in terms of increasing air movement and air pollution dispersion rate. According to the fieldwork findings, a two-meter dense hedgerow

between vehicular traffic and pedestrian areas can cut pollution exposure by half on the downwind side and behind the hedgerow (Fig.138).
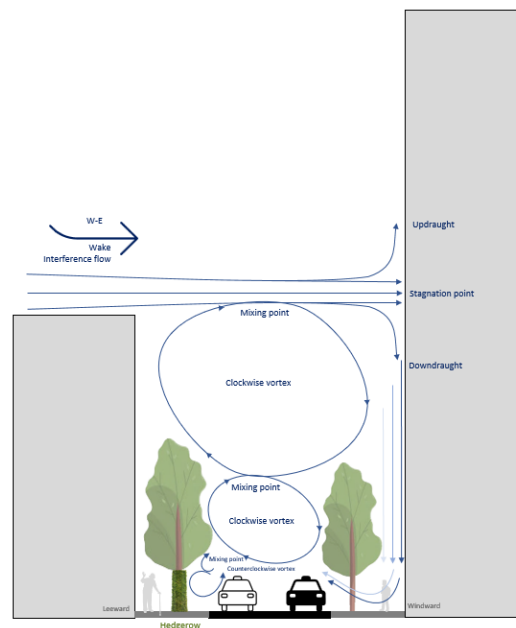
Fig.138 – Step-up narrow high street canyon with trees, summer period.

As it can be seen from Fig.138, the incoming wind splits after hitting the windward building, and the downdraught transports the pollution to the canyon's centre and leeward side. The 2-metre hedgerow at the leeward side of the canyon effectively recirculates pollution to the canyon centre, where it can be mixed with the two clockwise vortexes and eventually removed from the street canyon. Contrary to the hedgerows, trees with a stem height or canopy height of more than two metre elevated from the ground creates a clear zone and allow pollution from the source (street side) to flow freely into the pedestrian area. Whereas hedgerows are denser and their coverage begins from the ground surface and beyond the pedestrian height, therefore, more effective in protecting pedestrians from harmful air pollutants.

In terms of urban form, and based on the result it can be seen, that the shorter and denser the distance between buildings in urban canyons, the more uniform the pollution levels on both sides of the canyon; the wider the distance, the greater the complexity and the stronger the influence of other urban forms and meteorological parameters on air pollution concentrations within urban canyons.

As expected, the high sky view factor had a direct and positive effect on increasing air velocity and dispersing air pollution; additionally, it demonstrated that increased openness, fewer tree obstacles, and lower building heights reduced air pollution within urban canyons. The building height differentials had a similar magnitude of positive impact on air pollution reduction. Evidently, the greater the difference in height between leeward and windward buildings, the better the air pollution was in canyons. Surprisingly, and consistent with previous statements, tall buildings adjacent to lower or medium-height buildings in urban canyons were more effective at dispersing pollution, and as a result, almost all symmetric canyons had a much lower dispersion rate than their asymmetric canyon counterparts.

This finding indicates that in order to maximise air pollution dispersion and wind flow between spaces, tall buildings and urban canyons with varying heights are recommended to promote air movement between spaces. This is in particular more effective at the windward side of the canyons. As shown in Figs.139 and 140, the narrow high street step-up and step-down with trees have the highest air pollution dispersion and percentage change for leeward, while the worst configurations are highlighted as boulevard step-up with trees on three sides and in the middle. The leeward side identified High street step-up with and without trees as the best configuration out of the 30 canyon types and configurations, while the worst configurations are boulevard step-down and symmetric with trees on three sides of the canyon. With the exception of the step-up with trees on three sides, the boulevard canyon type and its various configurations were found to have the worst configurations. In both summer and winter, this boulevard canyon configuration had the highest pollution percentage change on its leeward side.

Fig.139 - Air pollution percentage change between all five urban street canyon types - leeward

side - (W=Winter, S=Summer, X=no tree configuration and ^=with tree configuration canyon)

Fig.140 – Air pollution percentage change between all five urban street canyon types - windward side - (W=Winter, S=Summer, X=no tree configuration and ^=with tree configuration canyon)

Finally, this thesis established that the buoyancy effect plays a significant role in modifying the air flow and vortex with street canyons. Computational modelling has demonstrated that when a surface in a street canyon heats up, the vortex flow characteristics change.

Additionally, heating different surfaces, such as the upwind wall, the downwind wall, or the canyon floor, alters the vortex flow in distinct ways. Moreover, it was discovered that the buoyancy effect continues to influence wind behaviour even as the distance between buildings increases, resulting in an increase in air pollution during colder months and increased dispersion of air pollution during warmer months.

On the basis of the foregoing and the findings of this thesis, the following recommendation matrix (Table.33) has been compiled to provide a set of recommendations on the most effective urban street canyon configuration capable of eliminating or reducing undesirable microclimate conditions in urban outdoor spaces, thereby reducing air pollution concentrations. The table provided recommendations for both existing contexts/scenarios and for new urban areas/streets. Recommendations that are applicable to existing scenarios are highlighted in one column and recommendations that can be applied or considered for new urban areas or streets are in a separate column. This set of recommendations can be used by urban planners and designers to consider their design implications in advance and make informed design decisions to encourage greater dispersion of air pollution within various urban street canyons, particularly in areas with high pedestrian traffic.

The matrix is divided into five sections based on the five major urban street canyons discussed in Chapter 3. Each urban street canyon is then subdivided based on its configuration, which can be symmetric or asymmetric. The asymmetric has also included configurations with both step-up and step-down canyon configurations. Wind velocity has been highlighted within each configuration; the levels range from low to moderate to high. This data assists designers in taking wind velocity into account and correlating it with the street canyon's sky view factor and aspect ratio. The recommendation matrix also emphasises and advises on which side of the canyon to locate high pedestrian activity. This information allows designers to avoid canyon side with potentially higher concentrations, thereby protecting pedestrians from harmful pollutants. Within the street canyons, there are also indications of possible green and

tree arrangements. It is worth mentioning that, based on manual for street (2007 & 2010) no tree or greenery arrangements highlighted for mews canyon type. Building heights and height differentials, as discovered, are critical for increasing turbulence and overall wind velocity, as well as its ability to disperse pollution from spaces. As a result, the recommendation matrix emphasises indications for increasing or decreasing building heights based on canyon types and configurations. The best and worst canyon configurations are also shown, and the air quality levels of each canyon type are RAG rated to highlight and encourage urban designers and environmental designers to use the least polluted configurations as the foundation of their design.

Table.33 (a) – Mews Street canyon configuration. Set of recommendations for both existing contexts/scenarios and for new urban areas/streets to mitigate air pollution at pedestrian height and increase air pollution dispersion.

235

Residential Street Canyon

Recommendation for existing contexts/scenarios

Configuration	Wind velocity	Where to locate / divert pedestrian traffic	Configuration with lowest pollution	Configuration with highest pollution	**Recommended configuration for new urban areas/streets** — Configuration

Symmetric (H1=H2)

W-E
Wake
Interference flow
SVF 0.62
H = 10 m
H/W=0.71
2 m
14 m
10 m

W-E
Wake
Interference flow
SVF 0.5
GCR 10%
H Tree = 15 m

W-E
SVF 0.62
❌ ✔

W-E
SVF 0.5
❌ ❌

H1 = H2 (summer)

H1= H2 with Trees (summer)

W-E
SVF 0.5
✔ ✔

- Low green cover ratio and greater distance between trees
- Leeward side trees should be lower than the building heights to encourage greater dispersion.
- 2-meter hedge row under the tree will block pollution and create a recirculation to disperse air pollution from the canyon.
- If the vehicle traffic is high, a lower height building is recommended.

Asymmetric (H1<H2, step-up)

W-E
Wake
Interference flow
SVF 0.68
H1 = 6 m
ΔH =4 m
H2 = 10 m
H/W=0.57
2 m
14 m
10 m

W-E
Wake
Interference flow
SVF 0.52
GCR 10%
H Tree = 15 m

W-E
SVF 0.68
✔ ❌

W-E
SVF 0.52
✔ ❌

H1<H2 (summer)

H1<H2 with tree (winter)

W-E
SVF 0.68
✔ ✔

- Low green cover ratio and greater distance between trees
- Windward side trees should be lower than the windward building height to encourage greater dispersion.
- No tree on the leeward side to increase the air velocity and a 2-meter hedge row to protect pedestrians from vehicle pollution and create recirculation and a counter-clockwise vortex to push the pollutant to above the roof air volume and disperse pollutants from the canyon.
- The lower the leeward side building, the lower the pollution level at the leeward side.
- The greater difference in building height the better the air quality within the canyon.

Asymmetric (H1>H2, step-down)

W-E
Wake
Interference flow
SVF 0.68
H1 = 10 m
ΔH =4 m
H2 = 6 m
H/W=0.57
2 m
14 m
10 m

W-E
Wake
Interference flow
SVF 0.52
GCR 10%
H Tree = 15 m

W-E
SVF 0.68
❌ ✔

W-E
SVF 0.52
GCR 10%
❌ ✔

H1>H2 (summer)

H1>H2 with tree (summer)

W-E
SVF 0.68
✔ ✔

- Low green cover ratio and greater distance between trees
- Windward side tree height and green coverage should be higher than leeward side to encourage higher airflow and dispersion rate.
- 2-meter hedge row on the leeward side can help to block pollution and create a recirculation to disperse air pollution from the canyon.
- The lower the windward side building, the lower the pollution level at the leeward side.
- The greater difference in building height the better the air quality within the canyon.

Legend

✔	Recommended
❌	Avoid
(wind icons)	Wind velocity form low to high
▼	Lower height building
▲	Higher height building
(trees)	Tall and short trees (Summer period)
(bare trees)	Trees (Winter period, no leaves)
(hedge)	Hedgerow
(orange block)	Building configuration (Summer period)
(dark block)	Building configuration (Winter period)
(blue-yellow-peach scale)	Lowest to highest pollution level (left to right, lowest, moderate, highest)
(green scale)	Best to reasonable configuration for lowest pollution level (left to right, best, moderate and reasonable)

Table.33 (b) – Residential Street canyon configuration. Set of recommendations for both existing contexts/scenarios and for new urban areas/streets to mitigate air pollution at pedestrian height and increase air pollution dispersion.

236

Table.33 (c) – High Street canyon configuration. Set of recommendations for both existing contexts/scenarios and for new urban areas/streets to mitigate air pollution at pedestrian height and increase air pollution dispersion.

Table.33 (d) – Narrow High Street canyon configuration. Set of recommendations for both existing contexts/scenarios and for new urban areas/streets to mitigate air pollution at pedestrian height and increase air pollution dispersion.

Table.33 (e) – Boulevard Street canyon configuration. Set of recommendations for both existing contexts/scenarios and for new urban areas/streets to mitigate air pollution at pedestrian height and increase air pollution dispersion.

7.4 Conclusion

This chapter applied Pearson correlation coefficient to all street canyons to summarise the strength and direction (negative or positive) of relationships between pollutants, meteorological conditions and urban morphological indicators which were extracted from the computational simulation in chapter 6. Each canyon type's data was analysed three times; once with summer data, once with winter data, and once with data from both seasons combined, Thus, some of the knowledge gaps identified in chapter 4 have been addressed. As it was mentioned, previous studies failed to account for seasonality in urban air pollution studies, but this study addressed this shortfall by taking summer and winter into account. This has contributed to our understanding of the dominant seasonal and annual parameters that influence the microclimate and air pollution concentration.

Interestingly, the correlation analysis identified relationship between various parameters of urban street canyons and offered new insights to explain some of the phenomena emerged during the fieldwork (chapter 5) and computational simulation (chapter 6). This has helped to signify the impact of urban form on microclimate and concentration of air pollution within various urban street canyons.

Based on the findings of fieldwork, computational simulation and correlation analysis, a set of recommendations has been devised and highlighted in Table.33 of this chapter. The matrix provided recommendations on the most effective urban street canyon configuration(s) capable of eliminating or reducing undesirable microclimate conditions in urban outdoor spaces to reduce air pollution concentrations. **The table provided recommendations for both existing contexts/scenarios and for new urban areas/streets.** Recommendations that are applicable to existing scenarios are highlighted in one column and recommendations that can be applied or considered for new urban areas or streets are in a separate column. This will assist urban planners and designers in considering their design implications in advance and making informed design decisions to encourage greater dispersion of air pollution within various urban street canyons, particularly in areas with high pedestrian traffic. Next chapter will conclude with a brief overview of the study, a summary of its key findings with reference

to the research objectives, and a discussion of their contribution to the knowledge as well as potential future research directions.

Part 3

Conclusions

Chapter 8

Chapter 8

Conclusion

The hypothesis that this thesis is based around, as stated in the introduction chapter, is that a well-designed urban street canyon can create a desirable microclimate capable of mitigating air pollution concentrations and respectively reducing its adverse impact on human health. The aim of this research was thus formed on the basis of providing evidence to confirm this hypothesis. The aim of the research was therefore to outline a set of recommendation strategies that can be used to motivate a positive impact on urban microclimate, encourage greater air pollution dispersion, and avoid air pollution concentration within urban street canyons, thereby reducing its adverse impact on human health.

According, this thesis investigated and analysed the impact of urban form on air pollutant dispersion in various urban canyon types and configurations using a variety of methods. The study of the literature review (chapters 2,3 and 4) and the results of fieldwork (chapter 5), computational modelling (chapter 6), and correlation analysis (chapter 7) deepened the understanding of air pollutants behaviour in various urban canyon types and provided much-needed knowledge and recommendations (refer to section 7.3) for urban designers and planners to consider to make informed design decisions to encourage greater dispersion of air pollution within various urban street canyons, particularly in areas with high pedestrian traffic to reduce and limit public exposure to harmful air pollution.

In response to the aim of this research, four main objectives were proposed in the introduction of this thesis and the following paragraphs conclude and highlight the key findings from the thesis with reference to these four objectives. The chapter then discusses the significance of this research and its contribution to knowledge, as well as the limitations of the current study and future research recommendations.

Objective 1: To demonstrate that air pollution has a significant impact on human health

This objective was accomplished by conducting a thorough literature review on the most recent findings indicating health problems caused by excessive pollution released into the air as a result of rapid urbanisation and man-made activities (refer to chapter 2). The review of **these studies confirmed that air pollution has a significant impact on human health, triggering and inducing a variety of diseases that result in high morbidity and mortality,**

particularly in urbanised areas. It was also established that NO_2 and PM_{10} and $PM_{2.5}$ are the most harmful pollutant to urban dwellers (refer to section 2.4). Furthermore, it was acknowledged that various governments around the world and in particular the UK government and the Mayor of London are actively introducing measures to control and reduce air pollution. However, it is unfortunate that most of these policies primarily focused on transportation and cars as the primary focal point for proposing strategies to rectify or diminish urban air pollutants and thus paid less attention to other potential factors such as urban physical form, urban planning, and microclimate (refer to section 2.5 & 2.6). These insights and findings demonstrated that **there is a clear knowledge gap in current regulations and standards, and this provided an opportunity to investigate and evaluate the impact of urban form on microclimate and air pollution concentration in order to propose a set of recommendations to fill this knowledge gap.**

Objective 2: To identify and explore the nexus between urban form and concentration of air pollution within urban street canyons

This objective was accomplished by conducting a literature review on relevant studies on human settlement and urbanisation, as well as issues related to urban population growth and activities that have exacerbated urban air pollution (refer to chapter 3). In addition to that, a number of urban form attributes that were investigated by authoritative urban morphologists were explored and discussed in detail (refer to section 3.3, table 06). Based on the aforementioned exploration, **this thesis established that specific attributes of urban form have a significant impact on the formation of undesirable microclimate, which increases the concentration of air pollution** in outdoor spaces, and that urban morphological indicators are essential for urban climatic analyses. As a result, a number of essential urban morphological and meteorological indicators identified to be used for study of air pollution and wind behaviour in urban street canyons. These are, **building site coverage, floor area ratio, aspect ratio, frontal area index, sky view factor, average building heights, building height differentials, green cover ratio, building and street orientation, temperature, relative humidity, wind speed and wind direction** (for definition of morphological indicators refer to section 3.3). According to studies on microclimate and air pollution, **the urban wind is the most important meteorological parameter in determining pollutants dispersion because wind can carry pollutants from one location to another, increasing or decreasing air**

pollution concentrations within various urban canyon configurations. It was also established that the aspect ratio (H/W) is one of the morphological indicators that can be used to categorise street canyons and wind behaviour. This is the most significant geometrical aspect of a street canyon, and depending on the geometrical configuration, a canyon might be called regular, avenue and deep canyon and can be divided into further classifications. These are mews, residential streets, high streets, narrow high streets and boulevard street canyons.

Objective 3: To identify those urban form attributes that have the greatest impact on air pollution concentration within urban street canyons

This objective was accomplished by comparing various urban canyon types and configurations through fieldwork and computational modelling. Based on the review of the relevant literature and studies, a list of potential meteorological and morphological indicators that influence the formation of undesirable microclimates, which increase the concentration of air pollution, was compiled (refer to section 3.5, table 09). Next, a fieldwork study was devised and implemented to inform the steps that must be taken to calibrate the computational model outputs. The comparison and correlation analysis of the fieldwork data and computational model outputs revealed that values are highly correlated, implying that the ENVI-met software (computational model) is a reliable tool for microclimate and air pollution research. It was also discovered that the output values from computational simulation were slightly different, being either higher or lower than the fieldwork measurement value necessitating the calibration of the ENVI-met application outputs. As a result of the calibration exercise, **this thesis for the first time provided series of equations for converting ENVI-met outputs to real-world spot measurements (refer to section 5.5 table 29). This has enabled any future simulation to be calibrated to real-world measurements based on weather conditions and seasons.**

Other interesting findings from the fieldwork included the evidence that NO_2, PM_{10}, and $PM_{2.5}$ **concentrations were highest on dry days and primarily during the summer and autumn seasons (refer to section 5.3).** Furthermore, and perhaps more interestingly, **locations with trees and vegetation were found to have the highest levels of pollution.** demonstrating the role of green infrastructure in influencing microclimate and thus air pollution concentrations. The only exception to this finding was **a 2-meter hedgerow placed between the polluted**

roadside and the pedestrian seating area which had effectively deposited and deflected air pollution away from the seating area, resulting in a significant decrease in pollutant levels. This discovery can be utilised as an effective mitigation strategy. And finally, the five urban street canyons were modelled by computational modelling software to investigate and evaluate those meteorological and morphological indicators that can have the potential to influence the concentration or dispersion of air pollutants in various street canyons. Each urban street canyon type was subdivided into six variations, each with a different aspect ratio (H/W) and tree arrangement. The symmetric urban canyon (H1=H2), asymmetric step-up canyon (H1≤H2), and asymmetric step-down canyon (H1≥H2) were the three variations used for this exploration. With the exception of mews street canyon, all other canyon configurations were simulated once with and once without trees. Based on this investigation, it was identified that ten meteorological and morphological indicators have the greatest impact on air pollution concentration within urban street canyons and must be considered when investigating the impact of urban form on microclimate and air pollution. These parameters are **floor area ratio, aspect ratio, sky view factor, average building heights, building height differentials, green cover ratio, building and street orientation, air and surface temperature, wind speed and direction.**

Objective 4: To outline a set of recommendations for improving air quality levels at pedestrian height within various urban street canyon types and configurations

This objective was accomplished by proposing a set of recommendations based on the findings of the fieldwork, computational modelling, and correlation analysis. Table 33 of chapter 7 outlined these recommendations in greater detail for each canyon type and configuration. **The correlation analysis revealed a number of interesting correlations between urban form, microclimate, and air pollution.** Based on the results of the correlation analysis, it appeared that **four of the parameters listed in table.09 of chapter 3 have a greater influence on wind behaviour and the dispersion or concentration of air pollution. These are building height differentials, average building heights, the green cover ratio and the sky view factor. In another words, these findings confirm the hypotheses stated in the introduction of this thesis and provided strong evidence that manipulation of urban form can create a desirable microclimate capable of mitigating air pollution concentrations** and respectively reduce its adverse impact on human health. Herein, a list of key recommendations

is included that can be considered by urban planners and designers prior to the start of and during any urban planning project. The recommendations mentioned here and in table 33 will enable the urban planners to make informed design decisions to encourage greater dispersion of air pollution within various urban street canyons, particularly in areas with high pedestrian traffic, in order to reduce and limit public exposure to air pollution.

Orientation first

- It is critical and strongly recommended that urban street canyons be oriented parallel to or 30 degrees to the prevailing wind in order to maximise air path, influence airflow, and increase air pollution dispersion. Additional measures such as the ones highlighted in table 33 must be taken into account to ensure adequate ventilation capacity when oriented perpendicular to the main wind direction.

It is all about the difference in building height

- As expected, the high sky view factor had a direct and positive effect on increasing air velocity and dispersing air pollution. Building height differentials had a similar magnitude of positive impact on air pollution reduction as the sky view factor. That means, the greater the difference in height between leeward and windward buildings, the better the air pollution is within canyons. Therefore, asymmetric configurations are preferred over symmetric canyons. Increasing the variance in building height increases turbulence, which in turn enhances the dilution of pollutants and ventilation within the canyon.

More tall buildings!

- Tall buildings adjacent to lower or medium-height buildings in urban canyons are recommended to promote air movement between spaces. This is in particular more effective at the windward side of the canyons if the street and building orientations are perpendicular to the upwind direction.

Expect the unexpected

- Unexpectedly, and with the exception of the step-up canyon configuration with trees on three sides (refer to Fig.120), the boulevard canyon type and its various configurations were found to have the worst air quality levels of any canyon type. This was found to be the case despite the fact that the boulevard canyon type has a low

aspect ratio and a large distance between leeward and windward buildings can mean better air ventilation and lower pollution concentrations. The result of this thesis challenge the common perception and implying that the greater the distance between two rows of buildings in a street canyon, the greater the complexity of the area, as well as the stronger the influence of other urban forms and meteorological parameters on the levels of air pollution that can be found within urban canyons.

Avoid symmetric canyon configuration

- With the exception of mews street canyon, the rest of the canyon showed the lowest mean pollution levels in a step-up canyon configuration, moderate mean pollution levels in a step-down canyon configuration, and the highest pollution levels in a symmetric canyon configuration. The latter also included mews street canyon. That means, as a general rule step-up canyon configuration must be encouraged.

Small details matter

- Trees and greenery, regardless of canyon type, may result in significantly higher pollution concentrations within urban canyons. Thus, more attention should be paid to the type, scale, species and, most importantly, the locations and distributions of trees within a given urban canyon in order to alleviate air quality problems.

Make way for active travel

- A well-planned tree arrangement and selection can block or redirect wind, directing it away from the canyon and protecting pedestrians from excessive exposure. A canyon with dense trees may be recommended, if vehicle traffic and pollution levels are extremely low within the canyon, as the tree canopy can help block incoming pollutants from above the rooftop (urban canopy layer) and keep the canyon's air pollution levels low, encouraging more active travel.

There is no one-size-fits-all solution

- If the air quality at the street level is better than the air quality above the building rooftop (urban canopy layer), trees should be encouraged; if the air quality at the street level is worse than the urban canopy layer, trees should be limited. This especially works in canyons with an aspect ratio greater than 0.5, such as mews, residential streets, and narrow and high streets. Therefore, the application of these

considerations is dependent on the type of urban canyon, tree arrangements, source of pollution, and volume of vehicle traffic.

Consider seasonality

- In urban canyons with a high pollution source, it is recommended to plant deciduous trees rather than evergreen trees. This is done to ensure that, at the very least, during the winter season, there is a greater sky view factor due to the lack of foliage on trees, which increases air pollution dispersion and lower pollution concentrations at pedestrian height.

It is not always about trees

- In a street canyon with high pollution levels and heavy vehicle traffic, a 2-metre-high hedgerow is more effective than trees with a stem height or canopy height of more than two metres elevated from the ground in protecting pedestrians from harmful air pollutants. It is important to note that the hedgerows should be planted close to the sources of pollution and should have a lower wind permeability so that they can serve as a barrier and reduce the amount of pollution that is inhaled by pedestrians.

The missing link, buoyancy effect!

- The buoyancy effect plays a significant role in modifying the flow and vortex. Computational modelling has demonstrated that when a surface in a street canyon heats up, the vortex flow characteristics change. Additionally, heating different surfaces, such as the upwind wall, the downwind wall, or the canyon floor, alters the vortex flow in distinct ways. Moreover, it was discovered that the buoyancy effect continues to influence wind behaviour even as the distance between buildings increases, resulting in an increase in air pollution during colder months and increased dispersion of air pollution during warmer months.

Based on the above findings and the results of the fieldwork, computational simulation, and correlation analysis, the hypothesis stated in the introduction chapter of this thesis has been addressed and confirmed, that means, manipulation of urban form can motivate a positive impact on urban microclimate and encourage greater air pollution dispersion, avoid air pollution concentration within urban street canyons, thereby reducing its negative impact on human health. The measures and recommendations mentioned here and in chapter 7 section 7.3 can be implemented as urban planning strategies and applied for new development or

urban regeneration projects. The new development offers the opportunity to manipulate the built form with greater flexibility and various urban morphological indicators such as sky view factor, aspect ratio and building heights can be controlled to achieve greater air pollution dispersion within the canyon, whereas urban regeneration may face some limitations in manipulating the built form, but there will be surly opportunities to introduce a well-planned green infrastructure to avoid high concentrations of pollution and to protect urban dwellers from polluted air.

8.1 Contribution to knowledge

The findings from this study make several contributions to the current literature and study.

This thesis has tackled some of the knowledge gaps identified in the systematic review of the literature and made several contributions to the current literature and knowledge. The specifics of these contributions are listed below:

- This thesis is the first comprehensive investigation of urban street canyons and the impact of microclimate on the concentration of air pollution. For 30 distinct urban street canyon configurations, recommendations are provided to increase dispersion and protect pedestrians from harmful levels of air pollution. Within each canyon type, this thesis identified canyon configurations with the highest and lowest levels of air pollution. This information can be used by urban planners, environmental designers, and other related and interested disciplines to avoid configurations and canyon sides with a high concentration of air pollution and simultaneously reduce pollution levels by implementing the recommendations.
- Given that most cities around the world have pledged to be significantly greener in the coming years, including expanding green spaces between buildings and increasing the number of street trees and greenery. The findings of this thesis add to the rapidly expanding field of urban green infrastructure and indicate an urgent need for effective tree-planting policy advice for urban planners in order to create better and more informed plans that ensure significant improvements in air quality without increasing pollution concentration or hot spots.

- Unlike many other computational modelling studies, this thesis considered the effect of tree trunks and leaf details including wet and dry deposition of air pollutants on trees in both summer and winter seasons. This has minimised potential errors and accurately calculated the interaction of tree leaf surface with respect to the actual meteorological, pollutants, and plant physiological conditions for each grid box of the plant canopy.

- Through a rigorous methodological calibration procedure, this study provided a series of equations for converting ENVI-met outputs to real-world spot measurement values. This will assist researchers to model and simulate idealised and future scenarios in a variety of urban settings in various seasons, while ensuring that the results are reliable and accurate predictions of real-world scenarios.

- This thesis study carried out seasonal fieldwork and computational modelling to ensure that seasonal changes in deciduous trees and meteorological conditions were accounted for when analysing the behaviour of air pollution. This has improved understanding of the confounding variables and prevented the generalisation of phenomena. It also provided finer data to be compared with the output of computational modelling (ENVI-met).

- Using correlation analysis, the study was able to identify relationships between various parameters in order to narrow down the ten identified morphological indicators (refer to section 3.5 table 09) to four indicators with the greatest impact on microclimate and air pollution levels, namely, building height differentials, average building heights, the green cover ratio and the sky view factor.

8.2 Limitations and recommendations for future research

This section discusses some overarching limitations of the research, as well as suggests potential areas for future research.

- Some of the limitations of this study are related to the computational modelling software used. For example, due to time constraints and increased modelling complexity, all building materials were assigned a single material, namely concrete, whereas building facades in a real urban canyon are made up of a variety of materials. An extension of the current research would be to simulate the same canyon types with

different materials with high and low albedo and measure their impact on buoyancy and wind flow and air pollution dispersion.

- Another limitation of the computational modelling was the difficulty in incorporating vehicle-induced turbulence, which is thought to affect the flow field in the street canyon. It's especially interesting to see how vehicles travelling at different speeds in one-way and two-way streets affect the flow field and pollution concentration or dispersion.

- Due to budget and facility constraints, fieldwork measurement had to be done with portable devices. Although, at the time of measurement, all protocols were followed to minimise error and capture as much data as possible within the spot measurement time frame. However, if the budget allows, it is far preferable to use continuous fixed air quality monitoring devices within each location of interest to measure pollution and meteorological parameters simultaneously and for a longer period of time, if possible, throughout the year.

- The current study did not account for the effect of street furniture during the computational modelling and simulation stages. An extension of this study would be to look at the role of street furniture such as parked cars, bus stops, and permanent sitting areas on concentration of pollution and, if possible, compare the results to the field measurement findings.

In the future, the primary goal will be to break through the above limitations, to achieve even higher accuracy and to model a further variety of realistic situations. Aside from the mentioned improvements, the next step in this study is to take one or more of the presented street canyons and generate a formula to relate gradual increases or decreases in building or tree heights to air pollution concentrations. In other words, to calculate the percentage change in pollution levels caused by meter-by-meter changes in building or tree heights within urban canyons. This will complement and broaden the scope of the current work and offer a more granular design recommendation. This will necessitate further computational simulation and correlation analysis similar to what has been presented in chapter 6 and 7.

References

Aarthi, A. et al. (2020). Air quality prediction through regression model. International Journal of Scientific and Technology Research, 9 (3), 923–928.

Abhijith, K. and Gokhale, S.: (2015) Passive control potentials of trees and on-street parked cars in reduction of air pollution exposure in urban street canyons, Environmental Pollution, 204, 99–108.

Abhijith, K. V. and Kumar, P. (2019). Field investigations for evaluating green infrastructure effects on air quality in open-road conditions. Atmospheric Environment, 201 (December 2018), 132–147. Available from https://doi.org/10.1016/j.atmosenv.2018.12.036.

Ahmad, K., Khare, M., Chaudhry, K.K., 2005. Wind tunnel simulation studies on dispersion at urban street canyons and intersections ? a review. J. Wind Eng. Indus. Aerodynamics 93, 697e717.

Air Quality England. (2022). London Borough of Camden Monitoring Data. Available from https://www.airqualityengland.co.uk/site/exceedence?site_id=CD009.

Albdour, M.S. and Baranyai, B. (2019). An overview of microclimate tools for predicting the thermal comfort, meteorological parameters and design strategies in outdoor spaces. Pollack Periodica, 14 (2), 109–118. Available from https://doi.org/10.1556/606.2019.14.2.10.

Allaby, M. (2009). Atmosphere : a scientific history of air, weather, and climate. New York : Facts on File. Available from https://www.worldcat.org/title/atmosphere-a-scientific-history-of-air-weather-and-climate/oclc/851098262&referer=brief_results#.WaVjKCwwBvY.mendeley [Accessed 29 August 2017].

Allegrini, J., Dorer, V. and Carmeliet, J. (2015). Journal of Wind Engineering In fl uence of morphologies on the microclimate in urban neighbourhoods. 144, 108–117. Available from https://doi.org/10.1016/j.jweia.2015.03.024.

Altshuller, A.P. (1956). Thermodynamic considerations in the interactions of nitrogen oxides and oxy-acids in the atmosphere. Journal of the Air Pollution Control Association, 6 (2), 97–100. Available from https://doi.org/10.1080/00966665.1956.10467740.

Amato, F., Pandolfi, M., Moreno, T., Furger, M., Pey, J., Alastuey, A., Bukowiecki, N., Prevot, A.S.H., Baltensberger, U. and Querol, X. (2011). Sources and variability of inhalable road dust particles in three European cities. Atmospheric Environment 45:6777-6787

Amorim, J.H., Rodrigues, V., Tavares, R., Valente, J., Borrego, C., 2013. CFDmodelling of the aerodynamic effect of trees on urban air pollution dispersion. Sci. Total Environ. 461–462, 541–551.

Ansys. (2020). Ansys. Available from https://support.ansys.com/AnsysCustomerPortal/en_us/Downloads/Current+Release.

AQMesh. (2019). Co-location comparison trials. Available from https://www.aqmesh.com/performance/co-location-comparison-trials/.

Arapakis, P. (2019). The use of 3D digital models in microclimatic studies: First steps in coupling CityGML with ENVI-met.

Arboit, M., Diblasi, A., Fernandezllano, J. and Derosa, C. (2008). Assessing the solar potential of low-density urban environments in Andean cities with desert climates: The case of the city of Mendoza, in Argentina. Renewable Energy. 33. 8. 1733-1748.

Assimakopoulos, V., Apsimon, H., & Moussiopoulos, N. (2003). A numerical study of atmospheric pollutant dispersion in different two-dimensional street canyon configurations. Atmospheric Environment,37(29), 4037-4049.

Baik, J.J., & Kim, J.J. (1999). A numerical study of flow and pollutant dispersion characteristics in urban street canyons, Journal of Applied Meteorology 38: 1576-1589.

Baik, J.J., Kang, Y.S. & Kim, J.K. (2007). Modeling reactive pollutant dispersion in an urban street canyon. Atmospheric Environment, 41(5), 934-949.

Balmes, J.R., Fine, J.M., Sheppard, D., 1987. Symptomatic bronchoconstric- tion after short-term inhalation of sulfur dioxide. Am. Rev. Respir. Dis. 136, 1117.

Bande, L. and Manandhar, P. (2019). DEFINITION OF LOCAL CLIMATE ZONES IN RELATION TO ENVI-MET AND SITE DATA IN THE CITY OF AL AIN , UAE DEFINITION OF LOCAL CLIMATE ZONES IN RELATION TO ENVI-MET AND SITE DATA IN THE CITY OF AL AIN , UAE. (December). Available from https://doi.org/10.2495/SC190191.

Barton, H. et al. (2015). Healthy urban planningWorld Health. Available from www.healthyurbandevelopment.nhs.uk.

Barwise, Y. and Kumar, P. (2020). Designing vegetation barriers for urban air pollution abatement: a practical review for appropriate plant species selection. npj Climate and Atmospheric Science, 3 (1), 1–19. Available from https://doi.org/10.1038/s41612-020-0115-3.

Bealey, W.J. et al. (2007). Estimating the reduction of urban PM10 concentrations by trees within an environmental information system for planners. Journal of Environmental Management, 85 (1), 44–58. Available from https://doi.org/10.1016/j.jenvman.2006.07.007.

Belcher, S., Coceal, O., Hunt, J. C. R., Carruthers, D. J., and a.G. Robins (2012). A re- view of urban dispersion modelling. Technical Report Report ADMLC-R7, Annex B, Atmospheric Dispersion Modelling Liaison Committee.

Bell, M.L., Davis, D.L. and Fletcher, T. (2008). A retrospective assessment of mortality from the london smog episode of 1952: The role of influenza and pollution. Urban Ecology: An International Perspective on the Interaction Between Humans and Nature, 6 (1), 263–268.

Berardi, U. and Wang, Y. (2016). The effect of a denser city over the urban microclimate: The case of Toronto. Sustainability (Switzerland), 8 (8), 1–11. Available from https://doi.org/10.3390/su8080822.

Billingsley, A. (2020). The challenges and benefits of using small sensor technology for local air quality monitoring. Envirotech. Available from https://www.envirotech-online.com/article/air-monitoring/6/environmental-instruments/the-challenges-and-benefits-of-using-small-sensor-technology-for-local-air-quality-monitoring/2679.

Blocken, B. et al. (2008). Numerical Study on the Existence of the Venturi Effect in Passages between Perpendicular Buildings. Journal of Engineering Mechanics, 134 (12), 1021–1028. Available from https://doi.org/10.1061/(asce)0733-9399(2008)134:12(1021).

Blocken, B., Defraeye, T., Derome, D., Carmeliet, J., 2009. High- resolution CFD simulations for forced convective heat transfer coefficients at the facade of a low-rise building. Building and Environment 44 (12), 2396–2412.

Blocken, B., Janssen, W.D., van Hooff, T., 2012. CFD simulation for pedestrian wind comfort and wind safety in urban areas: general decision framework and case study for the Eindhoven University campus. Environmental Modelling & Software 30, 15–34.

Bocquier, P. (2005). World urbanization prospects: An alternative to the UN model of projection compatible with the mobility transition theory. Demographic Research, 12 (4), 197–236. Available from https://doi.org/10.2307/2808041.

Boffetta, P., Merler, E. and Vainio, H. (1993). Carcinogenicity of mercury and mercury compounds. Scand. J. Work Environ Health, 19 (1).

Boningari, T. and Smirniotis, P.G. (2016). Impact of nitrogen oxides on the environment and human health: Mn-based materials for the NOx abatement. Current Opinion in Chemical Engineering, 13 (x), 133–141. Available from https://doi.org/10.1016/j.coche.2016.09.004.

Borna, M. and Schiano-phan, R. (2020). PLEA 2020 A CORUÑA Impact of vegetation on pollutants concentration at pedestrian level Improving Hyperlocal Air Quality in Cities. 0–5.

Borna, M. et al. (2022). A correlational analysis of COVID-19 incidence and mortality and urban determinants of vitamin D status across the London boroughs. Scientific Reports, (0123456789), 1–11. Available from https://doi.org/10.1038/s41598-022-15664-y.

Bosanquet, C.H. and Pearson, J.L. (1936). The spread of smoke and gases from chimneys. Transactions of the Faraday Society, 32 (0), 1249–1263. Available from https://doi.org/10.1039/TF9363201249.

Bottema, M. (1993). Wind climate and urban geometry. Eindhoven.

Bowden, R. (2007). Urbanization. London: Wayland. Available from https://www.worldcat.org/title/urbanization/oclc/166315097&referer=brief_results#.Wiash 81lktw.mendeley [Accessed 5 December 2017].

Britter, R.E. and S.R. Hanna, 2003: Flow and disper- sion in urban areas. Annual Review of Fluid Mechanics, Volume 35, pp. 469–496.

Brown, M. et al. (2006). Experimental and model-computed area-averaged vertical profiles of wind speed for evaluation of mesoscale urban canopy schemes. 86th AMS Annual Meeting, (January).

Bruse, M. (2012). ENVI-met 3. Available from http://www.envi-met.com.

Bruse, M. and H. Fleer (1998). Simulating Surface- Plant-Air Interactions Inside Urban Environments with a Three Dimensional Numerical Model, Environmental Software and Modelling, (13), S. 373–384

Buccolieri, R. et al. (2009). Aerodynamic effects of trees on pollutant concentration in street canyons. Science of the Total Environment, 407 (19), 5247–5256. Available from https://doi.org/10.1016/j.scitotenv.2009.06.016.

Buccolieri, R. et al. (2011). Analysis of local scale tree e atmosphere interaction on pollutant concentration in idealized street canyons and application to a real urban junction. Atmospheric Environment, 45 (9), 1702–1713. Available from https://doi.org/10.1016/j.atmosenv.2010.12.058.

Buccolieri, R. et al. (2019). Reprint of: Review on urban tree modelling in CFD simulations: Aerodynamic, deposition and thermal effects. Urban Forestry and Urban Greening, 37 (July 2018), 56–64. Available from https://doi.org/10.1016/j.ufug.2018.07.004.

Buccolieri, R. et al. (2022). Obstacles influence on existing urban canyon ventilation and air pollutant concentration: A review of potential measures. Building and Environment, 214 (February), 108905. Available from https://doi.org/10.1016/j.buildenv.2022.108905.

Buccolieri, R. et al. (2022). Obstacles influence on existing urban canyon ventilation and air pollutant concentration: A review of potential measures. Building and Environment, 214 (February), 108905. Available from https://doi.org/10.1016/j.buildenv.2022.108905.

Bühl, A. 2012. SPSS 20, 13., aktualisierte Auflage. München: Pearson. 142 s.

Bukowiecki, N., Gehrig, R., Lienemann, P., Hill, M., Figi, R., Buchmann, B., Furger, M., Richard, A., Mohr, C., Weimer, S., Prévôt, A. and Baltensperger, U. (2009a). PM10 emission factors of abrasion particles from road traffic (APART). Swiss Association of Road and Transportation Experts (VSS)

C R, A. et al. (2018). Detection and Prediction of Air Pollution using Machine Learning Models. International Journal of Engineering Trends and Technology, 59 (4), 204–207. Available from https://doi.org/10.14445/22315381/ijett-v59p238.

Cambridge Environmental Research. (2006). Modelling of Current and Future Concentrations of PM, NOx and O3 in London using ADMS-Urban Draft. (x).

Carrington, D. (2016). MPs: UK air pollution is a 'public health emergency'. The Guardian. Available from https://www.theguardian.com/environment/2016/apr/27/uk-air-pollution-public-health-emergency-crisis-diesel-cars [Accessed 18 August 2017].

Carrington, D. (2017). London breaches annual air pollution limit for 2017 in just five days. The Guardian. Available from https://www.theguardian.com/environment/2017/jan/06/london-breaches-toxic-air-pollution-limit-for-2017-in-just-five-days [Accessed 25 August 2017].

Chan, L.Y., & Kwok, W.S. (2000). Vertical dispersion of suspended particulates in urban area of Hong Kong, Atmospheric Environment 34: 4403-4412.

Chatzidiakou, L. et al. (2019). Characterising low-cost sensors in highly portable platforms to quantify personal exposure in diverse environments. Atmospheric Measurement Techniques, 12 (8), 4643–4657. Available from https://doi.org/10.5194/amt-12-4643-2019.

Chatzidimitriou, A. and Yannas, S. (2017). Street canyon design and improvement potential for urban open spaces; the influence of canyon aspect ratio and orientation on microclimate and outdoor comfort. Sustainable Cities and Society, 33 (June), . Elsevier85–101. Available from http://dx.doi.org/10.1016/j.scs.2017.05.019.

Chen, L. and Ng, E. (2011). Quantitative urban climate mapping based on a geographical database: A simulation approach using Hong Kong as a case study. International Journal of Applied Earth Observation and Geoinformation, 13 (4), 586–594. Available from https://doi.org/10.1016/j.jag.2011.03.003.

Chen, L., Ng, E. (2012). Outdoor thermal comfort and outdoor activities: a review of research in the past decade. Cities, 2 (29), 118–125.

Cheng, W.C., Liu, C.H. & Leung, D.Y.C. (2009). On the correlation of air and pollutant exchange for street canyons in combined wind-buoyancy-driven flow. Atmospheric Environment, 43(24), 3682-3690.

Chiaradia, A.J.F. (2019). UrbanMorphology/Urban Form. Available from https://doi.org/10.1002/9781118568446.eurs0382.

Claesen, J.L.A. et al. (2021). Associations of traffic-related air pollution and greenery with academic outcomes among primary schoolchildren. Environmental Research, 199 (March), 111325. Available from https://doi.org/10.1016/j.envres.2021.111325.

Clark, D. (1998). Interdependent Urbanization in an Urban World: an Historical Overview. The Geographical Journal, 164 (1), 85–95.

Clark, N. (2006). Industrial Revolution and the Standard of Living. Available from https://www.worldcat.org/title/industrial-revolution-and-the-standard-of-living/oclc/720033037&referer=brief_results#.WiU3-rymbi8.mendeley [Accessed 4 December 2017].

Cohen, A.J. et al. (2017). Estimates and 25-year trends of the global burden of disease attributable to ambient air pollution: an analysis of data from the Global Burden of Diseases

Study 2015. The Lancet, 389 (10082), 1907–1918. Available from
https://doi.org/10.1016/S0140-6736(17)30505-6.

Cole, R.J. (2009). Designing High-Density CitiesNg, E., ed. Designing High-Density Cities for
Social and Environmental Sustainability. Earthscan in the UK and USA in 2010. Available
from http://www.scopus.com/inward/record.url?eid=2-s2.0-
84905064368&partnerID=tZOtx3y1.

Communities and Local Government: London. (2011). Planning Policy Statement 3 (PPS3). 3
(June).

Conner, T. et al. (2018). How to Evaluate Low-Cost Sensors by Collocation with Federal
Reference Method Monitors. 45.

Cullen, F. and DCLG, (Department for Communities and Local Government) (2012). National
Planning Policy FrameworkCrown. www.communities.gov.uk. Available from
http://www.interreg4c.eu/uploads/media/pdf/7_Gateway_Methodology_Stages_of_herita
ge_led_regeneration_INHERIT.pdf%5Cnhttp://www.communities.gov.uk/documents/planni
ngandbuilding/pdf/2116950.pdf.

Cunningham, W.P. and Cunningham, M.A. (2017). Environmental science : a global concern,
Fourteenth edition. Available from https://www.worldcat.org/title/environmental-science-
a-global-concern/oclc/959228780&referer=brief_results#.War-X2GFA6c.mendeley
[Accessed 2 September 2017].

Daly, A. and Zannetti, P. (2007). Air Pollution Modeling – An Overview. Ambient Air
Pollution, I (2003), 15–28.

Davenport, A.G. (1960). Wind Loads on Structures, Technical Paper No. 88, Ottawa, Canada:
National Research Council.

Davim, J.P. (2017). Computational Methods and Production Engineering. Available from
https://doi.org/https://doi.org/10.1016/C2013-0-16281-2.

Davis, C. and Huxford, R. (2007). Manual for Streets. Available from
https://doi.org/10.1680/muen.2009.162.3.129.

Davis, D.L., Bell, M.L. and Fletcher, T. (2002). A look back at the London smog of 1952 and
the half century since. Environmental Health Perspectives, 110 (12), 734–735.

Davis, M. (2006). City of quartz : excavating the future in Los AngelesNew ed. London ;;New
York: Verso. Available from http://www.worldcat.org/title/city-of-quartz-excavating-the-
future-in-los-angeles/oclc/70402685&referer=brief_results#.Wt_4OXd5CHs.mendeley
[Accessed 25 April 2018].

DCLG, (Department for Communities and Local Government) (2007). Planning Policy
Statement: Planning and Climate Change. Policy,(December), 28. Available from
http://www.communities.gov.uk/documents/planningandbuilding/pdf/ppsclimatechange.p
df.

DEFRA. (2019). Emissions Factors Toolkit. Available from https://laqm.defra.gov.uk/air-quality/air-quality-assessment/emissions-factors-toolkit/.

DEFRA. (2021). Emissions Factors Toolkit. Available from https://laqm.defra.gov.uk/air-quality/air-quality-assessment/emissions-factors-toolkit/.

DEFRA. (2021a). National Bias Adjustment Factors. Available from https://laqm.defra.gov.uk/air-quality/air-quality-assessment/national-bias/.

DEFRA. (2021b). Precision and Accuracy. Available from https://laqm.defra.gov.uk/air-quality/air-quality-assessment/precision-and-accuracy/.

Denier Van der Gon, H., Jozwicka, M., Cassee, F., Gerlofs-Nijland, M,. Gehrig, R., Gustafsson, M., Hulskotte, J.; Janssen, N., Johansson, C., Ntziachristos. L. and Riediker, M., (2012). The policy relevance of wear emissions from road transport. now and in the future. TNO report. TNO-060-UT- 2012-00732

Department Environment For Affairs Food & Rural. (2020). National statistics Background to concentrations of air pollutants. Available from https://www.gov.uk/government/statistics/air-quality-statistics/background.

Department for Environment Food and Rural Affairs. (2018). Part IV of the Environment Act 1995 Local Air Quality Management Technical Guidance (TG16). Energy Resource Environmental and Sustainable Management, 2005 (NOV/DEC), 5.

Department for Transport. (2019). Road traffic statistics. Available from https://roadtraffic.dft.gov.uk/#6/55.254/-6.053/basemap-regions-countpoints.

Department of Transport. (2005). A guide to best practice on access to pedestrian and transport infrastructure. Inclusive Mobility, (December), 15. Available from https://www.gov.uk/government/publications/inclusive-mobility.

DePaul, F.T. and C.M. Shieh, 1986: Measurements of wind velocity in a street canyon. Atmospheric Environment, Volume 20, pp. 455–459.

Detwyler, T.R. (Thomas R. and Marcus, M.G. (Melvin G. (1972). Urbanization and environment; the physical geography of the city, 3. printing. Belmont Calif: Duxbury Press. Available from https://www.worldcat.org/title/urbanization-and-environment-the-physical-geography-of-the-city/oclc/472880479&referer=brief_results#.WiaeXfA_VFk.mendeley [Accessed 5 December 2017].

Di Bernardino, A. et al. (2018). Pollutant fluxes in two-dimensional street canyons. Urban Climate, 24 (July 2017), 80–93. Available from https://doi.org/10.1016/j.uclim.2018.02.002.

Di Sabatino, S. et al. (2008). Flow and pollutant dispersion in street canyons using FLUENT and ADMS-Urban. Environmental Modeling and Assessment, 13 (3), 369–381. Available from https://doi.org/10.1007/s10666-007-9106-6.

Dockery DW, Pope CA 3rd, Xu X, Spengler JD, Ware JH, Fay ME, Ferris BG Jr, Speizer FE. An association between air pollution and mortality in six U.S. cities. N Engl J Med. 1993 Dec 9;329(24):1753-9. doi: 10.1056/NEJM199312093292401. PMID: 8179653.

Dominski, F.H. et al. (2021). Effects of air pollution on health: A mapping review of systematic reviews and meta-analyses. Environmental Research, 201 (September 2020). Available from https://doi.org/10.1016/j.envres.2021.111487.

Edussuriya, P., Chan, A. and Ye, A. (2011). Urban morphology and air quality in dense residential environments in Hong Kong. Part I: District-level analysis. Atmospheric Environment, 45 (27), 4789–4803. Available from https://doi.org/10.1016/j.atmosenv.2009.07.061.

Edussuriya, P.S. and Chan, A. (2015). Analysis of urban morphological attributes and street level air pollution in high - density residential environments in Hong Kong467–476.

EEA. (2013). EMEP/EEA air pollutant emission inventory guidebook 2013: Technical guidance to prepare national emission inventories. EEA Technical report, (12/2013), 23. Available from http://www.eea.europa.eu/publications/emep-eea-guidebook-2013.

Ehrnsperger, L. and Klemm, O. (2022). Air pollution in an urban street canyon: Novel insights from highly resolved traffic information and meteorology. Atmospheric Environment: X, 13 (January), 100151. Available from https://doi.org/10.1016/j.aeaoa.2022.100151.

Emissions Analytics. (2022). The even more hidden life of tyres. Available from https://www.emissionsanalytics.com/news/the-even-more-hidden-life-of-tyres?utm_source=Emissions+Analytics+Newsletter&utm_campaign=92318d60d7-EMAIL_CAMPAIGN_2020_01_22_12_02_COPY_01&utm_medium=email&utm_term=0_c35 d8b9a1e-92318d60d7-60356753.

Enger, E.D. and Smith, B.F. (2016). Environmental science : a study of interrelationships, Fourteenth edition. Available from https://www.worldcat.org/title/environmental-science-a-study-of-interrelationships/oclc/889426104&referer=brief_results#.WasAVmhcNsw.mendeley [Accessed 2 September 2017].

ENVI-met. (2018a). ENVI-met guide. Available from https://envi-met.info/doku.php?id=kb:nesting#:~:text=As the Nesting Grids are,profiles (A and B).

ENVI-met. (2018b). Nesting Grids. Available from https://envi-met.info/doku.php?id=kb:nesting.

Erell, E., Pearlmutter, D. and Williamson, T. (2011). Urban Microclimate.

Esch, M.P. (2015). Designing the Urban Microclimate.

European Commission (2005). European air pollution policy. Available from http://ec.europa.eu/environment/air/clean_air/review.htm.

European Environment Agency. (2019). EMEP/EEA air pollutant emission inventory guidebook 2019: Technical guidance to prepare national emission inventories. EEA Technical report, (12/2019). Available from https://www.eea.europa.eu/publications/emep-eea-guidebook-2019.

European Environment Agency. (2020). Air quality concentrations. Available from https://www.eea.europa.eu/themes/air/air-quality-concentrations.

Evyatar, E., David, P. and Terry, W. (2011). Meterology and Urban Design Erelletal 1950_2010. Internet, (June), 23–24.

Eze, I.C., Schaffner, E., Fischer, E., Schikowski, T., Adam, M., Imboden, M., et al., 2014. Long-term air pollution exposure and diabetes in a population-based Swiss cohort. Envi- ron. Int. 70, 95–105.

Farrell, P. (2013). World's top problem is overpopulation, not climate. Market Watch (The Wallstreet Journal),.

Gallagher, J. et al. (2015). Passive methods for improving air quality in the built environment: A review of porous and solid barriers. Atmospheric Environment, 120, 61–70. Available from https://doi.org/10.1016/j.atmosenv.2015.08.075.

Gardner, M.W.; (1998) Dorling, S.R. Artificial Neural Networks (the Multilayer Perceptron)—-A Review of Applications in the Atmo- spheric Sciences. Atmos. Environ. 1998, 32, 2627–2636.

Gaspari, J. and Fabbri, K. (2017). A Study on the Use of Outdoor Microclimate Map to Address Design Solutions for Urban Regeneration. Energy Procedia, 111 (September 2016), 500–509. Available from https://doi.org/10.1016/j.egypro.2017.03.212.

Gauthier, P. and Gilliland, J. (2006). Mapping urban morphology: a classification scheme for interpreting contributions to the study of urban form. International Seminar on Urban Form, 10 (1), 41–50.

Givoni, B. (1998). Climate considerations in buildings and urban design. New York [etc.]: Van Nostrand Reinhold.

Glaeser, E.L. (Edward L. and James, L. (2011). Triumph of the city : how our greatest invention makes us richer, smarter, greener, healthier, and happier. Available from http://www.worldcat.org/title/triumph-of-the-city-how-our-greatest-invention-makes-us-richer-smarter-greener-healthier-and-happier/oclc/877879617&referer=brief_results#.Wt3KjJHLUps.mendeley [Accessed 23 April 2018].

Glover, N. (2015). Investigating the Impact of Trees on Airflow within Street Canyons through the use of CFD and Field Measurements. (August).

Gousseau, P., Blocken, B., van Heijst, G.J.F., 2011. CFD simulation of pollutant dispersion around isolated buildings: on the role of convective and turbulent mass fluxes in the prediction accuracy. Journal of Hazardous Materials 194, 422–434.

Goverment, U. (2019). Clean Air Strategy 2019: executive summary. Available from https://www.gov.uk/government/publications/clean-air-strategy-2019/clean-air-strategy-2019-executive-summary.

Greater London Authority. (2020). Air quality in London 2016-2020. London Environment Strategy: Air Quality Impact Evaluation, (October).

Grimm, N.B. et al. (2008). Global change and the ecology of cities. Science, 319 (5864), 756–760. Available from https://doi.org/10.1126/science.1150195.

Grimmond, C.S.B. et al. (2001). Rapid methods to estimate sky view factors applied to urban areas. Int. J. Climatol, 21 903–913.

Grimmond, S. (2007). Urbanization and global environmental change: Local effects of urban warming. The Geographical Journal, 173 (1), 83–88.

Gromke C, Buccolieri R, Di Sabatino S, Ruck B (2008) Dispersion modeling study in a street canyon with tree planting by means of wind tunnel and numerical investigations - Evaluation of CFD data with experimental data. Atmos Environ 42:8640–8650

Gromke, C. and Ruck, B. (2012). Pollutant Concentrations in Street Canyons of Different Aspect Ratio with Avenues of Trees for Various Wind Directions. Boundary-Layer Meteorology, 144 (1), 41–64. Available from https://doi.org/10.1007/s10546-012-9703-z.

Gromke, C., Ruck, B., 2007. Influence of trees on the dispersion of pollutants in an urban street canyon—experimental investigation of the flow and concentration field. Atmos. Environ. 41 (16), 3287–3302.

Gunnar, M. et al. (2013). Aerosols and their Relation to Global Climate and Climate Sensitivity. Nature, (May).

Halitsky, J., 1963. Gas diffusion near buildings. ASHRAE Transactions 69, 464–485.

Haughton, G., & Hunter, C. (2003). Sustainable Cities. New York; London: Routledge.,.

He, J. et al. (2017). Air pollution characteristics and their relation to meteorological conditions during 2014–2015 in major Chinese cities. Environmental Pollution, 223, 484–496. Available from https://doi.org/10.1016/j.envpol.2017.01.050.

Hu, T., and Yoshie, R. (2013). Indices to evaluate ventilation efficiency in newly-built urban area at pedestrian level'. Wind Engineering and Industrial Aerodynamics, 112 39–51.

Hua, C.H. & Wang, F. (2005). Using a CFD approach for the study of street-level winds in a built-up area. Building and Environment, 40, 617–31.

Huber, A.H., Snyder, W.H., 1982. Wind tunnel investigation of the effects of a rectangular shaped building on dispersion of effluent from short adjacent stacks. Atmospheric Environment 16 (12), 2837–2848.

Hueglin, C. et al. (2005). Chemical characterisation of PM2.5, PM10 and coarse particles at urban, near-city and rural sites in Switzerland. Atmospheric Environment, 39 (4), 637–651. Available from https://doi.org/https://doi.org/10.1016/j.atmosenv.2004.10.027.

Hunter, L.J., Johnson, G.T., & Watson, I.D. (1992). An investigation of three-dimensional characteristics of flow regimes within the urban canyon, Atmospheric Environment: 425-432.

Institute for Population Studies (2010). Overpopulation: Environmental and Social Problems.

Issakhov, A., Tursynzhanova, A. and Abylkassymova, A. (2022). Numerical study of air pollution exposure in idealized urban street canyons: Porous and solid barriers. Urban Climate, 43 (January), 101112. Available from https://doi.org/10.1016/j.uclim.2022.101112.

Jacobs, Jane. 1993. The Death and Life of Great American Cities. New York, NY: Vintage Books.

Jeanjean, A. et al. (2017). Air quality affected by trees in real street canyons: The case of Marylebone neighbourhood in central London. Urban Forestry and Urban Greening, 22, 41–53. Available from https://doi.org/10.1016/j.ufug.2017.01.009.

Jeanjean, A. et al. (2017). Air quality affected by trees in real street canyons: The case of Marylebone neighbourhood in central London. Urban Forestry and Urban Greening, 22, 41–53. Available from https://doi.org/10.1016/j.ufug.2017.01.009.

Jeanjean, A.P.R. et al. (2015). A CFD study on the effectiveness of trees to disperse road traffic emissions at a city scale. Atmospheric Environment, 120, 1–14. Available from https://doi.org/10.1016/j.atmosenv.2015.08.003.

Jerrett, M. et al. (2005). A review and evaluation of intraurban air pollution exposure models. Journal of Exposure Analysis and Environmental Epidemiology, 15 (2), 185–204. Available from https://doi.org/10.1038/sj.jea.7500388.

Jiang, D.; Jiang, W.; Liu, H.; Sun, J. (2008). Systematic influence of different building spacing, height and layouton mean wind and turbulent characteristics within and over urban building arrays. Wind Struct., 11 275–289.

Jimenez P., Baldasano, J. M., Dabdub D., 2003. Comparison of photochemical mechan- isms for air quality modeling. Atmospheric Environment. Vol.37: p.4179-4194.

Jin, H. et al. (2017). The effects of residential area building layout on outdoor wind environment at the pedestrian level in severe cold regions of China. Sustainability (Switzerland), 9 (12), 1–18. Available from https://doi.org/10.3390/su9122310.

Johnson, G.T., & I.D. Watson, 1984: The determination of view-factors in urban canyons. Journal ofClimate and Applied Meteorology, 23, 329–335.

Johnson, O. and More, D. (2004). Collins Tree Guide. Collins. Available from https://books.google.co.uk/books?id=%5C_rDlAAAACAAJ.

Johnson, W.B., Ludwig, F.L., Dabberdt, W.F. and Allen, R.J. (1973) 'An urban diffusion simulation model for Carbon Monoxide', Journal of Air Pollution Control Association, Vol. 23, pp.490–498.

Johnston, I. (2016). http://www.independent.co.uk/news/uk/air-quality-diesel-vehicle-car-emissions-clean-air-zones-charge-polluting-vehicles-mps-a7002611.html. Independent. Available from http://www.independent.co.uk/news/uk/air-quality-diesel-vehicle-car-emissions-clean-air-zones-charge-polluting-vehicles-mps-a7002611.html.

Jung, Y.R., Park, W.G. and Park, O.H. (2003). Pollution dispersion analysis using the puff model with numerical flow field data. Mechanics Research Communications, 30 (4), 277–286. Available from https://doi.org/10.1016/S0093-6413(03)00024-7.

Kalenderski, S. (2009). Stochastic Modeling of Space-Time Processes. an Air Pollution Problem. (April). Available from https://circle.ubc.ca/bitstream/id/18866/ubc_2009_fall_kalenderski_stoitchko.pdf.

Kastner-Klein, P. & Plate, E.J. (1999). Wind-tunnel study of concentration fields in street canyons. Atmospheric Environment, 33(24-25), 3973-3979.

Kelishadi R, Poursafa P. Air pollution and non-respiratory health hazards for children. Arch Med Sci. 2010 Aug 30;6(4):483-95. doi: 10.5114/aoms.2010.14458. Epub 2010 Sep 7. PMID: 22371790; PMCID: PMC3284061.

Kelly, M.J. (2012). Inclusive Mobilty. Neuroendocrinology, 96 (2), 101–102. Available from http://www.ncbi.nlm.nih.gov/pubmed/22987642.

Kemp, D.D. (2012). Exploring Environmental Issues. Routledge. Available from https://www.worldcat.org/title/exploring-environmental-issues/oclc/819508024&referer=brief_results#.WasMAVPXbC0.mendeley [Accessed 2 September 2017].

Kim, J.J. and Baik, J.J. (1999). A numerical study of thermal effects on flow and pollutant dispersion in urban street canyons. Journal of Applied Meteorology, 38 (9), 1249–1261. Available from https://doi.org/10.1175/1520-0450(1999)038<1249:ANSOTE>2.0.CO;2.

Kostof, Spiro. 1991. The City Shaped. Boston: Little, Brown.

Kottek, M. et al. (2006). World map of the Köppen-Geiger climate classification updated. Meteorologische Zeitschrift, 15 (3), 259–263. Available from https://doi.org/10.1127/0941-2948/2006/0130.

Krazter, P.A. (1956). The climate of cities. Braunschweig: Friedr. Vieweg and Sohn.

Kropf, K. (1996). Urban tissue and the character of towns. Urban Morphology,(19), 73–92.

Kropf, K. (2017). The handbook of urban morphology. Available from https://books.google.pl/books?id=g584DwAAQBAJ&dq=urban+fixation+line&hl=pl&source=gbs_navlinks_s.

Krüger EL, Minella FO, Rasia F (2011) Impact of urban geometry on outdoor thermal comfort and air quality from field measurements in Curitiba, Brazil. Build Environ 46(3):621–634. doi:10.1016/j. buildenv.2010.09.006 Int

Kubota, T. et al. (2008). Wind tunnel tests on the relationship between building density and pedestrian-level wind velocity: Development of guidelines for realizing acceptable wind environment in residential neighborhoods. Building and Environment, 43 (10), . Pergamon1699–1708. Available from https://www.sciencedirect.com/science/article/pii/S0360132307002028?via%3Dihub [Accessed 25 April 2018].

Kubota, T.; Miura, M.; Tominaga, Y.; Mochida, A. (2008). Wind tunnel tests on the relationship between building density and pedestrian-level wind velocity: Development of guidelines for realizing acceptable wind environment in residential neighborhoods. Build. Environ., 43 1699–1708.

Kuo, C.Y. et al. (2006). Accumulation of chromium and nickel metals in lung tumors from lung cancer patients in Taiwan. J. Toxicol. Environ. Health, A (69), 1337.

Kwak, K.H. et al. (2018). On-road air quality associated with traffic composition and street-canyon ventilation: Mobile monitoring and CFD modeling. Atmosphere, 9 (3), 1–13. Available from https://doi.org/10.3390/atmos9030092.

Landsberg, H.E. (1981). General climatology, 3. Amsterdam; New York: Elsevier Scientific Pub. Co.

Larkham, P. (1997). Typological Process and Design Theory. In: Urban morphology and typology in the United Kingdom., 159–177.

Lasley, S.M. and Gilbert, M.E. (2000). Glutamatergic components underlying lead induced impairments in hippocampal synaptic plasticity. Neurotoxicology, 21, 1057.

Lateb, M. et al. (2016). On the use of numerical modelling for near-field pollutant dispersion in urban environments - A review. Environmental Pollution, 208, 271–283. Available from https://doi.org/10.1016/j.envpol.2015.07.039.

Laville, S. et al. (2017). Thousands of British children exposed to illegal levels of air pollution. The Guardian. Available from https://www.theguardian.com/environment/2017/apr/04/thousands-of-british-children-exposed-to-illegal-levels-of-air-pollution [Accessed 18 August 2017].

Lawson, T. (2001). Building Aerodynamics. Singapore: Imperial College Press.

Leitl, B.M., Kastner-Klein, P., Rau, M., Meroney, R.N., 1997. Concentration and flow distributions in the vicinity of U-shaped buildings: wind-tunnel and computational data. Journal of Wind Engineering and Industrial Aerodynamics 67–68, 745–755.

Lelieveld, J., Evans, J.S., Fnais, M., Giannadaki, D., Pozzer, A., 2015. The contribution of outdoor air pollution sources to premature mortality on a global scale. Na- ture 525, 367e371.

Lelieveld, J., K. Klingmüller, A. Pozzer, U. Pöschl, M. Fnais, A. Daiber, T. Münzel, Cardiovascular disease burden from ambient air pollution in Europe reassessed using novel hazard ratio functions, Eur. Heart J. 40 (2019) 1590–1596. https://doi.org/10.1093/eurheartj/ehz135.

Lertxundi, A. et al. (2015). Exposure to fine particle matter, nitrogen dioxide and benzene during pregnancy and cognitive and psychomotor developments in children at 15months of age. Environment International, 80, 33–40. Available from https://doi.org/10.1016/j.envint.2015.03.007.

Li, H. et al. (2020). Evaluation of the performance of low-cost air quality sensors at a high mountain station with complex meteorological conditions. Atmosphere, 11 (2), 1–16. Available from https://doi.org/10.3390/atmos11020212.

Li, W., Meroney, R.M., 1983. Gas dispersion near a cubical model building—Part I. Mean concentration measurements. Journal of Wind Engineering and Industrial Aerodynamics 12, 15–33.

Lim, S.S., Vos, T., Flaxman, A.D., Danaei, G., Shibuya, K., Adair-Rohani, H., et al., 2012. A comparative risk assessment of burden of disease and injury attributable to 67 risk factors and risk factor clusters in 21 regions, 1990–2010: a systematic analysis for the Global Burden of Disease Study 2010. Lancet 380, 2224–2260.

Lin, M., Katul, G.G., Khlystov, A., 2012. A branch scale analytical model for predicting the vegetation collection efficiency of ultrafine particles. Atmos. Environ. 51, 293e302.

Lingard, J. et al. (2013). Statistical evaluation of the input meteorological data used for the UK air quality forecast (UK-AQF). (1), 28.

Liu, Z. et al. (2011). Real-world operation conditions and on-road emissions of Beijing diesel buses measured by using portable emission measurement system and electric low-pressure impactor. Science of the Total Environment, 409 (8), 1476–1480. Available from https://doi.org/10.1016/j.scitotenv.2010.12.042.

London Air. (2017). What do fireworks mean for health? Available from https://www.londonair.org.uk/londonair/guide/Fireworks.aspx.

London Air. (2019). Imperial College London. Available from https://www.londonair.org.uk/LondonAir/Default.aspx [Accessed 7 September 2021].

London Council. (2020). Demystifying Air Pollution in London full report.

Louka, P., Belcher, S. E. & Harrison, R. G. 2000. Coupling between air flow in streets and the well-developed boundary layer aloft. Atmospheric Environment, 34, 2613-2621

Lynch, K. (1981). A Theory of Good City Form. MIT Press,.

Lyons, T.J. et al. (2003). An international urban air pollution model for the transportation sector. Transportation Research Part D: Transport and Environment, 8 (3), 159–167. Available from https://doi.org/10.1016/S1361-9209(02)00047-0.

Macionis, J.J. and Parrillo, V.N. (2010). Cities and urban life, Seventh Ed. Available from https://www.worldcat.org/title/cities-and-urban-life/oclc/921240034&referer=brief_results#.WiaxLEGiQbQ.mendeley [Accessed 5 December 2017].

Mader, S.S., Windelspecht, M. and Carlson, J. (2016). Biology. [New York]: McGraw Hill. Available from https://www.worldcat.org/title/biology/oclc/912518987&referer=brief_results#.Wal1bUd2_Mc.mendeley [Accessed 1 September 2017].

Madiraju, S.V.H. and Kumar, A. (2022). Examination of the Performance of a Three-Phase Atmospheric Turbulence Model for Line-Source Dispersion Modeling Using Multiple Air Quality Datasets. J, 5 (2), 198–213. Available from https://doi.org/10.3390/j5020015.

Mandal, P.K. (2005). Dioxin: a review of its environmental effects and its aryl hydrocarbon receptor biology. J. Comp. Physiol., 175, 221.

Mannucci PM, Franchini M. Health Effects of Ambient Air Pollution in Developing Countries. Int J Environ Res Public Health. 2017 Sep 12;14(9):1048. doi: 10.3390/ijerph14091048. PMID: 28895888; PMCID: PMC5615585.

Mansoureh Tahbaz (2009) Estimation of the Wind Speed in Urban Areas - Height less than 10 Metres, International Journal of Ventilation, 8:1, 75 84, DOI: 10.1080/14733315.2006.11683833

Max Roser. (2021). An overview of published estimates of the death toll from air pollution. Our World in Data. Available from https://ourworldindata.org/data-review-air-pollution-deaths#:~:text=The WHO estimates that 4.2,(or ambient) air pollution.

Mayer, H. (1999). Air pollution in cities. Atmospheric Environment 33, 4029–4037

McKendry I.G., 2002. Evaluation of Artificial Neural Networks for fine particulate pollu- tion (PM10 and PM2.5) forecasting, J Air & Waste Manage Assoc 52, 1096–1101.

Meroney, R.N., Leitl, B.M., Rafailidis, S., Schatzmann, M., 1999. Wind tunnel and numerical modelling of flow and dispersion about several building shapes. Journal of Wind Engineering and Industrial Aerodynamics 81 (1–3), 333–345.

Met Office. (2020). UK climate averages. Available from https://www.metoffice.gov.uk/research/climate/maps-and-data/uk-climate-averages/gcpsvg3nc.

Met Office. (2021). climate statistics. Available from https://www.metoffice.gov.uk/services/transport/aviation/regulated/airfield-climate-stats#LondonCity.

Miao, C. et al. (2020). How the morphology of urban street canyons affects suspended particulate matter concentration at the pedestrian level: An in-situ investigation. Sustainable Cities and Society, 55 (December 2019), 1–7. Available from https://doi.org/10.1016/j.scs.2020.102042.

Mills IC, Atkinson RW, Kang S, et al. (2015). Quantitative systematic review of the associations between short-term exposure to nitrogen dioxide and mortality and hospital admissions. BMJ Open. Available from https://doi.org/10.1136/bmjopen-2014- 006946 Naess.

Mills, G. et al. (2010). Climate information for improved planning and management of mega cities (Needs Perspective). Procedia Environmental Sciences, 1 (1), 228–246.

Moonen, P. et al. (2012). Urban Physics: Effect of the micro-climate on comfort, health and energy demand. Frontiers of Architectural Research, 1 (3), 197–228. Available from https://doi.org/10.1016/j.foar.2012.05.002.

Moudon, A.V. (1997). Urban morphology as an emerging interdisciplinary field. Urban Morphology, 1 (1), 3–10.

Naboni E. Integration of outdoor thermal and visual comfort in parametric design. Sustainable habitat for developing societies. Ahmedabad: CEPT UNIVERSITY PRESS, 2014.

NAEI. (2019). UK Emissions data. Available from https://naei.beis.gov.uk/data/.

Nawrot, T. et al. (2006). Environmental exposure to cadmium and risk of cancer: a prospective population-based study. Lancet Oncol., (7), 119.

Nazarian, N. et al. (2018). Impacts of Realistic Urban Heating. Part II: Air Quality and City Breathability. Boundary-Layer Meteorology, 168 (2), 321–341. Available from https://doi.org/10.1007/s10546-018-0346-6.

Neft, I., M. Scungio, N. Culver, and S. Singh. 2016. Simulations of aerosol filtration by vegetation: Validation of existing models with available lab data and application to near-roadway scenario. Aerosol Science and Technology 50: 937–946.

Ng, E.& C. (2012). Urban human thermal comfort in hot and humid Hong Kong. Energy and Buildings, 55, 51–65.

"Ng, E., Yuan, C., Chen, L., Ren, C., & Fung, J.C.H. (2011). Improving the wind environment in high-density cities by understanding urban morphology and surface roughness: a study in Hong Kong. Landscape and Urban Planning, 1 (101), 59–74.

Ng, E. (2012). Towards planning and practical understanding of the need for meteorological and climatic information in the design of high-density cities: A case-based study of Hong Kong. International Journal of Climatology, 32 (4), 582–598.

Ng, E.& C. (2012). Urban human thermal comfort in hot and humid Hong Kong. Energy and Buildings, 55 51–65."

Ng, W.-Y., and C.-K. Chau. 2012. Evaluating the role of vegetation on the ventilation performance in isolated deep street canyons. International Journal of Environment and Pollution 50: S98– S110.

NHS London Healthy Urban Development Unit (2015). Healthy urban planning(2), 29. Available from www.healthyurbandevelopment.nhs.uk.

Nowack, P. et al. (2020). Towards low-cost and high-performance air pollution measurements using machine learning calibration techniques. Atmospheric Measurement Techniques Discussions, (December), 1–30.

Nowak, D.J., S. Hirabayashi, A. Bodine, and R. Hoehna. 2013. Modeled PM2.5 removal by trees in ten US cities and associated health effects. Environmental Pollution 178: 395–402.

Oke, T., Mills, G., Christen, A., & Voogt, J. (2017). Urban Climates. Cambridge: Cambridge University Press. doi:10.1017/9781139016476

Oke, T.. (1978). Boundary Layer Climates. Methuen & Co., New York, New York.,339–390.

Oke, T.R. (1977). The Energy Balance of an Urban Canyon. Applied Meteorology, 1 (16), 11–19.

Oke, T.R. (1981). Canyon geometry and the nocturnal heat island. Comparison of scale model and field observations. Climatology,237–254.

Oke, T.R. (1988). Street design and urban canopy layer climate. Energy and Buildings, 11 (1–3), 103–113.

Oke, T.R. (2004). Initial guidance to obtain representative meteorological observations at urban sites. World Meteorological Organization,(81), 51. Available from http://www.geog.ubc.ca/~toke/IOM-81-UrbanMetObs.pdf.

Oke, T.R. (2010). A holistic approach to energy efficient building forms. Energy and Buildings, 42 (9), 1437–1444.

Oke, T.R. et al. (2017). Urban Climates.

Ordnance Digimap Survey Collection. (2019). Euston Road. Available from https://digimap.edina.ac.uk/.

Ottosen, T.B. and Kumar, P. (2020). The influence of the vegetation cycle on the mitigation of air pollution by a deciduous roadside hedge. Sustainable Cities and Society, 53 (September 2019), 101919. Available from https://doi.org/10.1016/j.scs.2019.101919.

Owen, B. et al. (2000). Prediction of total oxides of nitrogen and nitrogen dioxide concentrations in a large urban area using a new generation urban scale dispersion model with integral chemistry model. Atmospheric Environment, 34 (3), 397–406. Available from https://doi.org/10.1016/S1352-2310(99)00332-5.

Oxford City Council. (2021). OxAir Air Quality Sensor Pilot. (April).

Pacyna, J.M. (2008). Atmospheric Deposition. Encyclopedia of Ecology, Five-Volume Set, 275–285. Available from https://doi.org/10.1016/B978-008045405-4.00258-5.

Whitehand, J.W.R. and Larkham, P.J. (1992). Urban landscapes: international perspectives. World Health Organization (WHO) (2014). Air quality deteriorating in many of the world's cities. Available fromhttp://www.who.int/mediacentre/news/releases/2014/air-quality/en/ [Accessed 24 November 2017].

Park, S.J. et al. (2020). Flow Characteristics Around Step-Up Street Canyons with Various Building Aspect Ratios. Boundary-Layer Meteorology, 174 (3), 411–431. Available from https://doi.org/10.1007/s10546-019-00494-9.

Pope, C.A. et al. (2020). Fine particulate air pollution and human mortality: 25+ years of cohort studies. Environmental Research, 183 (August 2019), 108924. Available from https://doi.org/10.1016/j.envres.2019.108924.

Pope, C.A., Ezzati, M. and Dockery, D.W. (2009). Fine-Particulate Air Pollution and Life Expectancy in the United States. New England Journal of Medicine, 360 (4), 376–386. Available from https://doi.org/10.1056/nejmsa0805646.

Pöschl, U. (2005). Atmospheric aerosols: Composition, transformation, climate and health effects. Angewandte Chemie - International Edition, 44 (46), 7520–7540.

Public Health England. (2022). Guidance Air pollution: applying All Our Health. Available from https://www.gov.uk/government/publications/air-pollution-applying-all-our-health/air-pollution-applying-all-our-health#:~:text=In the UK%2C air pollution,and 36%2C000 deaths every year.

Rådberg, J. (1996). Towards a Theory of Sustainability and Urban Quality A New Method for Typological Urban Classification.

Raithel, J. 2008. Quantitative Forschung, 2., durchges. Aufl. Wiesbaden: Verl. Für Sozialwiss. 213 s.

Randall D.A., 2006. Reynolds Averaging. http://kiwi.atmos.colostate.edu/group/dave/pdf/Reynolds_Averaging.pdf

Rapoport Amos, (1990), Vernacular Aechitecture, in Turan M., (eds); Current Challenges in the Environmental Social Sciences, Avebury, Aldershot, England.

Rasmussen, S.E. (1982). London, the unique cityRev. ed. Cambridge Massachusetts: M.I.T. Press. Available from https://www.worldcat.org/title/london-the-unique-city/oclc/638542003&referer=brief_results#.Wh7D8QVU3KQ.mendeley [Accessed 29 November 2017].

Ratnaike, R.N., 2003. Acute and chronic arsenic toxicity. Postgrad. Med. J. 79, 391.

Razak, A.A.; Hagishima, A.; Ikegaya, N.; Tanimoto, J. (2013). Analysis of airflow over building arrays for assessment of urban wind environment. Build. Environ, 59 56–65.

Reiminger, N. et al. (2020). CFD evaluation of mean pollutant concentration variations in step-down street canyons. Journal of Wind Engineering and Industrial Aerodynamics, 196 (June 2019). Available from https://doi.org/10.1016/j.jweia.2019.104032.

Ren, C., Ng, E. Y. Y., & Katzschner, L. (2011). Urban climatic map studies: A review. International Journal of Climatology, 31 (15), 2213–2233.

Ren, C., Spit, T., Lenzholzer, S., Yim, H. L. S., Heusinkveld, B., van Hove, B., ... Katzschner, L. (2012). Urban climate map system for Dutch spatial planning. International Journal of Climatology,.

Riediker, M., Cascio, W.E., Griggs, T.R., Herbst, M.C., Bromberg, P.A., Neas, L., Williams, R.W., Devlin, R.B., 2004. Particulate matter exposure in cars is associated with cardiovascular effects in healthy young men, Am. J. Respir. Crit. Care Med. 169, 934.

Rode, P. et al. (2014). Cities and Energy: Urban Morphology and Residential Heat-Energy Demand. Environment and Planning B: Planning and Design, 41 (1), 138–162. Available from https://doi.org/10.1068/b39065.

Rui, L. et al. (2019). Study of the effect of green quantity and structure on thermal comfort and air quality in an urban-like residential district by ENVI-met modelling. Building Simulation, 12 (2), 183–194. Available from https://doi.org/10.1007/s12273-018-0498-9.

Saathoff, P., Stathopoulos, T., Wu, H., 1998. The influence of freestream turbulence on nearfield dilution of exhaust from building vents. Journal of Wind Engineering and Industrial Aerodynamics 77–78, 741–752.

Saathoff, P.J., Stathopoulos, T., Dobrescu, M., 1995. Effects of model scale in estimating pollutant dispersion near buildings. Journal of Wind Engineering and Industrial Aerodynamics 54–55, 549–559.

Salata, F. et al. (2015). How high albedo and traditional buildings ' materials and vegetation affect the quality of urban microclimate . A case study. Energy & Buildings, 99, 32–49. Available from https://doi.org/10.1016/j.enbuild.2015.04.010.

Salizzoni, P., Soulhac, L., Mejean, P. & Perkins, R. J. 2008. Influence of a Two-scale Surface Roughness on a Neutral Turbulent Boundary Layer. Boundary-Layer Meteorology, 127, 97-110.

"Santamouris, M. (2000). Environmental Planning in Urban Areas. Generalisation based on least squared adjustments. Proceedings of International Archives of Photogrammetry and Remote Sensing,931–938.

Santamouris, M. (2001). Energy and climate in the urban built environment. London, James and James.,."

Santiago, J.L. et al. (2019). CFD modelling of vegetation barrier effects on the reduction of traffic-related pollutant concentration in an avenue of Pamplona, Spain. Sustainable Cities and Society, 48 (February), 101559. Available from https://doi.org/10.1016/j.scs.2019.101559.

Schatzmann, M., Leitl, B., 2011. Issues with validation of urban flow and dispersion CFD models. J. Wind Eng. Indus. Aerodynamics 99 (4), 169e186.

Schatzmann, M., Rafailidias, S., Britter, R. & Arend, M. (Editors): 1997: Database, monitoring and modelling of urban air pollution. Inventory of models and data sets. EC COST 615 Action. 109p.

Schell, L.M. et al. (2006). Effects of pollution on human growth and development: an introduction. J. Physiol. Anthropol., (25), 103.

Schellnhuber, H. J., M. Molina, N. Stern, V. Huber and S. Kadner (eds.) (2010) Global Sustainability - A Nobel CauseCambridge University Press, Cambridge, United Kingdom and New York, USA pp. 392 ISBN-13: 9780521769341

Shahriyari, H.A. et al. (2022). Air pollution and human health risks: mechanisms and clinical manifestations of cardiovascular and respiratory diseases. Toxin Reviews, 41 (2), 606–617. Available from https://doi.org/10.1080/15569543.2021.1887261.

Shannon, T.R., Kleniewski, N. and Cross, W.M. (2002). Urban problems in sociological perspective, 4th ed. Prospect Heights Ill.: Waveland Press. Available from https://www.worldcat.org/title/urban-problems-in-sociological-perspective/oclc/49522580&referer=brief_results#.Wia62yNk9XM.mendeley [Accessed 5 December 2017].

Sharag-Eldin, A. (2019). Impact of neighborhood morphology on air pollution dispersion patterns due to unplanned building demolition : a parametric STUDY Thesis Advisor : Dr . Adil Sharag-Eldin. (May).

Sharma, N., Chaudhry, K.K. and Chalapati Rao, C. V. (2004). Vehicular pollution prediction modelling: A review of highway dispersion models. Transport Reviews, 24 (4), 409–435. Available from https://doi.org/10.1080/0144164042000196071.

Sharmin, T. and Steemers, K. (2017). Understanding ENVI-met (V4) model behaviour in relation to environmental variables Understanding ENVI - met (V4) model behaviour in relation to environmental variables Behaviour and Building Performance Centre , The Martin Centre for Architectural and. (July).

Sini, J.F., Anquetin, S. & Mestayer, P.G. (1996). Pollutant dispersion and thermal effects in urban street canyons. Atmospheric Environment, 30(15), 2659-2677.

Smil, V. (1999). How many billions to go? Spagnolo, J. and de Dear, R. (2003). A field study of thermal comfort in outdoor and semi-outdoor environments in subtropical Sydney Australia. Building and Environment, 38 (5), 721–738.

Spagnolo, J. and de Dear, R. (2003). A field study of thermal comfort in outdoor and semi-outdoor environments in subtropical Sydney Australia. Building and Environment, 38 (5), 721–738. Available from https://doi.org/10.1016/S0360-1323(02)00209-3.

Sportisse, B. (2001). Box models versus Eulerian models in air pollution modeling. Atmospheric Environment, 35 (1), 173–178. Available from https://doi.org/10.1016/S1352-2310(00)00265-X.

Stathopoulos, T., Lazure, L., Saathoff, P., Gupta, A., 2004. The effect of stack height, stack location and roof-top structures on air intake contamination—a laboratory and full-scale study. IRSST report R-392, Montreal, Canada, 2004.

Stathopoulos, T., Lazure, L., Saathoff, P., Wei, X., 2002. Dilution of exhaust from a rooftop stack on a cubical building in an urban environment. Atmospheric Environment 36, 4577–4591.

Steadman, P. et al. (2000). A classification of built forms. Environment and Planning B: Planning and Design, 27 (1), 73–91.

Steeneveld, G. J., Koopmans, S., Heusinkveld, B. G., & Theeuwes, N.E. (2014). Refreshing the role of open water surfaces on mitigating the maximum urban heat island effect. Landscape and Urban, 121 92–96.

Steeneveld, G. J., Koopmans, S., Heusinkveld, B. G., & Theeuwes, N.E. (2014). Refreshing the role of open water surfaces on mitigating the maximum urban heat island effect. Landscape and Urban, 121 92–96.

Sutton O.G. (1932) A theory of Eddy Diffusion in the Atmosphere. Proc. Roy. Soc. A, 135:143.

Syafei, A.D., Fujiwara, A. and Zhang, J. (2015). Prediction Model of Air Pollutant Levels Using Linear Model with Component Analysis. International Journal of Environmental Science and Development, 6 (7), 519–525. Available from https://doi.org/10.7763/ijesd.2015.v6.648.

Tal, A. (2013). Overpopulation is still the Problem. TheHuffingtonPost.com, Inc.

Taleghani, M., Kleerekoper, L., Tenpierik, M., Van den Dobbelsteen, A., 2014. Out- door thermal comfort within five different urban forms in the Netherlands. Build. Environ. 83, 65–78. http://dx.doi.org/10.1016/j.buildenv.2014.03.014.

Tan, Z. et al. (2019). Impact of source shape on pollutant dispersion in a street canyon in different thermal stabilities. Atmospheric Pollution Research, 10 (6), 1985–1993. Available from https://doi.org/10.1016/j.apr.2019.09.005.

The Air Quality Expert Group. (2018). Ultrafine Particles (UFP) in the UK. Department for Environment, Food and Rural Affairs. Available from http://uk-air.defra.gov.uk.

The Tree Council. (2012). Tree Planting Guide. (December), 1–45. Available from https://treecouncil.org.uk/wp-content/uploads/2019/12/Tree-planting-guide.pdf.

Theurer W (1999) Typical building arrangements for urban air pollution modelling. Atmos Environ 33(24–25):4057–4066. doi:10.1016/ S1352-2310(99)00147-8

Timmers, V.R.J.H. and Achten, P.A.J., 2016. Non-exhaust PM emissions from electric vehicles. Atmospheric envir- onment. doi:10.1016/j.atmosenv.2016.03.017

Toparlar, Y. et al. (2017). A review on the CFD analysis of urban microclimate. Renewable and Sustainable Energy Reviews, 80 (May), 1613–1640. Available from https://doi.org/10.1016/j.rser.2017.05.248.

Trache, H. (2001). Promoting urban design in development plans : typo-morphological approaches in Montreuil , France. 157–172.

Tsiaras, A. (2018). unseen human body. Available from https://www.alexandertsiaras.com/.

Tsoka, S., Tsikaloudaki, K. and Theodosiou, T. (2017). Urban space's morphology and microclimatic analysis: A study for a typical urban district in the Mediterranean city of Thessaloniki, Greece. Energy and Buildings, 156, 96–108. Available from https://doi.org/10.1016/j.enbuild.2017.09.066.

Tsoka, S., Tsikaloudaki, K. and Theodosiou, T. (2017). Urban space's morphology and microclimatic analysis: A study for a typical urban district in the Mediterranean city of Thessaloniki, Greece. Energy and Buildings, 156, 96–108. Available from https://doi.org/10.1016/j.enbuild.2017.09.066.

Tsuang, B.J. (2003). Quantification on the source/receptor relationship of primary pollutants and secondary aerosols by a Gaussian plume trajectory model: Part I - Theory. Atmospheric Environment, 37 (28), 3981–3991. Available from https://doi.org/10.1016/S1352-2310(03)00471-0.

Tumini, I. (2015). The urban microclimate in open space. Case studies in Madrid. Cuadernos de Investigación Urbanística, (96). Available from https://doi.org/10.20868/ciur.2014.96.3022.

U.S. Environmental Protection Agency. (2015). Size comparisons for PM particles. Available from https://www.epa.gov/pm-pollution/particulate-matter-pm-basics.

Uematsu, Y., Isyumov, N., 1999. Wind pressures acting on low-rise buildings. Journal of Wind Engineering and Industrial Aerody- namics 82 (1), 1–25.

UNDESA Population Division. (2015). Population 2030: Demographic challenges and opportunities for sustainable development planning. United Nations, 58. Available from http://www.un.org/en/development/desa/population/publications/pdf/trends/Population2030.pdf%0Ahttp://www.un.org/en/development/desa/population/publications/pdf/trends/Population2030.pdf, date accessed 27th August, 2017.

United Nations. World Urbanization Prospects: The 2014 Revision, Highlights (ST/ESA/SER.A/352). New York (2014).

Uysal, N., Schapira, R.M., 2003. Effects of ozone on lung function and lung diseases. Curr. Opin. Pulm. Med. 9, 144.

Vachon, G., Louka, P., Rosant, J., Mestayer, P., and Sini, J.: Measurements of traffic-induced turbulence within a street canyon during the Nantes' 99 experi- ment, Water, Air and Soil Pollution: Focus, 2, 127–140, 2002.

Vallero, D.A. (2019). Chapter 14 - Air pollution dispersion models. In: Vallero, D.A.B.T.-A.P.C. (ed.). Elsevier, 429–448. Available from https://doi.org/https://doi.org/10.1016/B978-0-12-814934-8.00014-4.

Vallero, D.A. (2021). Chapter 10 - Environmental systems science models. In: Vallero, D.A.B.T.-E.S.S. (ed.). Elsevier, 463–507. Available from https://doi.org/https://doi.org/10.1016/B978-0-12-821953-9.00017-9.

Van Nes, A., Berghauser Pont, M., & & Mashhoodi, B. (2012). combination of space syntax with spacematrix and the mixed use index . The Rotterdam South test case. 8th International Space Syntax Symposium, Santiago de Chile, Jan. 3-6, 2012}.

Vardoulakis, S., Fisher, B.E.A., Pericleousa, K. & Gonzalez-Flesca, N. (2003). Modelling air quality in street canyons: a review, Atmospheric Environment 37: 155-182.

Vaughan, A. (2021). Rise of the electric cars. New Scientist, 249 (3317), 23. Available from https://doi.org/https://doi.org/10.1016/S0262-4079(21)00058-0.

Ventura, A. (2017). London Borough of Camden Air Quality Annual Status Report for 2017 Date of publication : 31 / 05 / 18. 2016 (16), 1–45.

Vigevani, I. et al. (2022). Particulate Pollution Capture by Seventeen Woody Species Growing in Parks or along Roads in Two European Cities. Sustainability (Switzerland), 14 (3), 1–20. Available from https://doi.org/10.3390/su14031113.

Vijay, P. et al. (2021). Performance Evaluation of UK ADMS-Urban Model and AERMOD Model to Predict the PM10 Concentration for Different Scenarios at Urban Roads in Chennai, India and Newcastle City, UK BT - Urban Air Quality Monitoring, Modelling and Human Exposure Assessment. In: Shiva Nagendra, S.M. Schlink, U. Müller, A. et al. (eds.). Singapore: Springer Singapore, 169–181. Available from https://doi.org/10.1007/978-981-15-5511-4_12.

Vincent, D. (2019). Airborne particulate matter and their health effects. Encyclopedia of the Environment. Available from https://www.encyclopedie-environnement.org/en/health/airborne-particulate-health-effects/.

Visser, G.T., Cleijne, J.W., 1994. Wind comfort predictions by wind tunnel tests: comparison with full-scale data. Journal of Wind Engineering and Industrial Aerodynamics 52, 385–402.

Voordeckers, D. et al. (2021). Guidelines for passive control of traffic-related air pollution in street canyons: An overview for urban planning. Landscape and Urban Planning, 207 (June 2020), 103980. Available from https://doi.org/10.1016/j.landurbplan.2020.103980.

Vos, P.E.J. et al. (2013). Improving local air quality in cities: To tree or not to tree? Environmental Pollution, 183, 113–122. Available from https://doi.org/10.1016/j.envpol.2012.10.021.

Wang, S. et al. (2020). Strategizing the relation between urbanization and air pollution: Empirical evidence from global countries. Journal of Cleaner Production, 243, 118615. Available from https://doi.org/10.1016/j.jclepro.2019.118615

Wania, A. et al. (2012). Analysing the influence of different street vegetation on traffic-induced particle dispersion using microscale simulations. Journal of Environmental Management, 94 (1), 91–101. Available from https://doi.org/10.1016/j.jenvman.2011.06.036.

weather spark. (2022). Climate and Average Weather Year Round in City of London United Kingdom. Available from https://weatherspark.com/y/45061/Average-Weather-in-City-of-London-United-Kingdom-Year-Round#Figures-Temperature.

Wen, H. (2017). The Effect of Urban Geometries and Roof Shapes on Airflow and Pollutant Dispersion : A CFD Investigation.

Whitehand, J.W.R. (1977) 'The basis for an historico-geographical theory of urban form', Transactions of the Institute British Geographers NS 2, 400-16.

Wieringa, J. (1993) 'Representative roughness parameters for homogeneous terrain', Boundary-Layer Meteorology, vol 63, no 4, pp323–363

Williams, M. and Barrowcliffe, R. (2011). Review of air quality modelling in Defra a report by the Air Quality Modelling Review Steering Group. (April). Available from https://uk-air.defra.gov.uk/assets/documents/reports/cat20/1106290858_DefraModellingReviewFinal Report.pdf.

Williams, R. et al. (2014). EPA Sensor Evaluation Report. US Environmental Protection Agency, (May), 40. Available from http://www.epa.gov/research/airscience/docs/sensor-evaluation-report.pdf%5Cnhttp://cfpub.epa.gov/si/si_public_record_report.cfm?dirEntryId=277270.

World Health Organization (2016). Ambient Air Pollution: A global assessment of exposure and burden of disease. World Health Organization,1–131. Available from www.who.int.org.

World Health Organization (2017). World Health Statistics 2017 : Monitoring Health for The SDGsWorld Health Organization.

World Health Organization (WHO) (2008). Our cities , our health , our future. Organization,1–199. Available from http://www.who.int/social_determinants/resources/knus_final_report_052008.pdf.

World Health Organization (WHO) (2014). Air quality deteriorating in many of the world's cities. Available from http://www.who.int/mediacentre/news/releases/2014/air-quality/en/ [Accessed 24 November 2017].

World Health Organization. (2018). World Health Organization: 9 our of 10 people worldwide breathe polluted air, but more countries are taking action. First WHO Global Conference on Air Pollution and Health Ginebra, 39 (6), 641–643. Available from https://www.who.int/news/item/02-05-2018

World Meteorological Organization. (2008). Guide to Meteorological Instruments and Methods of Observation.

Worsley, W. (2018). Urban tree manual. 33.

Xiaomin, X., Zhen, H. & Jiasong, W. (2006). The impact of urban street layout on local atmospheric environment. Building and Environment, 41(10), 1352-1363.

Xie, X., Liu, C.H. and Leung, D.Y.C. (2007). Impact of building facades and ground heating on wind flow and pollutant transport in street canyons. Atmospheric Environment, 41 (39), 9030–9049. Available from https://doi.org/10.1016/j.atmosenv.2007.08.027.

Xing, Y. and Brimblecombe, P. (2019). Role of vegetation in deposition and dispersion of air pollution in urban parks. Atmospheric Environment, 201 (August 2018), 73–83. Available from https://doi.org/10.1016/j.atmosenv.2018.12.027.

Xing, Y. et al. (2019). Tree distribution , morphology and modelled air pollution in urban parks of Hong Kong. Journal of Environmental Management, 248 (July), 109304. Available from https://doi.org/10.1016/j.jenvman.2019.109304.

Yamartino, R. J. & Wiegand, G. 1986. Development and evaluation of simple models for the flow, turbulence and pollutant concentration fields within an urban street canyon. Atmospheric Environment (1967), 20, 2137-2156.

Yang, F.; Lau, S.S.Y.; Qian, F. (2010). Summertime heat island intensities in three high-rise housing quarters in inner-city Shanghai China: Building layout, density and greenery. Build. Environ, 45 115–134.

Yoshie, R., Mochida, A., Tominaga, Y., Kataoka, H., Harimoto, K., Nozu, T., Shirasawa, T., 2007. Cooperative project for CFD prediction of pedestrian wind environment in the Architectural Institute of Japan. Journal of Wind Engineering and Industrial Aerodynamics 95 (9-11), 1551–1578.

Young, A. et al. (2010). Manual for Streets 2. Available from https://tsrgd.co.uk/pdf/mfs/mfs2.pdf.

Zhai, H. et al. (2022). Study of the Effect of Vegetation on Reducing Atmospheric Pollution Particles. Remote Sensing, 1–23. Available from https://doi.org/https://doi.org/10.3390/rs14051255 Academic.

Zhong, J. (2016). Modelling air pollution within a street canyon. (September), 255. Available from http://etheses.bham.ac.uk/6491/.

Zhu, X. et al. (2022). Urban Climate The influence of roadside green belts and street canyon aspect ratios on air pollution dispersion and personal exposure. Urban Climate, 44 (January), 101236. Available from https://doi.org/10.1016/j.uclim.2022.101236.

Appendices

Appendix 1
Publication

Title: Improving Hyperlocal Air Quality in Cities Impact of vegetation on pollutants concentration at pedestrian level. Planning Post Carbon Cities.
Published date: September 2020
Conference: 35th PLEA Conference on Passive and Low Energy Architecture. 1-3 September 2020, A Coruña: University of A Coruña, Spain.
Author: Mehrdad Borna
Co-author: Dr Rosa Schiano-Phan
Available from shorturl.at/atwy8

PLEA 2020
A CORUÑA

35th PLEA Conference on Passive and Low Energy Architecture

Planning Post Carbon Cities

Editors:
Jorge Rodríguez Álvarez
&
Joana Carla Soares Gonçalves

PLEA
Sustainable Architecture and Urban Design

UNIVERSIDADE DA CORUÑA

SC

SUSTAINABLE COMMUNITIES

Improving Hyperlocal Air Quality in Cities

Impact of vegetation on pollutants concentration at pedestrian level

MEHRDAD BORNA[1], ROSA SCHIANO-PHAN[1]

[1]School of Architecture and Cities, University of Westminster, London, United Kingdom

ABSTRACT: *Recent estimates published by WHO report that in 2016 outdoor air pollution caused 4.2 million premature deaths worldwide and urged urban planners, policymakers, and environmentalist to make health and wellbeing their number one priority when designing cities. In view of this, the current paper explores the effectiveness of trees and vegetation in dispersing air pollutants at pedestrian level by administering detailed fieldwork and spot measurement of both pollutants and microclimatic parameters close to one of the most polluted roads in London (Euston Road); followed by modelling a variety of real-life scenarios by using computational simulation application for validation and prediction. Whilst many studies agree in general on the mitigation of urban air pollutants by vegetation, the result of the current study contradicts this common understanding and demonstrates drastic increases in the concentration of particulate matters in the vicinity of trees. The results highlight that trees reduce wind velocity and air movement, causing pollutants to trap inside urban canyons. Therefore, planting more trees does not necessarily mean less pollution, at least locally. Instead, to alleviate air quality problems, more attention should be given to vegetation configuration, type, scale and most importantly, their locations and distributions within active urban pockets.*

KEYWORDS: *Air pollution, Vegetation, Urban form, ENVI-met, Particulate matters*

1. INTRODUCTION

The recent Lancet report (2018) highlighted air pollution as the major cause of cardiovascular and respiratory illnesses and premature death in the world today. For instance, in 2015 pollutants such as Nitrogen Dioxide (NO_2) and Particulate Matter (PM_{10}, $PM_{2.5}$) have caused 64,000 premature deaths in the UK, out of which, 9000 belongs to a developed city like London. The health impacts of outdoor and indoor air pollution are well researched and established by a substantial body of research worldwide. In contrast, relatively little research has investigated the role that the built environment can potentially have on the concentration and dispersion of air pollutants [1].

Whilst the best way to tackle air pollution is to reduce and stop the pollutants at their sources, which must always be the primary focus of air quality policies, a secondary method, and one which has been increasingly perceived as effectively removing pollutants and improving urban life, is urban greenery [2]. There is a large body of studies referring to trees and their air purifying power and the fact that planting more trees is a cost-effective way to tackle urban air pollution [3]. In view of this assumption, the current paper explores the effectiveness of trees and vegetation in dispersing air pollutants at pedestrian level by administering detailed fieldwork and spot measurement of both pollutants and

microclimatic parameters; followed by modelling a variety of real-life scenarios by using computational simulation software for validation and prediction.

2. METHODOLOGY

As an empirical basis for this investigation, this paper intentionally conducted its research far from the roadside and within an open courtyard (plaza) which was identified as a high-quality active pocket [4] which encourages the users to stay for longer periods of time, therefore increasing the risk of being exposed to pollutants. Accordingly, the Regent's Place pedestrian plaza which is located adjacent to one of the most polluted roads in London (Euston Road), was chosen as the fieldwork site for this paper. The fieldwork was conducted during a time when the Square was expected to be much busier than other times. In that respect, the on-site spot measurements were only carried out on the locations with the highest activities and a greater number of people density.

The Regent's Place characterised by street canyon configuration with an aspect ratio (height over width) of 1.81 and Sky View Factor of 0.35 and the built-up areas are 15 times greater than the green spaces (including trees, hedges, green roofs). Based on previous studies done by other researchers, the high aspect ratio and low SVF have a direct impact on the microclimate of a

particular urban location (at a hyperlocal scale) [5]; specifically, on wind speed and its direction and accordingly influence the rate of dilution and dispersion of pollutants. Based on a scheme (Local Climate Zone) developed by Stewart and Oke in 2012, the study site classified as 'compact high-rise' where tall buildings are tightly packed beside each other with little green spaces and a few trees between them.

Figure 1: The Regent's Place Plaza.
■ *Locations where the measurements were taken*
■ *Location of trees; description provided in table 02*
····· *Section A-A illustrated in figure 05*

In terms of population density and activities, close to 12,000 visitors, workers, and residents passing through the plaza each day. Despite its mixed-use, the square is mainly being used by office workers throughout the weekdays and getting populated during lunchtime (11:30 am – 3:00 pm). With its high quality and stylish sitting areas which have mainly sited under the trees, more people are attracted to stay, sit, eat, meet, enjoy, and interact with each other. The square also enjoys access to a number of restaurants, and during the summer/warmer season the restaurants offer more tables and chairs for people to have their meals in the outside open air. There is also an annual events programme, involving summer events during lunchtimes, charity events, farmers markets and other social events. For that reason, this study conducted during the lunchtime (11:00 am – 3:00 pm) and over the summer period (August 2018) where the square was expected to be much busier than other times. In that respect, the site divided into two characteristics and the on-site spot measurements were carried out on, first, locations with the highest activities and a greater number of people density, i.e. location b, c, and d, fig. 1. Second, locations which were seen to offer a better understanding of how air pollutants enter the site or disperse from the site, i.e. location a, e, f and g.

The concentration of particulate matter has increasingly become more significant inside the urban canyons where the urban form and urban features (i.e. solid and porous barriers) are intensifying the concentration of pollutants and increasing health problems [6]. For that reason, apart from Nitrogen Dioxide (NO_2) which is a major concern for Euston road; this study has considered to measure and evaluate two further key urban pollutants; these are particulate matter with a diameter of 10 microns (PM_{10}) and particulate matter with a diameter of 2.5 microns ($PM_{2.5}$).

2.1 Micro-meteorological observation and monitoring of street-level air pollutant concentration

In this study, two portable real-time monitoring devices have been used: Aeroqual Series 200, which is a Portable Air Quality Monitor and Vane Anemometer and Thermo hygrometer, Testo 410-2. Air pollutants and micro-meteorological parameters measured for the period of 30 minutes at each point with readings taken every 5 minutes and average values have been logged-in for further use in the computational analysis at modelling stage (Table 01).

location	Sunny Day		Meteorological conditions on 3rd August 2018 - Fri								Street-level air pollutant concentration					
	Time (hrs:mins)		Air Temperature (°C)		Relative Humidity (%)		Wind Velocity (m/s)		Wind Direction (m/s)		NO_2 (µg/m³)		PM_{10} (µg/m³)		$PM_{2.5}$ (µg/m³)	
			P*	S**	P	S	P	S	P	S	P	S	P	S	P	S
	11:00 – 11:30		29	27	56	54	2.2	2	SSW	SSW	119	94.6	34	23	14	14
	11:35 – 12:05		28	27	60	54	1.4	2	SSW	SSW	76	94.6	22	23	6	14
	12:10 – 12:40		25	28	63	51	0.4	2	-	SSW	51	137.3	47	21.3	29	18.1
	12:45 – 13:15		24	28	60	51	1.2	2	W	SSW	43	137.3	19	21.3	18	18.1
	13:20 – 13:50		24	29	67	43	1.0	2	S	SSW	52	94.9	31	24.6	20	19.3
	13:55 – 14:25		26	29	58	43	2.8	3	WSW	SW	57	94.9	26	24.6	9	19.3
	14:30 – 15:00		27	30	57	38	1.5	3	-	SW	101	72.5	30	30.4	16	16.3

*Table 01. Meteorological and air pollution data for 3rd August 2018. *P = Primary data, **S = Secondary data related to mereological conditions extracted from www.metoffice.gov.uk and air pollution data obtained from londonair.org.uk 'Westminster - Marylebone Road – kerbside' monitoring station operated by King's College London.*

Both air quality and microclimatic parameters have been compared and ratified against live official data from www.metoffice.gov.uk and the nearest fixed meteorological and air quality monitoring station to the study site. In this case, 'Westminster - Marylebone Road – kerbside' monitoring station *operated by King's College London* has been chosen, which sits within a kilometre distance from the study site. The equipment sets are placed with a reference height of 1.5 meter above ground level. The study also captured data in several days and weather conditions, i.e. sunny, rainy, and relatively windy day. However, in this paper, only data and results pertaining to the 3rd August are used for

illustration. On this particular day, the wind direction was the same as London prevailing wind direction, making this day a good representation of typical London wind behaviour for most of the year.

2.2 Computer simulations for validation and prediction

Parallel to the spot measurements and data collection, the complex microclimate phenomena and a range of issues, including air pollution dispersal/concentration, air movement in and around buildings, pedestrian level wind environment and the impacts of non-morphological features on air movement, i.e. vegetation, bus stops and cantilevered shading structures, which project at least one meter beyond the side of a building have been modelled and simulated on ENVI-met version 4.4.3. In order to correlate the relationship between vegetation and pollutants concentration, in addition to modelling the current scenario, a no-green scenario has also modelled and simulated for the plaza.

ENVI-met, which is a 3D CFD (Computational Fluid Dynamics) application, has been selected as air pollution dispersion simulation tool due to its proven reliable outcomes that were examined by previous researchers [7,8,9]. This Eulerian, time- dependant dispersion model uses RANS equation as its turbulence modelling and is capable of computing a large number of air plume particles as they emit from their original source [10]. Moreover, it uses the Finite Difference Method (FDM) to solve the multitude of partial differential equations in the model, which allows ENVI-met to use relatively large time steps but still remaining numerically stable. Moreover, with its fine resolution between half a meter to 10 meters and a typical time frame of 24-48 hours and a time step of 1-5 seconds, the model is able to simulate complicated scenarios and display the interactions between solid and porous barriers at various levels and resolutions in a very graphical format. The graphical representation of various scenarios created and produced by the LEONARDO tool included in ENVI-met package. As it was mentioned, the field spot measurement only conducted for 4 hours (11:00 am – 3:00 pm), therefore, in order to cover the total simulation time the data inserted in ENVI-met collected from 'Westminster - Marylebone Road – kerbside' monitoring station. The result of the ENVI-met simulation were thereafter compared with the field spot measurement values and further analysis and validation is provided in Result & Discussion section of this paper.

Data related to roads, buildings, vegetation, and surfaces material recorded and gathered through conventional field measurement, satellite-based measurement and official GIS documents/maps (Ordnance Survey which is the UK governmental mapping agency). Collected data from official GIS checked and verified against conventional field measurement data, and in some cases, aerial perspective published by Bing Maps and Google Maps used to minimise possible errors. Information related to vegetation characteristics such as species name, height, crown shape/size, clear stem height, and Leaf Area Density (LAD), leaf persistence and surface cover have been described in Table 02.

Vegetation Location	Vegetation Scientific name	Vegetation Common name	Vegetation Height (meter)	LAD (High/Low – Dense/Sparse)	Hairiness 0(Smooth) – 10 (silky)	Stickiness 0(Leathery) – 10 (highly viscid)	Evergreen /Deciduous	Trunk Size	Crown shape/Size	Clear Stem height (meter)
					Leaf Surface					
1	Buxus	Box Hedging	1	High	0	1	Evergreen	N/A	Hedge	0
2	Hedera helix	English Ivy	0.3	High	0	1	Evergreen	N/A	N/A	0
3	Platanus × acerifolia	London Plane	10	Low	5	3	Deciduous	Medium	Broadly Oval (Heart-Shaped)	2.5
4	Platanus × acerifolia	London Plane	10	Low	5	3	Deciduous	Medium	Broadly Oval (Heart-Shaped)	2.5
5	Prunus	Cherry Tree	4	Low	3	2	Deciduous	Small	Irregular (Heart-Shaped)	2
6	Tilia	Lime Tree	8	High	4	6	Deciduous	Medium	Broadly Round (Spherical)	2.5
7	Tilia	Lime Tree	8	High	4	6	Deciduous	Medium	Broadly Round (Spherical)	2.5
8	Platanus × acerifolia	London Plane	4	Low	5	3	Deciduous	Small	Irregular (Heart-Shaped)	2
9	Platanus × acerifolia	London Plane	10	Low	5	3	Deciduous	Medium	Broadly Oval (Heart-Shaped)	2
10	Quercus cerris	Turkey Oak	15	Low	2	2	Deciduous	Medium	Broadly Oval (Heart-Shaped)	4
11	Buxus	Box Hedging	2	High	2	1	Evergreen	N/A	Hedge	0

Table 02. Description of the study site's vegetation characteristic. Locations shown on fig. 01 in yellow numbered label

It is worth mentioning that the ENVI-met models are not working reliably at their model borders and the grids very close to them. For that reason, the nesting area of all simulation scenarios chosen sufficiently large to increase the accuracy and numerical stability of the simulation result [11]. Based on the guideline prescribed by previous researchers [12] five nesting grid cells were empirically set on each side of the model and accordingly the z-grid set to 3 times higher than the tallest building in the model site [13]. In order to accelerate the computational (rendering) time of the simulation, it was decided to lower the resolution to 4 for all axis (dx, dy and dz). Other setting and configuration considerations have been summarised in Table 03.

Modelling area file (.inx) settings		Simulation file (.sim) settings	
Model Location		**Start and duration of model run**	
Localisation	Central London	Start Date (DD.MM.YYYY)	03.07.2018
Latitude (deg,+N,–S)	51.49	Start time (HH:MM)	05:00
Longitude (deg,–W,+E)	-0.31	Total simulation time (h)	16
Model Geometry		**Initial meteorological conditions**	
Grid dimension (x, y, z)	75 x 75 x 60	Wind speed at 10m height (m/s)	2.5
Grid cells size (dx; dy; dz)	4m; 4m; 4m	Wind direction (deg)	225
Model rotation out of grid north	-19.00	Air Temperature (°C)	17 (min.) – 32 (max.)
		Relative Humidity in 2m (%)	38 (min.) – 94 (max.)
Nesting Grids	5	**Pollution Dispersion**	
Number of nesting grids		Operation mode	Multi Pollutant
		Chemistry (NO-O3-NO2)	Dispersion & Action Chemistry

Table 03. Study site input file in ENVI-met 4.4.3.

3. RESULTS & DISCUSSION

The first item revealed from the fieldwork spot measurement was that, 3rd August which was a sunny day recorded as the most polluted day in comparison to 9th (rainy day) and 24th August (windy day). This is more distinct when we look at the PM$_{10}$ and PM$_{2.5}$ levels and less noticeable in the case of NO$_2$ levels. Interestingly, the result of 9th August which was the rainy day scenario recorded PM$_{10}$ and PM$_{2.5}$ at even lower level than a windy day, but still, NO$_2$ was relatively high, and this has been identified as a reoccurring pattern for all other study days. In order to investigate this results further, the results of fieldwork spot measurements for the three study days of 3rd, 9th and 24th August 2018 were compared against the ENVI-met simulation of the same dates and times to firstly validate ENVI-met simulations and secondly to evaluate the effects of trees on the concentration of mentioned pollutants at the monitoring site (Regent's Place) (in this paper only data and results pertaining to the 3rd August are used for illustration). As Table 04 shows, there is a slight difference between the simulation values and measured data. The level and value of the various meteorological parameters and air pollutants simulated by ENVI-met are consistently lower than what has been measured on-site.

Sunny Day		Meteorological conditions on 3rd August 2018 - Fri								Street-level air pollutant concentration					
Location	Time (hrs:mins)	Air Temperature (°C)		Relative Humidity (%)		Wind Velocity (m/s)		Wind Direction (m/s)		NO$_2$ (µg/m³)		PM$_{10}$ (µg/m³)		PM$_{2.5}$ (µg/m³)	
		FM*	EM**	FM	EM	FM	EM	FM	EM	FM	EM	FM	EM	FM	EM
	11:00 – 11:30	29	27	56	54	2.2	1	SSW	SSW	119	90	34	15	14	9
	11:35 – 12:05	28	27	60	54	1.4	0.5	SSW	SSW	76	90	22	10	6	6
	12:10 – 12:40	25	25	63	57	0.4	0.5	-	NNW	51	30	47	10	29	6
	12:45 – 13:15	24	25	60	58	1.2	1	W	WSW	43	30	19	5	18	3
	13:20 – 13:50	24	25	67	59	1.0	1	S	SSW	52	30	31	5	20	3
	13:55 – 14:25	26	25	58	55	2.8	2.5	WSW	SW	57	30	26	5	9	3
	14:30 – 15:00	27	25	57	59	1.5	2	-	SSE	101	60	30	10	16	6

*Table 04. Comparison between data gathered during fieldwork measurement and data extracted from ENVI-met simulation result. *FM = Field measurements **EM= ENVI-met simulation.*

This ratio changes depending on the given meteorological conditions on the given days; however, in general, the pollution values in ENVI-met are always lower in value than the fieldwork spot measurement data. For example, the NO$_2$ and PMs concentration are respectively 1.4 and 3.2 times higher in recorded fieldwork spot measurements. In the case of meteorological parameters in most cases, the values are closely similar. These differences were expected as the background concentration data (for pollutants) and meteorological data which have been added in ENVI-met were extracted from the meteorological station which was located about a kilometre away from the study site ('Westminster - Marylebone Road – kerbside'), moreover, there were various simplification and assumption had to be made while modelling the site in ENVI-met. However, the most interesting aspect of this comparison which is also the main interest of this research is that the measured data and simulation data conclusively and broadly correspond to each other and more precisely confirmed and aligned over the pollution concentration zones.

In order to analyse the simulation results in more detail and understand the impact of trees on air pollution concentration, it was decided to compare the microclimate parameters both in the current urban configuration and in a scenario where there are no trees or vegetation. In this paper, the simulations with a greater significance have been presented in the next pages. For that reason, the data selected for illustration is also related to the busiest (activity and population wise) time of the plaza, which was 1 pm (lunchtime).

(a)   (b)   (c)
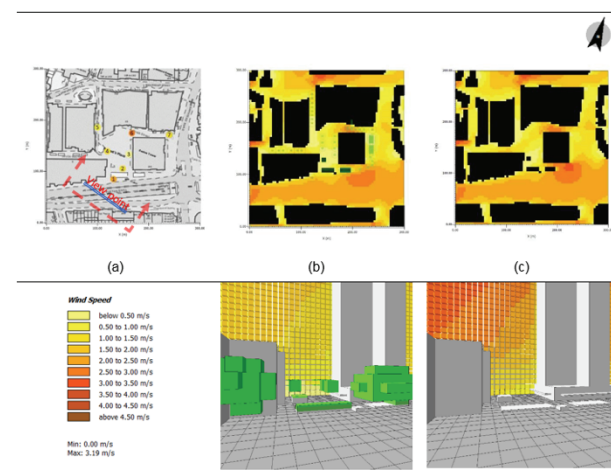
Figure 02. Snapshot of wind velocity and direction map at pedestrian level (1.5 m height from ground) for August 3rd, 2018, 13:00 h. (a) fieldwork spot measurements (b) ENVI-met simulation of current scenario (c) ENVI-met simulation of no-green scenario.

The simulation outcomes are quite revealing in several ways. First, the relative humidity is much lower in the no-green scenario, and this supports previous findings which have shown a decrease in relative humidity in no-green scenarios. Meanwhile, in the case of air temperature, the changes are not noticeable, and we do not see a great temperature difference between the two scenarios. This can be related to the low leaf area index of the trees and their clean stem height. This has been highlighted in Table 02. The wind aspect is the most interesting finding. Based on the result of the fieldwork and ENVI-met simulation, it is clear that trees in high and low density urban areas affect the wind velocity and its behaviour. As illustrated in Fig. 03 wind

velocity and vegetation have inverse correlation meaning that the wind velocity decreases with an increase in vegetation volume especially in the case of trees with high leaf area density (LAD). This drop of velocity has a direct impact on a higher concentration of pollutants, and in the case of Regent's Place, the high level of pollutants concentration can be found around the sets of trees which are located on the east and west side of the plaza (fig. 01 - location c and d). This scenario is exacerbated during the London prevailing wind direction of SSW and those trees planted in north and northeast of the square (fig. 01 – location e and f) slow down air velocity further and avoid pollutants to disperse from the plaza, therefore, led to a higher concentration of pollutants under the group of trees located in the east and west side of the plaza. Specifically, $PM_{2.5}$ is 120% greater around the group of trees in location (c) and PM_{10} values are even higher and stand at 175%. It has been noted that there is not much difference in NO_2 concentration values and the two scenarios (current and no-green) are almost the same but still around trees we can observe that the values are slightly higher than no-green scenario. It is worth mentioning that, the impact of trees on wind flow greatly depend on the vegetation shape and species, as well as the density of the urban context, i.e. planting high LAD heart-shape or spherical crown shape trees with low clear stem height and little space from each other, could slow down air velocity at pedestrian level (the urban canopy layer) and increase the concentration of pollutants. Previous research done by Edward NG [14] and several other studies [5,15,16] on designing for urban ventilation and urban thermal comfort, has established that a high-density urban area induces a weak wind flow and the current study shows that planting more trees will only exacerbate this already-slow wind speed reducing it even further.
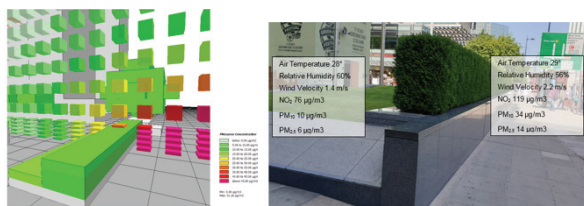
Figure 03. Snapshot of PM_{10} concentration map around hedgerow at the south side of the Regent's Place (left). Fieldwork spot measurements (right). August 3, 2018, 11:00 h.

Further analysis of the result showed that the large hedgerow located at the south side of the site (fig. 01 – location a) is the most effective element in dispersing or blocking (depositing) pollutants. In accord with the result of fieldworks, the ENVI-met simulation with the exception of NO_2, have indicated the same and showed

a substantial improvement in air quality in location (b) (immediately after the hedgerow) (Fig 04). Previous studies conducted by a number of researchers [16,17] are in support of the above findings. In addition to that, in 2018 similar experiment conducted by King's College London has found levels of NO_2 reduced by 23% when an ivy screen wall was installed and placed between school playground and a busy road [18]. For that reason, it has been decided to take this strategy a step further and pilot scenarios where hedgerows which have proven to be even more effective than ivy screen [19] can be employed as a barrier and stop the PMs from congregation under the group of trees at Location (c).
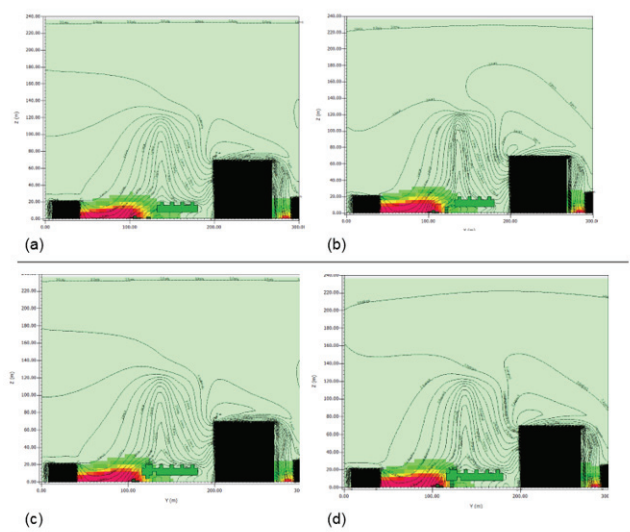
Figure 04. Section a-a illustrating PM_{10} concentration map at pedestrian level with (a) adding a 2-meter height hedgerow; (b) adding a 4-meter height hedgerow; (c) adding an 8 meter Tilia tree (lime tree); (d) adding a 2-meter height hedgerow and an eight-meter lime tree, immediately after the existing hedgerow on the south side of the site.

The first scenario (a) was to add a parallel hedgerow immediately after the 'near wake' of the existing hedgerow (fig 04 - a). the result shows a pronounced reduction in pollution level (PM_{10}) and has limited the distance which air pollution can travel (downwind). Furthermore, it has been noticed that the inlet airflow partly blocked by the two rows of hedges and partly separated upward and generated skimming flow. In the second attempt and in order to avoid the formation of skimming flow, the 2-meter hedgerow increased to 4-meter height. However, the simulation outcome showed that 4 meter height porous barrier is not enough to influence the flow turbulence as minimal reduction in terms of pollution level has been observed. In the third attempt, a 4 meter hedgerow has been replaced with an eight meter Tilia tree (lime tree, similar species as to the group of trees at East side of the site) to offer protection

over a larger distance downwind. The result showed a further reduction in the distance which air pollution can travel but not much difference in terms of air pollution concentration at pedestrian level. For that reason and as a final mitigation strategy, both hedgerow and tall trees put back in their suggested places to provide the maximum protection in terms of distance, downwind and pollution concentration at the pedestrian level (Fig 04 d).

4. CONCLUSION

Whilst many studies agree in general on the mitigation of urban air pollutants by vegetation through their deposition and dispersion properties, the result of the current research contradicts this common understanding and demonstrates drastic increases in the concentration of particulate matters in the vicinity of trees. The results highlight that trees reduce wind velocity and air movement, causing pollutants to settle around and under trees' canopy. This is more distinct when we look at the PM_{10} and $PM_{2.5}$ levels and less noticeable in the case of NO_2 levels. Therefore, planting more trees does not necessarily mean less pollution, at least locally. Instead, to alleviate air quality problems, more attention should be given to vegetation configuration, type, scale and most importantly, their locations and distributions within the given active urban pocket. The findings from this research provide a fruitful area for further work to determine the exact effectiveness of vegetation in urban spaces throughout the year (summer and winter scenarios). Further investigation and modelling in different urban form with diverse vegetation type and spatial quality are required to be conducted to establish a better understanding of this matter. Needless to say that, we need more effective tree planting policy which takes the above challenges into account, and urban planners need to consider the impact of urban trees and green spaces on air quality at hyperlocal scale.

REFERENCES

1. Hankey, S. and Marshall, J.D. (2017). Urban Form, Air Pollution, and Health. Environmental health reports, 4 (4): p. 491–503.
2. Berardi, U., G. Hoseini. 2013. State-of-the-art analysis of the environmental benefits of green roofs. *Journal of Applied Energy* 115: p. 411–428.
3. Nowak, D. and Heisler, G. (2010). Air Quality Effects of Urban Trees and Parks. *National Recreation and Park* Association, 1 (1), p. 48.
4. Gehl, J. (2011). Life between buildings: using public space. Washington, DC: Island Press, 200.
5. Edussuriya, P., Chan, A. and Malvin, A. (2014). Urban morphology and air quality in dense residential environments: Correlations between morphological parameters and air pollution at street-level. Journal of Engineering Science and Technology, 9 (1), p. 64–80.
6. WHO (2018), Ambiant (outdoor) Air Pollution, available from https://www.who.int/news-room [June 2019]
7. Jin, H. et al. (2017). The effects of residential area building layout on outdoor wind environment at the pedestrian level in severe cold regions of China. Sustainability (Switzerland), 9 (12), p. 1–18.
8. Vos, P.E.J. et al. (2013). Improving local air quality in cities: To tree or not to tree? Environmental Pollution, 183. Elsevier Ltd113–122.
9. Tsoka, S., Tsikaloudaki, K. and Theodosiou, T. (2017). Urban space's morphology and microclimatic analysis: A study for a typical urban district in the Mediterranean city of Thessaloniki, Greece. Energy and Buildings, 156. Elsevier B.V.96–108.
10. Bruse, M. (2004). ENVI-met 3.0: Updated Model Overview (March), p. 1–12.
11. ENVI-met (2019). Nesting Grids. envi-met.info. available from http://www.envi-met.info/doku.php?id=kb:nesting [June 2019]
12. Conry, P. et al. (2015). Chicago's heat island and climate change: Bridging the scales via dynamical downscaling. Journal of Applied Meteorology and Climatology, 54 (7), 1430–1448.
13. Evyatar, E., David, P. and Terry, W. (2011). Meteorology and Urban Design Erelletal 1950_2010., p. 23–24.
14. Ng, E. et al. (2011). Improving the wind environment in high-density cities by understanding urban morphology and surface roughness: A study in Hong Kong. Landscape and Urban Planning, 101 (1), Elsevier B.V.59–74.
15. Chatzidimitriou, A. and Yannas, S. (2017). Street canyon design and improvement potential for urban open spaces; the influence of canyon aspect ratio and orientation on microclimate and outdoor comfort. Sustainable Cities and Society, 33 (June), Elsevier85–101.
16. Abhijith, K. V. et al. (2017). Air pollution abatement performances of green infrastructure in open road and built-up street canyon environments – A review. Atmospheric Environment, 162, Elsevier Ltd71–86.
17. Hewitt, C.N., Ashworth, K. and MacKenzie, A.R. (2019). Using green infrastructure to improve urban air quality (GI4AQ). Ambio,. Springer Netherlands.
18. Temper, A.H. and Green, D.C. (2018). The impact of a green screen on concentrations of nitrogen dioxide at Bowes Primary School, Enfield Prepared for the London Borough of Enfield (January), 1–19.
19. Chen, L. et al. (2017). Variation in Tree Species Ability to Capture and Retain Airborne Fine Particulate Matter (PM2.5). Scientific Reports, 7 (1), Springer US1–11.

Appendix 2
Publication

Title: A correlational analysis of COVID-19 incidence and mortality and urban determinants of vitamin D status across the London boroughs
Published date: July 2022
Journal: Scientific Reports
Author: Mehrdad Borna
Co-author: Dr Maria Woloshynowych, Dr Rosa Schiano-Phan, Dr Emanuela V. Volpi & Dr Moonisah Usman
Available from https://doi.org/10.1038/s41598-022-15664-y.

scientific reports

OPEN

A correlational analysis of COVID-19 incidence and mortality and urban determinants of vitamin D status across the London boroughs

Mehrdad Borna[1✉], Maria Woloshynowych[2], Rosa Schiano-Phan[1], Emanuela V. Volpi[3] & Moonisah Usman[4]

One of the biggest challenges of the COVID-19 pandemic is the heterogeneity in disease severity exhibited amongst patients. Among multiple factors, latest studies suggest vitamin D deficiency and pre-existing health conditions to be major contributors to death from COVID-19. It is known that certain urban form attributes can impact sun exposure and vitamin D synthesis. Also, long-term exposure to air pollution can play an independent role in vitamin D deficiency. We conducted a correlational analysis of urban form and air quality in relation to the demographics and COVID-19 incidence and mortality across 32 London boroughs between March 2020 and January 2021. We found total population, number of residents of Asian ethnicity, 4-year average PM_{10} levels and road length to be positively correlated with COVID-19 cases and deaths. We also found percentage of households with access to total open space to be negatively correlated with COVID-19 deaths. Our findings link COVID-19 incidence and mortality across London with environmental variables linked to vitamin D status. Our study is entirely based on publicly available data and provides a reference framework for further research as more data are gathered and the syndemic dimension of COVID-19 becomes increasingly relevant in connection to health inequalities within large urban areas.

The SARS-Cov-2 virus has caused a worldwide pandemic that has been spreading at an alarming rate. At present, COVID-19 has been linked to approximately 21 million cases and over 172,000 deaths in the United Kingdom[1]. Several risk factors including age, gender, ethnicity, body mass index and pre-existing conditions have been suggested to play a role in contributing to a more severe course of the disease[2]. Reviews of pandemics with a similar magnitude indicate that the physical configuration of the built environment can also play a significant role in supporting human health and subsequently impacting the severity of disease[3–5]. Therefore, a critically important objective is to identify the major modifiable variables that may contribute to poorer COVID-19 health outcomes.

Currently, over half of the world's population lives in urban areas, a proportion that is expected to grow by 2.5 billion by 2050. Urban populations are faced with an array of health threats, including climate change, infectious and non-communicable diseases, ageing populations, and newly evolved airborne diseases[6]. However, our built environment has a long history of evolving and adapting in the aftermath of crises[7–9]. Throughout history, the built environment has played a key role in influencing population health, and urban designers have had a considerable impact on improving or exacerbating a variety of health outcomes through their design choices. For example, the 1918 Spanish flu epidemic, followed by typhoid, polio, and tuberculosis outbreaks had a huge impact on the development of contemporary architecture as we understand it today. As a result of these diseases and in order to combat them, urban designers and planners were urged to eliminate slums and pass waste management and tenement reform legislation[7,10]. Additionally, architectural design witnessed an age of demand for more simple, modern and precise geometry and materials in order to establish a cleaner, physically and symbolically, urban environment. These included an increase in the size of windows to allow for greater solar

[1]School of Architecture and Cities, University of Westminster, 35 Marylebone Road, London NW1 5LS, UK. [2]School of Social Sciences, University of Westminster, London, UK. [3]School of Life Sciences, University of Westminster, London, UK. [4]Centre for Education and Teaching Innovation, University of Westminster, London, UK. ✉email: m.borna@westminster.ac.uk

gain, open balconies to encourage connection to nature and improved ventilation, flat facades that would not accumulate dust, and white paint to convey the idea of cleanliness[7,11]. Against this backdrop, the current health crisis necessitates the development of our built environment in order to increase the capability of our cities to aid in the prevention of infection and disease spread. Multiple areas of research addressing COVID-19 are required in this setting and in relation to human behaviour.

Human activities have resulted in a widespread increase in a variety of hazardous pollutants, posing a serious threat to human health[12]. Each year, 4.6 million people die as a result of diseases and illnesses caused by poor outdoor air quality, according to the World Health Organization[13]. Numerous studies have established a link between air pollution and health, including infectious and chronic respiratory illnesses, cardiovascular disease, neurocognitive disease, and pregnancy outcomes[13–15]. Long-term exposure to common road transport pollutants like nitrogen dioxide and Particulate Matter (PM) can cause inflammation in the airways and oxidative stress, leading to the development and exacerbation of asthma, diabetes and cardiovascular disease and chronic obstructive pulmonary disease[15,16]. Furthermore, airborne PM has been shown to increase SARS-CoV-2 survival, implying that the risk of infection is increased in highly polluted areas[17]. Although the epidemiology of COVID-19 is still developing, there is substantial evidence linking the pathological characteristics of COVID-19 critical illness and the causes of death in COVID-19 patients with the conditions caused and/or exacerbated by long-term exposure to air pollutants like NO_2 and PMs. The hypothesis of a COVID-19 air pollution link has been supported by a fast-growing body of literature reporting evidence of positive association between outdoor air pollution and COVID-19 morbidity and mortality in different parts of the world[18]. It is reasonable to suggest that since chronic air pollution has a negative impact on the cardiovascular and respiratory systems, and immune function, it increases the risk of mortality, exacerbates COVID-19 infection symptoms and worsens COVID-19 patients' prognosis[19–21]. Given that the majority of air contaminants in the UK, particularly in London, remain far higher than WHO recommendations and the majority of air pollutants are expected to exceed the limits set by European Union and UK directive beyond 2030[22,23], investigating the link between air pollution exposure and COVID-19 mortality and infectivity at borough level in London, in addition to other modifiable factors, should be a priority.

Recent studies indicate that vitamin D deficiency is a modifiable risk factor for COVID-19 infection and mortality, with a strong environmental link. Vitamin D is primarily synthesised in the skin as a result of the conversion of 7-dehydrocholesterol to cholecalciferol (vitamin D3) following exposure to ultraviolet B (UVB) radiation from the sun. An epidemiological association has been identified between vitamin D deficiency and the rate of COVID-19 infection and mortality across several European countries[24]. Associations between viral disease and vitamin D are not new. For long, research has linked vitamin D deficiency with an increased risk of influenza, Human Immunodeficiency Virus, Epstein-Barr virus, and hepatitis B[25]. Additionally, it has been suggested that vitamin D deficiency contributes to the pathogenesis of chronic respiratory diseases such as asthma and chronic obstructive pulmonary disease (COPD)[26–29]. It is well known that vitamin D plays a role in controlling viral replication and resolving hyper-inflammation—a marked feature of the immune response to COVID-19[29]. Several randomised controlled clinical trials support vitamin D supplementation to prevent acute respiratory tract infections and reduce the risk of pneumonia associated death[30]. More recent evidence suggests that vitamin D supplementation may also reduce the risk of COVID-19 infection and death[31]. It is important to explore whether environmental modifications to enhance vitamin D synthesis may also mitigate the risks associated with vitamin D deficiency.

In the UK, it is estimated that a third of the population have hypovitaminosis D, with the deficiency possibly higher in ethnic minorities[32]. The most efficient, cost-free way of acquiring vitamin D is via sensible exposure to sunlight. The Greenspace Index identified that nearly 2.8 million people across the UK do not live within a ten-minute walk of a greenspace[33]. Furthermore, there are also disparities in access to total open space across London neighbourhoods, for instance with respect to private gardens[34]. Other environmental factors that can impact vitamin D levels include air pollution. Increased atmospheric pollution from industrial and vehicular sources may result in UVB photon absorption, thereby decreasing cutaneous vitamin D synthesis[35]. Recently, a cross-sectional analysis of vitamin D levels across nearly 0.5 million adults in the UK revealed increased $PM_{2.5}$, PM_{10}, NO_x, and NO_2 exposure to be associated with a reduction in vitamin D serum concentrations[36]. It is also of relevance that the amount of indoor sunlight exposure may be affected by urban typology; additionally, advances in high-performance window glazing have made them UVB-protective, with glasses that completely block UVB radiation[37].

The aim of our research was to explore the relationship between built environment configuration, air pollution, ethnic composition and COVID-19 incidence and mortality at borough-level in London. For that purpose, we conducted a correlational analysis of urban form attributes, air quality and demographics across 32 London boroughs. Our findings support the hypothesis that differences in air pollution and aspects of the built environment which exacerbate vitamin D deficiency could underlie the increased severity of COVID-19 in certain urban areas.

Methods

A correlation study was conducted to investigate associations between ethnic composition, urban form attributes and levels of air pollution with total COVID-19 deaths and cases across the 32 boroughs of London. All methods were performed in accordance with the relevant guidelines and regulations. Table 1 summarises the publicly available data sources used for this analysis. The variables or data type subcategories analysed in this study are also specified in Table 1.

Data type	Data type subcategory	Source	Download date	Measuring units
COVID-19	COVID-19 Deaths	Public Health England (https://coronavirus.data.gov.uk/details/download)	March 2020 up until January 2021	Cumulative deaths counts per London boroughs
	COVID-19 Cases	Public Health England (https://coronavirus.data.gov.uk/details/download)	March 2020 up until January 2021	Cumulative cases counts per London boroughs
Urban Form & air pollution	Mean percentage of households with access to total open spaces	Greenspace Information for Greater London (GiGL) (http://www.gigl.org.uk/)	Feb 2021	Percentages
	Total road length	Department for Transport (DFT) https://www.gov.uk/government/statistical-data-sets/road-length-statistics-rdl	Feb 2021	Miles
	Air quality data {NO$_2$, PM$_{10}$]	London Air Quality Network (https://www.londonair.org.uk/)	Oct 2020	Air Quality values μgm^{-3}—4 years average (2016–2019)
Demographics	Population data	Office for National Statistics (https://www.ons.gov.uk)	Oct 2020	Numbers (persons by single year of age and sex for local authorities in London, data created mid-2019)
	Ethnic group	Office for National Statistics (https://www.ons.gov.uk) https://data.london.gov.uk/dataset/ethnic-groups-borough	Feb 2021	Population number by Ethnic Group by London borough, data created mid-2019

Table 1. Summary of data sources.

Data sources for demographics. We used the Office for National Statistics (ONS) mid-year population estimate for 2019, which is considered to be the official source of population size in-between censuses, covering the populations of local authorities, counties, regions, and countries in the United Kingdom by age, sex and ethnicity. The ethnicities covered in this study are White, Black, Asian and Mixed/Other, as defined by the ONS[38].

Data sources for COVID-19 deaths and cases. COVID-19 deaths and cases for 32 London boroughs and City of London were sourced from Public Health England (PHE). The cumulative number of deaths and cases in each London borough was collected from the first death on the week ending 6 March 2020 to 29 January 2021 which marked the beginning of the third national lockdown and also the time when free rapid home tests were made available to the public. During this period, the cumulative data recorded was 13,148 deaths and 216,743 laboratory-confirmed cases for London boroughs, including the City of London. It's worth noting that the death counts are based on PHE's definition of COVID-19 related death, which states that any person who died within (equal to or less than) 28 days of receiving a laboratory-confirmed positive COVID-19 test[39]. According to PHE, the number of cases is equivalent to the number of people who have at least one positive COVID-19 test result, whether obtained via PCR or a rapid lateral flow test. Individuals who tested positive more than once are only counted once, on the date of their first positive test.

Data sources for air quality levels. Borough-level air pollution data were sourced from the London Air Quality Network (LAQN) website[40] which is operated by the Environmental Research Group (ERG) of Imperial College London and quality assured (QA) and controlled (QC) by King's College London. We included in our analysis data for Nitrogen Dioxide (NO$_2$), a highly reactive gas mainly formed from the burning of fuel and a significant outdoor air pollutant, and PM$_{10}$, which is an inhalable particulate matter with an aerodynamic diameter of 10 microns. Each air pollutant value is expressed in μgm^{-3} and represents a four year average (2016–2019) of the yearly level in each borough. There have been reports suggesting that the intermittent lockdowns in 2020 and 2021 led to behavioural changes and fluctuations in air pollution levels[41], thus data for these years was omitted. The average over the four years leading to the pandemic in 2020 was used to adjust for historical changes in air pollution levels, as well as to identify a link between COVID-19 incidence and mortality and long-term air pollution exposure. Only ratified and available data for the aforementioned period were collected from 32 London boroughs' air quality monitoring stations. The City of London was omitted due to the lack of demographic data and concerns about the limitation of the number of ratified air pollution data. Similarly, due to a lack of availability of ratified, long-term data from borough level official air quality stations, PM$_{2.5}$ values were not included in our analysis.

Data source for urban form attributes. In our study, two attributes were defined and calculated to represent the urban form. Firstly, we used the mean percentage of households with access to total open space as several studies conducted prior and during the COVID-19 pandemic highlighted the insufficient and unequal access to green spaces and discovered a significant association between urban nature and physical and mental health[42–45]. Data on households with access to total open space were extracted from Greenspace Information for Greater London (GiGL)[46]. Table 8.1 of the London Plan 2021[47] contains a detailed and comprehensive definition of public open space types. The analysis of total open space is based on access to designated green/public open space and for that reason, farmland, private gardens, and other types of green space, which are not included in the London Plan's public open space category definitions, are excluded. Secondly, we used 'total road length' as
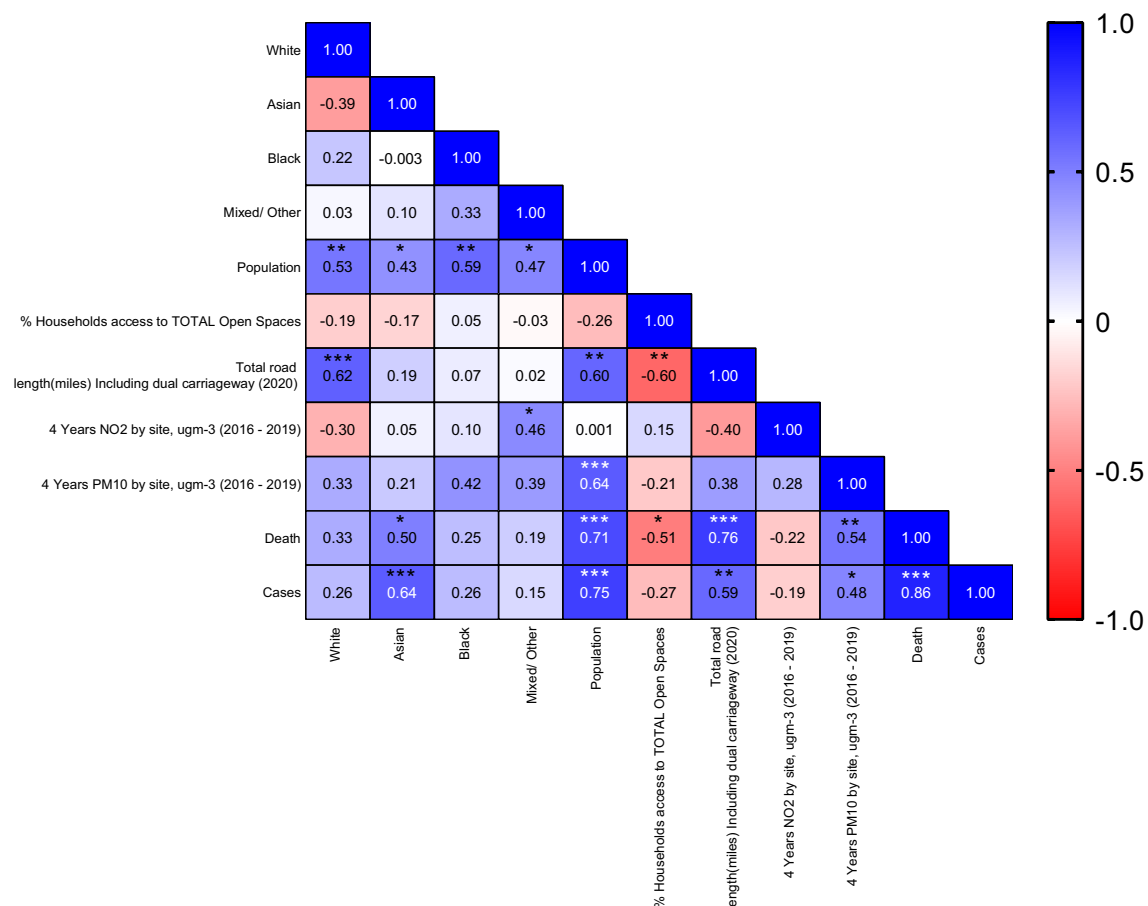
Figure 1. Heatmap displaying Pearson correlation analysis R values and p-values between all variables across 32 London boroughs (p* ≤ 0.0137, ** ≤ 0.001, *** ≤ 0.0001).

a proxy for built density, open space distribution, and their relationship to traffic-related pollution levels[48,49]. Another reason for choosing total road length was that no other researcher had ever used it in conjunction with COVID-19 and exploring this area can help us gain a better understanding of this parameter and its relationship to COVID-19 severity. The total road length data for each borough were obtained from the Department for Transport (DfT), and it includes dual carriageways and is measured in miles.

Data analysis. Pearson correlation analysis was conducted to explore the relationship between two urban form attributes, two air pollutants and two demographic indices (Table 1) and the total number of COVID-19 cases and deaths reported by Public Health England (PHE) across the 32 London boroughs. Microsoft Excel and GraphPad Prism version 9 were used for all statistical analyses, including the creation of graphs and heatmaps. Due to the nature of the study and the assumption of a linear relationship, the Pearson correlation coefficient was chosen to summarise the strength and direction (negative or positive) of relationships between variables. Statistical significance was defined as $p < 0.05$. However, because a large number of hypotheses tests were conducted concurrently, and to reduce the risk of a Type I error we calculated the False Discovery Rate (FDR) using the Benjamin and Hochberg procedure[50].

Ethical approval. This research was granted ethical approval from the University of Westminster Research Ethics Committee (Reference: ETH2021-0440).

Results
Pearson correlation analysis was applied to all variables to investigate possible relationships between borough demographics, air pollution, urban form and COVID-19 deaths and cases across 32 London boroughs (see Fig. 1).

Total population and Asian ethnicity are positively correlated with COVID-19 incidence and mortality. We identified a statistically significant positive correlation between population and COVID-19 cases and deaths ($p \leq 0.0001$) (Fig. 2a. We also identified a significant positive correlation between the number of residents of Asian ethnicity and the number of COVID-19 cases ($p < 0.0001$) and deaths ($p < 0.0137$) (Fig. 2b).
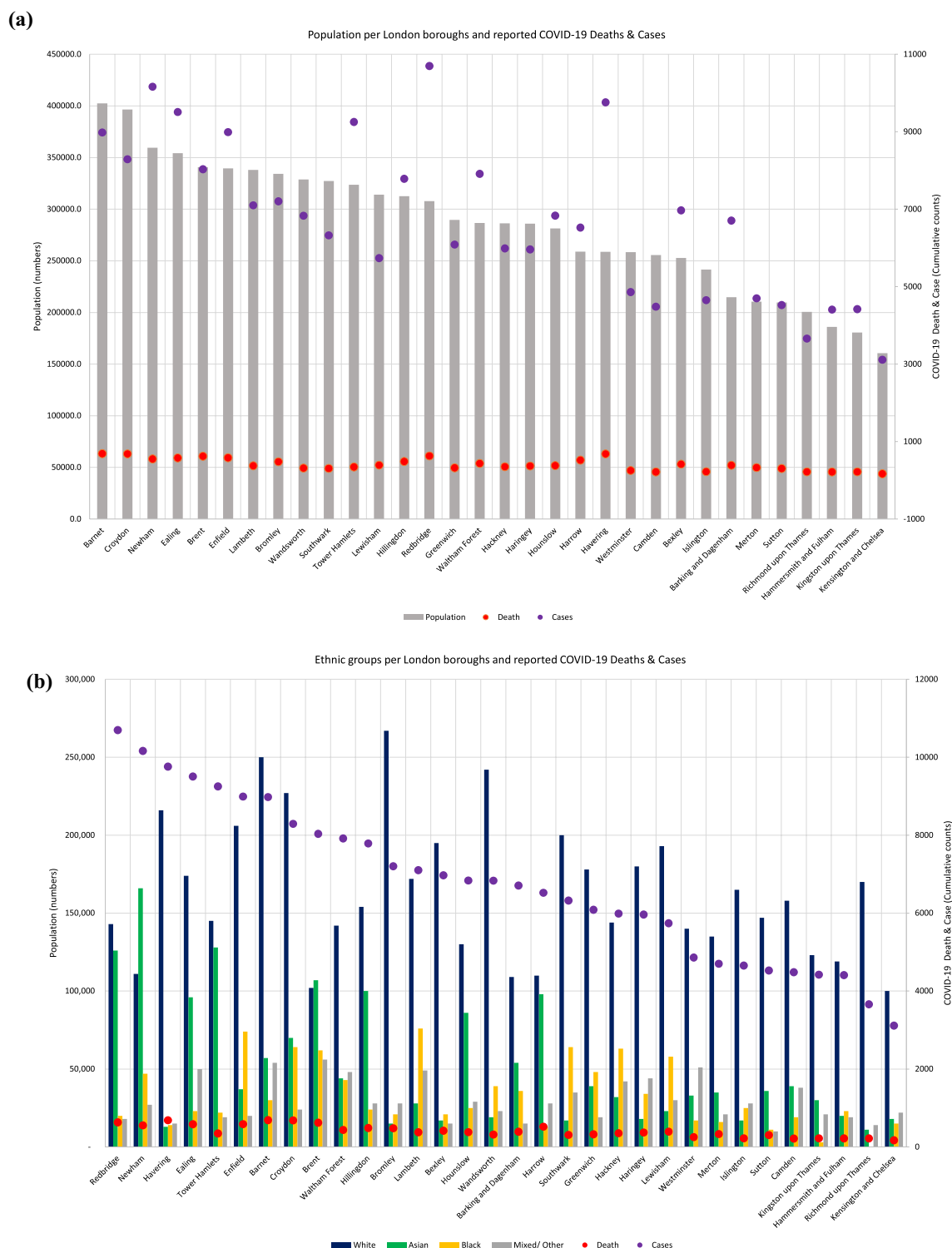
Figure 2. (**a**) Relationship between total population (numbers) and COVID-19 case and death rate in each London borough. (**b**) Relationship between total population (numbers) and ethnicity (numbers) and COVID-19 case and death rate in each London borough.

Levels of PM$_{10}$ are positively correlated with the rate of COVID-19 deaths and cases. We identified a statistically significant positive correlation between 4-year average PM$_{10}$ levels and COVID-19 cases ($p < 0.0137$) and deaths ($p < 0.001$) (Fig. 3a). The London borough of Lambeth had the highest level of average 4-year PM$_{10}$ at 31.8 μgm-3. The borough with the lowest levels of 4-year average PM$_{10}$ was Richmond upon Thames, at 6.0 μgm-3. PM$_{10}$ levels were almost twice as high in Lambeth compared to Richmond upon Thames. We found a similar trend in COVID-19 cases between the London borough of Lambeth (7103) and Richmond

(a)

(b)

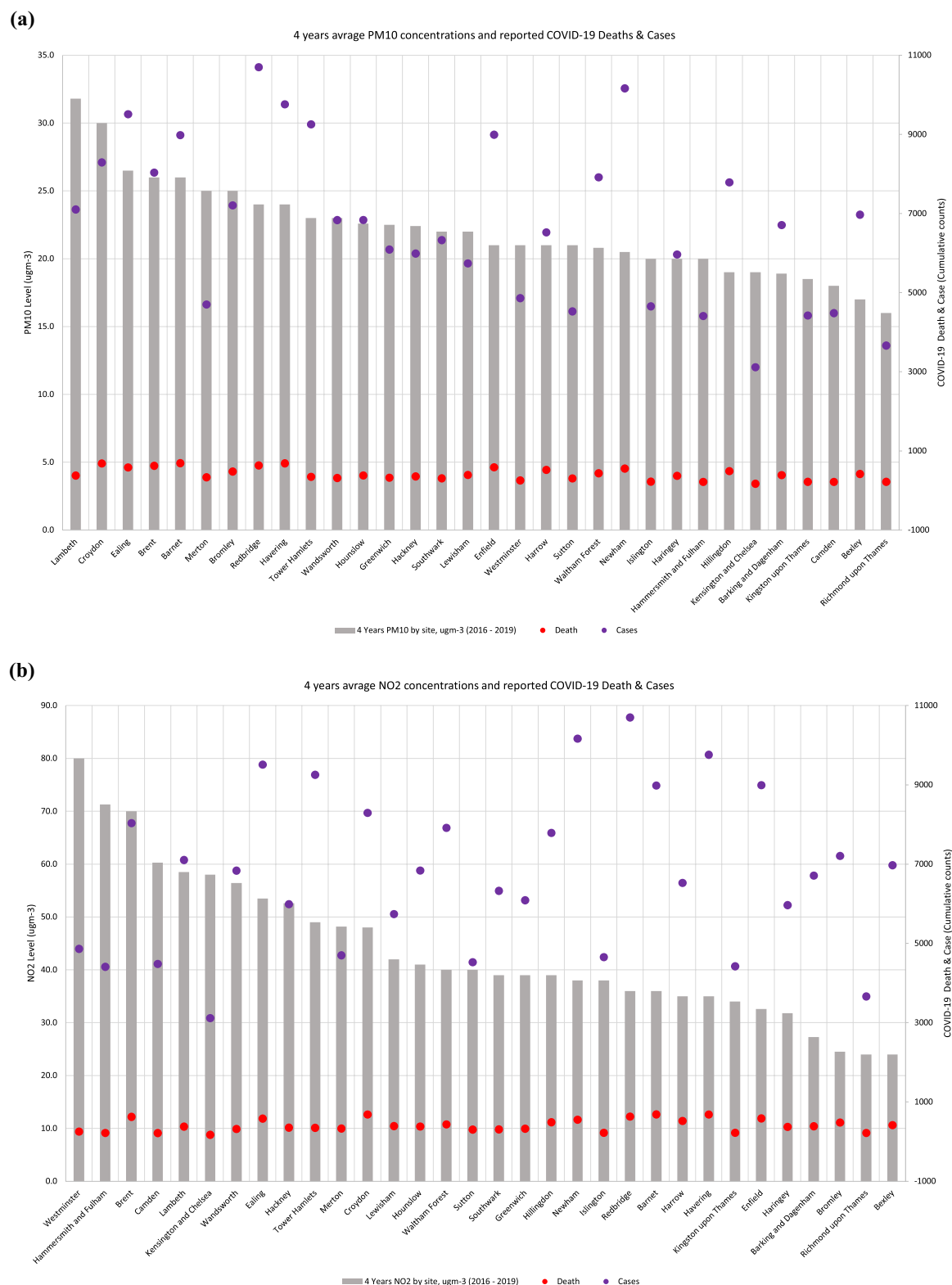**Figure 3.** (**a**) Relationship between PM10 (μgm-3) and COVID-19 case and death rate in each London borough. (**b**) Relationship between NO2 (μgm-3) concentrations and COVID-19 case and death rate in each London borough.

upon Thames (3663). No significant correlations were identified between 4-year average levels of NO_2 and COVID-19 cases and deaths (Fig. 3b).

Urban form attributes are correlated with the rate of COVID-19 deaths. We identified a statistically significant negative correlation between the percentage of households with access to total open space and the rate of COVID-19 deaths ($p < 0.0137$), but not cases (Fig. 4a). The borough with the highest percentage of households with access to total open space was Hackney at 67%. The borough with the lowest percentage of households with access to total open space was Barnet at 26%. We also found that Barnet had 64% more deaths from COVID-19 compared to Hackney.

Furthermore, our analysis revealed a statistically significant positive correlation between total road length (miles) and the rate of COVID-19 deaths ($p < 0.0001$) and cases ($p < 0.001$) (Fig. 4b). The borough with the longest total road length (567.6 miles) was Bromley and the borough with the shortest total road length was Kensington and Chelsea (132 miles). We observed the number of deaths and cases to be 94% higher in Bromley compared to Kensington and Chelsea.

Discussion

We report the first research to explore associations between demographics, urban form attributes and air pollution levels with COVID-19 deaths and cases at borough level across London. Our study shows that total population, number of residents of Asian ethnicity, 4-year average PM_{10} levels and road length are positively correlated with COVID-19 cases and deaths, while percentage of households with access to total open space is negatively correlated with COVID-19 deaths.

Our findings indicate that COVID-19 incidence and mortality are higher in London boroughs with a higher proportion of Asian residents which is consistent with previously published research on COVID-19 risk and outcome disparities[51,52]. In 2020 Public Health England[53] released a report that re-confirmed health inequalities and found that Black and Asian minority ethnic groups have a higher risk of COVID-19 infection and admission to ICU and death than White ethnic group. Asians and other ethnic minorities are more likely than other groups to live in urban areas[54]. This alone increases the risk that they might live in relatively smaller dwellings with limited open space, overcrowded households and public spaces, each of which can increase the risk of contracting an infectious disease[55,56]. However, it is important to note that an analysis of over 10,000 patients with COVID-19 admitted to intensive care units in UK hospitals indicated that when patient characteristics such as age, sex, obesity, and comorbidities were considered, there was no increased risk of mortality or HDU/ICU admissions between ethnic groups[57]. In contrast to the PHE report, we did not find a significant positive correlation between Black minorities and COVID-19 deaths and cases. This discrepancy could be explained on the basis that the PHE report incorporated analysis on the entire UK, whereas our research was focused on the London boroughs. All considered, it is becoming increasingly obvious that the relationship between ethnicity and COVID-19 morbidity and mortality is complex, and it is most likely the result of multiple factors.

Our results also indicate that long-term exposure to higher levels of PM_{10} is associated with increased COVID-19 incidence and mortality. Our findings that across the London boroughs levels of PM_{10}, COVID-19 incidence and mortality correlate with total population suggest that population per borough could be a confounding factor. However, it is important to note that other studies have identified an association between long term exposure to PM_{10} levels and increased incidence of COVID-19, independent to population levels, suggesting that correlations with PM_{10} should not be ignored[58]. During the COVID-19 pandemic, numerous international studies were conducted to assess the impact of air pollution on COVID-19 severity, including in Italy[59,60], Europe[61,62], and the United States[19,63–66]. The majority of these studies found a link between COVID-19 morbidity and mortality and exposure to air pollution. Similarly, in the UK studies have analysed links between air pollution and COVID-19 and found that NO_x and $PM_{2.5}$ levels were a major contributor to COVID-19 cases and mortality[67,68]. Of specific relevance, an ecologic study by Sasidharan and colleagues[69] looked at short-term (one month, March 2020) air pollution levels (NO_2 and $PM_{2.5}$) and increased risk of COVID-19 transmission across 15 boroughs in London and discovered a significant positive correlation between short-term NO_2 exposure and COVID-19 deaths and cases. In contrast, by looking at long-term NO_2 levels we found no significant correlation with COVID-19 incidence or mortality. A particular strength of our study is that we are the first to use a four-year annual average (2016 to 2019) of daily measurements for NO_2 and PM_{10} data collected from air quality monitoring stations across all London boroughs, which increases the reliability of the air pollution data, better represents actual pollution levels within each borough and offers a long-term view of possible health impacts.

Our findings contribute to the growing body of evidence demonstrating the harmful effects of air pollution on human health. Whilst our observational study cannot confirm causative biological links between exposure to air pollutants and increased risk of COVID-19, previous research has highlighted that PM_{10} promotes lung inflammation, and plays a pathological role in the development of lung disorders such as asthma, but also respiratory viruses[70,71]. Furthermore, increased exposure to PM_{10} has also been linked with reduced systemic vitamin D levels[36,72], and vitamin D has been suggested to have a direct role in reducing complications from COVID-19 via several biological mechanisms[73]. Therefore, increased exposure to PM_{10} could contribute in multiple ways to a higher risk of acquiring COVID-19 with more severe outcomes.

Our findings also indicate that urban form attributes can have an effect on COVID-19 incidence and mortality, emphasising the importance of critical reflection on the role of cities and how they are shaped to improve quality of life and protect their inhabitants. While the recent acceleration and densification of urban areas have put a strain on greenspaces and outdoor spaces, new research suggests that urban growth should seriously consider the consequences of a lack of open space and ensure that future development addresses this critical need, as doing so will have numerous short- and long-term health benefits. For example, across all London boroughs, our study discovered a negative correlation between the mean percentage of households with access to total open space and the COVID-19 mortality. These findings corroborate pre-COVID research indicating that exposure to natural environments is associated with improved health and well-being, particularly among urban

(a)

(b)
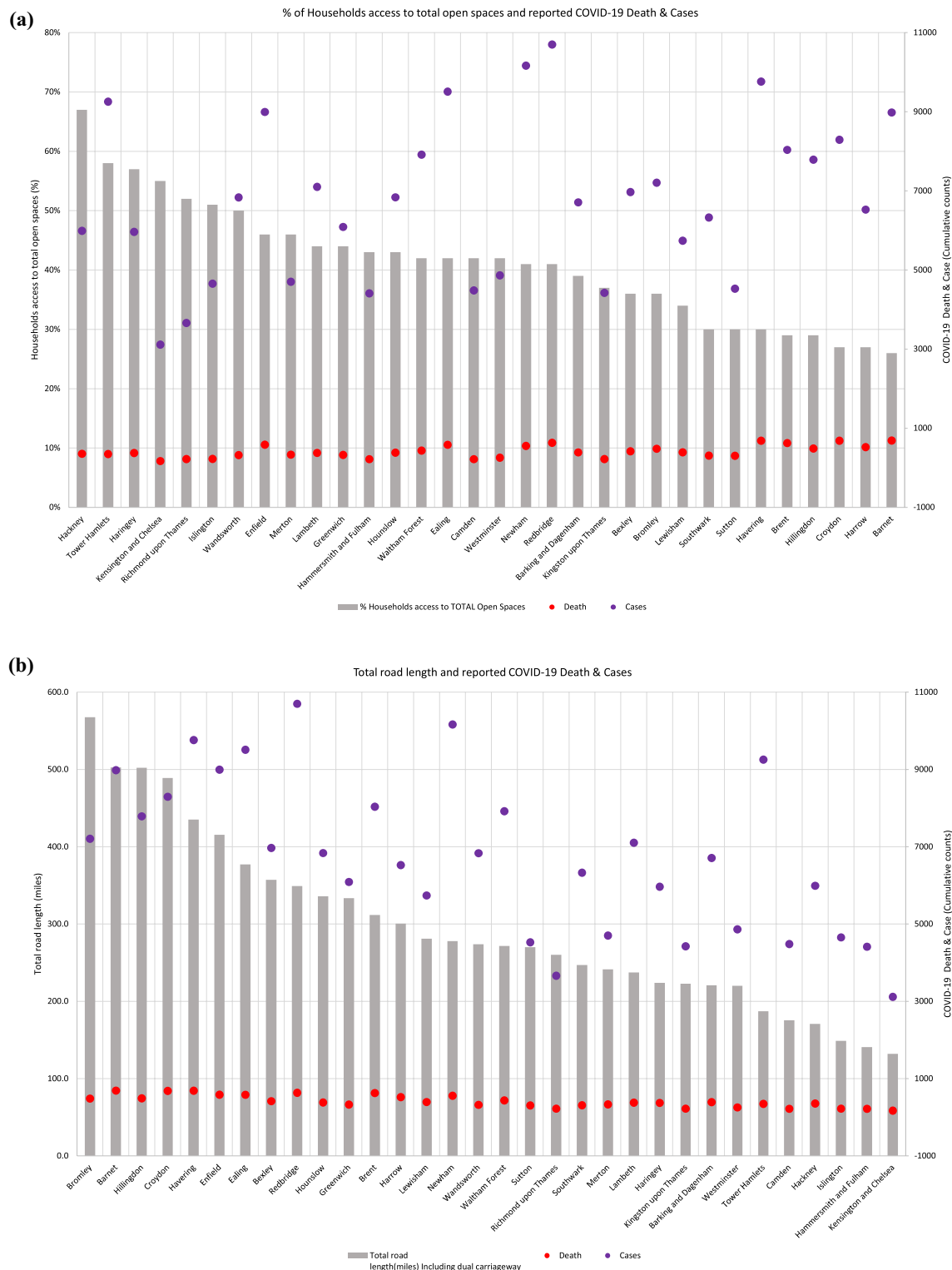
Figure 4. (**a**) Relationship between mean households' access to total open spaces (percentage) and COVID-19 case and death rate in each London borough. (**b**) Relationship between total road length (miles) and COVID-19 case and death rate in each London borough.

populations[74–77]. It has been suggested that when outdoor spaces are insufficient or of poor quality, the majority of gatherings must inevitably take place indoors[78], with significant risks for the spread of COVID-19, given the increased possibility of airborne transmission indoors[79]. Our research is the first to demonstrate an inverse association between access to open space and COVID-19 mortality across the London boroughs. We postulate that

reduced access to outdoor space might impact COVID-19 severity by reducing exposure to ultraviolet radiation (UV) with implications for vitamin D deficiency and other pre-existing morbidities.

Finally, we found a statistically significant positive correlation between total road length (miles) and COVID-19 deaths and cases. In comparison to the twenty outer London boroughs, eight of the twelve inner London boroughs have shorter road lengths and a smaller population, and fewer reported deaths and cases. Similarly, these eight inner boroughs demonstrated greater access to total open space than the rest of the London boroughs. When this aspect is analysed in detail, the inner London boroughs reveal to have a significantly higher percentage of access to public open space and local parks, which may make it easier for residents to visit these spaces because they are within 400 m (walking distance) of their households[46]. The further the distance from central London, the fewer local parks there are, and the distance between public open spaces and greenery is significantly greater, resulting in longer road length which may require vehicle access[80]. Furthermore, the London Underground has substantial infrastructure, with a greater number of stations located close together within inner London boroughs, reducing the need for road transportation.

Conclusion

Our findings support the hypothesis that urban form characteristics and exposure to air pollutants, which can impact vitamin D synthesis, are associated with an increased risk of COVID-19 and subsequent mortality across the London boroughs. Importantly, our study relies on publicly available data to allow for future expansion of these analyses as the pandemic progresses and more data becomes available. Our findings call for further research on the impact of urban form and air quality on vitamin D deficiency as a modifiable risk factor for COVID-19 and other common pathologies to suggest built environment modifications and inform localised public health interventions.

References

1. Public Health England. Coronavirus (COVID-19) in the UK [Internet]. 2021. https://coronavirus.data.gov.uk/.
2. Williamson, E. J. et al. Factors associated with COVID-19-related death using OpenSAFELY. Nature [Internet] 584(7821), 430–436. https://doi.org/10.1038/s41586-020-2521-4 (2020).
3. Tornero-Molina, J., Sánchez-Alonsoc, F., Fernández-Pradaa, M., Bris-Ochaitaa, M.-L. AS-GY JV-F. Urbanisation and infectious diseases in a globalised world. Ann. Oncol. 19–22 (2020).
4. Connolly, C., Keil, R. & Ali, S. H. Extended urbanisation and the spatialities of infectious disease: Demographic change, infrastructure and governance. Urban Stud. 58(2), 245–263 (2021).
5. Neiderud, C. J. How urbanization affects the epidemiology of emerging infectious diseases. Afr. J. Disabil. 5(1), 1–9 (2015).
6. Standards, T., Design, U. & Table, S. World Urbanization Prospects The 2018 Revision [Internet]. https://population.un.org/wup/Publications/Files/WUP2018-Report.pdf.
7. Chang, V. The Post-Pandemic Style [Internet]. https://slate.com/business/2020/04/coronavirus-architecture-1918-flu-cholera-modernism.html.
8. Dejtiar, F. Is Coronavirus Pandemic Accelerating the Digitalization and Automation of Cities? [Internet]. https://www.archdaily.com/936064/is-coronavirus-pandemic-accelerating-the-digitalization-and-automation-of-cities.
9. Muggah, R. & Ermacora, T. Opinion: Redesigning the COVID-19 City [Internet]. https://www.npr.org/2020/04/20/839418905/opinion-redesigning-the-covid-19-city.
10. Lubell, S. Commentary: Past pandemics changed the design of cities. Six ways COVID-19 could do the same [Internet]. https://www.latimes.com/entertainment-arts/story/2020-04-22/coronavirus-pandemics-architecture-urban-design.
11. Budds, D. Design in the age of pandemics [Internet]. https://archive.curbed.com/2020/3/17/21178962/design-pandemics-coronavirus-quarantine.
12. Sharma, S., Zhang, M., Gao, J., Zhang, H. & Harsha, S. Effect of restricted emissions during COVID-19 on air quality in India (2020).
13. Cohen, A. J. et al. Estimates and 25-year trends of the global burden of disease attributable to ambient air pollution: An analysis of data from the Global Burden of Diseases Study 2015. Lancet [Internet]. 389(10082), 1907–18. https://doi.org/10.1016/S0140-6736(17)30505-6 (2017).
14. Wellenius, G. A. et al. Ambient air pollution and the risk of acute ischemic stroke. Arch. Intern. Med. 172(3), 229–34 (2012).
15. Pope, C. A., Ezzati, M. & Dockery, D. W. Fine-particulate air pollution and life expectancy in the United States. N. Engl. J. Med. 360(4), 376–386 (2009).
16. Strak, M. et al. Long-term exposure to particulate matter, NO2 and the oxidative potential of particulates and diabetes prevalence in a large national health survey. Environ. Int. [Internet] 108(2), 228–36. https://doi.org/10.1016/j.envint.2017.08.017 (2017).
17. Setti L. et al. SARS-Cov-2RNA found on particulate matter of Bergamo in Northern Italy: First evidence. Environ Res. 188, 109754. https://doi.org/10.1016/j.envres.2020.109754 (2020).
18. Aloisi V, Gatto A, Accarino G, Donato F, Aloisio G. The effect of known and unknown confounders on the relationship between air pollution and Covid-19 mortality in Italy: A sensitivity analysis of an ecological study based on the E-value. Environ Res. 207, 112131. https://doi.org/10.1016/j.envres.2021.112131 (2022).
19. Brook, R. D. et al. Particulate matter air pollution and cardiovascular disease: An update to the scientific statement from the American heart association. Circulation 121(21), 2331–2378 (2010).
20. Pope, C. A. et al. Cardiovascular mortality and long-term exposure to particulate air pollution: Epidemiological evidence of general pathophysiological pathways of disease. Circulation 109(1), 71–77 (2004).
21. Ciaula, A. D. et al. Nitrogen dioxide pollution increases vulnerability to COVID-19 through altered immune function. Environ. Sci. Pollut. Res. [Internet] https://doi.org/10.1007/s11356-022-19025-0 (2022).
22. Goverment U. Clean Air Strategy 2019: Executive summary [Internet] (2019). https://www.gov.uk/government/publications/clean-air-strategy-2019/clean-air-strategy-2019-executive-summary.
23. Font, A., Guiseppin, L., Blangiardo, M., Ghersi, V. & Fuller, G. W. A tale of two cities: Is air pollution improving in Paris and London?. Environ. Pollut. 249(10), 1–12 (2019).
24. Ilie, P. C., Stefanescu, S. & Smith, L. The role of vitamin D in the prevention of coronavirus disease 2019 infection and mortality. Aging Clin. Exp. Res. [Internet] 32(7), 1195–8. https://doi.org/10.1007/s40520-020-01570-8 (2020).
25. Beard, J. A., Bearden, A. & Striker, R. Vitamin D and the anti-viral state. J. Clin. Virol. 50(3), 194–200 (2011).

26. Litonjua, A. A. & Weiss, S. T. Is vitamin D deficiency to blame for the asthma epidemic?. *J. Allergy Clin. Immunol.* **120**(5), 1031–1035 (2007).
27. Litonjua, A. A. Childhood asthma may be a consequence of vitamin D deficiency. *Curr. Opin. Allergy Clin. Immunol.* **9**(3), 202–207 (2009).
28. Janssens, W. *et al.* Vitamin d beyond bones in chronic obstructive pulmonary disease: Time to act. *Am. J. Respir. Crit. Care Med.* **179**(8), 630–636 (2009).
29. Janssens, W. *et al.* Vitamin D deficiency is highly prevalent in COPD and correlates with variants in the vitamin D-binding gene. *Thorax* **65**(3), 215–220 (2010).
30. Martineau AR. *et al.* Vitamin D supplementation to prevent acute respiratory tract infections: systematic review and meta-analysis of individual participant data. *BMJ.* **356**, i6583. https://doi.org/10.1136/bmj.i6583 (2017).
31. Grant, W. B. *et al.* Evidence that vitamin d supplementation could reduce risk of influenza and covid-19 infections and deaths. *Nutrients* **12**(4), 1–19 (2020).
32. Crowe, F. L. *et al.* Trends in the incidence of testing for Vitamin D deficiency in primary care in the UK: A retrospective analysis of the Health Improvement Network (THIN), 2005–2015. *BMJ Open* **9**(6), 1–8 (2019).
33. Fields in Trust [Internet]. [cited 2021 Sep 7]. https://www.fieldsintrust.org/green-space-index.
34. Public Health England. *Improving Access to Greenspace: A New Review for 2020 About Public Health England* 1–112 (2020).
35. Mousavi, S. E., Amini, H., Heydarpour, P., Amini Chermahini, F. & Godderis, L. Air pollution, environmental chemicals, and smoking may trigger vitamin D deficiency: Evidence and potential mechanisms. *Environ. Int. [Internet].* **2019**(122), 67–90. https://doi.org/10.1016/j.envint.2018.11.052 (2018).
36. Yang, C., Li, D., Tian, Y. & Wang, P. Ambient air pollutions are associated with vitamin D status. **2** (2021).
37. Duarte, I., Rotter, A., Malvestiti, A. & Silva, M. The role of glass as a barrier against the transmission of ultraviolet radiation: An experimental study. *Photodermatol. Photoimmunol. Photomed.* **25**(4), 181–184 (2009).
38. Office for National Statistics. Popuation by Ethnic Group by borough [Internet]. ONS Annual Population Survey. [cited 2021 Sep 7]. https://data.london.gov.uk/dataset/ethnic-groups-borough.
39. Cases by specimen date [Internet]. Public Health England. 2020 [cited 2021 Sep 7]. https://coronavirus.data.gov.uk/details/cases.
40. London Air [Internet]. Imperial College London. [cited 2021 Sep 7]. https://www.londonair.org.uk/LondonAir/Default.aspx.
41. Frühauf, A., Schnitzer, M., Schobersberger, W., Weiss, G. & Kopp, M. Jogging, nordic walking and going for a walk—interdisciplinary recommendations to keep people physically active in times of the covid-19 lockdown in Tyrol, Austria. *Curr. Issues Sport Sci.* **5**, 3–6 (2020).
42. Burnett, H., Olsen, J. R., Nicholls, N. & Mitchell, R. Change in time spent visiting and experiences of green space following restrictions on movement during the COVID-19 pandemic: A nationally representative cross-sectional study of UK adults. *BMJ Open* **11**(3), 1–10 (2021).
43. Soga, M., Evans, M. J., Tsuchiya, K. & Fukano, Y. A room with a green view: The importance of nearby nature for mental health during the COVID-19 pandemic. *Ecol. Appl.* **31**(2), 1–10 (2021).
44. Gray, S. & Kellas, A. Covid-19 has highlighted the inadequate, and unequal, access to high quality green spaces [Internet]. The BMJ. [cited 2021 Sep 7]. https://blogs.bmj.com/bmj/2020/07/03/covid-19-has-highlighted-the-inadequate-and-unequal-access-to-high-quality-green-spaces/.
45. WHO Regional Office for Europe. *Urban Green Spaces and Health* 92 (2016).
46. Greenspace Information for Greater London. Access to public open space and nature by ward [Internet]. Greater London Authority. [cited 2021 Sep 7]. https://www.gigl.org.uk/.
47. The London Plan [Internet]. Greater London Authority; 2021. www.london.gov.uk.
48. Wirth, L. "Urbanism as a way of life": A review and an agenda. *Am. J. Sociol.* **44**(1), 1–24 (1938).
49. Behar, A., Manners, P. & Nelson, B. D. *Roads and Urban Growth* 439. Department of economics discussion paper series exports and logistics (2018).
50. Chen, S. Y., Feng, Z. & Yi, X. A general introduction to adjustment for multiple comparisons. *J. Thorac. Dis.* **9**(6), 1725–1729 (2017).
51. El-Khatib, Z., Jacobs, G. B., Ikomey, G. M. & Neogi, U. The disproportionate effect of COVID-19 mortality on ethnic minorities: Genetics or health inequalities?. *EClinicalMedicine* **23**, 10–11 (2020).
52. Sze, S. *et al.* Ethnicity and clinical outcomes in COVID-19: A systematic review and meta-analysis. *EClinicalMedicine [Internet]* **29–30**, 100630. https://doi.org/10.1016/j.eclinm.2020.100630 (2020).
53. Public Health England. *Disparities in the Risk and Outcomes of COVID-19* 89 (PHE Publication, 2020). https://www.gov.uk/government/publications/covid-19-review-of-disparities-in-risks-and-outcomes.
54. O'Brien, O. & Cheshire, J. Interactive mapping for large, open demographic data sets using familiar geographical features. *J. Maps [Internet]* **12**(4), 676–83. https://doi.org/10.1080/17445647.2015.1060183 (2016).
55. Matheson, J., Nathan, M., Pickard, H., & Vanino, E. Why has coronavirus affected cities more than rural areas? [Internet]. Economics Observatory. https://www.economicsobservatory.com/why-has-coronavirus-affected-cities-more-rural-areas.
56. Holden, J. & Kenway, P. Self-isolation doesn't work for crowded households—Government needs to take the WHO's advice and respond [Internet]. Housing and Homelessness. https://www.npi.org.uk/blog/housing-and-homelessness/self-isolation-doesnt-work-crowded-households-government-needs-take-whos-advice-and-respond/.
57. Harrison, E., Docherty, A. & Semple, C. Investigating associations between ethnicity and outcome from COVID-19. *Sage [Internet]* 1–13 (2020). https://www.ethnicity-facts-figures.service.gov.uk/uk-population-by-ethnicity/national-and-regional.
58. Marquès M. *et al.* Long-term exposure to PM10 above WHO guidelines exacerbates COVID-19 severity and mortality. *Environ Int.* **158**, 106930. https://doi.org/10.1016/j.envint.2021.106930 (2022).
59. Zoran, M. A., Savastru, R. S., Savastru, D. M. & Tautan, M. N. Assessing the relationship between surface levels of PM2.5 and PM10 particulate matter impact on COVID-19 in Milan, Italy. *Sci. Total Environ. [Internet]* **738**, 139825. https://doi.org/10.1016/j.scitotenv.2020.139825 (2020).
60. Fattorini, D. & Regoli, F. Role of the chronic air pollution levels in the Covid-19 outbreak risk in. *Environ. Pollut. [Internet]* **264**, 114732. https://doi.org/10.1016/j.envpol.2020.114732 (2020).
61. Cole, M. A., Ozgen, C. & Strobl, E. Air pollution exposure and Covid-19 in Dutch municipalities. *Environ. Resour. Econ. [Internet]* **76**(4), 581–610. https://doi.org/10.1007/s10640-020-00491-4 (2020).
62. Ogen, Y. Assessing nitrogen dioxide (NO2) levels as a contributing factor to coronavirus (COVID-19) fatality. *Sci. Total Environ. [Internet]* **726**, 138605. https://doi.org/10.1016/j.scitotenv.2020.138605 (2020).
63. Chakrabarty, R. K. *et al.* Ambient PM2.5 exposure and rapid spread of COVID-19 in the United States. *Sci. Total Environ [Internet].* **760**, 143391. https://doi.org/10.1016/j.scitotenv.2020.143391 (2021).
64. Petroni, M. *et al.* Hazardous air pollutant exposure as a contributing factor to COVID-19 mortality in the United States. *Environ. Res. Lett.* **15**(9), 0940a9. https://doi.org/10.1088/1748-9326/abaf86 (2020).
65. Liang D, Shi L, Zhao J, Liu P, Schwartz J, Gao S, Sarnat J, Liu Y, Ebelt S, Scovronick N, Chang HH. Urban air pollution may enhance COVID-19 case-fatality and mortality rates in the United States. medRxiv [Preprint]. 2020 May 7:2020.05.04.20090746. https://doi.org/10.1101/2020.05.04.20090746. Update in: Innovation (N Y). 2020 Sep 21:100047.
66. Wu, X., Nethery, R. C., Sabath, M. B., Braun, D. & Dominici, F. Exposure to air pollution and COVID-19 mortality in the United States: A nationwide cross-sectional study. *medRxiv* 1–13 (2020).

67. Konstantinoudis, G. *et al.* Long-term exposure to air-pollution and COVID-19 mortality in England: A hierarchical spatial analysis. *Environ Int [Internet]* **146**, 106316. https://doi.org/10.1016/j.envint.2020.106316 (2021).
68. Travaglio, M., Yu, Y., Popovic, R., Selley, L., Leal, N. S. & Martins, L. M. Links between air pollution and COVID-19 in England (2020).
69. Sasidharan, M., Singh, A., Eskandari, M. & Kumar A. A. vulnerability-based approach to human-mobility reduction for countering COVID-19 transmission in London while considering local air quality (2020).
70. Mishra, R., Krishnamoorthy, P., Gangamma, S., Raut, A. A. & Kumar, H. Particulate matter (PM10) enhances RNA virus infection through modulation of innate immune responses. *Environ. Pollut. [Internet]* **266**, 115148. https://doi.org/10.1016/j.envpol.2020.115148 (2020).
71. Morales-Bárcenas, R. *et al.* Particulate matter (PM10) induces metalloprotease activity and invasion in airway epithelial cells. *Toxicol. Lett. [Internet]* **237**(3), 167–173. https://doi.org/10.1016/j.toxlet.2015.06.001 (2015).
72. Zhao, Y. *et al.* Particulate air pollution exposure and plasma vitamin D levels in pregnant women: A longitudinal cohort study. *J. Clin. Endocrinol. Metab.* **104**(8), 3320–3326 (2019).
73. Gilani, S. J., Bin-Jumah, M. N., Nadeem, M. S. & Kazmi, I. Vitamin D attenuates COVID-19 complications via modulation of proinflammatory cytokines, antiviral proteins, and autophagy. *Expert. Rev. Anti Infect. Ther. [Internet]* **10**, 1–11. https://doi.org/10.1080/14787210.2021.1941871 (2021).
74. Hartig T, Kahn PH Jr. Living in cities, naturally. *Science.* **352**(6288), 938–940. https://doi.org/10.1126/science.aaf3759 (2016).
75. Hartig, T., Mitchell, R., De Vries, S. & Frumkin, H. Nature and health. *Annu. Rev. Public Health* **35**, 207–228 (2014).
76. Douglas, I. Urban ecology and urban ecosystems: Understanding the links to human health and well-being. *Curr. Opin. Environ. Sustain. [Internet]* **4**(4), 385–392. https://doi.org/10.1016/j.cosust.2012.07.005 (2012).
77. McKinney, M. L. & VerBerkmoes, A. Beneficial health outcomes of natural green infrastructure in cities. *Curr. Landsc. Ecol. Rep. [Internet]* **5**(2), 35–44. https://doi.org/10.1007/s40823-020-00051-y (2020).
78. Kleinschroth, F. & Kowarik, I. COVID-19 crisis demonstrates the urgent need for urban greenspaces. *Front Ecol Environ.* **18**(6), 318–319 (2020).
79. Hyde, Z., Berger, D. & Miller, A. Australia must act to prevent airborne transmission of SARS-CoV-2. *Med. J. Aust.* **215**(1), 7-9.e1 (2021).
80. Greenspace Information for Greater London. Access to public open space by ward [Internet]. Greater London Authority. 2015. https://data.london.gov.uk/dataset/access-public-open-space-and-nature-ward

Acknowledgements

Author contributions

All authors contributed to the study conception, planned the research and devised the methodology. Funding acquisition, M.U., R.S.-P. and E.V.; data collection and visualisation, M.B.; data analysis, all authors; statistical analysis, M.B., M.U. and M.W.; first draft of the manuscript, M.B. and M.U. All authors discussed the results and contributed to the final manuscript. All authors read and approved the final manuscript. Mehrdad Borna (M.B.) Maria Woloshynowych (M.W.) Rosa Schiano-Phan (R.S.-P.) Emanuela V Volpi (E.V.) Moonisah Usman (M.U.).

Funding

Competing interests

The authors declare no competing interests.

Additional information

Correspondence and requests for materials should be addressed to M.B.

Reprints and permissions information is available at www.nature.com/reprints.

Publisher's note Springer Nature remains neutral with regard to jurisdictional claims in published maps and institutional affiliations.

Appendix 3
National air quality objectives

The national Air Quality Objectives and Air Quality Standards Regulations limit and target values with which the UK must comply. These limits and targets are summarised in the National air quality objectives. Source: The Air Quality Standards Regulations 2010

National air quality objectives and European Directive limit and target values for the protection of human health						
Pollutant	**Applies**	**Objective**	**Concentration measured as**	**Date to be achieved by (and maintained thereafter)**	**European Obligations**	**Date to be achieved (by and maintained thereafter)**
Particles (PM$_{10}$)	UK	50 µg/m^3 not to be exceeded more than 35 times a year	24 hour mean	31 December 2004	50 µg/m^3 not to be exceeded more than 35 times a year	1 January 2005
	UK	40 µg/m^3	annual mean	31 December 2004	40 µg/m^3	1 January 2005
	Indicative 2010 objectives for PM$_{10}$ (from the 2000 strategy and Addendum) have been replaced by an exposure reduction approach for PM$_{2.5}$ (except in Scotland – see below)					
	Scotland	50 µg/m^3 not to be exceeded more than 7 times a year	24 hour mean	31 December 2010	50 µg/m^3 not to be exceeded more than 35 times a year	1 January 2005
	Scotland	18 µg/m^3	annual mean	31 December 2010	40 µg/m^3	1 January 2005
Particles (PM$_{2.5}$)	UK (except Scotland)	20 µg/m^3	annual mean	1 January 2020	Stage 1 Limit - 25 µg/m^3 Stage 2 Limit - 20 µg/m^3	1 January 2015 1 January 2020
	Scotland	10 µg/m^3	annual mean	31 December 2020		
Exposure Reduction	UK urban areas	Target of 15% reduction in concentrations at urban background		Between 2010 and 2020	Target of 20% reduction in concentrations at urban background.	Between 2010 and 2020

National air quality objectives and European Directive limit and target values for the protection of human health						
Pollutant	**Applies**	**Objective**	**Concentration measured as**	**Date to be achieved by (and maintained thereafter)**	**European Obligations**	**Date to be achieved by (and maintained thereafter)**
Nitrogen dioxide	UK	200 µg/m^3 not to be exceeded more than 18 times a year	1 hour mean	31 December 2005	200 µg/m^3 not to be exceeded more than 18 times a year	1 January 2010
	UK	40 µg/m^3	annual mean	31 December 2005	40 µg/m^3	1 January 2010
Ozone	UK	100 µg/m^3 not to be exceeded more than 10 times a year	8 hour mean	31 December 2005	Target of 120 µg/m^3 not to be exceeded by more than 25 times a year averaged over 3 years	31 December 2010
Sulphur dioxide	UK	266 µg/m^3 not to be exceeded more than 35 times a year	15 minute mean	31 December 2005	-	-
	UK	350 µg/m^3 not to be exceeded more than 24 times a year	1 hour mean	31 December 2004	350 µg/m^3 not to be exceeded more than 24 times a year	1 January 2005
	UK	125 µg/m^3 not to be exceeded more than 3 times a year	24 hour mean	31 December 2004	125 µg/m^3 not to be exceeded more than 3 times a year	1 January 2005
Polycyclic Aromatic Hydrocarbons	UK	0.25 ng/m^3 B[a]P	as annual average	31 December 2012	1.0 ng/m^3	31 December 2012

National air quality objectives and European Directive limit and target values for the protection of human health						
Pollutant	Applies	Objective	Concentration measured as	Date to be achieved by (and maintained thereafter)	European Obligations	Date to be achieved by (and maintained thereafter)
Benzene	UK	16.25 µg/m³	running annual mean	31 December 2003	-	-
	England and Wales	5 µg/m³	annual average	31 December 2010	5 µg/m³	1 January 2010
	Scotland, Northern Ireland	3.25 µg/m³	running annual mean	31 December 2010	-	-
1,3-butadiene	UK	2.25 µg/m³	running annual mean	31 December 2003	-	-
Carbon monoxide	UK	10 mg/m³	maximum daily running 8 hour mean/in Scotland as running 8 hour mean	31 December 2003	10 mg/m³	1 January 2005
Lead	UK	0.5 µg/m³	annual mean	31 December 2004	0.5 µg/m³	1 January 2005
		0.25 µg/m³	annual mean	31 December 2008	-	-

National air quality objectives and European Directive limit and target values for the protection of vegetation and ecosystems						
Pollutant	Applies	Objective	Concentration measured as	Date to be achieved by (and maintained thereafter)	European Obligations	Date to be achieved by (and maintained thereafter)
Nitrogen oxides	UK	30 µg/m³	annual mean	31 December 2000	30 µg/m³	19 July 2001
Sulphur dioxide	UK	20 µg/m³	annual mean	31 December 2000	20 µg/m³	19 July 2001
	UK	20 µg/m³	winter average	31 December 2000	20 µg/m³	19 July 2001
Ozone: protection of vegetation and ecosystems	UK	Target value of 18,000 µg/m³ based on AOT40 to be calculated from 1 hour values from May to July, and to be achieved, so far as possible, by 2010	Average over 5 years	1 January 2010	Target value of 18,000 µg/m³ based on AOT40 to be calculated from 1 hour values from May to July, and to be achieved, so far as possible, by 2010	1 January 2010